OLFACTORY ENSHEATHING CELLS FOR CENTRAL NERVOUS SYSTEM REPAIR: A VENTRAL ROOT MODEL FOR INTRASPINAL CERVICAL ROOT REPAIR IN THE RAT

PRATIPAL SINGH KALSI

Thesis undertaken for the degree of Doctor of Philosophy

University College London

October 2020

Department of Brain Repair & Rehabilitation, Spinal Repair Unit, Institute of Neurology, Queen Square, London.

DECLARATION

I, Pratipal Singh Kalsi, confirm that the work presented in this thesis is my own. Where information has been derived from other sources, I confirm that it has been indicated as such in the thesis.

Pratipal Singh Kalsi

ABSTRACT

Brachial plexus avulsion injuries occurring at the central nervous system and peripheral nervous system transition zone are often referred to as longitudinal spinal cord injuries. A number of surgical procedures, including intraspinal ventral root reimplantation, have been devised to treat these injuries but hand function rarely recovers and there is no cure.

A number of preclinical and clinical studies have attempted to use cellular therapies for spinal cord injury repair. To this regard the olfactory ensheathing cell, obtained from the olfactory pathways, has shown promise but remains controversial. These cells have not previously been investigated in a brachial plexus repair model but their reparative and regenerative properties gives them investigative potential.

In order to replicate a brachial plexus injury affecting the human hand, we have devised a rodent model of C8 ventral root repair. We used histological analysis and immunohistochemistry staining with neurofilament and glial fibrillary acidic protein to assess the repair. Tests were developed to assess neuronal continuity across the repair site using retrograde tracers. Functional tests were developed to quantify forepaw injury and recovery.

Once a model was established, four experimental study groups consisting of left C8 ventral root avulsion, reimplantation, and transplantation of mucosal and bulb olfactory ensheathing cells were devised. Our results demonstrate that reimplantation of the ventral root after avulsion led to a significantly improved left paw spread recovery and survival of motor neurones compared to the avulsion group. Transplantation of mucosal and bulb olfactory ensheathing cells led to a significantly improved recovery

in paw spread, increased survival of motor neurones, and less forepaw deformity and autotomy, compared to the reimplantation group. These results suggest that olfactory ensheathing cells can promote central nervous system recovery in adult rats and add promise to their translational potential for brachial plexus repair in humans.

IMPACT STATEMENT

The work carried out in this thesis has led to the development of a C8 ventral root brachial plexus injury model in a rat. A considerable amount of work went into developing the surgical model, functional tests to assess the injury and recovery after surgery, and methods to assess continuity of motor neurones across the injury and repair site. These are novel techniques which have not been described in this context before and they should be utilised to further study the effects of these cells on neural repair and regeneration after brachial plexus injury.

Although there are a number of controversies and challenges regarding olfactory ensheathing cells, our model could be used to investigate other cellular, pharmacological and nanomaterial strategies to treat focal longitudinal spinal cord injuries.

If we assume that olfactory ensheathing cells are beneficial for central nervous system repair, the next logical step would be to consider their utilisation in patients with brachial plexus injury. These cells can safely be obtained from the nasal mucosa of the olfactory epithelium and direct autologous transfer of these cells in patients undergoing brachial plexus repair remains a realistic therapeutic intervention for this devastating injury.

ACKNOWLEDGEMENTS

First and foremost, I would like to thank Professor David Choi, my supervisor, for inviting me to come to his laboratory and carry out this work. Without his persistent energy, time, support and motivation I would not have been able to do any of this work.

I would like to thank Daqing Li and Karen Oprych for their invaluable scientific advice and encouragement when my experiments were not going to plan!

I would also like to thank Stuart Law for the technical and logistical support he gave me. Without his skills and laboratory expertise my experiments would have been impossible to do.

This work would not have been possible without the constant support and encouragement from my family.

TABLE OF CONTENTS

LIST OF FIGURES

CHAPTER 1

CHAPTER 2

CHAPTER 3

CHAPTER 4

CHAPTER 5

CHAPTER 6

LIST OF TABLES

CHAPTER 1

CHAPTER 3

CHAPTER 6

LIST OF ABBREVIATIONS

ASIA: American Spinal Injury Association

ASD: avulsion Sprague Dawley group

BPI: brachial plexus injury

BDA: biotinylated dextran amine

BSD: bulb olfactory ensheathing cell Sprague Dawley group

bOEC: bulb olfactory ensheathing cells

CNS: central nervous system

CNTF: ciliary neurotrophic factor

DREZ: dorsal root entry zone

E-NCAM: embryonic neural cell adhesion molecule

erbB3: receptor tyrosine kinase erbB3

FB: FastBlue®

FD: Dextran conjugated to fluorescein

FGFR1: fibroblast growth receptor receptor 1

FGF2: fibroblast growth factor 2

FG: fluoro-gold

FR: fluoro-ruby

GFP: green fluorescent protein

GFAP: glial fibrillary acidic protein

H&E: haematoxyllin & eosin

HRP: horseradish peroxidase

ITS: intermediate toe spread

L1 CAM: L1 neural adhesion molecule

MRC: Medical Research Council

MSD: mucosal olfactory ensheathing cell Sprague Dawley group

mOEC: mucosal olfactory ensheathing cells

NCAM: neural cell adhesion molecule

NF: neurofilament

NSPCs: neural stem progenitor cells

O4: oligodendrocyte marker O4

OEC: olfactory ensheathing cell

OCT: optimal cutting temperature compound

ONF: olfactory nerve fibroblasts

PA: paw angle

PS: paw spread

PFA: paraformaldehyde

PEG: polyethylene glycol

PNS: peripheral nervous system

PACAP: pituitary adenylate cyclase activating peptide

PDGF-B: platelet derived growth factor B

PN-1: protease nexin 1

RSD: reimplantation Sprague Dawley group

S100β: S100 calcium-binding protein β

SMA: smooth muscle actin

SD: Sprague Dawley rats

VEGF: vascular endothelial growth factor

PUBLICATIONS

Kalsi P, Thom M, Choi D. The histological effects of fibrin glue and tissue adhesives on the spinal cord: Are they safe to use? British Journal of Neurosurgery 2017 Dec;31(6): 695-700

Gladwin K, Kalsi P, Choi D. Rat brachial plexus ventral root repair model. Plast Reconstr Surg Glob Open. 2016 Jan 7;3(12):e576

PRESENTATIONS

Kalsi P, Oprych K, Choi D. Olfactory Ensheathing Cells for Central Nervous System Repair: An Experimental Ventral Root Model for Intraspinal Brachial Plexus Repair. Global Spine Congress, Rio, Brazil, 2020 (Accepted - Conference cancelled due to Covid-19)

Kalsi P, Thom M Choi D. The histological effects of fibrin glue and synthetic adhesives on spinal cord. Society of British Neurological Surgeons, Romford, Autumn 2013.

CHAPTER ONE

CHAPTER 1: INTRODUCTION

1.1 Introduction

Traumatic brachial plexus injuries (BPI) are rare injuries afflicting young adult males, having an incidence of 0.64-3.9/100000/year and prevalence of 1.2%. High velocity motorcycle accidents account for 67% of BPI with other causes including car accidents, sports injuries and gunshot wounds. (Kaiser et al., 2020) These injuries tend to occur when the abducted arm is forcefully extended behind the body. Depending on the precise anatomical location and severity of the injury, patients may be left with a flail, senseless and extremely painful arm which can have a devastating impact on quality of life. A number of surgical procedures have been developed to help improve symptoms and functional outcomes. However, there is currently no curative treatment.

A BPI can be either a peripheral (PNS) or central nervous system (CNS) injury. A central brachial plexus avulsion injury is a type of longitudinal spinal cord injury (SCI) occurring at the junction between the central and peripheral nervous system. (Carlstedt, 1997, Carlstedt, 2007, Berthold and Carlstedt, 1977) Any injury which leads to the avulsion of a ventral root through its central nervous system component will lead to a rapid death of motor neurones. (Koliatsos et al., 1994) Injury proximal to the dorsal root ganglion, whether it is in the central or peripheral part of the nerve, is also considered a central nervous system injury. (Carlstedt, 1997) If untreated, the affected spinal cord segments deteriorate rapidly over a few weeks, with death of sensory, motor and autonomic neurones. (Bergerot et al., 2004, Chew et al., 2008, Hoang et al., 2008) Axonal regeneration at this focal injury point is affected by the same factors

inhibiting spinal cord repair, namely a reactive astrocytosis, leading to formation of an inhibitory glial scar, hindering axonal propagation and repair. (Reier, 1983)

A number of investigators have tried to minimise the effects of the inhibitory components of the glial scar to promote CNS regeneration. (Li et al., 1995, Novikova et al., 1997a, Bergerot et al., 2004, Blits et al., 2004, Son, 2015, Goncalves et al., 2015) Other groups have aimed to provide a neuroprotective environment and promote plasticity, repair and/or regeneration by providing a protective environment for axonal regeneration with cell therapies. (Chong et al., 1999, Kliot et al., 1990, Ramer et al., 2002, Wang et al., 2008)

One of these cells is the olfactory ensheathing cell (OEC). OECs are found in the olfactory pathways of mammalian species. A number of investigators have explored the possibility of using OECs as a cellular strategy to promote axonal regeneration in the spinal cords of adult rats. (Ramon-Cueto and Nieto-Sampedro, 1994, Li et al., 1997, Li et al., 2004, Barnett and Riddell, 2007)

Repair of clinical brachial plexus injuries by transplantation of human OECs presents a practicable target for CNS repair because the damage to the nervous tissue in these injuries is focal and the injuries have a predictable outcome. (Kachramanoglou et al., 2011b)

We therefore developed a rat brachial plexus ventral root avulsion injury model and devised reproducible functional and immunohistopathological tests to quantify the injury. (Oprych et al., 2015) This model will be used to assess the safety and efficacy of autologous Sprague Dawley rat OECs to promote CNS repair and/or regeneration after brachial plexus injury.

1.2 Brachial plexus avulsion injury in humans

Traumatic brachial plexus injuries are rare injuries often occurring after high-speed motor vehicle accidents. They can result in nerve roots being contused, stretched, or ruptured after the nerves have either left the foramen or completely avulsed at the spinal cord level. Dorsal root injuries occurring distal to the dorsal root ganglion are referred to as post-ganglionic injuries. Pre-ganglionic injuries can be either a central or peripheral type depending on the location of the avulsion. Nevertheless, dorsal root injuries proximal to the ganglion do not recover. (Carlstedt, 1997) Similarly, when the ventral root is pulled out of its CNS connection this is also considered a longitudinal CNS injury. In a central type plexus injury the nerve rootlets are avulsed from the cord, either proximal to or at the transition zone of the spinal cord. (Carlstedt, 1997)

At the nerve root spinal cord junction, each spinal nerve consists of a short segment of central nervous tissue and a longer segment of peripheral nervous tissue. The central component of the spinal nerve has a dense concentration of astrocytes and astrocytic foot processes, which project around 100 micrometres into the CNS-PNS interface. This region is known as the transition zone. (Berthold and Carlstedt, 1977) It is usually the site of root avulsion in BPI. (Livesey and Fraher, 1992) At this transition zone, the CNS tissue forms a growth-inhibitory scar preventing axonal growth from the PNS. (Reier, 1983)

After a complete brachial plexus avulsion injury affecting all roots from C5 to T1, patients will usually have a flail, senseless arm and severe, intractable pain. (Berman, Birch, & Anand, 1998a; Htut, Misra, Anand, Birch, & Carlstedt, 2006) These patients may also develop an ipsilateral Horner's syndrome due to damage of the sympathetic plexus and in pre-ganglionic injuries pseudomeningocoeles can develop due to

rupture of the dural sac. The injury can have a devastating impact on quality of life and although a number of surgical interventions have helped improve functional outcomes there remains no cure. (Kachramanoglou et al., 2017)

1.3 Brachial plexus repair strategies in humans

Nerve transfer or neurotization techniques are used in an attempt to relieve arm pain and improve function. Letivant first described neurotization in 1873. The principle involves sacrificing the function of a lesser valued donor muscle or sensory nerve in order to improve function of the recipient nerve and muscle undergoing attempted reinnervation. (Narakas and Hentz, 1988) A functional recovery of elbow flexion was seen in 60-80% of patients having these procedures. (Bentolila et al., 1999, Gu and Ma, 1996, Waikakul et al., 1999) However, reinnervation of forearm muscles and restoration of hand function was poor. Other nerve and muscle transfer techniques have attempted to restore hand function, but outcomes remain similarly poor. (Berger et al., 1990, Doi et al., 2000)

Other researchers have developed techniques in an attempt to improve hand function. One such technique is intraspinal ventral root reimplantation for BPI. This technique was first performed by Carlstedt and Noren. (Carlstedt and Noren, 1995) The procedure involves opening the dura and inspecting the spinal cord under direct vision. Depending on the timing of surgery, ventral roots that have been avulsed may remain within the subdural space but more often are displaced outside the spinal canal and have migrated into the arm. Under these circumstances a nerve graft from a sensory nerve in the arm is used to connect the detached nerve root to the spinal cord. An opening is made in the pia and the nerve graft is reimplanted directly into the anterolateral aspect of the spinal cord and retained in position using tissue glue

(Tisseel®, Baxter, Illinois, US). The graft is then then pulled through or around the intervertebral foramen and connected to the distal stumps, which have usually migrated into the neck by the time of surgery. (Carlstedt and Noren, 1995)

1.4 Clinical outcomes of brachial plexus repair after intraspinal ventral root reimplantation

Successful recovery of function following spinal ventral root reimplantation is thought to depend on motor neurone survival, regrowth of interneurons and migration of axons through the spinal cord in to the reimplanted ventral root to re-establish connections within target muscles. The timing of surgical intervention is crucial with motor neurones being rapidly killed by nerve avulsion (Koliatsos et al., 1994) a further 50% being killed within 2 weeks followed by a progressive loss over time. (Bergerot et al., 2004)

When patients have surgery within a month of the injury, they may start to recover muscle function in the proximal arm within a year. Over time strength in the proximal arm muscles can return to near normal power in some (MRC 4-5/5) and forearm muscles can reach MRC 2/5. (Kachramanoglou et al., 2017) However, similar to previously described neurotization techniques, functional recovery in the hand remains poor. Surgery after a month from injury invariably produces poor functional results. (Carlstedt et al., 2000, Carlstedt et al., 1995) However, ventral root reimplantation after a complete avulsion injury in a preadolescent child did result in recovery of hand function as well as good recovery of power in proximal arm muscles. (Carlstedt et al., 2004)

Nevertheless, after a complete C5-T1 avulsion injury and ventral root reimplantation, proprioception and sensation do not usually recover. Although some patients have a return of some sensory function the improvement of pain is difficult to explain when

only ventral surgery has been performed. This is thought to correlate with the return of muscle activity rather than the quality of muscle function in the arm. (Berman et al., 1998, Htut et al., 2006)

Although intraspinal ventral root reimplantation is an established technique for patients with brachial plexus avulsion injuries, the lack of functional recovery in the hand means that there is still no cure for BPI. This has led to the development of newer experimental treatments including OEC transplantation in combination with surgery to promote the regeneration of CNS axons in spinal cord injury. (Feron et al., 2005, Huang et al., 2003a, Lima et al., 2006)

1.5 Cell transplants for the treatment of central nervous system injuries in animal models

Over the last two decades a number of preclinical animal studies have been conducted to try to establish an ideal cell type to use for spinal cord repair and/or regeneration. (Carlstedt, 2008, Raisman et al., 2011, Carlstedt, 2016)

Schwann cells have been extensively studied and their neurotrophic extracellular matrix and cell adhesion properties make them a candidate for nerve regeneration in the PNS. Tello, Ramón y Cajal, and David & Aguayo demonstrated long-distance axonal regeneration from CNS neurons when presented with a PNS environment. (David and Aguayo, 1981, Ramon Y Cajal, 1928, Tello, 1911b)

Several authors have shown that peripheral nerve grafts can promote axonal regeneration from the CNS over long distances. (Bray et al., 1987, Li and Raisman, 1994) Functional improvements using Schwann cells in rodent models have also been described. (Barakat et al., 2005, Takami et al., 2002) However, Schwann cell

transplants stay within the lesion cavity, and are unable to migrate into the spinal cord. This leads to a growth of axons through the Schwann cell bridge but the regenerating axons are unable to enter the spinal cord. (Novikova et al., 2011)

Other cell types to have been studied include neural stem progenitor cells (NSPCs), which are thought to be precursors of neurons, astrocytes and oligodendrocytes. These precursor cells differentiate into predominantly astrocytes and oligodendrocytes but differentiation into neuronal cells is unusual. (Karimi-Abdolrezaee et al., 2006, Parr et al., 2007) However, functional improvements have been demonstrated with this cell type in a spinal injury model. (Iwanami et al., 2005) Although embryonic cells theoretically have a promising role a number of ethical issues prevent routine use in experimental models.

Other groups have attempted spinal cord repair by using neural and glial restricted precursors, but functional improvements have been limited. (Cao et al., 2005)

More recently OECs have become popular as an experimental cell for spinal cord repair. A number of investigators have explored the possibility of using OECs as a cellular strategy to promote axonal regeneration in the damaged spinal cords of adult rats. (Feron et al., 2005, Huang et al., 2003a, Lima et al., 2006) Cultures of OECs have been grafted into the injured spinal cord of adult rats and have resulted in axonal sprouting and regeneration, reduced cavitation at the injury site and improved functional recovery. (Boyd et al., 2003, Bunge, 2001, Franklin and Barnett, 2000, Raisman, 2001, Ramon-Cueto and Valverde, 1995, Richter and Roskams, 2008, Ruitenberg et al., 2006)

1.6 Olfactory ensheathing cells

OECs were first recognised by Blanes (1898) but their ability to ensheath multiple olfactory axons was described by Doucette. (Doucette, 1984) These cells are unique in that they are found in both the CNS and the PNS and have the ability to regenerate continuously throughout adulthood.

The olfactory bulbs and olfactory system are derived embryologically from the cranial telencephalon. Cells in the nasal placodes differentiate to form the primary neurosensory cells of the olfactory epithelium during the 4^{th} and 5^{th} weeks of life. The cells send axons to the cranial end of the telencephalon and the subsequent ossification of the anterior skull base creates the axonal passage into the cribriform plate. The olfactory bulb is formed at the base of each cerebral hemisphere at around 6 weeks gestation and axons sprouting from the bulb which form connections with the primary sensory cells from the epithelial mucosa differentiate to become second order neurones of the olfactory system. These axons synapse in the olfactory centres in the brain and as the cerebral hemispheres develop the pathways elongate to form the olfactory tracts. (Larsen, 1998)

Throughout development and in adult life, the regeneration of nerve cells occurs in the olfactory epithelium, where cells in the basal layer continually proliferate to generate new sensory neurons every 1 to 3 weeks. (Graziadei and Graziadei, 1979, Leung et al., 2007) This ability to regenerate is attributed to OECs, which therefore play a pivotal role in not only the development of the olfactory system but also in the continuous axonal regeneration and organisation of the olfactory system. (Chuah and Zheng, 1992)

1.6.1 Anatomical organisation of the olfactory system

All mammals have a central and peripheral component to their olfactory system. The olfactory nerves are comprised of primary olfactory neurons which originate in the nasal olfactory epithelium. These peripheral axons have the ability to undergo continual renewal. (Schwob, 2002) Neurons in the olfactory mucosa give rise to axons which pass through the lamina propria of the olfactory mucosa and enter the cranium through the cribriform plate to synapse with second order neurons of the olfactory bulb. (Calof et al., 2002, Schwob, 2002) From here axons pass through the olfactory nerve fibre layer to synapse with second order olfactory neurons in the glomerular layer in the olfactory bulb. (see Figure 1.1)

1.6.2 Histological organisation of the olfactory system

Primary olfactory neurons send thin unmyelinated axons from the basal olfactory epithelium to the glomeruli in the olfactory bulbs. Throughout this pathway these peripheral nerve fibres are intricately associated with OECs. In the lamina propria the OECs completely ensheath the fascicles of olfactory axons. (Boyd et al., 2005, Doucette, 1995, Raisman, 1985, Ramon-Cueto and Avila, 1998) As the axons penetrate the olfactory nerve fibre layer of the olfactory bulbs, the organisation between OECs and these fibres becomes a dense meshwork of bundles juxtaposed by clusters of OECs. (Figure 1.1)

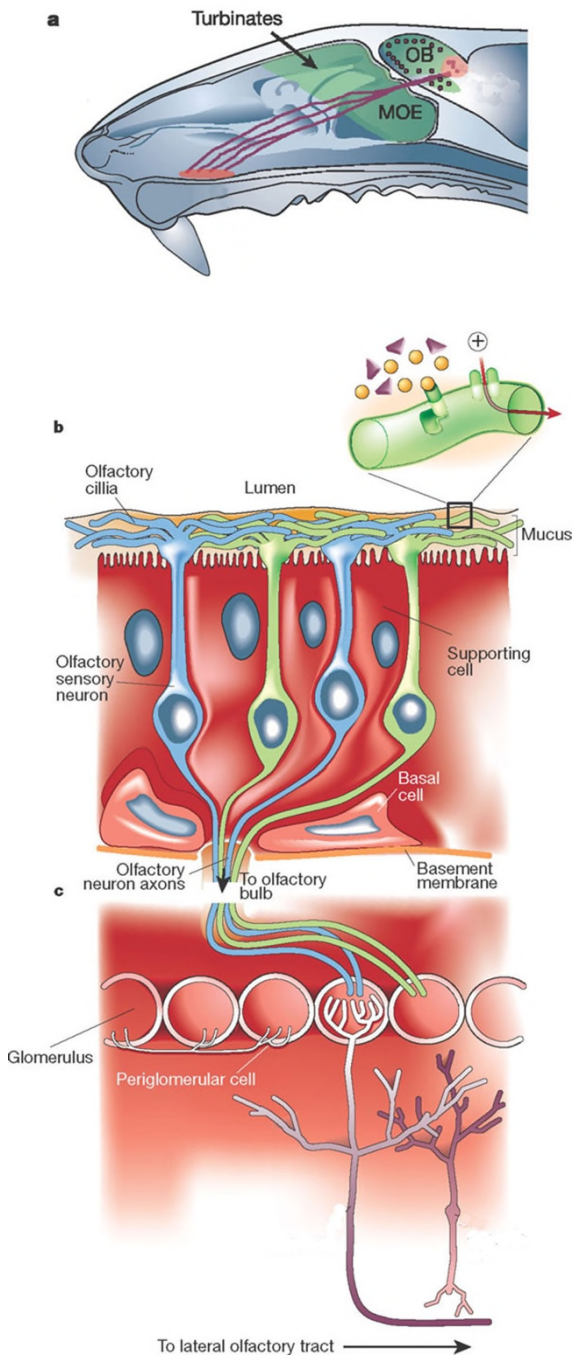

Figure 1.1. Organisation of the rat olfactory system. a) Schematic of a rat head sagittal section showing the main olfactory epithelium underlying the nasal turbinate's and olfactory bulb. b) The cells of the olfactory mucosa send axons trough the basal lamina to the glomeruli of the olfactory bulb. c) The olfactory bulb is shown with primary axons synapsing with the glomerular layer, before second order neurons leave in the olfactory tract. (From Firestein, 2001(Firestein, 2001))

1.6.2.1 Olfactory mucosa

The olfactory mucosa is composed of a superficial epithelial layer and a deeper lamina propria. The olfactory epithelium is located closest to the air space of the nasal cavities. It contains primary olfactory nerve fibres and associated support cells and basal stem cells. Axons from this primary layer pass through the basal lamina to enter the underlying lamina propria. The lamina propria is comprised of loose connective tissue and has multiple olfactory nerve fascicles of different sizes and is attached to the underlying turbinate's and septum by thick periosteal connective tissue.

The olfactory axons pass through the lamina propria in olfactory nerve fascicles. These fascicles have a high density of mucosal OECs which send numerous processes amongst the thin unmyelinated olfactory nerve fibres. However, the mucosal lamina propria also contains peripheral nerves composed of myelinated and unmyelinated nerve axons which are closely associated with Schwann cells.

1.6.2.2 Olfactory bulb and nerve fibre layer

The outermost layer of the olfactory bulb, the olfactory nerve fibre layer, is the transition point between PNS and CNS. At this point fascicles of the olfactory axons penetrate the bulb and innervate second-order neurons. The olfactory bulb is composed of six demarcated cell layers, which include from outermost to innermost: olfactory nerve fibre layer, glomerular layer, external plexiform layer, mitral cell layer, internal plexiform layer and granule layer. On approaching the olfactory bulb, the olfactory nerve fibres merge into larger bundles which penetrate the olfactory bulb in a criss-cross meshwork fashion. Here, groups of bulb OECs are clustered together, each extending processes around the multiple bundles of olfactory axons. However, peripheral nerves are also found in the nerve fibre layer of the olfactory bulb. Schwann

cell-containing nerves embedded within the CNS component of these olfactory tissues have been reported in a number of mammalian species. (Doucette, 1991, Kawaja et al., 2009)

1.7 Phenotypic features of olfactory ensheathing cells in vivo

A number of studies have detailed the characteristics of OECs in the olfactory mucosa and bulbs of mammals. (see Table 1.1) Barber & Lindsay first reported that these cells express glial fibrillary acidic protein (GFAP). (Barber and Lindsay, 1982) Other investigators showed that human OECs stained positive for S100ß, cell adhesion molecules NCAM, NCAM180 and L1 in adult mouse OECs, p75 neurotrophin receptor ($p75^{NTR}$) in embryonic and adult rat OECs, O4 and neuropeptide Y in embryonic rat OECs. (Franceschini and Barnett, 1996, Gong et al., 1994, Miragall et al., 1988, Takahashi et al., 1984, Ubink and Hokfelt, 2000)

OECs in vivo co-express $p75^{NTR}$, GFAP and S100ß. Although a large number of antibodies have been used to positively label OECs in vitro, none of these have been successful at labelling OECs in the olfactory mucosa or bulbs of mammals.

In addition, $p75^{NTR}$, GFAP and S100β can be used to label Schwann cells in vivo and/or in vitro. (Guenard et al., 1996, Li et al., 1996, Li et al., 2003a, Li et al., 2003b, Pixley, 1992)

	Olfactory Mucosa	Olfactory Bulb
Antigens expressed by OECS in vivo	S100β, GFAP, NCAM, PN-1, galectin, L1CAM, vimentin, neuroligin-3, PACAP, erbB3, integrins, VEGF, FGFR1	**Outer nerve layer:** $p75^{NTR}$ & E-NCAM **Inner nerve layer:** NPY & TROY **Both layers:** S100β, GFAP, NCAM, galectin, L1CAM, vimentin, PN-1, neuroligin-3, PACAP, erbB3, FGF2, PDGF-B, CNTF

Table 1.1. Molecules expressed by OECs in the olfactory mucosa and bulb. S100β, S100 calcium-binding protein β; OECs, olfactory ensheathing cells; GFAP, glial fibrillary acidic protein; NCAM, neural cell adhesion molecule; L1CAM, L1 neural cell adhesion molecule; PN-1, Protease nexin-1; PACAP, pituitary adenylate cyclase activating peptide; erbB3, receptor tyrosine-protein kinase erbB3; VEGF, vascular endothelial growth factor; FGFR1, fibroblast growth factor receptor 1; $p75^{NTR}$, low affinity neurotrophin receptor; E-NCAM, embryonic neural cell adhesion molecule; NPY, neuropeptide Y; FGF2, fibroblast growth factor 2; PDGF-B, platelet derived growth factor B; CNTF, ciliary neurotrophic factor. Adapted from Vincent et al (Vincent et al., 2005)

1.8 Phenotypic features of OECs *in vitro*

Ramon-Cueto and colleagues demonstrated three distinct cell types in bulb OEC cultures from adult rats: 1) fusiform Schwann cell-like OECs that resembled non-myelinating Schwann cells; 2) flattened multipolar astrocyte-like OECs resembling

astrocytes; and 3) macrophage like cells. (Pixley, 1992, Ramon-Cueto and Nieto-Sampedro, 1992, Ramon-Cueto et al., 1993)

The Schwann cell like OECs have avid $p75^{NTR}$ but weak GFAP immunostaining but the astrocyte-like OECs have avid GFAP and weak $p75^{NTR}$ staining. (Franceschini and Barnett, 1996, Franklin and Barnett, 1997, Huang et al., 2008, Pixley, 1992) However, detection of OECs with S100ß, 04 and Thy 1.1 have not yielded consistent results. (Nash et al., 2001, Sonigra et al., 1999, Wewetzer et al., 2005) In addition to these markers a large number of other markers have also been detected in OEC mucosal and bulb cultures.

However, OECs and Schwann cells express variable levels of $p75^{NTR}$, and this point is important when considering the OEC source (namely bulb versus mucosal) and the age of the olfactory tissue being utilised.

Cultures of OECs from the olfactory nerve fibre layer of embryonic rats express SMA and a number of other proteins. (Boyd et al., 2006, Jahed et al., 2007) Consequently, the use of $p75^{NTR}$ as a single biomarker for OECs is insufficient to exclude contamination of OEC cultures by Schwann cells. It is therefore suggested that markers including SMA and calponin should be used in combination with $p75^{NTR}$ to establish the proportions of OECs and Schwann cells in a culture. (see Figure 1.2)

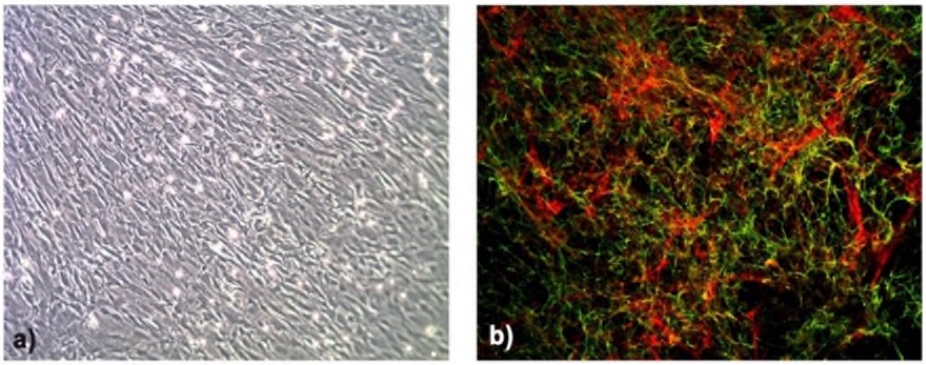

Figure 1.2. Microscopic appearance of OECs. a) Light microscopy showing a culture of bulb cells at Day 17 (x40). b) Bulb cultures characterised with $p75^{NTR}$ (green) and fibronectin (red) at Day 17

1.9 Bulb or mucosal olfactory ensheathing cells?

There is debate as to whether mucosal or bulb OECs are more effective in promoting repair and/or regeneration within the CNS. Recent studies suggest that mucosal and bulb OECs have different characteristics. Following spinal cord transplantation, mucosal OECs have superior ability to migrate and can promote nerve axon growth. (Richter et al., 2005) Other studies indicate that bulb OEC transplantation into corticospinal tract lesions leads to regeneration of nerve axons and restoration of function. (Li et al., 1998) However, other studies have shown that mucosal OECs transplanted into the same lesions produced functional recovery without regeneration of damaged nerve fibres, suggesting that mucosal OECs may be able to promote plasticity. (Yamamoto et al., 2009) However, there are controversies around the methods for culturing mucosal and bulb tissue and the proportion of OECs and other cell types may confound the results of these studies.

1.10 OECs in spinal repair in animal models

A number of studies have investigated the ability of OECs to promote repair and regeneration in dorsal and ventral root and spinal cord injury models.

In the adult, injury to the dorsal roots results in a situation where the PNS-CNS interface acts as a barrier through which regenerating axons of an injured nerve are not able to re-enter the CNS. (Li et al., 2004)

Some authors have reported that cut dorsal roots can be triggered to regenerate into the CNS by transplantation of glial cells, conditioning of nerve injuries peripheral to the dorsal root ganglion, or by use of various growth factors. (Chong et al., 1999, Kliot et al., 1990, Ramer et al., 2002)

The dorsal roots of the rat brachial plexus were one of the first sites where OECs were tested. (Ramon-Cueto and Nieto-Sampedro, 1994, Barnett and Riddell, 2007) Adult rat bulb OECs transplanted at the site of re-apposition of the cut dorsal lumbar roots survived forming a bridge between the severed roots and the dorsal horn of the cord, thereby allowing axons to cross the glia-pial barrier, re-enter the dorsal horn and continue into the dorsal horns. (Li et al., 2004) Transplanted OECs in the dorsal root of the rat brachial plexus have been shown to restore grasp function of the forepaw. (Ibrahim et al., 2009a) OECs have also shown promise in repair of damaged corticospinal tracts. (Li et al., 1997, Keyvan-Fouladi et al., 2003)

Another author has shown that reimplantation of an avulsed lumbar ventral root can recruit parasympathetic fibres and addition of OECs may be a target for impaired bladder function. (Hoang et al., 2008)

However, in other studies transplantation of OECs into crushed or sectioned dorsal roots have not shown any regeneration of sensory fibres into the spinal cord. (Ramer et al., 2002) However, it is unclear whether this finding is due to differences in cell culture, presence of other cell types, and/or differences in surgical technique. (Li et al., 2004)

With regards to ventral roots, a proportion of axons are able to enter reimplanted ventral roots, regenerate through the brachial plexus, and reinnervate proximal muscles, without the presence of OECs. The additional benefits of transplanting OECs in such a reimplantation therefore provide a theoretical target for brachial plexus repair.

In a series of rat experiments, bulb OECs have been shown to survive and migrate into the peripheral nerve after lumbosacral ventral roots surgery. (Li et al., 2007)

However, despite successful reports of CNS regeneration with OEC transplantation, a number of negative studies raises concerns about their efficacy. The method of application may play a significant role in the regenerative potential of these cells, as demonstrated by studies where OECs were injected into the site of injury in the spinal cord or applied topically in a cell matrix. (Ibrahim et al., 2009a, Ramon-Cueto and Nieto-Sampedro, 1994)

Another source of controversy is the composition of the OEC cultures. Many groups have used purified OEC cultures but others report that co-transplantation with unpurified OECs with a fibroblast component have an enhanced regenerative effect. (Li et al., 2005) The length of time the OECs are cultured may also impact OEC regenerative potential. Studies suggest that they should be cultured for at least one-week prior to transplantation, so that they are converted into active regeneration

promoting cells but if they are cultured for more that 14-17 days this potential may be lost. (Novikova et al., 2011, Raisman, 2001) Noviokova et al. also demonstrated that OEC culture methods could affect the regenerative potential of these cells. (Novikova et al., 2011) Other studies suggest that the source of OECs impacts the reparative properties, such that mucosal OECs have an increased migratory ability, exhibit less cavitation and have potential to stimulate growth of different axons compared with bulb OECs. (Richter et al., 2005)

1.11 OEC mechanism of repair

The precise way in which OECs enhance spinal repair is unknown. A number of studies have reported enhanced neural repair after transplanting OECs into spinal injury in rodents, but it is uncertain as to what role OECs play and to what degree other cell types are involved. (Barnett and Riddell, 2007, Boyd et al., 2004, Andrews et al., 1988, Ruitenberg and Vukovic, 2008, Wewetzer and Brandes, 2006) Other controversies include purity of OEC cultures prior to transplantation and identification of OECs following transplantation. (Boyd et al., 2006, Jahed et al., 2007)

Some studies have shown that transplanted OECs transform into Schwann cell-like cells and synthesize myelin around the axons at the site of spinal injury. (Barnett et al., 2000, Dunning et al., 2004, Imaizumi et al., 1998, Kato et al., 2000, Lakatos et al., 2003, Li et al., 1997, Sasaki et al., 2006a, Sasaki et al., 2006b, Smith et al., 2001) However, other groups have shown that this is not the case and that they form a scaffold, in which myelinated and unmyelinated axons with invading Schwann cells can be identified. (Boyd et al., 2004, Boyd et al., 2005, Boyd et al., 2006) With regards to dorsal root repair, OECs ensheath and support elongation of the axon and mediate

their entry into the CNS. The regenerating axons that have crossed the OEC 'bridge' are able to regenerate for substantial distances within the CNS.

1.12 Clinical prospects for repair of traumatic brachial plexus injury

Traumatic brachial plexus avulsion injury results in a localised, focal spinal cord injury that has a poor outcome if untreated. Reimplantation of avulsed ventral roots via a peripheral nerve graft into the anterolateral spinal cord is an established technique which improves function in the proximal arm and pain. (Carlstedt and Noren, 1995) However, hand function rarely recovers and there is still no cure for a central or longitudinal type of BPI.

A number of preclinical studies have attempted to improve function following spinal cord injury by transplantation of OECs. (Feron et al., 2005, Huang et al., 2003a, Lima et al., 2006). However, the results from these studies are controversial and there are a number of potential drawbacks to each of these studies.

In human studies, Feron et al. performed a phase I clinical study to assess feasibility and safety of autologous transfer of OECs to three paraplegic patients with complete spinal cord injury (ASIA A). However, ASIA scores did not improve, there was no overgrowth or increase in spinal cord volume as measured by MRI scan but there was also no deterioration in neurological function. (Feron et al., 2005) Lima et al. also performed a phase I study involving transfer of autologous OECs in 7 ASIA A patients (Lima et al., 2006). Neurological improvements were observed in every patient and 2 patients improved from ASIA A to C, but other studies have showed improvements in neurological outcome with conservative management and no cellular therapies. (Katoh and el Masry, 1994, Katoh and el Masry, 1995) The study by Huang et al. is the largest study of transplanted embryonal OECs and although this study reported

variable improvement in neurological outcomes the study group consisted of a heterogenous population, results were not statistically significant and the conclusions limited by poor methods. (Huang et al., 2003a) Other authors have demonstrated an improvement in ASIA motor scores after decompression and insertion of autologous OECs in a chronic spinal injury model, but this was in a single patient and there is controversy regarding the ethical approval of this study (Tabakow et al., 2014)

Another potential model where OECs can be tested is a brachial plexus avulsion injury which is a focal longitudinal spinal cord injury. Current models of intradural ventral nerve root implantation into the spinal cord in humans are helpful but not curative. (Kachramanoglou et al., 2017) Application of OECs, particularly mucosal OECs which can be sourced more easily compared with bulb OECs, therefore presents a potential target to allow nerve generation across the CNS-PNS interface and could potentially lead to improvement of distal limb function. However, it may well be the case that OEC therapy in combination with other agents may be more efficacious than OECs alone. (Pearse et al., 2007)

1.13 Study objectives

1. The initial objective of this thesis is to devise a rodent model of brachial plexus ventral root avulsion and repair.

2. Perform histological and immunohistochemistry analyses using haematoxylin & eosin (H&E), glial fibrillary astrocytic protein (GFAP) and neurofilament (NF) to assess the model.

3. To devise a technique for assessing nerve root continuity across the ventral root repair site. This model will be used to establish the number of motor neurone cell

bodies supplying each cervical ventral root, and the number of surviving motor neurone cell bodies when the root has been avulsed. Subsequently we will use this model to compare the surviving motor neurone pool after ventral root reimplantation and OEC transplantation.

4. To develop behavioural studies to establish quantifiable and reproducible functional outcomes for the brachial plexus ventral root model.

5. Once a model is established, we endeavour to augment the repair with autologous rat mucosal and bulb OECs and assess outcomes using histology, immunohistochemistry techniques, labelling of motor neurones and functional tests.

CHAPTER TWO

CHAPTER 2: DEVELOPMENT OF THE BRACHIAL PLEXUS VENTRAL ROOT AVULSION MODEL

2.1 Introduction

Brachial plexus avulsion injury is common after road traffic accidents and other high velocity trauma. A popular treatment modality involves reimplantation of avulsed ventral roots back into the spinal cord. (Carlstedt et al., 2000) The reimplantation of ventral roots improves proximal muscle strength, functional outcomes and pain. (Carlstedt et al., 2004, Htut et al., 2007) As hand function rarely returns to normal our objective was to devise a model for the lower brachial plexus ventral roots innervating the rat forepaw. (Carlstedt et al., 2004)

Once a stable, reproducible and quantifiable model of brachial plexus ventral root avulsion injury has been established it could be used to assess outcomes for ventral root repair and augmentation with cellular therapies, including rat bulb and mucosal OECs, as well as other potential cell types.

After a model has been devised it should assessed by performing histology, immunohistochemistry with GFAP and NF, as well as studies to assess survival of the motor neurone pool in the anterior horn of the cervical cord. Behavioural tests are also essential to quantify the injury and to assess functional outcomes in parallel with the other tests. However, before we can do this, a reliable and reproducible rat brachial plexus ventral root injury model has to be devised.

2.1.1 Rat Vertebral Anatomy

The rat vertebral column is composed of seven cervical, thirteen thoracic, six lumbar, four sacral and about 28 caudal vertebrae. A typical vertebra has a large ventral part called the body. The vertebral arch is attached to the body with the two enclosing the spinal canal, through which the spinal cord passes. The two horizontal plates forming the roof of the arch are called the laminae. These are attached to the body by pedicles. The region where the laminae meet the pedicles is the pars interarticularis. The spinous process projects upwards from the junction of the two laminae in the midline, which are all comparable to human cervical vertebrae. (Figure 2.1)

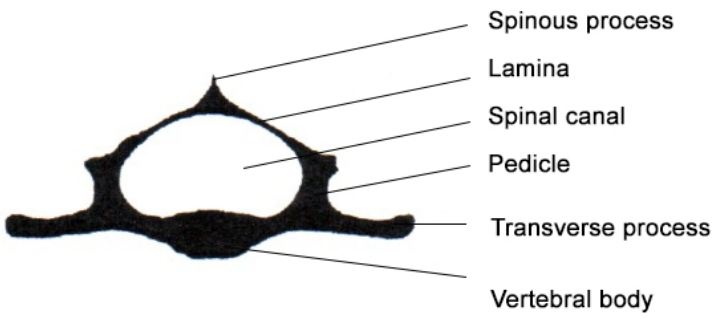

Figure 2.1. Cross-section of a typical rat cervical vertebra showing anatomical landmarks. (Adapted from Greene (Greene, 1968))

The seven cervical vertebrae are similar to each other, except for the first two, the atlas and the axis, similar to that in humans. The spinous process of the second thoracic vertebra is longer than that of any other vertebra and is an important landmark.

A number of unique distinguishing features between individual cervical and upper thoracic vertebrae are helpful when sectioning & processing the spine for histology. (Figure 2.2)

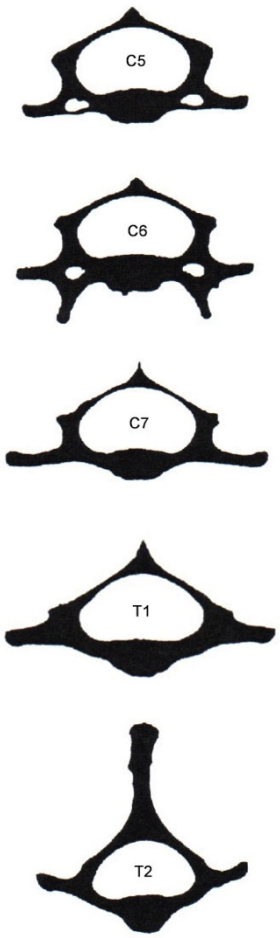

Figure 2.2. Cross-sections of the rat C5, C6, C7, T1 and T2 vertebrae. The C5 and C6 vertebrae both have a transverse foramen for the vertebral artery but C7, T1 and T2 do not. C5 and C6 can be distinguished from each other in that C6 has an anterior projection from the junction between the body and the transverse process and C5 does not. C7 and T1 have a similar shape. However, the T2 vertebra has the largest spinous process due to its attachment of muscles running between the occiput and back and can easily be identified in cross-sections. (Adapted from Greene (Greene, 1968))

2.1.2 Rat Brachial Plexus Anatomy

The rat brachial plexus is similar anatomically to the human brachial plexus. A similar nomenclature is used to identify the spinal cord and various nerves supplying the rat upper limb. The rat spinal cord extends from the foramen magnum to the fourth lumbar vertebra, unlike in humans where it usually ends at L1. It has a cervical and lumbar enlargement. In the cervical spine there are eight paired cervical nerves, which contribute to the cervical and brachial plexus on each side. (Greene, 1968)

The rat brachial plexus is formed by the inferior primary divisions of the last four cervical nerves and part of the first thoracic nerve, and in some cases a contribution from the second thoracic nerve. The plexus is more flattened in the rat and is not divisible into lateral, medial and posterior cords comparable to those in humans. (Figures 2.3 a & b) (Greene, 1968)

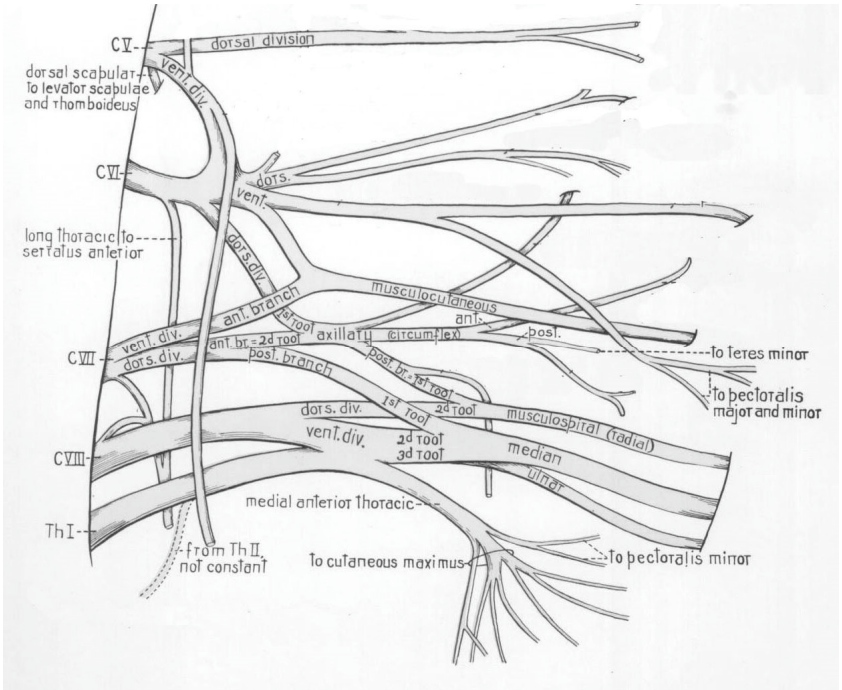

Figure 2.3a. The rat brachial plexus. (from Greene, (Greene, 1968))

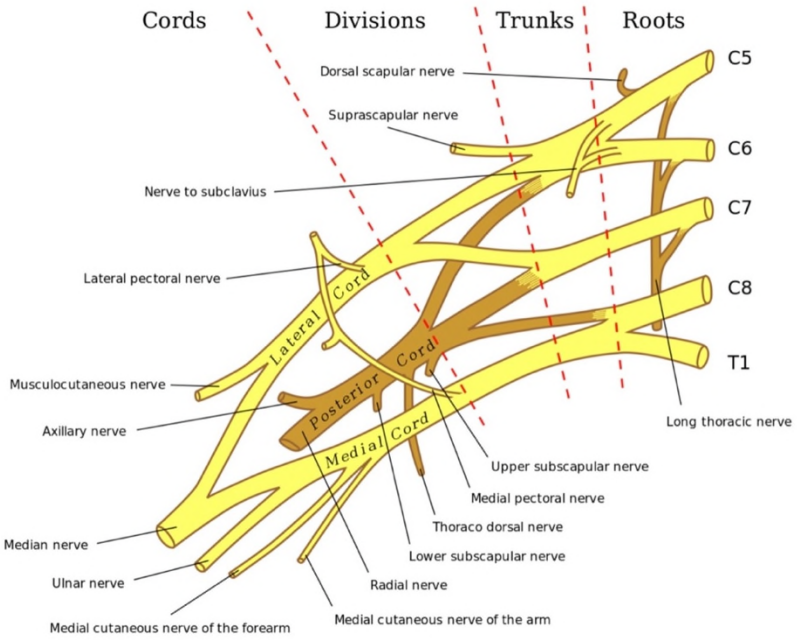

Figure 2.3b. The human brachial plexus (from Wikipedia)

The eighth cervical nerve (C8) divides into a dorsal and larger ventral part. The ventral portion is in two parts, one passing outward to form the second head of the median nerve, the other passing backwards to join the ventral division of the first thoracic nerve. The dorsal smaller portion of the eighth nerve contributes to the long thoracic nerve and then forms the second, larger root of the radial nerve.

The first thoracic nerve (T1) divides into a number of branches giving rise to the third root of the median nerve and the ulnar nerve. The median nerve is the largest nerve of the rat brachial plexus and is formed by the ventral divisions of the seventh and eighth cervical nerves and the first thoracic nerve. The ulnar nerve is composed of branches of the eighth cervical and first thoracic nerve. (Greene, 1968)

The median nerve innervates the extrinsic flexor muscles of the fingers and controls rat grip strength. (Bertelli and Mira, 1994) The ulnar nerve innervates the intrinsic

muscles of the forepaw and controls fine movements of the fingers and grip precision. (Greene, 1968)

Rat forepaw innervation has a number of similarities and differences to the human hand. Like in man, both intrinsic and extrinsic muscles work synergistically under the control of the median and ulnar nerves to coordinate grip strength. The intrinsic muscles (interossei, lumbricals, thenar and hypothenar muscles) are important for providing the precision and fine control of grip whereas the extrinsic muscles (palmaris longus, flexor digitorum sublimis and profundus) provide strength. In humans the median and ulnar nerves contribute to innervate both extrinsic and intrinsic muscles of the hand. (Kozin et al., 1999) However, in the rat there is a clear distinction in the innervation of paw muscles. The median nerve innervates all the extrinsic flexor muscles, while the ulnar nerve controls most intrinsic muscles of the paw with the exception of flexor pollicis brevis. (Bertelli and Mira, 1994, Greene, 1968)

It is therefore envisaged that the ventral roots of C8, T1 or a combination of C8 and T1 will lead to neurological deficit in the rat forepaw such that a functional test can be devised to quantify the injury.

2.2 Practical issues of operating on rat brachial plexus

There are a number of issues to consider when working with the rat brachial plexus compared to the human brachial plexus. The rat is considerably smaller, with a restricted operative field that makes surgery technically demanding. The small circulating blood volume means minimal blood loss can lead to death. The rat dura is thin and translucent making it difficult to open without damaging the cord, which is very sensitive and swells with minimal trauma. Working with rat brachial plexus ventral

roots is therefore challenging and other structures in the vicinity leave a small margin for error.

Firstly, a number of structures in the anterior of the neck and the small size and anatomy of the cervical vertebral bodies makes an anterior approach and corpectomy extremely difficult. In theory an anterior approach to the cervical spine would make access to the ventral roots more feasible, without having to transect the dorsal roots, but this approach is notoriously difficult. In contrast, the posterior approach to the cervical spine requires only incision and retraction of the paraspinal muscles prior to removal of posterior vertebral elements. However, if bone removal is not done adequately the spinal cord may have to be retracted and/or rotated to provide access to the ventral roots, and this can lead to neurological injury or even death, especially if epidural blood vessels are lacerated.

Secondly, in comparison to lumbar roots the intervertebral portion of the cervical ventral roots is short and immobile. As well as limiting access this makes it hard to manipulate individual roots. This makes lumbar ventral roots more convenient for applying anterograde and retrograde tracers and for measuring the rate of progress of growing axons through the reimplanted roots with motor neurone labelling methods.

Thirdly, although there is information on the peripheral nervous system innervation of the rat arm and forepaw, there is limited data on the neurological and functional deficits, which occur following intradural avulsion of individual cervical ventral roots. This probably explains the limited number of studies looking at CNS repair and/or regeneration in the rat brachial plexus and makes outcomes of brachial plexus repair difficult to assess.

However, the majority of plexus injuries in clinical practice affect the brachial plexus. A rat brachial plexus ventral root avulsion model therefore has an obvious advantage over a lumbar plexus model in that it may more closely mimic injuries seen in clinical practice.

A small number of rat brachial plexus ventral root studies have been described in the literature. Some of these studies have used the anterior approach. For example, Jivan et al. performed an anterior approach to avulse the C7 spinal nerve 10mm distal to the dorsal root ganglion. (Jivan et al., 2006) Similarly, Sananpanich et al. used an anterior approach to access the extradural nerves of the brachial plexus. (Sananpanich et al., 2007) However, dorsal approaches to the cervical spine have also been previously described. In their study Bertelli and Mira used a dorsal approach to perform a laminectomy and partial C5 corpectomy before avulsing the ventral and dorsal roots and repairing them with a peripheral nerve graft and fibrin glue. (Bertelli and Mira, 1994) However, corpectomy can be associated with a significant blood loss and because rats have a small circulating blood volume, this can lead to death, even with minimal blood loss. Chuang et al. performed a laminectomy via the posterior approach and avulsed the C6 and C7 ventral roots before using nerve graft to perform an intradural repair. (Chuang et al., 2002) Haninec et al. (Haninec et al., 2003) Huang et al. used a dorsal approach to perform hemi-laminectomies before avulsing the C6 and C7 roots. (Huang et al., 2003b, Huang et al., 2007, Huang et al., 2009) Similarly, Liu et al. used this posterior approach with hemi-laminectomies to access the C5-7 ventral roots. (Liu et al., 1997) Pinter et al. used a posterior approach to cervical laminectomy and avulse the C7 ventral root before reimplanting it into the cord. (Pinter et al., 2010) Because human brachial plexus repair leads to poor return of hand function we wanted to develop a model for rat C8 or T1 ventral root avulsion. (Kachramanoglou et al.,

2017) We have made a number of small adaptations to the approaches described in the literature to make what we believe is a reliable and reproducible model of brachial plexus ventral root avulsion injury in the rat.

2.3 Developing a ventral nerve root avulsion model: The posterior approach to the cervical spine

All the work performed in this chapter was approved by the Animal Welfare Ethical Review Body (AWERB). All experiments in this study were conducted in accordance with the UK's Animals (Scientific Procedures) Act 1986 with ethical approval from Institute of Neurology, University College London. We followed the ARRIVE Guidelines when conducting these experiments.

Although the majority of clinical ventral root injuries affect the upper limb, most ventral root animal studies have focused on lumbar models of CNS repair as the lumbar ventral roots are more accessible. (Novikova et al., 1997a, Li et al., 1997, Li et al., 1998) A number of approaches have been used to access the ventral roots of the brachial plexus in rats including anterior and posterior, as described above. In the most economical animal model, the rat, accurate intradural avulsion and reimplantation of avulsed ventral nerve roots is technically difficult. A number of studies using the posterior approach have been described but Cao & Ling described an anatomical posterior approach to the rat brachial plexus. (Cao and Ling, 2003) They stated that extensive bone work was associated with significant and sometimes fatal bleeding. We have made some adaptations to this and other previously described models to describe the anatomic basis and technical aspects of our brachial plexus ventral root injury model in the rat. We used a custom-made animal support moulded from plasticine to flex the rat cervical spine to increase the interlaminar space and reduce damage to the cervical cord. In addition, we devised a custom-made nerve hook by

filing a tungsten needle, so that we could safely open the dura, manipulate, avulse and transect cervical nerve roots. (Oprych et al., 2015)

2.3.1 Animal subjects

Female Sprague Dawley (SD) rats weighing 200-250g (of age 8-10 weeks) were used for this study (Harlan Laboratories, UK).

2.3.2 Animal positioning

The anaesthetised rat was placed prone and supported using our custom-made plasticine device. (see Figure 2.4) The main purpose of this device was to ensure flexion of the cervical spine, thereby increasing the inter-laminar space, improving access to the spinal cord and nerve roots and minimising blood loss by reducing venous pressure. The device was also important for securing the mouthpiece for delivering and maintaining anaesthesia during the procedure. The rat was anaesthetised with isoflurane (IsoFlo®, Abbott Laboratories Ltd, UK) and positioned such that the left side, the operated side, was closest to the surgeon. The fur was clipped, skin prepared with Tamodine® iodine antiseptic solution (Vetark Animal Health, UK) and the rat draped to maintain a sterile field.

Figure 2.4. Custom-made plasticine support for the rat and anaesthetic delivery device. This has been made to accommodate the anaesthetic administration device and to keep the rat cervical spine in a stable, flexed position to allow access to the spinal cord and nerve roots and to minimise blood loss by reducing venous pressure in cervical epidural vessels.

2.3.3 Posterior approach to the spine

In the rat the second thoracic (T2) vertebra has the most prominent spinous process and is an important surgical landmark. (Cao and Ling, 2003) With the spine flexed on the custom-made device, this landmark is easily palpable. A midline skin incision was made from rostral to the T2 spinous process to the lower cervical spine. An operating microscope (Carl Zeiss Ltd, Cambridge, UK) was positioned and the posterior midline neck muscles, including the trapezius and levator auris longus, were split to reach the posterior elements of the vertebrae. A consistent deep vascular fat pad exists just proximal to the laminae. This can bleed profusely but can be controlled with direct pressure and/or bipolar coagulation. (TDB60, Eschmann, West Sussex, UK) By using an operating microscope, meticulous surgical technique and by staying close to the midline excessive blood loss can be minimised at this stage.

2.3.4 Bone removal

Muscle dissection exposed the hemi-laminae, facet joints and the transverse process at the appropriate level. (Figure 2.5) Adequate bone removal must be performed to access the spinal cord and ventral roots.

Initial attempts to expose the C8 ventral root by removing the C7 & T1 hemi-laminae were fraught with problems. The ventral roots arise close to the midline on the anterior

surface of the cord and pass in a vertical fashion towards the intervertebral foramen. It was quickly established that a greater degree of bone removal was necessary for access to the ventral root on the anterior surface of the spinal cord.

Partial removal of the C7 and T1 facet joint is extremely important. Without this it is impossible to approach the ventral root from the dorsal spine. In addition, removing the lower part of the facet between C6 and C7 and the upper part of the facet between T1 and T2 improves visibility and access to the ventral root.

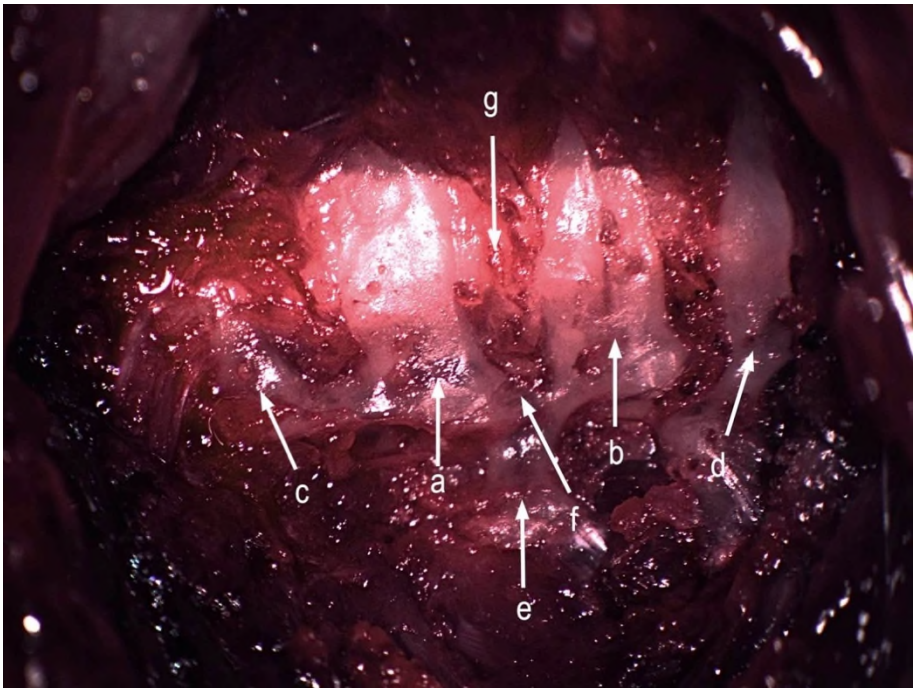

Figure 2.5. Midline posterior approach to the cervical spine. All muscles are stripped and retracted off the vertebrae. The C7 hemi-lamina (a) and the T1 hemi-lamina (b) are shown. The hemi-lamina of C6 above (c) and T2 below (d) are also labelled. The transverse process of T1 (e) is shown. The facet joint between C7 and T1 (f) is indicated.

The pedicle of C7 must be completely drilled to a stump otherwise irrespective of the facetectomy it will be impossible to retract the dura sufficiently to obtain access to the ventral root. The pedicle stump should be level with the posterior aspect of the

corresponding vertebral body. It is also important to expose or at least visualise the caudal border of the C6 hemi-lamina and the cranial border of the T2 hemi-lamina as this ensures the largest possible dural opening can be made to improve access to the T1 ventral root.

The facet joints and pedicle are drilled away using a handheld burr and a 0.7mm drill bit. (Fine Science Tools, Foster City, CA, USA) Smaller drill bits have the propensity to slip and may cause spinal cord damage and soft tissue injury with bleeding. Removal of the facet and pedicle should not result in any significant blood loss if done correctly. If operating on the cervical spine above C7, care must be taken whilst drilling the pedicle to ensure the foramen transversarium is not penetrated, as this can damage the vertebral artery causing fatal injury. The remaining hemi-lamina, which is attached to the midline, is removed using a fine bone rongeur. (FST, Foster City, CA, USA) It is best removed from the free lateral edge towards the midline otherwise the free edge can pierce the dura and damage underlying nerve roots and spinal cord. (Figure 2.6) The application of Floseal® (Baxter, CA, USA) can also be used to control bleeding from vessels which cannot be cauterised.

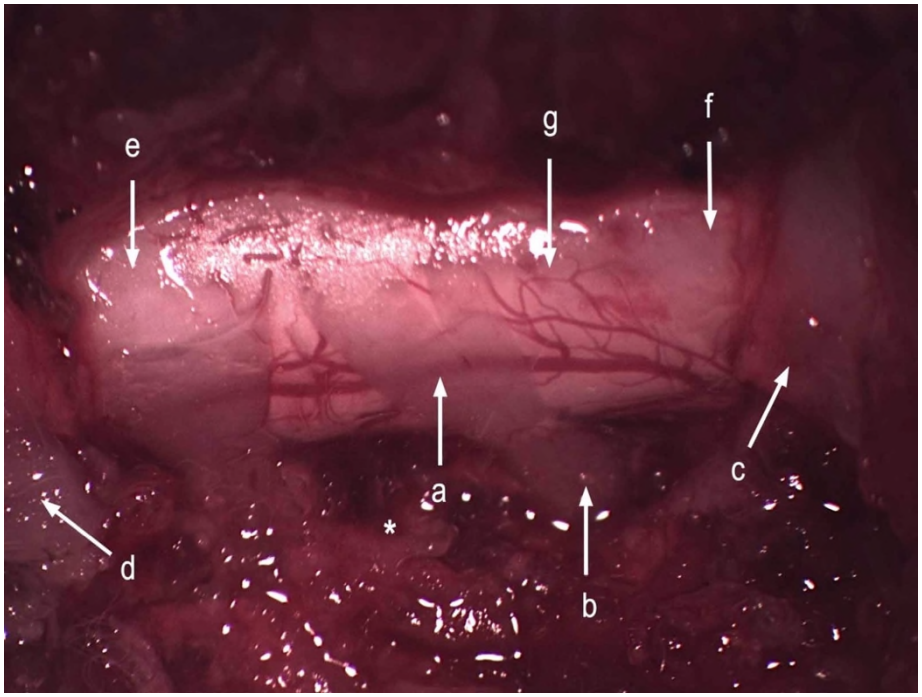

Figure 2.6. Cervical spinal cord following hemi-laminectomies. The hemi-laminae of C7 and T1 have been removed, together with the facet joint between C7 & T1, as well as the lower part of the facet joint between C6 & C7 and the upper part of the facet between T1 & T2. The hemi-laminae of C6 (d) and T2 (c) are indicated. The pedicle of T1 has been completely drilled away (*). The T1 dorsal root (a), which has two rootlets and T1 nerve root (b) are shown. The C8 and T2 dorsal root (e & f) are identified. The spinal cord (g) is shown with the overlying dura mater intact.

If more than one ventral root needs to be accessed, more extensive bone work will need to be undertaken. If two adjacent ventral roots are to be avulsed three hemi-laminae and the appropriate facet joints, and pedicles will need to be removed. It is important to note that with increasing levels of muscle dissection and bone work the incidence of fatal blood loss can increase so care must be taken to avoid blood loss even at a single level surgery.

2.3.5 Dural opening

The dural opening should be made medially. A custom-made tungsten hook and a 30G needle are used. (BD Microlance, Ireland; see Figure 2.7) The underlying dorsal roots are visible through the thin dura. Care must be taken not to cut into the spinal cord. To avoid this the initial dural puncture with the 30G needle should be made directly over a dorsal root. The needle is gently passed from a cranial to caudal direction until the dural space is entered. If possible, the arachnoid layer should be kept intact until the dural flap has been created. Entry into the subarachnoid space is marked by egress of cerebrospinal fluid into the operating field. The sharp hook is positioned into the subdural space, the dura tented up and the 30G needle used to cut the dura from lower border of C6 to the upper border of T2. However, a linear dural incision is insufficient because it does not allow retraction laterally enough to obtain access to the anteriorly placed ventral roots.

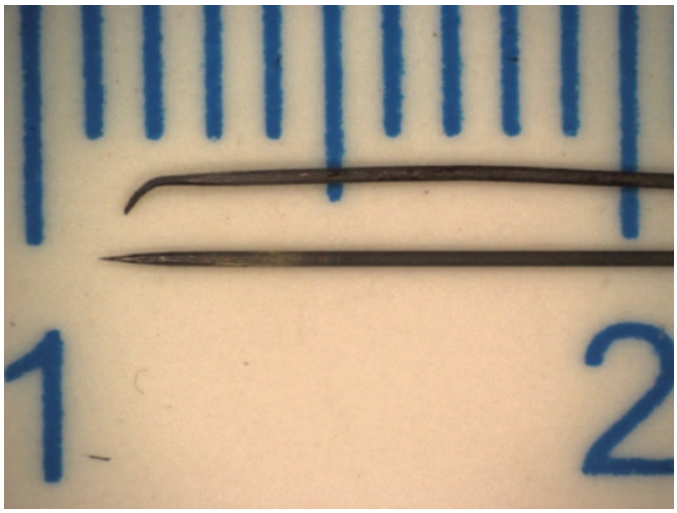

Figure 2.7. Custom-made tungsten nerve hook. We devised this to open the dura safely and to avulse the nerve roots from the cord.

2.3.6 Creating a dural flap and using forceps to retract the dura

A rectangular or c-shaped dural flap should be created. At either end of the incision the dura is cut from a medial to lateral direction to create a trap door type of opening. This flap can then be lifted laterally. Providing the facet joints and pedicles have been removed adequately this will allow good exposure to the anterior aspect of the spinal cord and the ventral root. If the dura is initially opened too laterally one can damage underlying epidural vessels and there isn't enough of a dural edge to grasp with a pair of forceps.

Initial attempts to retract the dura using a pair of No.5 forceps proved difficult. Holding the dura with one hand whilst manipulating, transecting initially the dorsal and then avulsing the ventral rootlets was technically challenging. Because one hand was always required to retract the dura it was hard to control bleeding, and this made visibility of the operating field difficult.

The forceps technique for dural retraction led to a large number of intradural peripheral ventral root avulsions as well as a large number of spinal cord injuries. Although this technique was useful to initially develop the model other techniques were trialled to improve access to the ventral roots.

2.3.7 Creating a dural flap for retraction using hitch stitches

A single dural hitch stitch using a 10.0 Ethilon (Johnson & Johnson, UK) was the initial preferred technique for this. A single stitch passing through the dura at the level of the dorsal root was used. The dura was stitched to the paraspinal muscles using a slipknot, which was secured with a surgeon's knot thus providing a strong durable hitch stitch, improving access to the ventral root.

However, a two dural hitch stitch technique with a suture applied to the dura on either side of dorsal root provided improved retraction of the dura and access to the ventral root. This has become our method of choice for our brachial plexus ventral root avulsion model. (Figure 2.8)

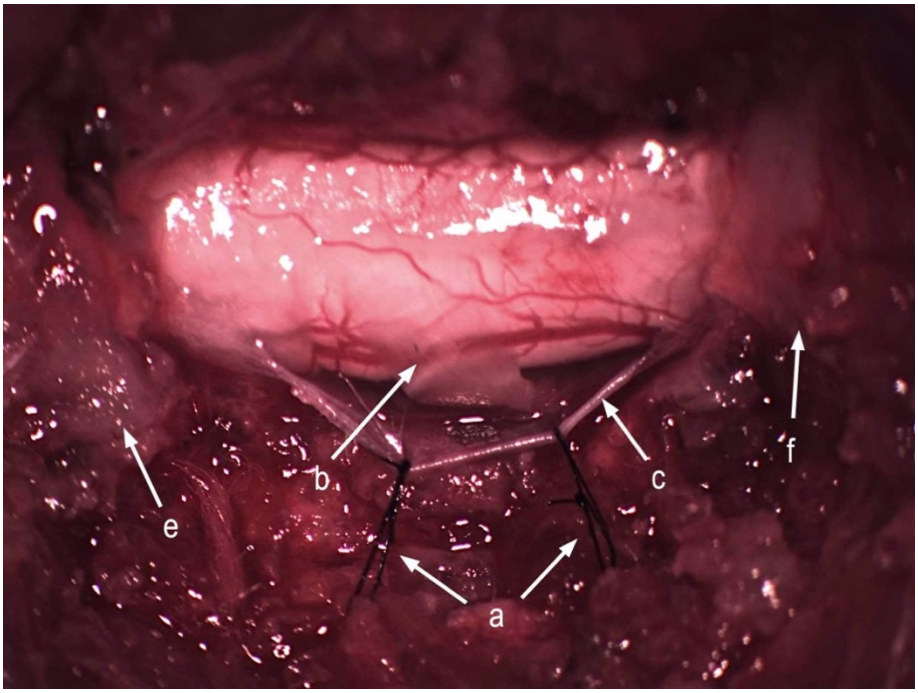

Figure 2.8. Dural opening and hitching. Th dura mater has been opened using a sharp hook and needle. Two dural hitch stitches (a) have been placed to improve access to the ventral root (not shown). The T1 dorsal root (b), as well as the lower border of the C6 hemi-lamina (e) and the T2 hemi-lamina (f) is indicated.

2.3.8 Dorsal root transection

Once the dura has been adequately opened the operating microscope is repositioned to focus on the dorsal root. The C8 dorsal root, which lies perpendicular to the spinal cord, is transected adjacent to the dorsal root entry zone, using a sharp hook to lift the root and a 30G needle to cut it. Care was taken not to pull the dorsal root out of the spinal cord to avoid a spinal cord injury. The transected end is placed over the dural

edge. (Figure 2.9) In the majority of cases there is a large blood vessel associated with the dorsal root and bipolar coagulation must be used to cauterize this vessel prior to dorsal root transection.

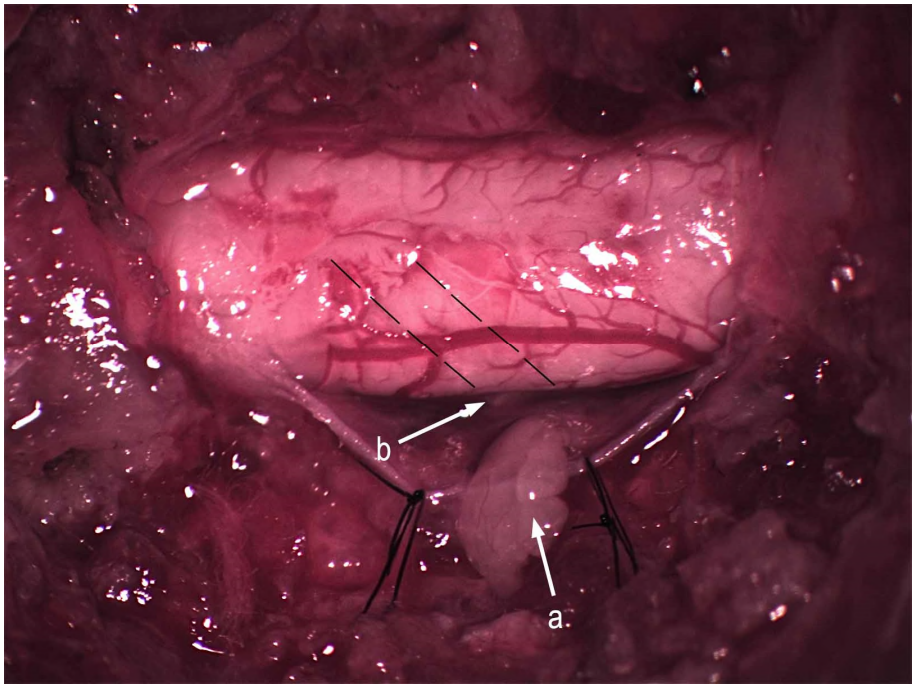

Figure 2.9. Dorsal root transection to identify ventral root. The dorsal root (a) has been transected adjacent to the dorsal root entry zone and laid over the edge of the hitched dura. The ventral root (b) can be seen as it joins the dorsal root to make the C8 nerve root (not visible). The direction of the ventral root under the ventral aspect of the spinal cord is indicated with a broken black line.

2.3.9 Ventral root avulsion

Once the C8 dorsal root has been transected the dentate ligaments above and below the root should be identified and cut to provide better access to the ventral root. The C8 ventral root arises close to the midline on the ventral surface of the cord and pass tangentially towards the intervertebral foramen, where they merge with the dorsal root and become the C8 nerve root. The ventral root can be exposed with gentle retraction

of the cord, although this must be kept to a minimum to prevent spinal cord damage. (Figure 2.10)

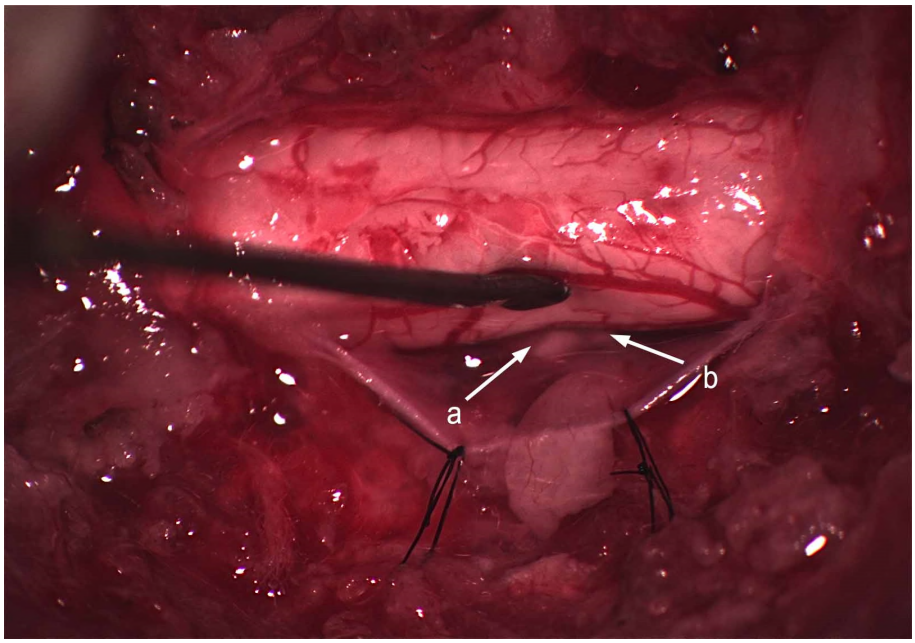

Figure 2.10. Gentle manipulation of spinal cord to reveal ventral rootlets. The spinal cord is retracted to show the two ventral rootlets of the T1 ventral root. (a & b) The dentate ligaments above and below have been cut (not shown) but the protective pia still covers the spinal cord.

The ventral root is usually made up of one or two large roots with multiple small rootlets attaching it to the spinal cord. Once the ventral rootlets are visualised, the sharp hook is placed underneath them under direct vision and swept from a caudal to cranial direction with gentle traction, to avulse the ventral rootlets as they emerge from the spinal cord surface. The avulsed ventral root is placed on the dorsolateral surface of the spinal cord. (Figure 2.11)

From our experience the rat ventral root is often associated with at least one large blood vessel. It is vital to cauterise any vessels prior to attempting to avulse the ventral

root otherwise excessive bleeding will be encountered, leading to either poor visibility, suboptimal ventral root avulsion, poor reimplantation or fatal blood loss.

To reimplant the ventral root the pia of the spinal cord is gently opened with a sharp new 30G needle and the avulsed ventral root gently placed into the dorsolateral aspect of the cord. Any cellular or pharmacological treatments can be applied at this stage.

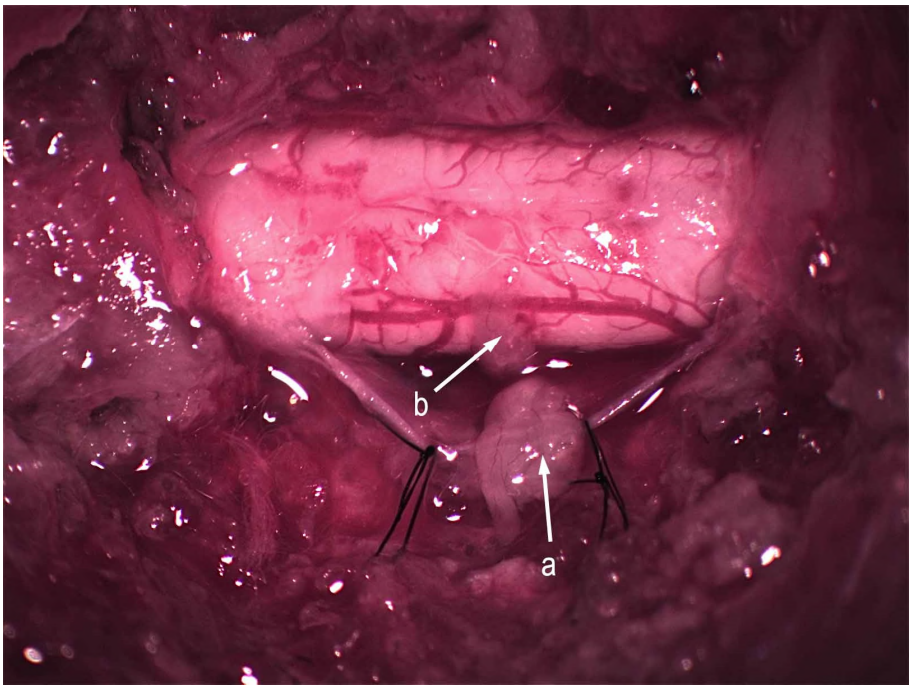

Figure 2.11. Ventral root avulsion. The ventral root (b) has been hooked and avulsed close to its insertion on the ventral surface of the spinal cord. It has been reimplanted on the dorsolateral surface of the spinal cord.

2.3.10 Application of tissue glue to ventral roots

The dorsal root is laid over the avulsed ventral root and a drop of Tisseel® is applied to keep the nerve roots in place on the spinal cord. (Figure 2.12)

In our initial surgery's histology showed that avulsed ventral roots were not always being held in place on the dorsolateral aspect of the spinal cord and there was suspicion that they may be being washed away by cerebrospinal fluid.

In clinical models of brachial plexus repair Tisseel® (Baxter, Illinois, US) fibrin glue is used to adhere reimplanted nerve roots to the spinal cord. It is impossible to suture them as this may cause spinal injury and outweigh any benefits of repair. As a result, we started to experiment with a number of commercially available tissue glues before we decided on the optimum tissue glue to use in our study.

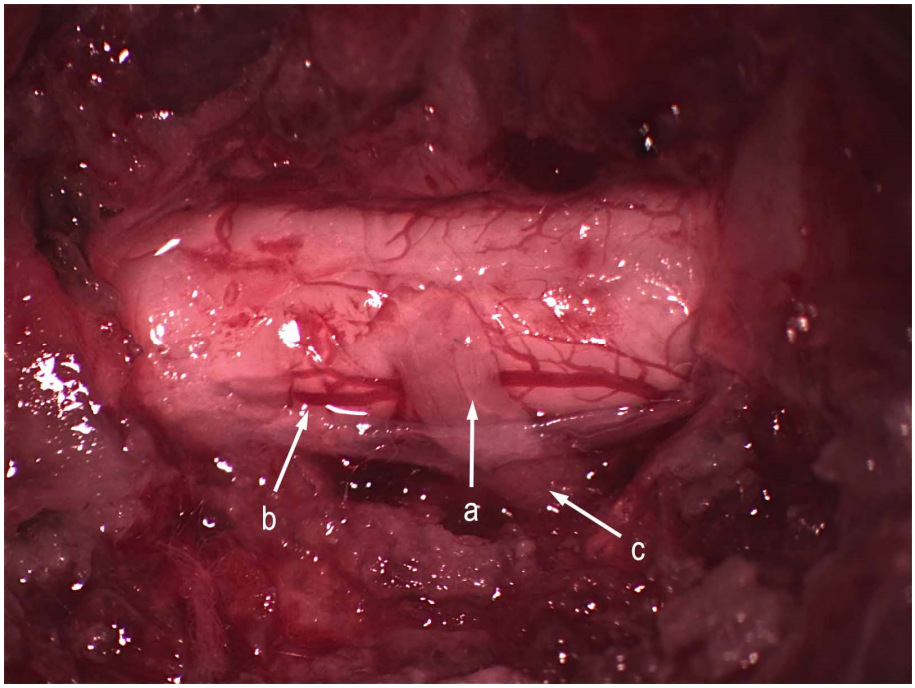

Figure 2.12. Application of Tisseel® to keep reimplanted rootlets in position. The dorsal root (a) is laid over the ventral root to protect it and to keep it in place. A small drop of Tisseel® is applied to keep nerve roots in place. The dural hitch stitches are removed and the dural edge (b) can be seen adjacent to the spinal cord. The C8 nerve root (c) can be seen.

2.3.11 Skin and fascial closure

The fascia and muscle layer is closed with continuous absorbable sutures and the skin is closed with interrupted 4.0 Vicryl. (Johnson & Johnson, UK) The rat is placed in the recovery cage, injected with Novox® (Vedco, MO, USA) analgesia and fed a wet mash diet for three days.

2.4 Anatomy of the rat cervical cord & ventral root reimplantation

The rat spinal cord is comprised of a central column of grey matter surrounded by white matter. Incoming or sensory fibres have their cell bodies in the dorsal root ganglion. From here fibres project peripherally and centrally towards the spinal cord. The dorsal root projects centrally towards the dorsolateral aspect of the spinal cord before splitting into multiple rootlets before, which further split into multiple rootlets before entering the spinal cord at the dorsal root entry zone (DREZ). This region is the area where the peripheral nervous system (PNS) joins with the central nervous system (CNS) and is referred to as the PNS-CNS transition zone. This region is typified by an abutment of CNS tissue from the cord together with PNS tissue in the most proximal region of the nerve root, with a dome shaped projection of CNS tissue towards the nerve. At this point, the Schwann cells and their associated collagen cross into the central abutment of the spinal cord which is rich in glial cells and astrocytes. (Carlstedt, 2007)

Similarly, the ventral or motor roots arise as a series of small rootlets which emerge from the anterolateral surface of the cord to coalesce into the ventral nerve root. The region where the CNS tissue merges with the PNS tissue is referred to as the ventral root entry zone, and this is again typified by oligodendrocytes and astrocytes on the

CNS side and Schwann cells and collagen as the nerve root leaves the CNS to enter the PNS and become the ventral root.

Neurofilaments provide structural support to myelinated axons by forming a dense continuous, cablelike structure, which are aligned in the same orientation along the axon. Astrocytes are star shaped glial cells found in the CNS. The have a number of important roles such as biomechanical support of surrounding cells, nutrient supply, maintenance of extracellular ion concentrations and play a role following neurological injury and scar formation. (Lobsiger, 2009)

Nevertheless, there are number of controversies of ventral root avulsion and reimplantation into the dorsolateral aspect of the spinal cord. Nerve fibre regrowth is unable to take place across the PNS–CNS transition zone, but regeneration of severed nerve fibres has been demonstrated in the immature animal before the transition zone has been established. (Carlstedt et al., 1987)

It has been demonstrated that spinal cord motor neurones will regrow into spinal roots following injury. (Ramon Y Cajal, 1928) Axonal regrowth occurs from spinal motor neurones after spinal cord lesioning. (Risling et al., 1983) This regenerative capacity of motor neurons was subsequently demonstrated in a rat ventral root avulsion model. When avulsed lumbar ventral roots were reimplanted into the ventrolateral aspect of the cord there was connectivity between the motor neurones and target muscles. (Carlstedt et al., 1986) Regrowth via other routes was excluded because the experimental procedures involved excision of adjacent roots and labelling of regenerated neurones. (Cullheim et al., 1989) The regenerated axons had grown from CNS to PNS tissue for some distance before reaching the target muscle. It has also been shown that the glial cells migrate into the implanted root, thereby extending the zone of CNS axon regeneration into the replanted ventral root. (Cullheim et al., 1989)

In the adult mammal, there is no regeneration of motor neurones from the CNS to the PNS. However, regrowth of motor neurones from the CNS to the PNS via a newly established transition zone has been demonstrated. (Carlstedt, 1997, Carlstedt et al.,

2000, Carlstedt et al., 1993) This growth is not necessarily by growing a new axon but also by collateral sprouting of axons. (Havton and Kellerth, 1987)

A number of nerve growth factor receptors such as trkA, trkB and p75 were demonstrated in the scar tissue and nerve growth factors may be a thnerapeutic target for similar models. (Risling et al., 1993)

We therefore aimed to re-establish connectivity between the spinal cord and the PNS by disrupting the transition zone.

2.5 Histological and immunohistochemistry assessment of the brachial plexus avulsion model

The normal and avulsed ventral root specimens were processed and stained with Haematoxylin and Eosin (Merck, Darmstadt, Germany) and immunohistochemistry using glial fibrillary acid protein (GFAP) and neurofilament (NF). The avulsed ventral roots show a marked degeneration of their neurofilaments. The normal and avulsion group sections are shown in Figure 2.13.

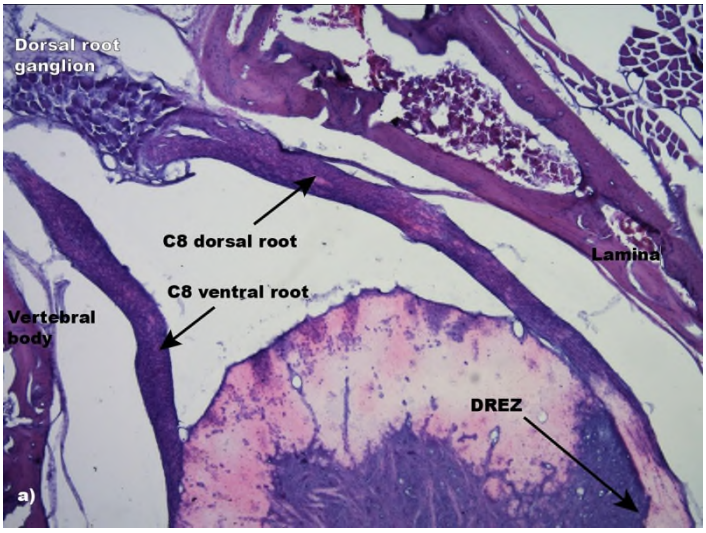
Dorsal root ganglion
C8 dorsal root
Lamina
C8 ventral root
Vertebral body
DREZ
a)

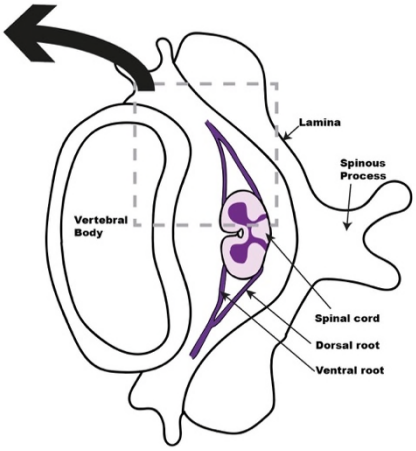
Lamina
Spinous Process
Vertebral Body
Spinal cord
Dorsal root
Ventral root

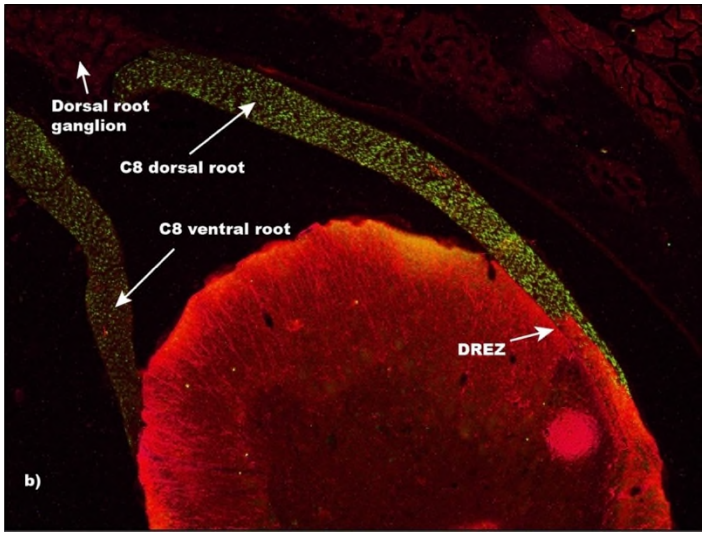
Dorsal root ganglion
C8 dorsal root
C8 ventral root
DREZ
b)

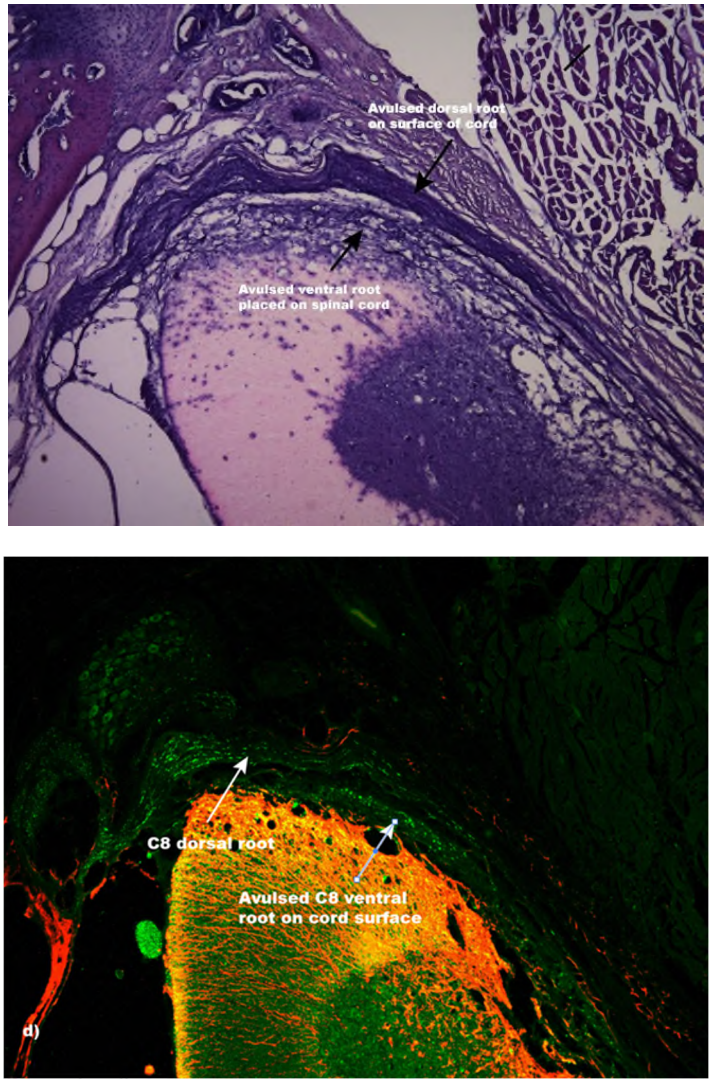

Figure 2.13. Histology and immunochemistry of spinal cord sections at the C8 level in an intact and avulsion rat. a) Haematoxylin & Eosin (H&E) (x10) section of the intact rat cervical cord at the C8 level. Ventral and dorsal roots are anotated. The DREZ and the PNS-CNS transition zone is identified. The dorsal root ganglion is also visible as well as the lamina and the vertebral body. A schematic of the spinal cord with the area shown on the H&E section is illustrated. b) Fluorescent antibody labelleling with glial fibrillary acidic protein (GFAP, red) and neurofilament (NF, green)(x10). The nerufilament in the intact ventral and dorsal nerve roots is organised in a regular pattern along the nerve axis. The DREZ and the PNS-CNS transition zone is well demarcated with a dome of concave CNS tissue projecting from the spinal cord to the PNs and the C8 dorsal nerve root. c) H&E section of an avulsed ventral root which has been placed on the spinal cord with the dorsal root positioned on top. Gliosis characterised by vaculoation and cavitation is visible in the dorsolateral cord. d) The neurofilament in the ventral and the dorsal root has lost it's regular organised structure

but the the ventral and overlying dorsal roots are visible on the dorsilateral aspect of the spinal cord at 8 weeks.

2.6 Summary

We have developed a model of brachial plexus ventral root avulsion injury. A custom-made support and nerve hook, meticulous haemostasis and careful drilling of bone, and carefully fashioning a dural flap with the use of hitch stitches, significantly improve access and visibility of the ventral root from a dorsal approach. With our modified technique, accurate ventral root avulsion close to the spinal cord surface is easier to achieve in a reproducible manner.

CHAPTER THREE

CHAPTER 3: ASSESSMENT OF OPTIMAL TISSUE GLUES FOR BRACHIAL PLEXUS REIMPLANTATION

3.1 Introduction

Fibrin glues have a number of uses in neurological surgery. (de Vries et al., 1998, Schafer et al., 1985, Liguori et al., 1984) Before they became established in clinical practice a number of safety studies were performed to establish their safety profile and efficacy. (de Vries et al., 2002, Ghulam Muhammad et al., 1997) Tisseel® (Baxter, Illinois, US) has been used in primate models of ventral root reimplantation after brachial plexus injury as well as brachial plexus reconstruction in humans, where reimplanted nerves cannot be sutured directly to the spinal cord. (Carlstedt et al., 1993, Hallin et al., 1999)

More recently, a variety of synthetic glues and dural sealants have become popular in neurosurgery, including polyethylene glycol (PEG) hydrogels such as Adherus® and glutaraldehyde sealants such as BioGlue®. (see Figure 3.1) Although these compounds are licensed for extradural use, they have found intradural applications, where they may contact the brain and spinal cord. (Kumar et al., 2003) However, there is very little information on the effectiveness or adverse effects of these substances on CNS tissue.

The main purpose of brachial plexus reimplantation after traumatic avulsion injury is to improve sensation, pain and function. (Carlstedt et al., 2004) The procedure requires placement of the nerve through a pial defect created on the surface of the cervical cord and application of tissue glue to hold the nerve in place, as the reimplanted nerve cannot be directly sutured the cord. Animal models of brachial

plexus injury aim to improve our understanding of this condition and allow us to investigate experimental treatments, which may in time be translated to clinical practise. Although the manufacturers of BioGlue® and Adherus® do not recommend intradural spinal application, we wanted to assess their efficacy in keeping the reimplanted nerve in position and their histological effects on the spinal cord.

a)

b)

c)

Figure 3.1. Tissue glues used to augment ventral root reimplantation. a) Tisseel® (Baxter, Illinois, US), b. BioGlue® (CryoLife Inc. Georgia, US) and c) Adherus® (HyperBranch medical Technologies Inc., North Carolina, US)

Tisseel® fibrin glue is a two-component sealant composed a sealer protein and a thrombin solution. The sealer consists of purified human fibrinogen and aprotinin, which aims to stop premature fibrinolysis. The thrombin component is formed of human thrombin and calcium chloride. When Tisseel® is applied the two components mix forming a clot which mimics the end stage of the clotting cascade. Tisseel® has been safely used in spinal intradural procedures and is completely absorbed within 10-14 days. It is licensed to control bleeding and prevent fluid leaks.

BioGlue® (CryoLife Inc. Georgia, US) is another two-component sealant comprised of bovine albumin and a glutaraldehyde solution, which has been popularised in cardiovascular surgery. (Bavaria et al., 2002, Passage et al., 2002, Hewitt et al., 2001) However, it has increasingly been used in neurosurgery to obtain a watertight dural closure. (Kumar et al., 2003) The two separate components are dispensed in a pre-determined ratio through an applicator tip, where cross linkage between the albumin and the glutaraldehyde occurs. The glutaraldehyde also covalently binds to extracellular matrix proteins on the tissue to produce a watertight seal. The manufacturers advise against the use of BioGlue® in close proximity to neural tissue and a study has demonstrated that the glue can expand and damage adjacent structures. (Lemaire et al., 2007)

Adherus® (HyperBranch Medical Technologies Inc., North Carolina, US) is also a two-component dural sealant. It is composed of a synthetic absorbable hydrogel, which is an activated PEG ester solution, and polyethyleneimine. On application the two

solutions mix within the applicator tip, cross-linking to form a hydrogel sealant. The hydrogel breaks down into water-soluble molecules within ninety days. The manufacturers recommend the use of Adherus® on the dura mater but stipulate that it should not be used in confined spaces. This is likely to be due to the fact that it is a hydrogel and has a theoretical risk of expansion with compression of adjacent structures.

The use of PEG hydrogel and glutaraldehyde sealants has increased in neurosurgery, but there remains a paucity of information on their effects on central nervous system tissue. The commercial recommendations for them not to be used intradurally are based on expansion risk, and not direct toxicity. We therefore wanted to compare the efficacy and histological effects of Tisseel®, BioGlue® and Adherus®, in our rat model of intradural brachial plexus repair .

3.2 Materials & Methods

All the work performed in this chapter was approved by the Animal Welfare Ethical Review Body (AWERB). All experiments in this study were conducted in accordance with the UK's Animals (Scientific Procedures) Act 1986 with ethical approval from Institute of Neurology, University College London. We followed the ARRIVE Guidelines when conducting these experiments.

Forty-one female Sprague-Dawley rats weighing 200-250g (Harlan Laboratories, UK) were anaesthetised with 2.5L/min Vetflurane (Abbott Laboratories Ltd, UK). The rats were positioned on a custom-made plasticine device (see Chapter 2) to maintain anaesthesia and to flex the cervical spine. The fur was clipped and the skin cleaned with antiseptic solution. A posterior midline cervical incision was made and cervical muscles split to expose the left C7 & T1 hemi-laminae. Under direct vision using an operating microscope (Carl Zeiss Ltd, Cambridge, UK) C7 & T1 hemi-laminectomies

were performed using a high-speed drill and a fine bone rongeur. The dural opening was made using a custom-made hook and 30G needle (see Chapter 2) and the dura hitched back with 10.0 vicryl. The custom-made sharp hook was placed under the C8 dorsal root and the nerve cut distal to the DREZ, taking care to ensure the underlying spinal cord was not damaged. (Figure 3.2) The cut C8 dorsal root was then re-positioned on the spinal cord, without disrupting the pia, and two drops of either Tisseel®, Adherus®, BioGlue® or no glue (control) were applied. The dura was left open as this is our preferred method for our brachial plexus repair model but also to allow for any potential glue expansion and associated cord compression. The fascia, muscle layer and skin were closed in a standard fashion with absorbable sutures. All animals were recovered in a standard cage and given Novox® (Vedco, MO, USA) analgesia for three days after the surgery.

The Tisseel® was purchased for these experiments by the laboratory. BioGlue® and Adherus® were obtained from the UK distributors free of charge.

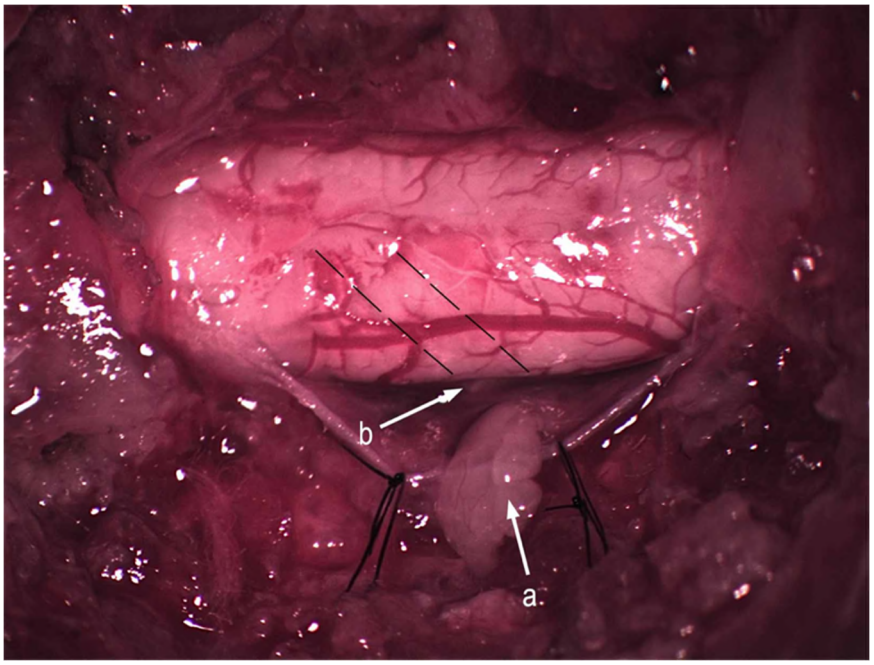

Figure 3.2. Transection of the C8 dorsal root. The left side C7 & T1 hemi-laminae have been removed. A dural opening has been made and the dura hitched to allow access to the spinal cord. The C8 dorsal root (a) has been transected and lifted laterally, distal to the DREZ. The attached ventral root (b) is also visible. Broken black lines shown position of the dorsal root before it was cut.

For the study, four experimental groups were established. In the control group (n = 9), the C8 dorsal root was transected and positioned on the spinal cord without application of any fibrin glue or sealant. In the Tisseel® group (n = 8), Tisseel® was applied to the C8 dorsal root and spinal cord to hold the cut root on the cord. In BioGlue® (n = 10) and Adherus® groups (n = 14), BioGlue® and Adherus® were applied in equal quantities to the cut C8 root and spinal cord.

At days 7, 14 and 28, two or three rats from each group were culled for histological analysis. The rats were pericardially perfused and fixed with 4% PFA (Appendix 1, 2 & 3) after terminal anaesthesia with CO_2. The cervical vertebral column with associated musculature, vertebrae, cord and rootlets was carefully dissected and placed in PFA for 24 hours before being decalcified overnight. (Decalcifier-II, Surgipath Europe Ltd., Cambridgeshire, Great Britain) Samples were then cryopreserved by sequentially placing them in 10% and 20% sucrose solution. They were then embedded in optimum cutting temperature media (OCT) (Bright Cryo-M-Bed; Jencons Scientific Ltd, Leighton Buzzard, UK) prior to being frozen with dry ice, mounted and cut in axial sections at 20μm thickness. (Appendix 4) In total, each rat had around 150 cross sections on 30-40 slides, from the area of the avulsed root where tissue glue had been applied. All sections were stained with H&E (Appendix 5) and slides representing the mid-section of the avulsed root slides from each rat in each group were selected for blind evaluation by a neuropathologist.

3.3 Results

By day 7, a marked acute inflammatory response was evident in the cord of the Tisseel® group but only a mild inflammatory reaction was identified in the Adherus® and BioGlue® groups, which was similar to control. By day 14, the control group did not show an acute inflammatory response, but the other three groups demonstrated a mild acute inflammatory reaction. By the final time point, day 28, there was no evidence of acute inflammation in the spinal cord in any group. (See Table 3.1)

	Day 7				Day 14				Day 28			
	Control	Tisseel	Adherus	BioGlue	Control	Tisseel	Adherus	BioGlue	Control	Tisseel	Adherus	BioGlue
Acute inflammation *	+	+++	+	+	-	+	+	+	-	-	-	-
Lymphocytic infiltrate *	+	+	++	++	+	++	++	++	+	+	+	+
Foreign body giant cell reaction *	+	+++	+	++	++	+++	+++	+++	-	-	+	++
Soft tissue necrosis *	-	-	-	-	-	-	-	-	-	-	-	-
Fibroblastic reaction *	++	+++	+++	++	+	++	+++	+++	+	+	+	+
Spinal cord changes **	+	+	++	++	+	+	+	++	+	+	++	++

Table 3.1. Histopathological response of the spinal cord in the control, Tisseel®, Adherus® and BioGlue® groups at days 7, 14 and 28. **+, ++ & +++ denote a mild, moderate and severe response. – denotes not visible.**

By day 7 there was mild lymphocytic infiltration in the control and Tisseel® groups compared to a moderate response in the Adherus® and BioGlue® groups. By day 14 the control group had a mild lymphocytic infiltrate, but all other groups showed a moderate infiltrate. By day 28 a mild lymphocytic response was identified in all four groups.

By day 7, a mild foreign body giant cell reaction was noted in the control and Adherus® groups. The Tisseel® group showed an extensive giant cell reaction but the BioGlue® group demonstrated a moderate reaction. At day 14 the control group had a moderate foreign body giant cell reaction, but all the other groups demonstrated extensive reaction. At the final time point the giant cell reaction had almost resolved in the control and Tisseel® groups but some giant cells were visible in the Adherus® group and a moderate reaction remained in the BioGlue® group.

By day 7, there was a moderate fibroblastic reaction noted in the control and BioGlue® groups. However, the Tisseel® and Adherus® groups showed a severe fibroblastic reaction. However, by day 14 there was only a mild reaction in the control group, a moderate reaction in the Tisseel® group and a severe fibroblastic response in the BioGlue® and Adherus® groups. At day 28 all groups displayed a mild fibroblastic reaction which was similar to control.

Whereas rats in the control and Tisseel® groups showed only focal inflammation in the cord at all time points (Figure 3.3) the Adherus® and BioGlue® groups showed histological evidence of cord degeneration. (Figure 3.4)

The control and Tisseel® groups showed no histological evidence of pressure or mass effect on the spinal cord at any of the time points during the study. The BioGlue® and Adherus® groups demonstrated cord compression from the glue mass at all time points although the majority of rats did not show any neurological deficit.

One rat in the BioGlue® group did not wake up at the end of the procedure but the cause for this is unknown. Two rats in the BioGlue® and one in the Adherus® group had a left sided hemiplegia. (Figure 3.4) One Adherus® group rat had a left hind limb

paresis but no left forepaw abnormality. No neurological complications were observed in the Tisseel® or control groups.

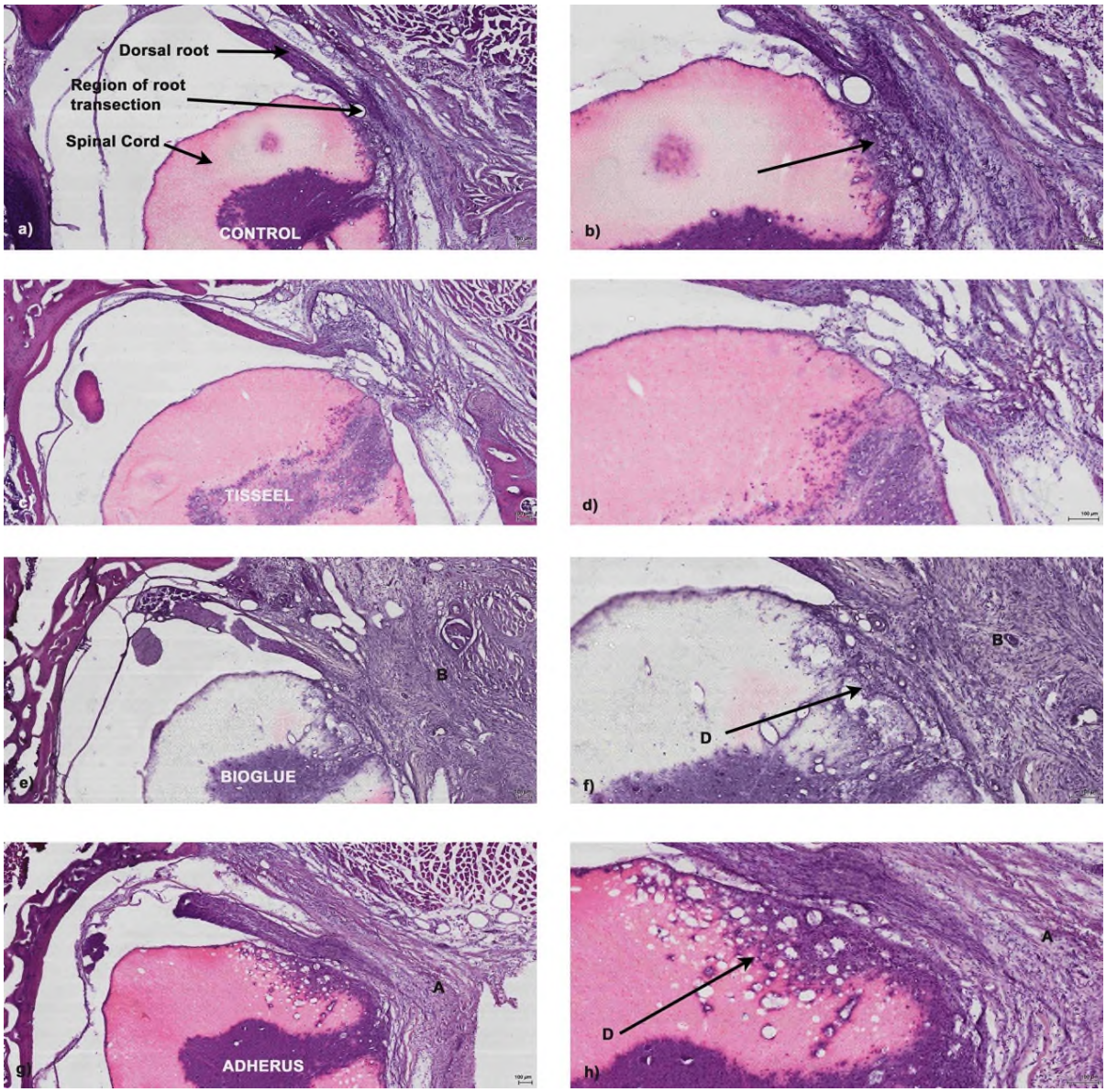

Figure 3.3. H&E stained cervical spinal cord sections in the four different test groups at day 28. a & b) Low and medium power images of the control group. The C8 dorsal root, area of root transection, spinal cord (arrows) and paraspinal musculature are identified. Medium power image (b) demonstrating focal inflammatory infiltration on the cord surface (arrow). c & d) Low and medium power images of the Tisseel® group demonstrating mild inflammatory response in the cervical spinal cord. No evidence of spinal cord compression or degeneration can be identified and Tisseel® has been absorbed. e & f) Low and medium power images of the BioGlue® group. BioGlue®

(B) is seen as an acellular, amorphous substance which has not been absorbed at day 28. Spinal cord degeneration is identified (arrows, D) and there is an eosinophilic infiltrate between the glue mass and cord. g & h) Low and medium power images of the Adherus® group. In this image Adherus® (A) glue is seen compressing the spinal cord, with spinal cord degeneration (arrows, D) and a chronic inflammatory response characterised by eosinophils is noted in the spinal cord.

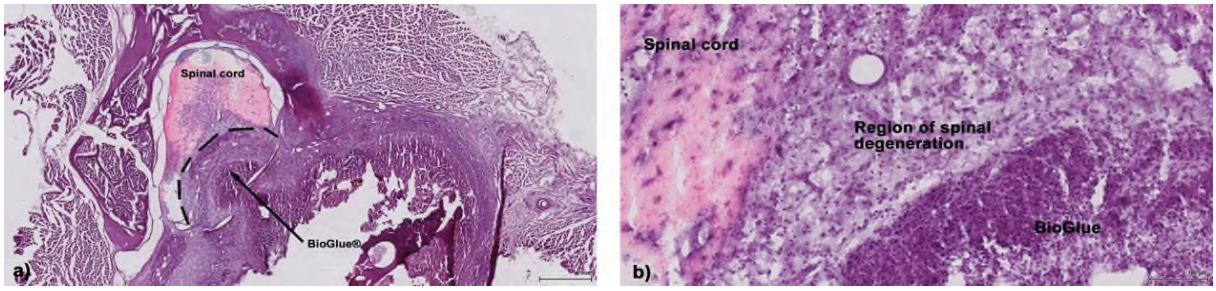

Figure 3.4. Spinal cord compression caused by BioGlue®. a) BioGlue® has caused significant spinal cord compression and pressure necrosis in the left hemicord. b) At high power a significant inflammatory infiltrate, typified by an eosinophilic response, is evident and spinal cord degeneration is seen. The BioGlue® material is infiltrated with eosinophilic cells at the margin between the glue and cord and is to be compressing the cord.

3.4 Discussion

Fibrin glues such as Tisseel® have been utilised in neurosurgery for over three decades and have a variety of applications. (Liguori et al., 1984, Schafer et al., 1985) A number of studies were conducted to confirm their safety and efficacy before they became established in clinical practice. (de Vries et al., 2002, Ghulam Muhammad et al., 1997) However, there is a paucity of information about the histological effects on CNS tissue of the more recently introduced glues and sealants, including Adherus® and BioGlue®, which are widely used in a number of surgical disciplines. The purpose

of this study was to compare Tisseel®, BioGlue® and Adherus® on the cervical spinal cord using our rat brachial plexus repair model.

Any implanted material is likely to undergo a tissue response when it is placed in vivo. The resulting reaction leads to an acute inflammation which is typified by an acute neutrophilia. Neutrophils have a short lifespan and rapidly disappear from the inflammatory exudate, in contrast to macrophages which may persist for several weeks or months, which coincides with the chronic inflammatory response. A foreign body reaction with granulation tissue is the response to an implanted material and is caused by proliferation of fibroblasts and vascular endothelial cells, leading to fibrous encapsulation.

The main role of Tisseel® in neurosurgery is to augment dural closure but other uses include, but are not limited to treating cerebrospinal fluid leaks, nerve repair, reinforcing muscle wrapping around aneurysms and to protect cranial nerves during skull base surgery. (de Vries et al., 1998, Menovsky et al., 1999, Narakas, 1988, Uzan et al., 1996) Tisseel® has been used for intradural brachial plexus repair in animal models and clinical practice. (Carlstedt et al., 1993, Hallin et al., 1999, Carlstedt, 2007)

Histological safety studies of fibrin glue on CNS tissue demonstrated a marked acute inflammatory reaction with on day 7 but by day 28 it had subsided, which suggests that it did not lead to CNS damage in a rodent model. (de Vries et al., 2002) Muhammed et al. demonstrated that although fibrin glues elicited an acute inflammatory response in rat brain, juxtaposed and surrounding CNS tissue was not damaged. (Ghulam Muhammad et al., 1997) Our results are consistent with these studies and showed a severe acute inflammatory response at day 7 when Tisseel® was applied, but by day 14 the response was mild and by day 28, there was no acute

inflammation in this group. Similarly, a mild to moderate chronic lymphocytic infiltrate was seen in all groups across at the different time points but this was comparable to control by day 28. All groups demonstrated a moderate to severe fibroblastic reaction by days 7 & 14 but at the final timepoint this response was similar to control.

BioGlue® has been used to reconstruct the sellar floor following transphenoidal procedures. It rapidly solidifies on application to a dry surface and the manufacturers state that it should not be used in confined spaces as there is a risk it can expand and lead to neural compression. In a major study, BioGlue® in was used as a dural sealant in 114 supratentorial, 53 infratentorial, 41 transphenoidal and 8 spinal procedures with no serious complications. Kaye et al., safely used BioGlue® to repair the sellar floor in 32 transphenoidal procedures and reported no CSF leaks. (Kumar et al., 2003)

A study to investigate the effect of BioGlue® on the cerebral cortex showed the presence of inflammatory infiltrate overlying the pia-arachnoid with gliosis but the glue did not expand or cross into the brain substance unless the pial surface had been disrupted. (Stylli et al., 2004) In our model, although care was taken not to disrupt the pia-arachnoid interface, in some cases it may have been disrupted but gliosis and cord degeneration to varying degrees was identified in all the Adherus® or BioGlue® rats.

Another laboratory study with BioGlue® on vascular tissue demonstrated that up to 2 months post-operatively it did not induce a chronic inflammatory response. However, in some specimens it demonstrated a minor foreign body reaction but no granulation tissue was identified. (Hewitt et al., 2001) However, several cardiac, thoracic and vascular studies have demonstrated varying inflammatory responses, including fibrosis, necrosis and giant foreign body reaction. (Babin-Ebell et al., 2010, Khan et al., 2011, Luk et al., 2012, Schiller et al., 2007a, Schiller et al., 2007b) Other clinical

studies have reported increased wound infections when BioGlue® is utilised to close the dura following intracranial procedures. (Gaberel et al., 2011, Klimo et al., 2007, Ito et al., 2013)

PEG hydrogels have had many applications as medical implants and delivery devices as they are easy to work with and in theory, biocompatible. (Kim et al., 2010) A number of studies suggest that that local environment has an important role in augmenting the inflammatory response when hydrogels are implanted. (Reid et al., 2015, Mathis and Shoelson, 2011, Hillel et al., 2011, Bjugstad et al., 2010) Preul et al. demonstrated inflammatory cells within the dura, arachnoid and pia of experimental animals. (Preul et al., 2003, Preul et al., 2007) However, importantly, the study by Bakar et al. suggested that Adherus® did not show any neurotoxicity in vivo. (Bakar et al., 2013)

A foreign body giant cell reaction is the typical healing response to an implanted material. Our results demonstrate a severe foreign body giant cell reaction with BioGlue® at day 14, which was moderate by day 28. There was a mild foreign body giant cell reaction in the Adherus® group at day 28 but no foreign body reaction was identified in the Tisseel® and control groups. Although the giant cell reaction with Tisseel® was severe at days 7 & 14, by the final time point in the study this could not be detected.

The Tisseel® and control groups showed only focal cord inflammation suggesting that the application of Tisseel®, irrespective of whether the pia-arachnoid interface had been disrupted, was similar to the control group. The Adherus® and BioGlue® groups however, demonstrated gliosis and cord degeneration histologically but the majority of rats in these groups did not show neurological deficits. (Figure 3.3) However, it

remains unclear whether cord degeneration in these groups was due to pressure necrosis, neurotoxicity, ischaemic injury or a combination of the aforementioned.

Histological sections of the two hemiparetic BioGlue® rats demonstrated glue material compressing the cervical cord, leading to a marked cord degeneration. Severe acute inflammation was seen with a moderate soft tissue necrosis and fibroblastic reaction. (Figure 3.3) Some researchers suggest that BioGlue® can cause direct nerve injury because of the glutaraldehyde component and state direct neural contact must be avoided. (Lemaire et al., 2007)

Similarly, one Adherus® rat developed a hindlimb paralysis and another developed a hemiparesis, with both having left hemicord compression. This could be due to inadvertent application of copious sealant due to the sensitivity of the applicator or from expansion of the hydrogel in vivo. Some clinical studies suggest a delayed cauda equina compression after dural repair with BioGlue®, possibly due to expansion after application. (Lauvin et al., 2015)

In these examples the exact mechanism of cord injury remains unclear, but it would be advisable to follow manufacturers guidelines and not apply BioGlue® and Adherus® in close proximity to CNS tissue. (Kalsi et al., 2017)

3.5 Conclusion

Tisseel® can be safely used on the spinal cord and CNS tissues. BioGlue® and Adherus® should only be applied sparingly to the outside of the dura to form a watertight seal but intradural application and contact with CNS tissue must be avoided. Tisseel® can be safely used to reimplant spinal nerve roots into the cord.

CHAPTER FOUR

CHAPTER 4: DEVELOPING A MODEL TO ASSESS NEURONAL CONTINUITY ACROSS THE SITE OF VENTRAL ROOT AVULSION AND REPAIR, USING A NEURAL TRACER.

4.1 Introduction

The demonstration of axonal regeneration in models of spinal cord injury is important to assess repair and regeneration. Several anterograde and retrograde axonal tracers have been used over the past decades. Anterograde transport is from the cell body to the periphery whereas retrograde transport is from the periphery back to the cell body. An ideal tracer should be able to demonstrate regeneration, reliably label the majority

of axons or cell bodies, should be easy to apply, survive in animal tissues for the duration of the planned study, be compatible with processing techniques and be relatively easy to visualize.

A number of techniques using unidirectional or bidirectional anterograde and retrograde axonal labelling have been described in the literature. (Huang et al., 1999, Cheng et al., 1996, Choi et al., 2002) Simultaneous bidirectional tracing in the same animals in theory allows a more complete examination of the regenerating axonal fibres and reduces the number of animals required in animal studies. (Tsai et al., 2001) However, the practicalities of doing this in a cervical ventral root repair model mean that an optimal unidirectional tracer needs to be established.

Anterograde tracers are useful for labelling long tracts. Biotinylated dextran amine (BDA) is an anterograde which can label tracts originating in the cerebral cortex and traversing the spinal cord. Although this is a useful axonal tracer it does not cross synapses and additional compounds, such as viruses, are required to assess pathways across synapses. (Kristensson et al., 1974)

Retrograde labelling is an important method to accurately distinguish between motor neurones and sensory neurones in the relationship between the peripheral nerve and spinal cord. Sensory neurone cell bodies are located in the dorsal root ganglion whereas alpha motor neurones projecting motor fibres into peripheral nerves are located in the anterior horn of the spinal cord grey matter. Retrograde labelling can be performed with single agents or dual agents at the same time in the same animal. (Fritz et al., 1986a, Fritz et al., 1986b, Gordon and Richmond, 1990, Hoover and Durkovic, 1991) By applying different agents to separate targets, different populations of motor neurones can be compared in the same histological sections. Multiple

labelling methods are also advantageous when tracers need to be applied to nerves which are difficult to isolate.

The first documented retrograde labelling of motor neurone cell bodies in the central nervous system was with horseradish peroxidase (HRP). (Kristensson and Olsson, 1971) HRP was initially used as a sole agent to assess the distribution of motor neurones one muscle at a time. Although HRP can be detected using light microscopy it is considered an historical tracer. (Berretta et al., 1991) This is primarily because labelling of motor neurone cell bodies by this tracer is highly variable. (Richmond et al., 1994)

Fluorescent retrograde tracers have been used for retrograde labelling of axonal projections since the late 1970s. (van der Kooy et al., 1978) They have been utilised to compare pre- and post-injury motor neurone populations in axons projecting to the injury site. (Horikawa and Powell, 1986, Haase and Payne, 1990, Richmond et al., 1994, Puigdellivol-Sanchez et al., 2000) A variety of compounds have been studied in animal models under different settings and each has its specific benefits and drawbacks.

Fluro-Gold (FG) is a water soluble crystalline tracer. (Schmued et al., 1990) It is effective for experiments which require fast neuronal labelling. (Richmond et al., 1994, Choi et al., 2002) Fast Blue® (FB), alternatively known as diamidino compound 253/50, is a fluorescent retrograde tracer which is carried rapidly and efficiently by retrograde axonal transport over long distances. FB has been shown to safely label motor neuron cell bodies in several animal models, including rats. It labels the cytoplasm of the cell bodies and dendrites, which fluoresce bright blue and silver respectively, on excitation with wide band ultraviolet light (excitation: 360nm; emission:

420nm). (Bentivoglio et al., 1980) However, FG has been shown to label a significant number of cells both within and outside the spinal segments of interest and may therefore not be as accurate. Furthermore, the yield of labelled cells has been highly unpredictable when both FG and FB were administered intramuscularly. (Richmond et al., 1994)

Dextran conjugated to fluorescein (FD) and dextran conjugated to rhodamine (Fluro-ruby, FR) have not been used commonly to label motor neurones. (Gimlich and Braun, 1985) They have been used primarily to assess CNS pathways in mammals. (Nance and Burns, 1990) In one study these tracers were shown to only label motor neurone cell bodies when applied to cut nerves and not to muscle or intact nerve. (Richmond et al., 1994) This contradicts earlier work, which suggested they could do so. (Glover et al., 1986) Despite this, FD and FR may be useful for nerve injection as leakage into muscle may not lead to contamination.

The aims of this study were firstly to accurately assess the C8 & T1 motor neurone cell body pool in the intact nerves. Secondly, we wanted to determine the ideal site of injection of retrograde tracer into a rat peripheral nerve, so as to selectively label motor neurone cell bodies associated with the C8 nerve root pool. Thirdly, we wanted to quantify motor neurone population survival following ventral root avulsion so that we could establish a baseline for our ventral root repair model. We opted to assess the efficacy of a single retrograde tracer, Fast Blue® for the purpose of this study.

4.2 Materials and Methods

All the work performed in this chapter was approved by the Animal Welfare Ethical Review Body (AWERB). All experiments in this study were conducted in accordance with the UK's Animals (Scientific Procedures) Act 1986 with ethical approval from

Institute of Neurology, University College London. We followed the ARRIVE Guidelines when conducting these experiments.

The aim of this study was to assess the efficacy of Fast Blue® tracer to accurately label motor neurone cell bodies when applied to a peripheral nerve, so as to determine the C8 motor neurone pool in our rat brachial plexus model. The animals were all locally bred isogenic and phenotypically identical adult female Sprague-Dawley (SD) rats weighing 200-250g at the start of the experiments. (Harlan Laboratories, UK) Throughout the experiments, all rats had free access to food and water. Appropriate measures were taken to minimise discomfort and pain and experiments were terminated early if the animal subjects showed any symptoms of pain or self-harm.

The first study group involved injecting Fast Blue® tracer into the median nerve of five intact rats (n = 5) and five rats who had a undergone a left C8 ventral root avulsion, (n = 5) at 56 days after the avulsion surgery (chronic injury). The second study group involved injecting tracer into the ulnar nerve of five intact rats (n = 5) and five rats who had a undergone a left C8 ventral root avulsion at the 56-day point. The third study group involved injection of tracer into the extraforaminal left and right C8 nerve roots in rats who had had a left C8 ventral root avulsion (n=5) and those who had undergone a left C8 nerve root reimplantation (n=5) at 56-days after initial surgery.

For the peripheral nerve injections, the rats were anaesthetised with intraperitoneal injection of 2% tribromoethanol. (Sigma-Aldrich, UK) They were positioned supine and the shoulder externally rotated. The skin was shaved in the cubital fossa, cleaned with Tamodine® iodine antiseptic solution (Vetark Animal Health, UK) and draped. An incision was made parallel to humerus continuing in the cubital fossa and proximal forearm. A heavy toothed forceps and sharp scissors were used to dissect the median

nerve. A 25 µl Hamilton syringe was used to inject 5 µl of 2% FastBlue® retrograde tracer on to the undamaged median or ulnar nerve sheath epineurium, and excess tracer blotted away after 10 seconds. The skin was closed with 4.0 Vicryl (Johnson & Johnson, UK).

For injection of the extraforaminal C8 nerves, anaesthetised rat was placed prone on the custom-made plasticine device allowing anaesthesia and the posterior approach to the cervical spine. The fur was clipped, skin prepared with Tamodine® iodine antiseptic solution (Vetark Animal Health, UK) and the rat draped to maintain a sterile field. A skin incision was made in the midline from C6-T2. A bilateral muscle strip to expose the lateral facet joint, extraforaminal space and bilateral C8 nerve roots, distal to the site of initial surgery. A 25 µl Hamilton syringe was used to inject 5 µl of FastBlue® retrograde tracer on to the undamaged nerve sheath epineurium, and after 10 seconds any excess tracer was blotted away. The fascia and muscle layer were closed with continuous absorbable sutures and the skin closed with interrupted vicryl. (Johnson & Johnson, UK).

The animals recovered from anaesthesia without side effect and their forelimb function had not changed. After 1 week the rats were anaesthetised with a terminal dose of CO_2. Through a wide thoracotomy the heart was exposed, and an incision made in the right atrium and left ventricle. A blunt hypodermic needle (0 gauge; cut flat and polished smooth) was inserted into the ascending aorta through the left ventricle. The circulating blood volume was flushed out by perfusion with 100ml of 0.1M phosphate-buffered saline (PBS) followed by pericardial perfusion with 4% PFA. (Appendices 1 & 2)

The cervical spinal cords from the region C4 to T2 were obtained for section. Under a dissecting microscope the cervical spine was dissected to remove excess muscle and trimmed down to a size to fit the cryotome. The dissected tissue was placed in Decalcifier-II (Surgipath Europe Ltd., Cambridgeshire, UK) for 18 hours followed by suspension in 10% and 20% sucrose overnight for cryopreservation.

The sample was then placed in OCT (Bright Cryo-M-Bed; Jencons Scientific Ltd, Leighton Buzzard, UK) on an agitator for 30 minutes before being rapidly frozen with crushed dry ice. It was then mounted on a specimen holder in OCT (Bright Cryo-M-Bed); Jencons Scientific Ltd, Leighton Buzzard, UK) and cut in axial sections with a plane thickness of 25 μm. (Appendix 4) The sections were mounted on to slides, covered and left in a dark room to dry for at least 4 hours prior to viewing under the fluorescence microscope (Zeiss Axiophot fluorescence microscope) using a standard UV filter and wavelength of 360nm.

In each spinal section corresponding to the ventral root motor neuron pool, the total number of labelled cell bodies was counted twice by eye. The microscope focus was varied throughout the depth of the section. Only cells where the nucleus was completely visible were counted. Statistical testing was carried out using SPSS Statistics 22.0. (IBM, Armonk, NY, USA)

4.3 Results

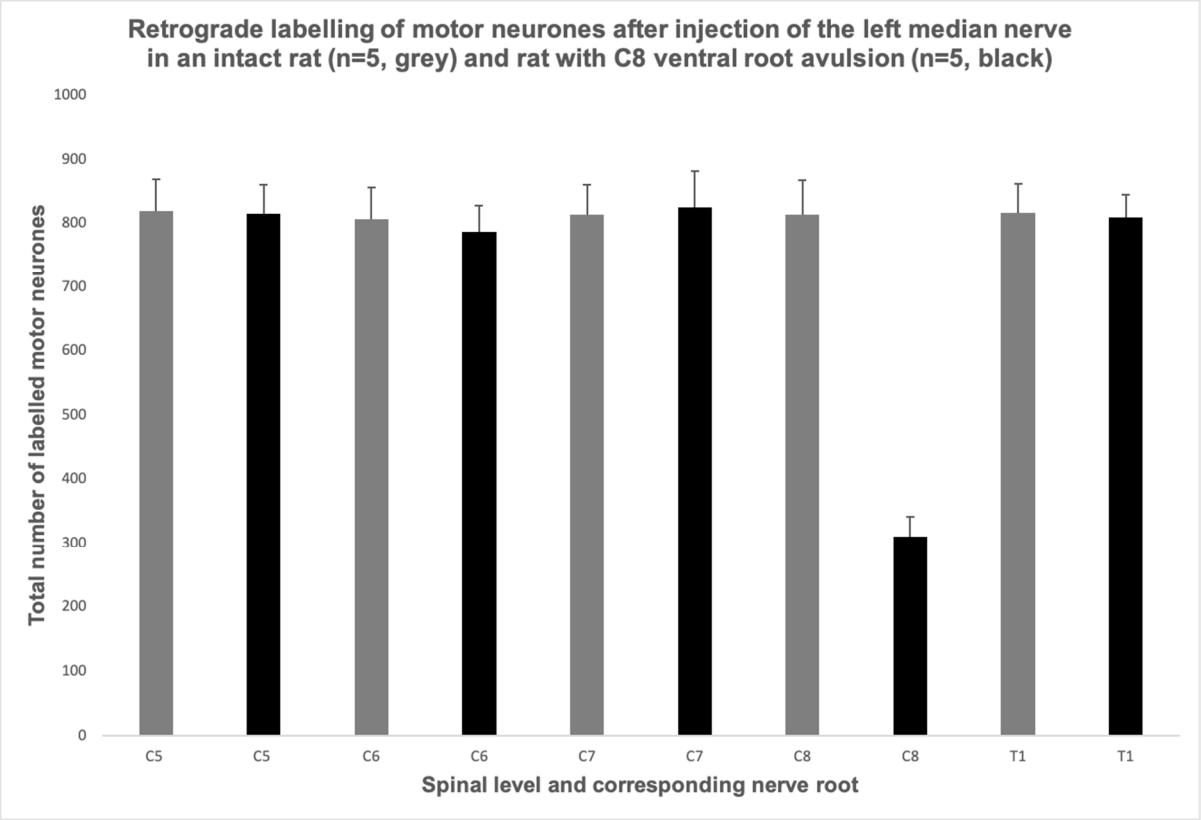

Figure 4.1. Graph showing retrograde labelling of cervical motor neurons in an intact rat (grey) and a rat with left C8 ventral root avulsion (black) following median nerve injection with Fast Blue® in the left cubital fossa. (Error bars indicate mean ± SD)

The results were analysed using a one-way analysis of variance. (ANOVA, SPSS Statistics 22.0) There was no difference in the mean number of motor neuron cell bodies labelled at the C5, C6, C7, C8 and T1 levels, when the median nerve was injected in the intact rat ($p = 0.18$) (see Figure 4.1). However, in the group where the rats had avulsion of the C8 ventral root, ($n = 5$) injection of Fast Blue® tracer in to the median nerve showed a significant difference in the uptake of tracer at the level of

motor neuron pool of the C8 ventral root compared with the motor neuron pools of the other nerves contributing to the brachial plexus. ($p<0.05$) (Figure 4.1)

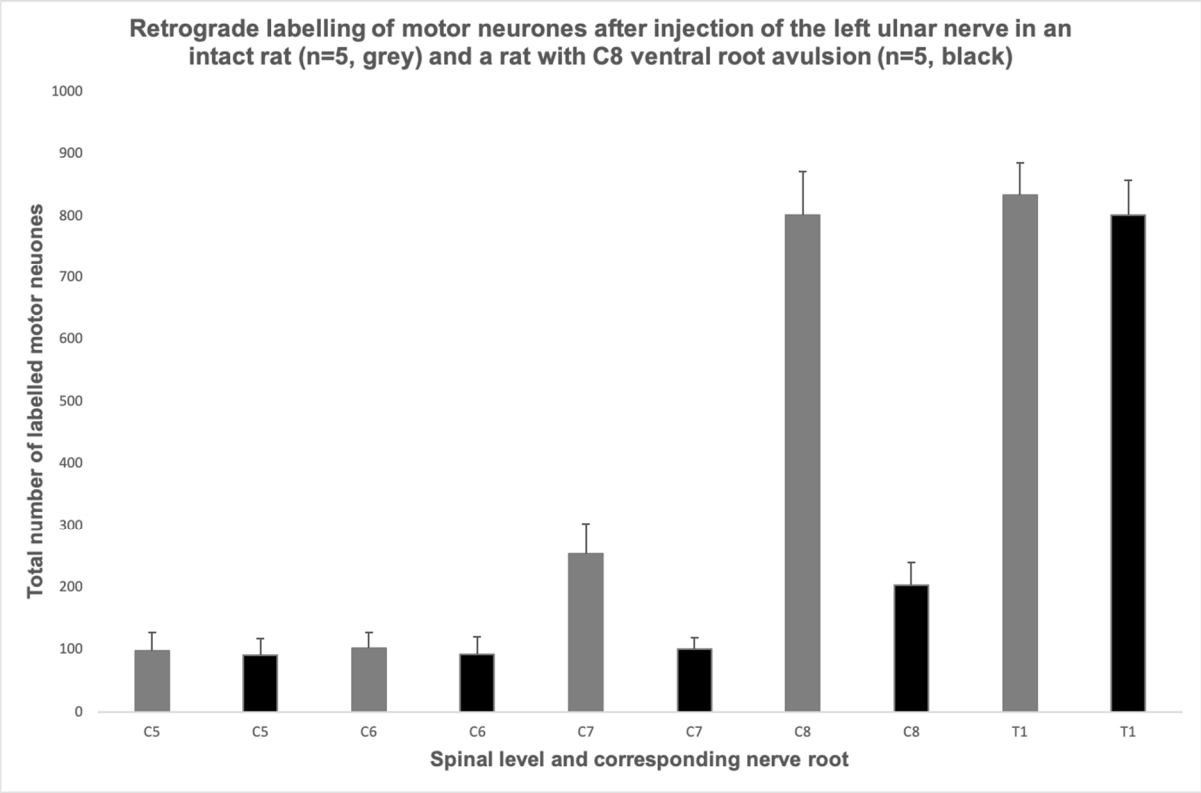

Figure 4.2. Graph showing retrograde labelling of cervical motor neurons in an intact rat and a rat with C8 ventral root avulsion, when the ulnar nerve was injected in the cubital fossa with Fast Blue®. (Error bars indicate mean ± SD)

The results were analysed using a one-way analysis of variance. (ANOVA, SPSS Statistics 22.0) There was a significant difference in the mean number of motor neurone cell bodies labelled in the C8 and T1 motor neurone pools compared with the C5, C6 and T1 pools, when the ulnar nerve was injected in the intact rat ($p<0.05$). (Figure 4.2) There was no difference between the C8 and T1 motor neurone pools. (paired T-test, $p = 0.23$) In the group where the rats had avulsion of the C8 ventral

root, injection of Fast Blue® tracer showed a significant difference in the uptake of tracer between the motor neurone pool of the C8 ventral root compared with the motor neurone of the T1 root. (Paired T-test, $p<0.05$) (Figure 4.2)

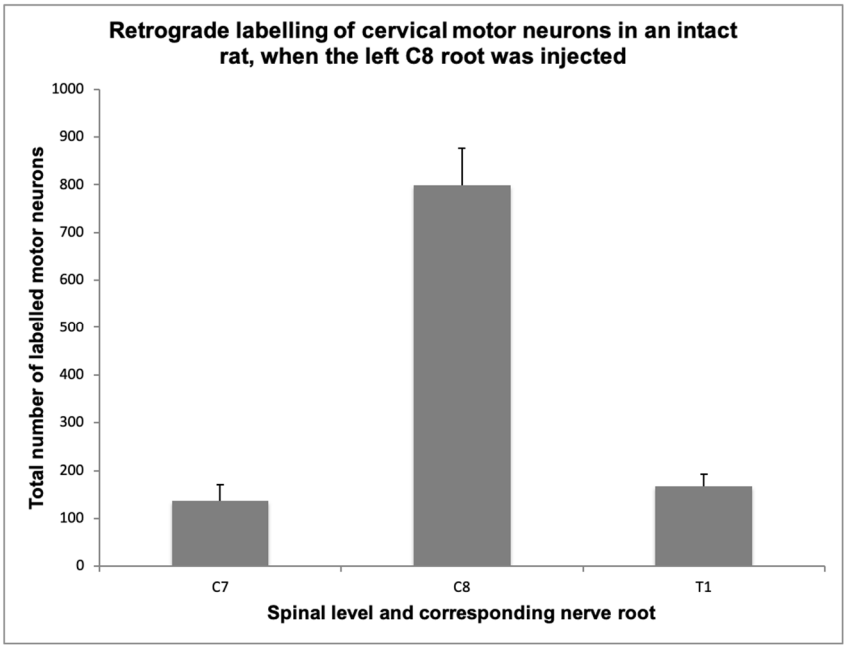

Figure 4.3. Graph showing retrograde labelling of cervical motor neurones in an intact rat when the C8 nerve was injected with Fast Blue® as it emerges from the foramen. (Error bars indicate mean ± SD)

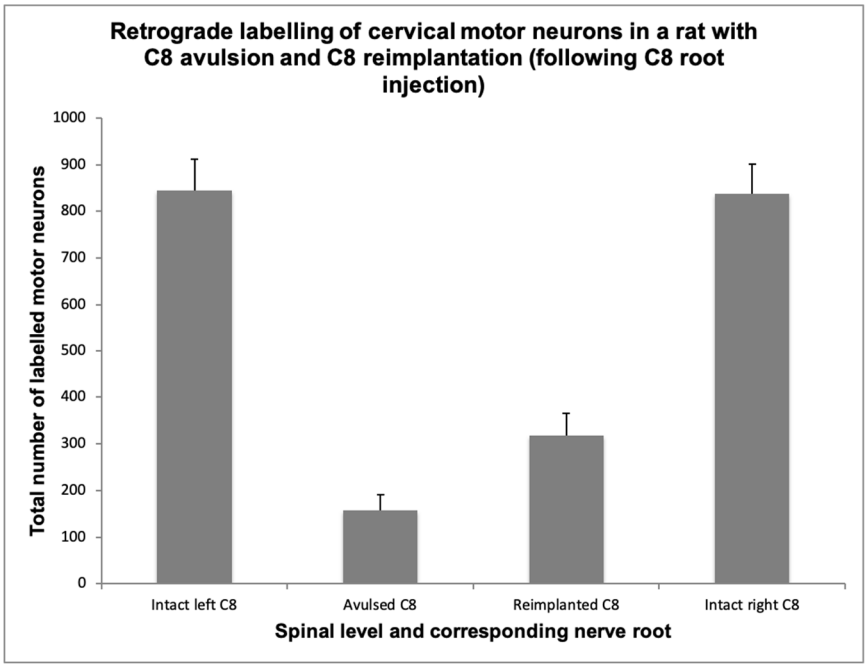

Figure 4.4. Graph showing retrograde labelling of cervical motor neurones in a rat when the C8 nerve root was injected with Fast Blue®. The graph shows tracer uptake in an intact left C8 root, an avulsed and reimplanted C8 root and the contralateral right sided intact C8 root. (Error bars indicate mean ± SD)

The results were analysed using a one-way analysis of variance. (ANOVA, SPSS Statistics 22.0) There was a significant difference in the mean number of motor neurone cell bodies labelled with Fast Blue® when the intact C8 nerve was injected compared with the C7 and T1 roots (ANOVA, $p<0.05$). (Figure 4.3) In the group where the rats had avulsion of the C8 ventral root, and reimplantation of the C8 ventral root, there was a significant difference between the intact and surgery rats (one-way ANOVA, $P<0.05$) and a significant difference between the avulsed and reimplanted ventral root ($p<0.05$) (paired T-test). (Figure 4.4)

A representative image of the appearance of labelled motor neurone cell bodies as seen under the fluorescent microscope, following injection of the extraforaminal C8 nerve root is presented in Figure 4.5.

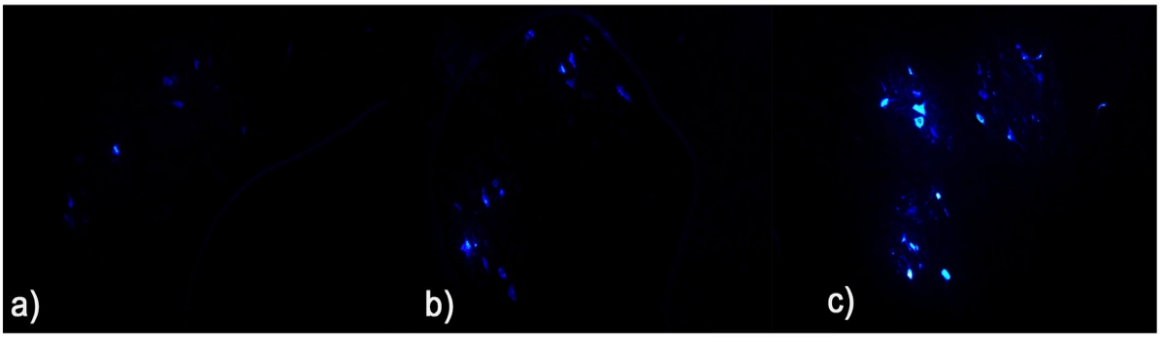

Figure 4.5. Spinal cord cross sections (25μm) after the C8 nerve root was injected with Fast Blue®. Labelling of motor neurone cell bodies in the anterior horn of the cervical spinal cord. a) The left C8 ventral root was avulsed and injected with Fast Blue® at day 56. b) The C8 ventral root was reimplanted and injected with Fast Blue® at day 56. c) A non-lesioned C8 ventral root with retrograde tracer injected in to the C8 nerve root extraforaminally.

4.4 Discussion

The main aims of this study were to firstly establish the motor neurone pool of the C8 nerve in an intact rat. Secondly, we wanted to determine the ideal site of injection of Fast Blue® into a rat peripheral nerve to assess the motor neurone pool of the C8 nerve. Thirdly, we wanted to quantify the population pool of surviving motor neurones in a chronic model of C8 ventral root avulsion in order to establish a baseline for our rat brachial plexus C8 ventral root repair model.

Previous studies established that Fast Blue® can consistently and effectively label motor neurones over long distances and has adequate fluorescent longevity for the purposes of this study, namely analysis one week after injection. (Horikawa and Powell, 1986, Novikova et al., 1997b, Choi et al., 2002)

There was significant motor neurone survival after ventral root reimplantation compared with ventral root avulsion. advantage ($p<0.05$). The number of motor neurone cell bodies labelled in the C8 nerve tracer injection compared with the median and ulnar nerve injections was significantly lower ($p < 0.05$). The results also suggest there is a slight cross over with motor neurone cell bodies at adjacent levels supplying on average 100 motor neurones to the adjacent motor neuron cell pool.

In theory, the ideal injection site of Fast Blue® would be the peripheral component of C8 nerve root as close as possible to the injury site. However, in a chronic injury model, where the rat has had a previous posterior approach to the cervical spine and surgery of the C8 root, a revision surgery at the same level could potentially be fraught with problems. Firstly, the scar tissue could preclude easy access to the nerve root and secondly, by trying to obtain access we could potentially damage the reimplantation or cause spinal cord injury.

In order to overcome this potential problem, we initially attempted to inject Fast Blue® into the median and ulnar nerves of intact rats in the cubital fossa. This method labelled all the motor neurone pool of the nerves in the anterior horn of the spinal cord from C5 to T1 and C8 to T1, respectively. In the C8 ventral root avulsion group, injection of Fast Blue® in to the median and ulnar nerves at the cubital fossa lead an indiscriminate labelling of all the motor neurone pool from C5 to T1 and C8 to T1 in the two peripheral nerve models. Although there was a significant reduction in labelling of the motor neurone pool of the avulsed C8 nerve in this model we could not be entirely sure how many of the C8 pool of motor neurones had survived following ventral root avulsion and how much of the labelling was due to crossover from adjacent levels.

We subsequently devised a surgical approach to specifically target the C8 nerve as it emerged from the intervertebral foramen, where we could safely apply the retrograde tracer. In rats who had not had previous posterior cervical injury this method was straight forward, as it was relatively easy to perform a posterior approach to the extraforaminal region, identify and inject the C8 nerve root with tracer. However, the approach to the extraforaminal C8 root after rats had undergone a posterior cervical approach to avulse or reimplant the C8 root was more challenging. In this group, the skin incision was easily recognisable, but we did not want to perform a midline muscle strip because scarring and revisional surgery could potentially disrupt the ventral root repair which was going to be analysed histologically when the rats were culled 1 week after tracer injection. We therefore developed a posterior approach through the paraspinal musculature using anatomical landmarks, (Cao and Ling, 2003) which allowed direct access to the lateral facet joint, foramen, and extraforaminal C8 nerve root.

Injection of Fast Blue® tracer on to the C8 nerve at intervertebral foramen resulted in tracer uptake predominantly by the motor neurone pool of the C8 nerve. In an intact C8 nerve root we established that the motor neurone pool was significantly higher than the avulsion group. However, the reimplantation group showed significant motor neurone survival compared to the avulsion group.

As a pilot study, the number of rats used in this study was kept to a minimum whilst providing helpful data to plan the rest of our study. The rats in the study were injected with equal volumes of Fast Blue® and were culled after exactly 1 week of addition of the tracer, meaning that any decrease of efficacy of the tracer or labelling of motor neurone cell bodies would not be a variable. (Soreide, 1981) The use of bilateral

tracers in the left and right C8 nerves served as controls for counting the number neurones on the avulsed/reimplanted and intact sides.

Fast Blue® has been shown to label cells with good intensity and can persist in cell bodies for up to 8 weeks. (Choi et al., 2002) In other studies it has been shown to persist for up to 6 months. (Novikova et al., 1997b) In a study of the cat peripheral nerve, labelling at 3 days after operation was shown to be inconsistent. (Illert et al., 1982) However, other studies where the injection of tracer and axonal transport has been over shorter distances in smaller animal models have not shown this to be the case. (Choi et al., 2002, Horikawa and Powell, 1986) In our study there was no difference in retrograde labelling of motor neurone cell bodies at the median nerve or the C8 nerve root one week after injection of Fast Blue®.

Counting the nuclei in a 25 μm section is likely to overestimate the cell bodies in the spinal cord as some nuclei may be counted twice on consecutive slices. However, the aim of this study was to analyse the raw data in an uncorrected form because we were comparing groups with the same error rather than accurately establishing absolute motor neurone cell body numbers. Since the thickness of the slice was many times greater than the actual size of the motor neurone cell body it was assumed that counting error would be negligible and Abercrombie's correction factor did not need to be applied to the data. (Clarke, 1992) For absolute counts, unbiased stereological methods can be applied to accurately count cell numbers. (Gundersen et al., 1988) These can help to provide an accurate cell count, avoiding counting errors when absolute numbers are being evaluated. (Coggeshall and Lekan, 1996)

4.5 Conclusion

Our study supports the use of Fast Blue® retrograde tracer to label pre- and post-injury neuronal populations in a C8 ventral root avulsion model. We can conclude that carefully re-opening the posterior cervical incision, paraspinal muscle dissection to expose the extraforaminal C8 nerve followed by injection of tracer, provided the optimal results for assessment of surviving C8 motor neurone pools.

CHAPTER FIVE

CHAPTER 5: DEVELOPING A FUNCTIONAL TEST TO QUANTIFY VENTRAL ROOT INJURY IN THE RAT BRACHIAL PLEXUS AVULSION MODEL

5.1 Introduction

The purpose of this study was to identify which functional tests could be used to assess our rat brachial plexus ventral root model. As our study objective was to replicate a model of human brachial plexus repair, where there is poor recovery of hand function, we wanted to devise functional tests to quantify rat forepaw recovery for our model.

Functional tests can be used to quantify the effect of a nerve lesion and then to monitor the recovery and compare the effects with an experimental intervention. As nerve regeneration after repair does not occur in a standardised way, recovery of function may not always correlate with histological or electrophysiology evidence of nerve regeneration. (Brushart and Mesulam, 1980, Dellon and Mackinnon, 1989) A number of rat behavioural tests have therefore been devised to test forelimb reinnervation and function following injury to the spinal cord and peripheral nerves. (Nichols et al., 2005) However, there are no specific tests to assess functional outcome after focal ventral nerve root lesions in the lower brachial plexus.

The rat forelimb is innervated by branches of the brachial plexus. The median nerve is solely responsible for forepaw grip unlike in humans where both the median and ulnar nerves play a critical role in wrist and hand flexors. (Bertelli and Mira, 1995) Similar to humans the rat median nerve comprises the ventral rami of the C5 through to T1 nerves, receiving contributions from the lateral, posterior and medial cords. The

nerve passes into the axilla and then the forearm to innervate all the forepaw flexor muscles.

Due to ease of access, the sciatic nerve is the most commonly tested peripheral nerve in rats and the majority of functional tests are designed for spinal cord injury and hind limb deficits. However, over 40 functional tests have been developed to test and quantify forepaw function in normal and nerve injured rat models in the context of spinal cord and peripheral nerve injury models. (Nichols et al., 2005)

The key characteristic of the rat forelimb is the ability to grasp. (Ivanco et al., 1996) The dexterity of the rat forepaw with regards to grasping movement as when feeding has been studied and quantified whilst doing skilled forepaw movements. (Whishaw and Gorny, 1994) As rats are traditionally cheap to house, handle and train this makes them ideal candidates for testing repetitive trained movements. However, the effect of C8 or T1 avulsion on median and ulnar nerve function in the rat forelimb has not been studied. There are no functional tests to assess these specific nerve roots in isolation. We therefore assessed the efficacy of a number of functional tests to develop behavioural tests to quantify the injury in our rat model.

5.2 Functional tests overview

Behavioural tests for forelimb function in rodent models can broadly be divided into tests for locomotion, motor skill tests, sensory tests, sensory-motor tests, autonomic tests, and also electrophysiology and functional MRI.

5.2.1 Tests for locomotor function

Normal locomotion in a rat requires both forepaw and hind paw function. The BBB test, named after the scientists who developed it, namely Basso, Beatie and

Bresnahan is the commonest test used test for spinal cord injured rats. (Basso et al., 1995) Similarly, kinematic analysis, thoracolumbar height test and the swim test can be used for this purpose. (Gale et al., 1985, Metz et al., 1998, van de Meent et al., 1996) However, all these tests assess hindlimb locomotion in predominantly thoracic level cord injury rats and are not applicable to our study, where we were trying to measure forelimb and more specifically lower brachial plexus root function.

The Forelimb Locomotor Assessment Scale (FLAS) is a test of forelimb function in cervical spinal cord injured rats. (Anderson et al., 2009) In this test rats who have received cervical cord injury are videoed whilst walking. A score is given based on a number of parameters including forepaw movements or lack of. A score range between 0-64 is ascribed, with 0 denoting no function and 64 meaning normal forelimb function. This test is validated for cervical cord injury in the rat and would probably not be useful in our focal longitudinal injury model.

Another test for locomotion is the Catwalk® system which uses a long glass walkway and fluorescent light to capture gait, paw prints and paw pressure, as well as a number of other parameters, which can be videoed and analysed by Catwalk® software. (Hamers et al., 2006, Hamers et al., 2001) The DiGiGait™® system (Mouse Specifics Inc., Boston, USA) is also available for gait analysis and this allows a number of measurements, including limb rotation, paw and digit spread to be assessed using computer software.

These tests are based on gait analysis work initially described by de Medinaceli at al. and later modified by others. (de Medinaceli et al., 1982, Chan et al., 2005, Metz et al., 2000) The rats are trained to walk on a narrow paper covered wooden beam, their paws dipped in non-toxic water soluble ink and various measurements including paw

spread, digit spread, and limb rotation angle are manually measured from the derived footprints. (de Medinaceli et al., 1982) Such tests are the forbearers of the modern digital tests and are cheaper to perform although analysis is time consuming and requires at least two researchers to independently verify the results.

5.2.2 Tests for motor function

These are tests for specific skeletal muscle functions, but they do not assess locomotion. The limb hanging test is used to assess primarily rat forepaw function after cervical spinal cord injury. (Diener and Bregman, 1998, Pearse et al., 2005) However, in severely injured forelimb animals who have no paw function, this test only provides a binary yes or no answer and therefore needs to be used in combination with other tests.

The paw grip strength is a test of the peak force an animal applies on grasping. This test can be used for both forelimb and hindlimb testing. It requires a grip strength meter, which is constructed on the basis of the Meyer Method. (Meyer et al., 1979) Similar to the limb hanging test this test is unable to measure the grip strength in severely damaged limbs but if the animal is able to grip, this test can give a precise and unique measurement.

Another useful test for forepaw function is the forelimb asymmetry test. This is sensitive to a number of central nervous system insults and uses the rat's preference to stand on its hindlimbs and reach out with the forepaw. (Gharbawie et al., 2004) This test can take the form of either the cylinder test, limb use asymmetry test or paw preference test. However, these tests require functional shoulder flexion and elbow extension, so may not be as useful in rats with a normal C5, C6 and C7 nerve root.

Food pellet reaching tests are also validated in rat cervical spinal cord injury. In this test the rat is trained to grasp a specific sized food pellet and the success rate is calculated by the number of times the rat grasps the pellet divided by the number of attempts required. (Whishaw, 2000) A modification of this test is the paw reaching or staircase test, but this predominantly used as a behavioural tests in stroke models. (Montoya et al., 1991)

5.2.3 Sensory-motor tests

Although one of these tests was devised for brachial plexus evaluation, the majority of these tests would unlikely be applicable in our model as sensory-motor tests require competent sensory and motor systems. A number of tests including the rope walking test, narrow beam test and the foot slip test can be used to assess sensory-motor hindlimb and forelimb function. (Chan et al., 2005, Hicks and D'Amato, 1975, Kim et al., 2001) The Grooming test was initially devised to assess a C5 brachial plexus lesion, by way of assessing the rat's ability to abduct the shoulder. (Bertelli and Mira, 1993) However, this test is now more commonly used for cervical spinal cord injury. (Gensel et al., 2006) The grid walk, foot fault test is a sensitive test for evaluating the sensory-motor control of the limbs and we wanted to try this test to see whether dorsal root avulsion before avulsion of the ventral root would have an impact on paw placement and errors. (Metz et al., 2000) Although our model requires the avulsion of dorsal roots in order to access the ventral root, other authors have used sensory functional tests to assess repair of the cervical dorsal roots. (Ibrahim et al., 2009a, Collins et al., 2017)

5.2.4 Other functional tests in spinal injury models

Reflex response-based tests, such as the toe spread and righting reflex, and autonomic tests such as urinary bladder function and autonomic dysreflexia testing are more useful in the context of spinal cord injury. Functional MRI testing is a very precise test but requires specialist and expensive MRI equipment. Motor evoked potentials either by transcranial electrical stimulation or direct motor cortex stimulation can provide additional information about neurological recovery. (Nichols et al., 2005) However, the disadvantage of these techniques is that they require familiarity with neurophysiological equipment and techniques and are not routinely available in all laboratories.

5.3 The use of functional tests to assess forelimb nerve root lesions in published studies

Although the Forelimb Locomotor Assessment Scale (FLAS) is the only validated test to evaluate forelimb function during quadrupedal motion in rats, it is more pertinent to rats subjected to midline cervical spinal cord injury and not a focal brachial plexus lesion. (Bertelli and Mira, 1995, Yang et al., 2019, Anderson et al., 2009) Yang et al., they tested their extradural C7 repair model by using the grooming test devised by Bertelli and Mira. (Bertelli and Mira, 1995) Similarly, Yang et al. and Guo et al. assessed their end-to-side C5 and C6 nerve repair and intradural C6 nerve root repairs respectively, with the grooming test. (Bertelli and Mira, 1993, Yang et al., 2015, Guo et al., 2019) Wang et al. tested their C7 end to side neurotization with direct observation of recovery of elbow flexion. (Wang et al., 2011) Stossel et al. tested their median nerve injury repair model by assessing grip strength, and the staircase test, whereas Jager et al. tested their mouse median nerve model with the grasping test.

(Bertelli and Mira, 1995, Galtrey and Fawcett, 2007, Jager et al., 2014, Meyer et al., 1979, Stossel et al., 2017) In the study by Papalia et al. transection of the ulnar nerve in the axilla had no effect on the grasp test, but it affected the extensors on the forepaw. (Papalia et al., 2006)

Thus, it is clear that no functional tests have been utilised to assess either the C8 or the T1 ventral root in isolation. We therefore set out to evaluate a range of commonly used functional tests in the literature to assess our brachial plexus ventral root model.

5.4 Materials & Methods

Based on our review of the literature we decided to assess the efficacy of gait analysis, grip strength, cage walk faults and preferential paw placement. We wanted to establish whether we could quantify a C8, T1 and combined C8 and T1 ventral root injury and establish which functional tests to use in our brachial plexus repair model.

All the work performed in this chapter was approved by the Animal Welfare Ethical Review Body (AWERB). All experiments in this study were conducted in accordance with the UK's Animals (Scientific Procedures) Act 1986 with ethical approval from Institute of Neurology, University College London. We followed the ARRIVE Guidelines when conducting these experiments.

5.4.1 Animal testing conditions

For all the experiments we used genetically identical Sprague-Dawley female rats weighing 200-250 grams and of similar ages, as there is evidence that rodents of differing weights and ages have differing rates of neurological recovery. (Brailowsky and Knight, 1987) The same strain of rat was used in all experiments as it is known that functional outcomes differ between strains. (Mills et al., 2001) Testing conditions

were set out at the start of the experiments in order to ensure that functional tests were done in a reliable, reproducible and useful manner.

All animals were housed in cages of five to help social interaction and create a stimulating and stress free environment. (Tatlisumak, 2006) The cages contained straw bedding, which was changed at regular intervals, and rats had access to water and food pellets at all times. The rats were kept on a standard sleep wake cycle with lights being dimmed in the evenings and turned on during the daytime.

All rats were handled in a standard manner by placing a hand under their body or by holding the tail. The tester spent time handling the rats so that they could become accustomed to being handled prior to any behavioural tests being performed.

Behavioural testing was performed in a quiet, warm and well-ventilated room in a similar environment to the rodent housing area. In order to maintain the rodent sleep night cycle and circadian rhythms testing was done during a set time in the morning throughout the study. (Kriegsfeld et al., 1999) There were regular air changes in the testing areas for animal welfare and tester safety. Background noise was kept to a minimum at all times in order to ensure animals were not distracted or startled. No music was played, although there is no evidence to suggest that music impairs functional performance in rats. (Tatlisumak, 2006) All behavioural testing equipment was set-up prior to bringing the rats into the testing room within their cages. At the end of the functional testing the equipment was cleaned, with non-toxic cleaning equipment so as not to leave any residue or smells which could harm the rats or affect the outcome of functional tests.

All rats underwent pre-training with the functional tests prior to having surgery. This ensured that the animal was performing a trained manoeuvre, was acclimatised to the test and minimised stress during the testing period during and after surgery.

Acclimatisation to the tests was performed by two independent handlers who were familiar with the functional tests and comfortable handling the rats. Each handler performed the tests on consecutive days at pre-determined timepoints. This was done to compare scores, eliminate bias and to ensure that the same small relative error was consistent throughout the study and to reduce the absolute error. (Basso, 2004) All animals were weighed on a regular basis and locomotion tested prior to behavioural testing. (Farooque, 2000, Urdzikova and Vanicky, 2006) By training all the animals we ensured that the rats were performing a learned behaviour to their best functional ability, before and after surgery, which helps to further standardise the functional tests. (Muir and Webb, 2000)

It is not known whether a C8, T1 or a combination of C8 & T1 ventral root avulsion leads to a functional loss of forepaw function. Having reviewed the existing literature, we assessed a number of functional tests to establish whether a root deficit or recovery could be recorded. After this we endeavoured to establish functional tests that were quantifiable, reliable and reproducible for our brachial plexus ventral root model.

5.4.2 Gait assessment after ventral root surgery

This functional test was based on the work by Medinaceli et al. Several adaptations to this initial work have been made to modify the test. (Chan et al., 2005, Metz et al., 2000, de Medinaceli et al., 1982) We trained rats to walk on a purpose built 1.5m long and 8cm wide platform made of wood, which had a strip of white paper measuring 1 metre by 7cm placed on it. The platform was balanced at one side by an empty cage

and at the other by a cage housing the other rats in the group, providing a stimulus for the rat to return back to the cage. Initial training involved placing the rat on the platform and waiting for it to walk at least eight steps volitionally and without stopping. No rewards were required for this procedure. Once the rats were able to this, both forepaws were dipped in a non-toxic water-based paint. The rat was then placed on the platform and volitionally walked from the empty cage towards its housing cage. (Figure 5.1)

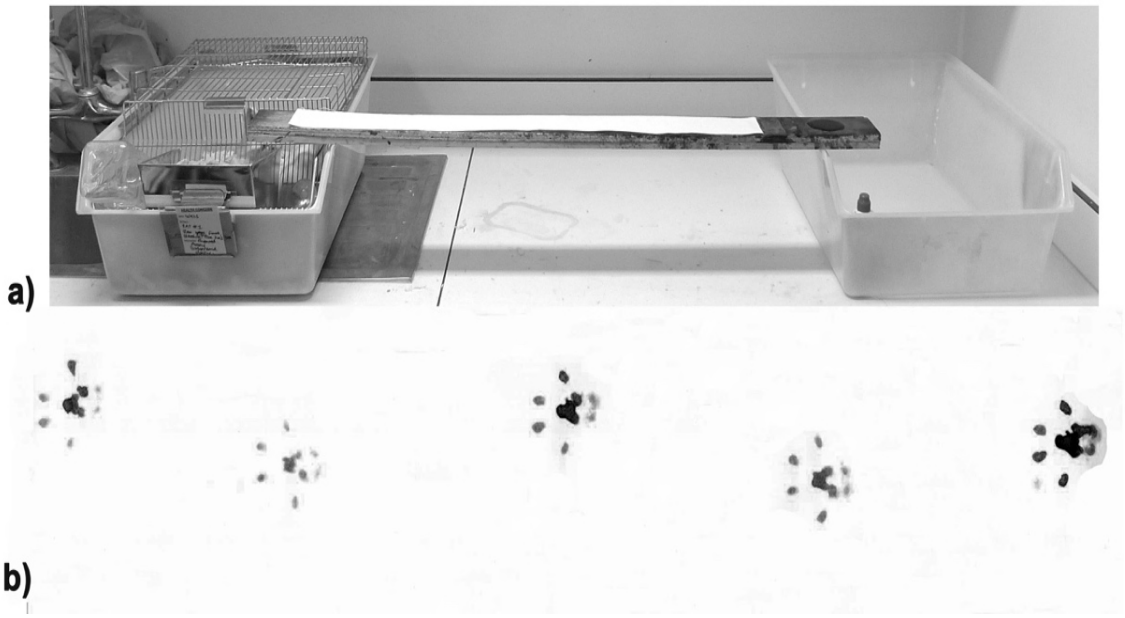

Figure 5.1. Locomotor tests for gait assessment. a) Wooden platform measuring 1 metre in length and 8 cm wide. The platform is balanced at one end on an empty cage and at the other end on the cage housing the group of rats. Paper to record forepaw prints is placed on the platform, along with water-soluble paints at one end. b) Sprague Dawley rat gait strip showing left and right forepaw prints in an intact rat (no root avulsion)

Rats were divided into a number of groups namely intact, C8, T1 and combined C8 & T1 avulsion, and C8, T1 and combined C8 & T1 reimplantation. (n = 5 in each group)

The forepaw prints generated allowed us to analyse a number of measurements including paw spread (PS), intermediate toe spread (ITS) and paw angle (PA), which represents limb rotation. (Figure 5.2) These were measured at weekly timepoints from before the surgery and every week up to 8 weeks post-surgery.

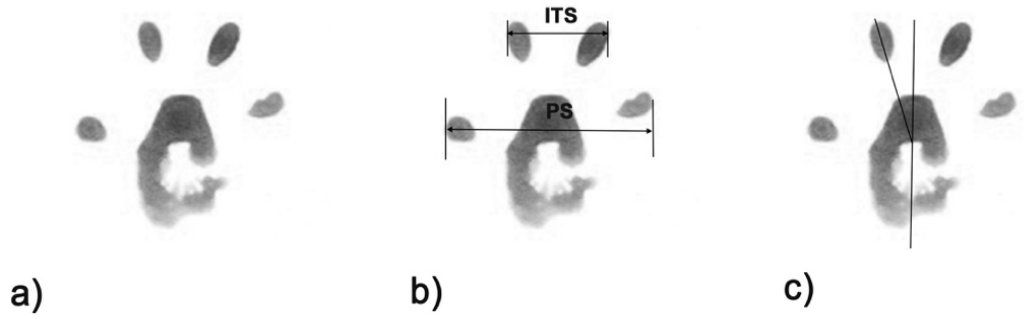

Figure 5.2. Forepaw prints in an intact rat. a) Left paw-print of a non-lesioned rat. b) The paw-print is annotated to show intermediate toe spread (ITS) and paw spread (PS) in a normal rat. c) Paw-print showing the paw angle (PA) in a normal rat.

5.4.3 Grip Strength Measurements

Grip strength testing is a validated test for motor function of the forepaw in prehensile mammals. (Anderson et al., 2005, Meyer et al., 1979) In order to reliably assess grip strength all rats need to be pre-trained. Our initial training sessions were dedicated to handling the animals and subsequent sessions involved familiarising the rats with the grip strength meter, holding them from their midsection, and allowing them to grasp the Grip Strength Meter (GSM) (TSE Systems Inc, Chesterfield, MO) with both forepaws. (Figure 5.3) Once the rats were comfortable using both forepaws to grasp the GSM, the right paw was gently tucked into their chest wall with the testers index finger and the rats innately attempted to grasp the bar with their left paw.

After training rats were divided into a number of groups namely intact, C8, T1 and combined C8 & T1 avulsion, and C8, T1 and combined C8 & T1 reimplantation. (n = 5 in each group). Left paw and bilateral paw grip were measured at weekly timepoints from before the surgery and every week up to 8 weeks post-surgery.

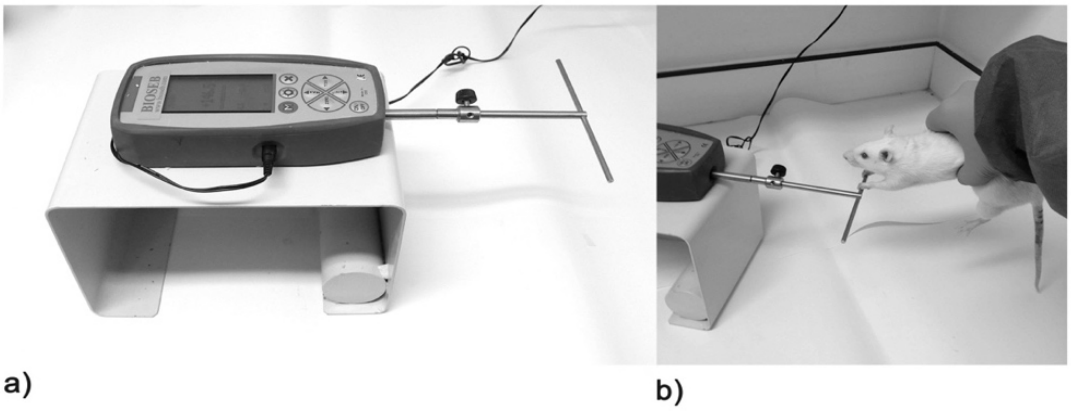

Figure 5.3. Analysis of grip strength. a) Grip strength meter. b) Rat being held at waist with both paws gripping the bar and giving a reading for bilateral paw grip strength.

5.4.4 Cage Walk Faults

It was observed that lesioned rats placed on top of a cage had difficulty walking on the cage following surgery. The grid walk test or the cage-walk faults test are an important test of sensorimotor function. (Metz et al., 2000) We tested cage-walk faults in our model of brachial plexus avulsion injury by using a purpose-built grid to simulate a cage. The grid was a metre long and made of horizontal bars welded together 5cm apart and vertical bars 1cm apart. The bars were 1.36mm in thickness. (Figure 5.4) The rats walked from one end of the platform to the other. No incentive was needed for the rats to do this. Rats were videoed as they walked across this frame and recordings from both forepaws analysed. The faults were graded as normal, or

whether the forepaw went through the grid to the level of the wrist, elbow or shoulder. Rats with a C8, T1 and a combined C8 & T1 avulsion and reimplantation were tested in this way on a weekly basis for eight weeks after surgery. (n = 5 in each group)

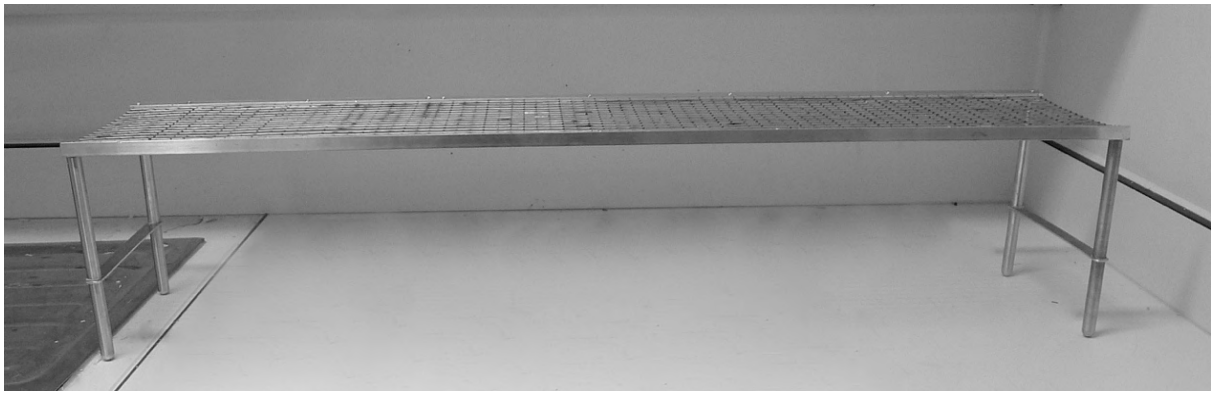

Figure 5.4. Walking grid to assess cage walk faults in rats. A purpose made walking grid to simulate the exterior surface of a rat housing cage. The rats were placed at one end and walked towards the other side, where the video camera filming their faults was placed.

5.4.5 Vertical Paw Placing

Rats were placed in a clear Plexiglas cylinder and videotaped for 2 minutes. The number of paw placements, the forepaw that was placed and any asymmetry between the two sides was noted, in rats that had had a C8, T1 and a combined C8 &T1 ventral root avulsion. These were measured pre-operatively and on a weekly basis for eight weeks after surgery (n = 5 in each group). (Ballermann et al., 2001)

5.5 Results

5.5.1 Paw spread, intermediate toe spread and limb rotation angle in an intact rat

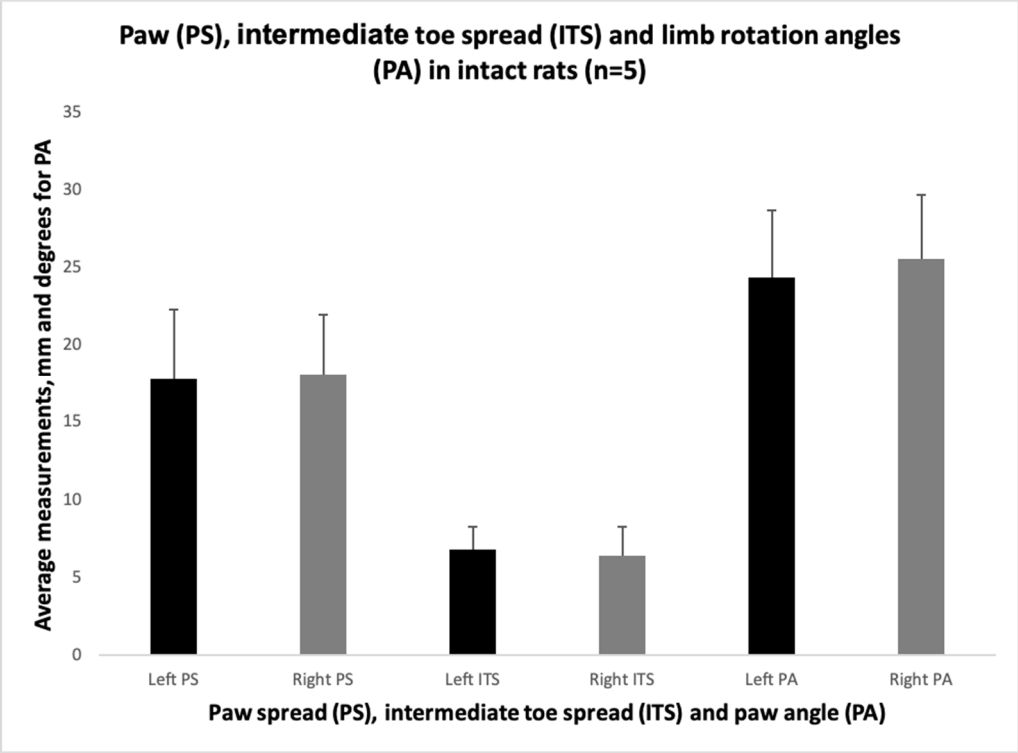

Figure 5.5. Graph demonstrating the average paw spread (PS), average intermediate toe spread (ITS) and paw angle (PA) in degrees, in an intact rat. (mean ± SD)

Paired t-test showed that there was no significant difference between left and right paw spread in intact rats, mean 17.1 ± 2.7mm v 17.4 ± 3.3mm ($p = 0.13$, $n = 5$), intermediate tow spread 6.7 ± 1.4 v 6.3 ± 1.9mm ($p = 0.22$, $n = 5$) and limb rotation angle 23 ± 3.2^0 v 25 ± 2.9^0 ($p = 0.39$, $n = 5$) (Figure 5.5)

5.5.1.1 Paw spread following left C8 ventral root avulsion

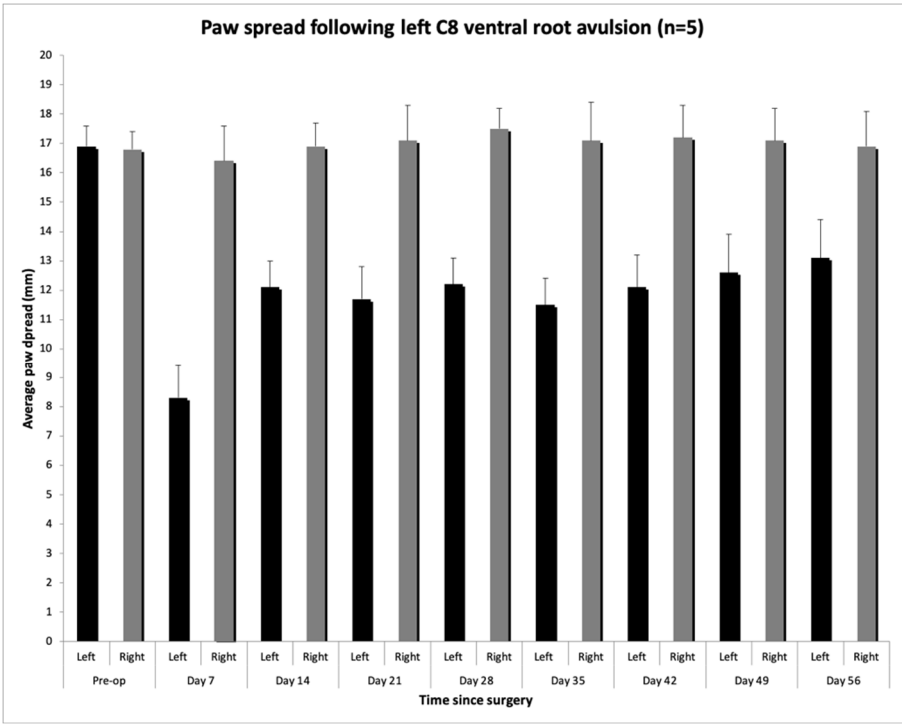

Figure 5.6. Left (black) and right (grey) paw spread following left C8 ventral root avulsion over a period of 8 weeks. The left paw spread reduced significantly after the surgery and recovered to a degree before plateauing and remaining significantly lower than the control right side at all time points. (mean ± SD shown on graph)

There was no difference in pre-operative left paw spread between the left and right paws (mean left 17.4 ± 2.3mm v right 17.2 ± 2.1mm, ($p = 0.12$). (Figure 5.6) After left C8 ventral root avulsion the mean paw spread significantly reduced to 8.3 ± 1.6mm ($p<0.05$) on day 7. At all time-points the paw spread remained significantly less than the control right side. At day 56 the left paw spread was 12.4 ± 2.1mm which was significantly lower than the right-side control (18.1 ± 2.9mm, $p<0.05$)

5.5.1.2 Paw spread following left T1 ventral root avulsion

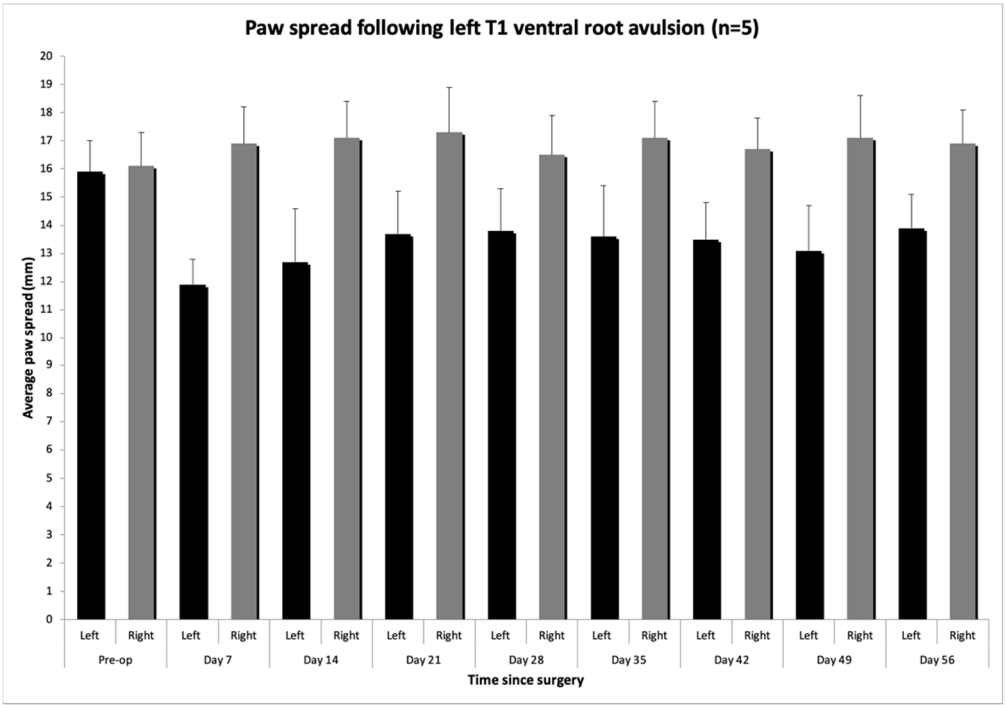

Figure 5.7. Left and right paw spread changes following left T1 ventral root avulsion over a period of 8 weeks. The left paw spread reduced significantly after the surgery and recovered to a degree before plateauing and remaining significantly lower than the control right side at all time points. (mean ± SD shown on graph)

Preoperatively there was no significant difference between left and right paw spread. (left 17.5 ± 2.3mm v right 17.6 ± 2.4mm, $p = 0.34$) (Figure 5.7) Left PS significantly reduced one week after T1 ventral root avulsion compared to the right side and the preoperative value (left side 12.1 ±1.4 mm, v right side 17.5 ± 2.1mm, $p<0.05$). The decrease in paw spread was however, significantly less than in the C8 avulsion group. (8.3 ± 1.6mm v 12.1 ± 1.4, $p<0.05$) At all time points the paw spread was significantly lower in the T1 avulsion group ($p<0.05$) compared to the right-side control. Compared

with the C8 avulsion group the paw spread was greater in the T1 avulsion group at all time points and at day 56 the Paw spread in the C8 avulsion and T1 avulsion group was 12.6 ± 2.1mm v 13.9 ± 1.8mm, but this was not a significant difference. (p = 0.48)

5.5.1.3 Paw spread following combined left C8 & T1 avulsion

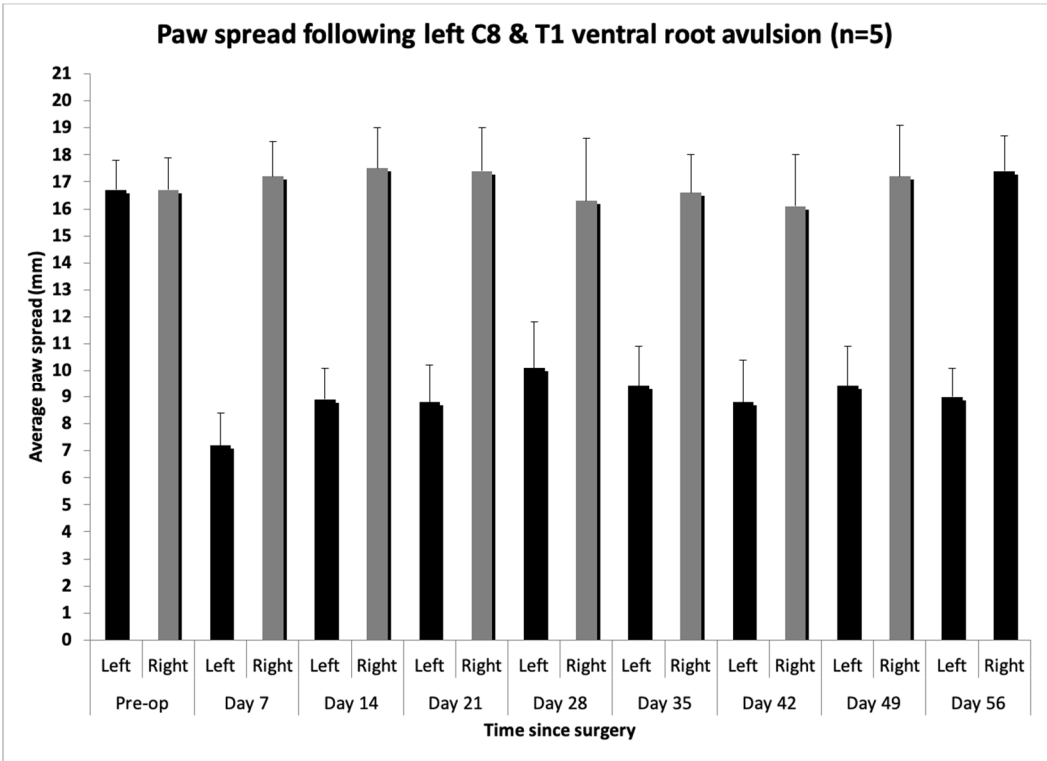

Figure 5.8. Left and right paw spread following combined C8 & T1 ventral root avulsion over a period of 8 weeks. The left paw spread reduced significantly after the surgery and never really recovered before plateauing and remaining significantly lower than the control right side at all time points. At day 56 the combined C8 & T1 avulsion paw spread was statistically lower than on the intact right side. (8.2 ± 1.4mm v 18.1 ± 2.4mm, $p<0.05$) (mean ± SD shown on graph)

Preoperatively there was no significant difference between left and right paw spread. (left 17.5 ±1.9mm v right 17.6 ± 2.3mm, p = 0.39) (Figure 5.8) On day 7 the left paw spread was 8.1 ± 1.5mm which was significantly lower than the intact right paw (17.6 ± 2.3 p <0.05) The paw spread in the combined C8 & T1 avulsion group remained around 8mm at all time points and this was significantly different to the right side control, and on day 56 it remained significantly lower than in the left C8 and left T1 avulsion groups. (p<0.05)

5.5.1.4 Paw spread following C8 ventral root reimplantation

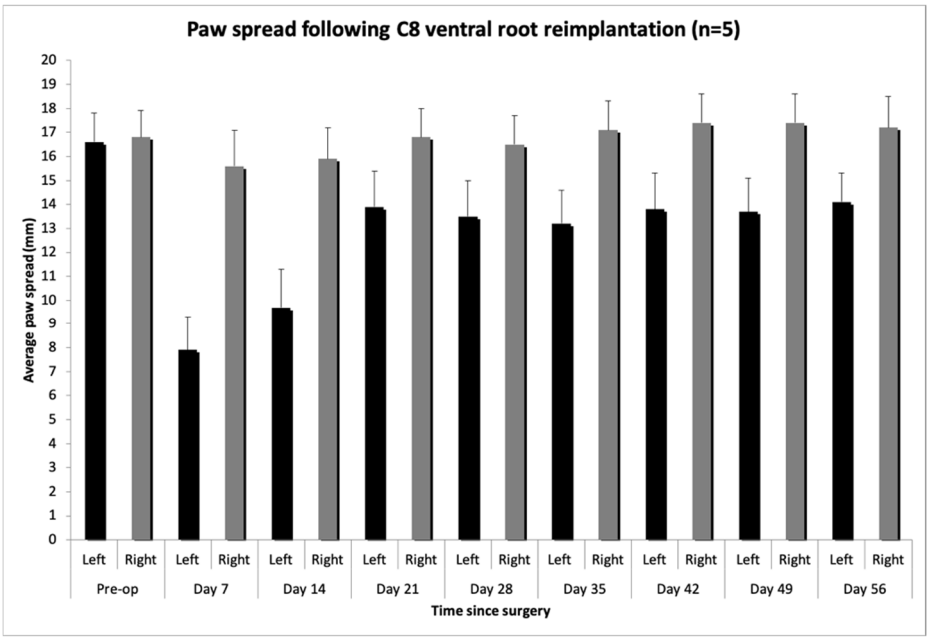

Figure 5.9. Graph showing paw spread following C8 ventral root reimplantation over the eight-week testing period. (mean ± SD shown on graph)

Preoperatively there was no significant difference between left and right paw spread. (left 17.4 ± 2.3mm right 17.3 ± 2.5mm p = 0.40) (Figure 5.9) On day 7 the left paw spread was 7.1 ± 1.5mm which was lower than in the C8 and T1 avulsion groups but

not significantly (p = 0.37) The paw spread in the reimplantation group was significantly lower than in the avulsion group on day 14 and day 21 ($p<0.05$). By day 28 there was no significant difference in paw spread between the C8 avulsion and reimplantation groups (12.3 ± 2.1mm v 13.7 ± 1.5mm, p = 0.47), although there was a trend towards significance. However, over the next 4 weeks the paw spread significantly improved in the C8 reimplantation group and at day 56 it was 14.8 ± 1.7mm compared with 12.6 ± 2.1mm in the avulsion group (p = 0.034). C8 ventral root reimplantation therefore lead to an improvement in paw spread over the 8-week testing period compared to the C8 avulsion group.

5.5.1.5 Paw spread following left T1 ventral root reimplantation

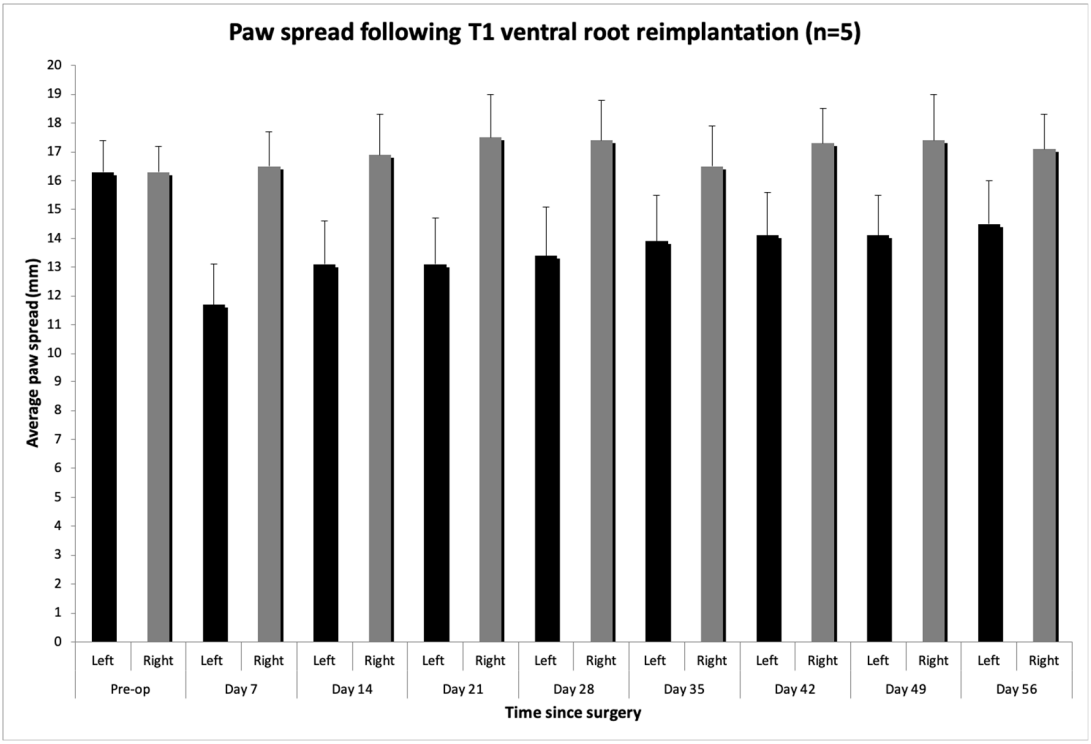

Figure 5.10. Paw spread following T1 ventral root reimplantation over the 56-day testing period. (error bars indicate mean ± SD)

Preoperatively there was no significant difference between left and right paw spread. (left 17.5 ± 2.3mm right 17.4 ± 2.6mm p = 0.40) (Figure 5.10) At day 7 the left paw grip was significantly lower than compared to preoperatively and to the right paw control (11.3 ± 1,8mm v 17.3 ± 2.6mm, p<0.05). The paw spread continued to improve over the next few weeks before reaching a plateau and was 13.8 ± 1.9mm at day 56. In the T1 avulsion group it was 13.9 ± 1.8mm, which was not significantly different (p = 0.29). Thus in the T1 root model the paw spread test did not lead to a significant difference in paw spread in the avulsion and reimplantation groups.

5.5.1.6 Paw spread following C8 & T1 left ventral root reimplantation

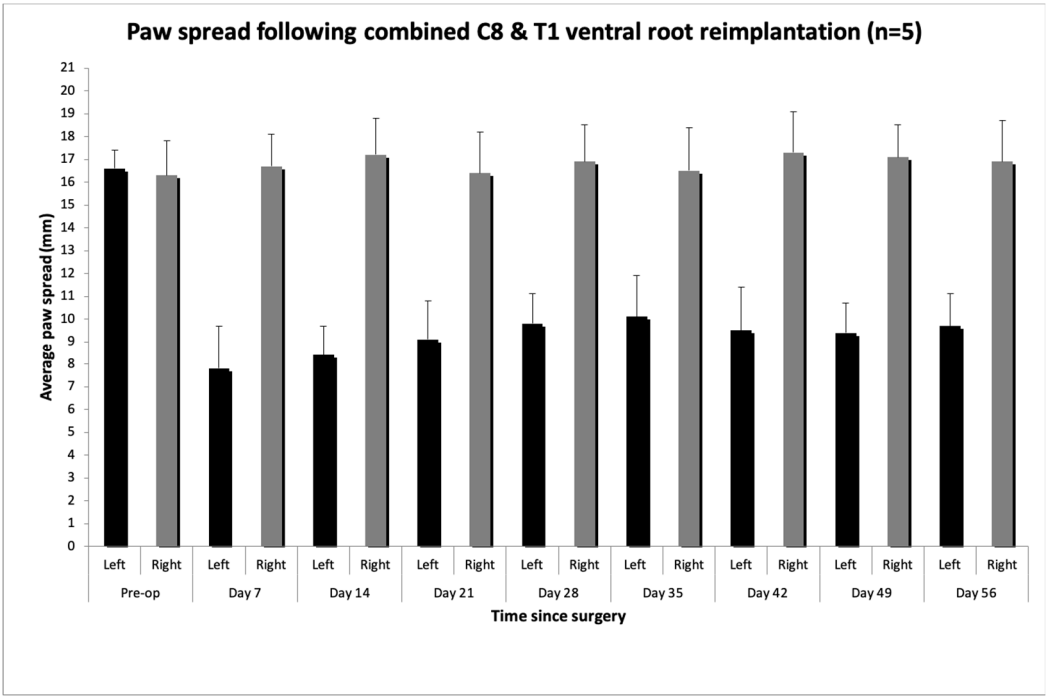

Figure 5.11. Paw spread following C8 & T1 ventral root reimplantation. (Bars indicate standard mean ± SD)

Left paw spread in this group significantly reduced a week after surgery 8.1 ± 2.3mm. (p<0.005) compared with right side control and the left C8 and T1 root models. (Figure

5.11) Paw-spread remained significantly less than controls at all points and did not improve, such that by day 56 it was 8.5 ± 2.1mm in the reimplantation group. This was not statistically significant compared to the combined C8 and T1 avulsion group. However, the paw morphology with two roots operated on was significantly different compared to a single root injury and harder to measure. In addition, these rats demonstrated high rates of paw injury autotomy.

Rat gait paw images showing paw spread in the avulsion and reimplantation groups at Day 56 are shown in Figure 5.12.

Figure 5.12. Forepaw gait analysis at 56-days post-surgery. a) Fore-paw prints following left C8 ventral root avulsion. There is a difference in the morphology of the left paw print on the lesioned side (left, upper paw print) and the paw spread is visibly less than the normal, right side (lower image). b) Fore-paw prints following left C8 ventral root reimplantation. Although there is a difference in morphology of paw spread in the left paw, this is visibly less than in (a) and also compared to the rat's right paw.

5.5.1.7 Intermediate toe spread after ventral root surgery

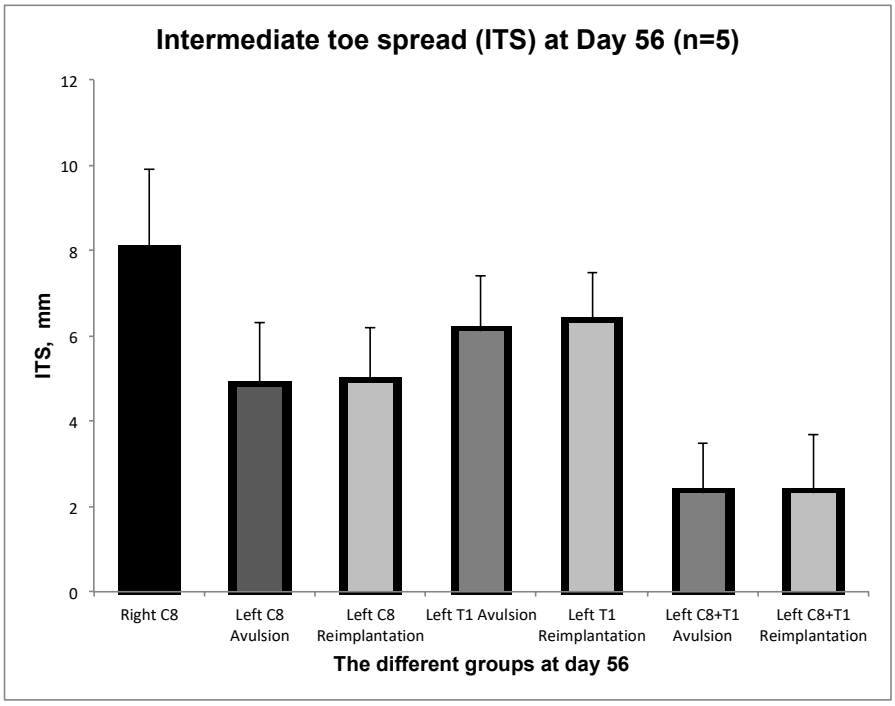

Figure 5.13. Intermediate toe spread (ITS) in the different test groups. Graph showing ITS in the control, right C8, left C8 avulsion and C8 reimplantation, left T1 avulsion and reimplantation and left combined C8 & T1 avulsion and reimplantation groups. (n = 5 in each group)

The differences in intermediate paw spread (ITS) between the groups were small, and in some cases difficult to accurately measure. (Figure 5.13) At day 56, there was a significant reduction in the ITS in the C8 avulsion and the reimplantation groups compared to control (4.8 ± 1.5mm v 4.9 ± 1.6mm, $p<0.05$). However, the difference between the avulsion and reimplantation groups was not significant. ($p = 0.167$) Similarly, there was a significant reduction in the ITS between the T1 avulsion and reimplantation groups compared to control but the difference in between these groups was not significant. (6.1 ± 1.3mm v 6.3 ± 1.2mm, $p = 0.234$) In the groups having bilateral C8 and T1 avulsion and reimplantation the ITS was very small, due to the

paw deformity and could not be accurately measured but was not significantly different in the two groups ($p = 0.39$)

5.5.1.8 Paw angle after ventral root surgery

The differences in paw angle (PA) between the groups were small, and in some cases difficult to accurately measure. At day 56, there was a significant reduction in the PA in the C8 avulsion and the reimplantation groups compared to control (13.4 ± 2.3 degrees v 15.1 ± 3.1 degrees, $p<0.05$). However, the difference in paw angle between the avulsion and reimplantation groups was not significant. ($p = 0.328$) Similarly, there was a significant reduction in the PA between the T1 avulsion and reimplantation groups compared to control but the difference in between these groups was not significant. (16.3 ± 3.1 degrees v 15.4 ± 4.2 degrees, $p = 0.234$) In the groups having bilateral C8 and T1 avulsion and reimplantation the PA was small, partly due to the paw deformity, and could not be accurately measured.

5.5.2 Grip Strength Measurements

Average left paw grip strength and bilateral forepaw grip strength in an intact rat were measured and there was no significant difference in left paw and right paw grip (mean 193.6 ± 17.5g v 201 ± 19.3g , $p=0.38$) and bilateral forepaw grip strength was on average 415.6 ± 37.5g.

5.5.2.1 Grip strength after left C8 ventral root avulsion and root reimplantation

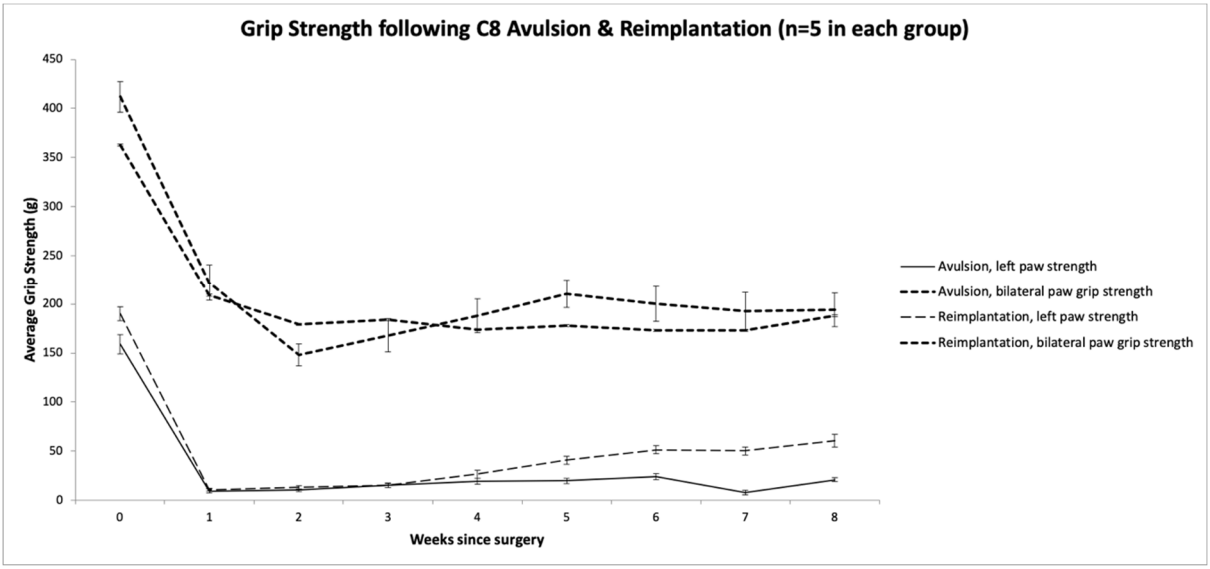

Figure 5.14. Grip strength following C8 ventral root surgery. Graph showing average left paw grip strength (below) and bilateral grip strength (above) following C8 avulsion and reimplantation. (mean ± SD is shown on the graphs)

Following left C8 ventral avulsion surgery the grip strength reduced significantly in the left paw and bilaterally ($p<0.05$) at week 1, compared to baseline. The left grip remained poor for the first three weeks after surgery in the avulsion and reimplantation groups and there was no significant difference at these time points ($p = 0.33$). At 5 weeks left grip strength improved in the reimplantation groups and at 8 weeks there was a significant improvement in the reimplantation group. (20.9 ± 5.1g v 60.5 ± 7.3g, $p<0.05$, $n = 5$) Bilateral grip strength in the C8 avulsion and reimplantation groups was similar at eight weeks (188 ± 13.7g v 194 ± 21.9g, $p=0.19$, $n=5$). (Figure 5.14)

5.5.2.2 Grip strength after left T1 ventral root avulsion and reimplantation

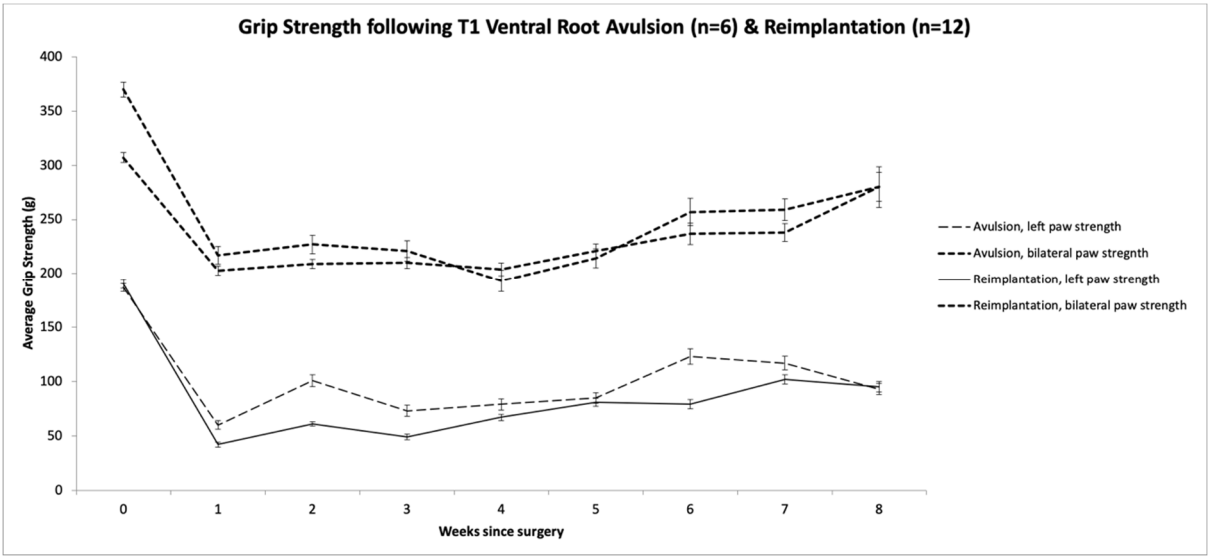

Figure 5.15. Grip strength following T1 ventral root surgery. Graph showing average grip strength following T1 avulsion and reimplantation. Left paw (below) and bilateral paw (above) strength following T1 avulsion and reimplantation are shown. (mean ± SD is shown on the graphs)

After T1 ventral root surgery the grip strength reduced significantly in the left paw and bilaterally ($p<0.05$) compared with preoperatively. (Figure 5.15) At eight weeks the left grip strength in the avulsion and reimplantation groups was not statistically different. (93 ± 5.1g v 95 ± 4.8g, $p = 0.45$, $n = 5$). Bilateral grip strength in the T1 avulsion and reimplantation groups was similar throughout the 8-week testing period and at 8-weeks (280 ± 13.4g v 280 ±1 8.6g, $p = 0.71$, $n = 5$).

5.5.2.3 Grip strength after C8 & T1 ventral root avulsion and reimplantation

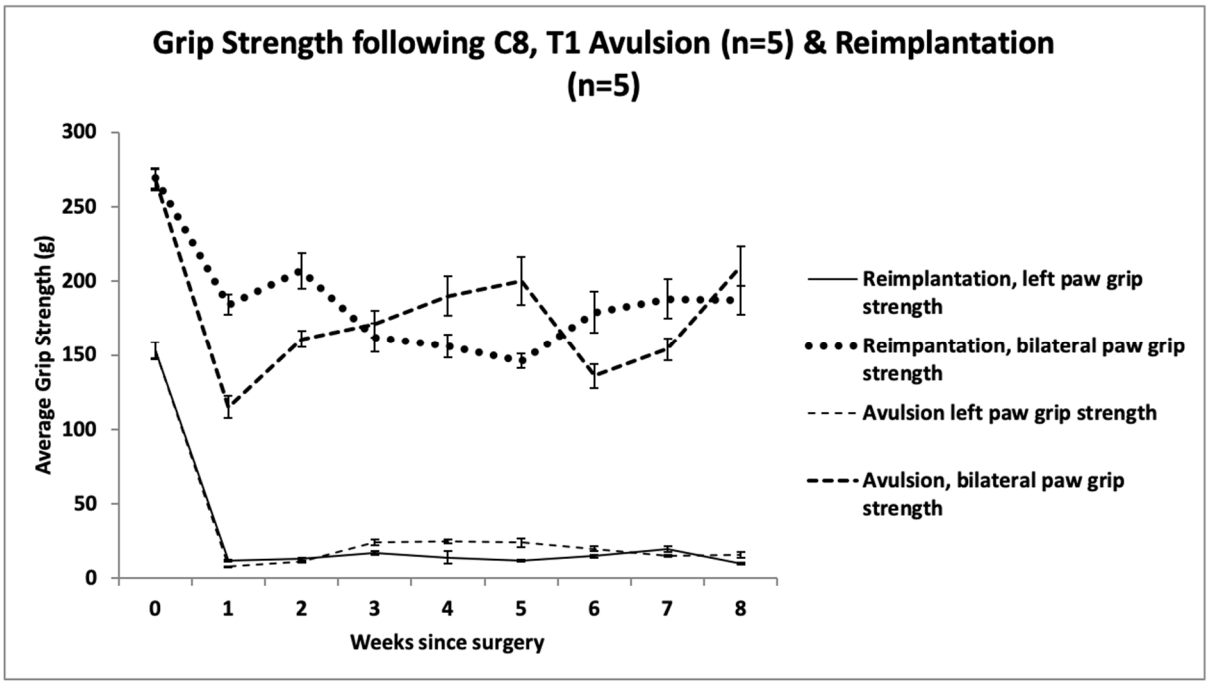

Graph 5.16. Grip strength following combined C8 and T1 ventral root surgery. Graph showing average grip strength following C8 & T1 avulsion and reimplantation. Left paw (below) and bilateral paw (above) strength following C8 & T1 avulsion and reimplantation are shown. (mean ± SD is shown on the graphs).

Following combined left C8 and T1 ventral root surgery the grip strength reduced significantly in the left paw ($p<0.05$) in both the avulsion and reimplantation groups. (Figure 5.16) There was no significant difference between left paw grip strength in the avulsion and reimplantation groups. (16 ± 1.9g v 10 ± 0.8g, $p = 0.13$) Similarly, there was no significant difference in bilateral grip strength in the C8 and T1 avulsion and reimplantation groups. (210 ± 13.2g v 187 ± 9.6g, $p = 0.15$) This test also confirmed that a two-root avulsion/reimplantation model could not be quantified with grip strength tests, because the forepaw injury was such that the animal subjects were not able to make a quantifiable recovery. In addition, rats with two injured nerve roots had a higher

level of autotomy and digit deformities and this likely affected the ability to grip, compared to those with single root lesions.

5.5.3 Cage Walk Faults

By week three there was no difference in cage walk faults in the C8 and T1 groups ($p = 0.31$). In the C8 & T1 combined lesion group there was a difference in that the rats had more faults at all time points. However, this group had a higher degree of autotomy as well.

5.5.3.1 Cage walk faults after C8 ventral root avulsion and reimplantation

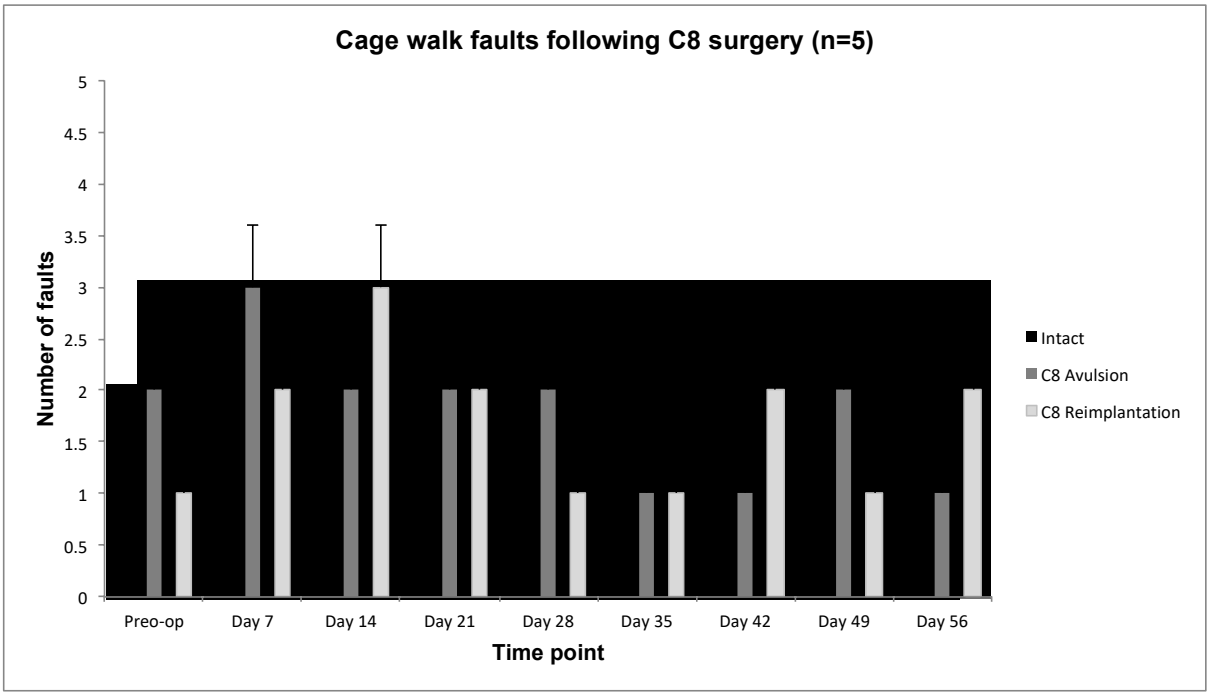

Figure 5.17. Cage walk faults following C8 ventral root surgery. Graph showing number of cage-walk faults in intact, C8 avulsion and C8 ventral root reimplantation groups over the 56-day period (n = 5 in each group)

After C8 ventral root surgery there was no significant difference in cage walk faults between the control, avulsion and reimplantation groups overall. Although the avulsion

and group had more cage faults at days 7 (3 ± 0.7 faults, p = 0.39) compared with control and reimplantation this was not significant. At day 56 in the control, avulsion and reimplantation groups there were 1 ± 0.3, 1 ± 0.3, and 2 ± 0.4 faults, which was not a significant difference between the groups. (p = 0.39) (Figure 5.17)

5.5.3.2 Cage walk faults after T1 ventral root avulsion and reimplantation

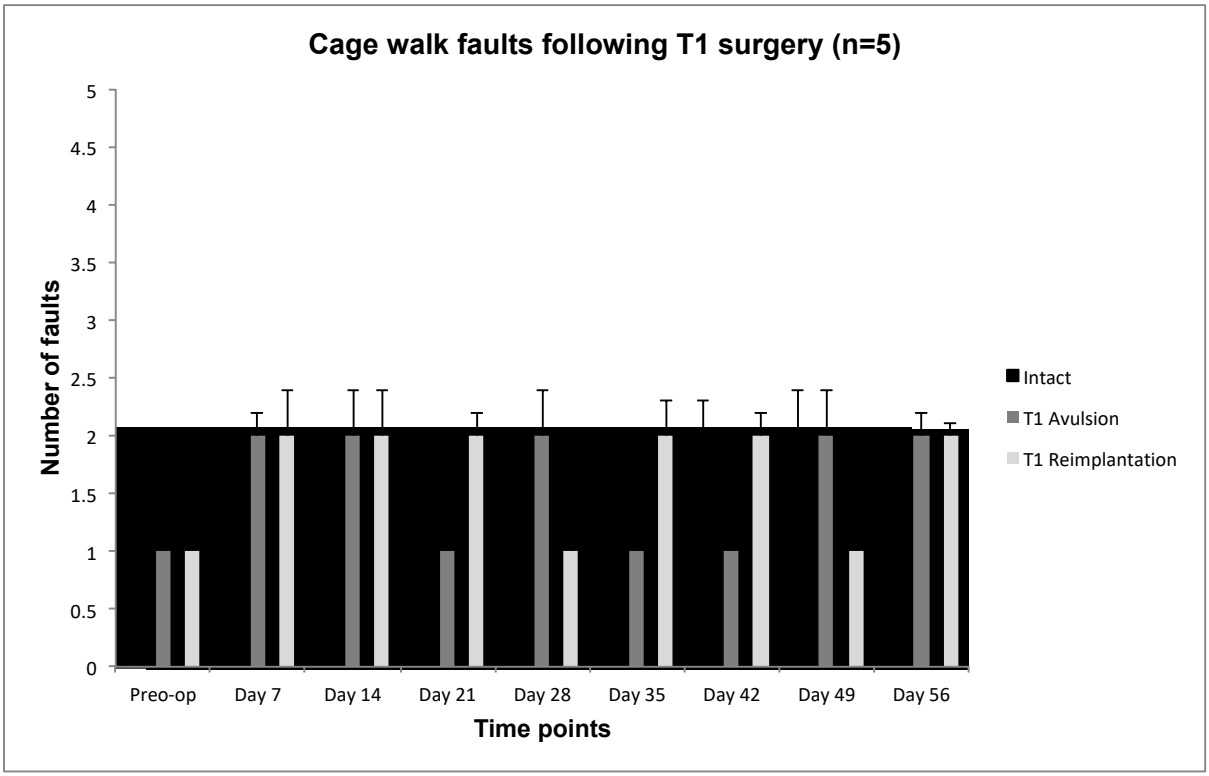

Figure 5.18. Cage walk faults after T1 ventral root surgery. Graph showing number of cage-walk faults in intact, T1 avulsion and T1 ventral root reimplantation groups over the 56-day period (n = 5 in each group)

After T1 ventral root surgery there was no significant difference in cage walk faults between the control, avulsion and reimplantation groups overall. Although the avulsion and reimplantation group had more cage faults at days 7 (2 ± 0.3 and 2 ± 0.4 faults respectively, p = 0.39) there was no statistically significant difference. At all-time points

over 56-day period there was no significant difference between control in the T1 avulsion and reimplantation groups. (Figure 5.18)

5.5.3.3 Cage walk faults after combined C8 & T1 ventral root avulsion and reimplantation

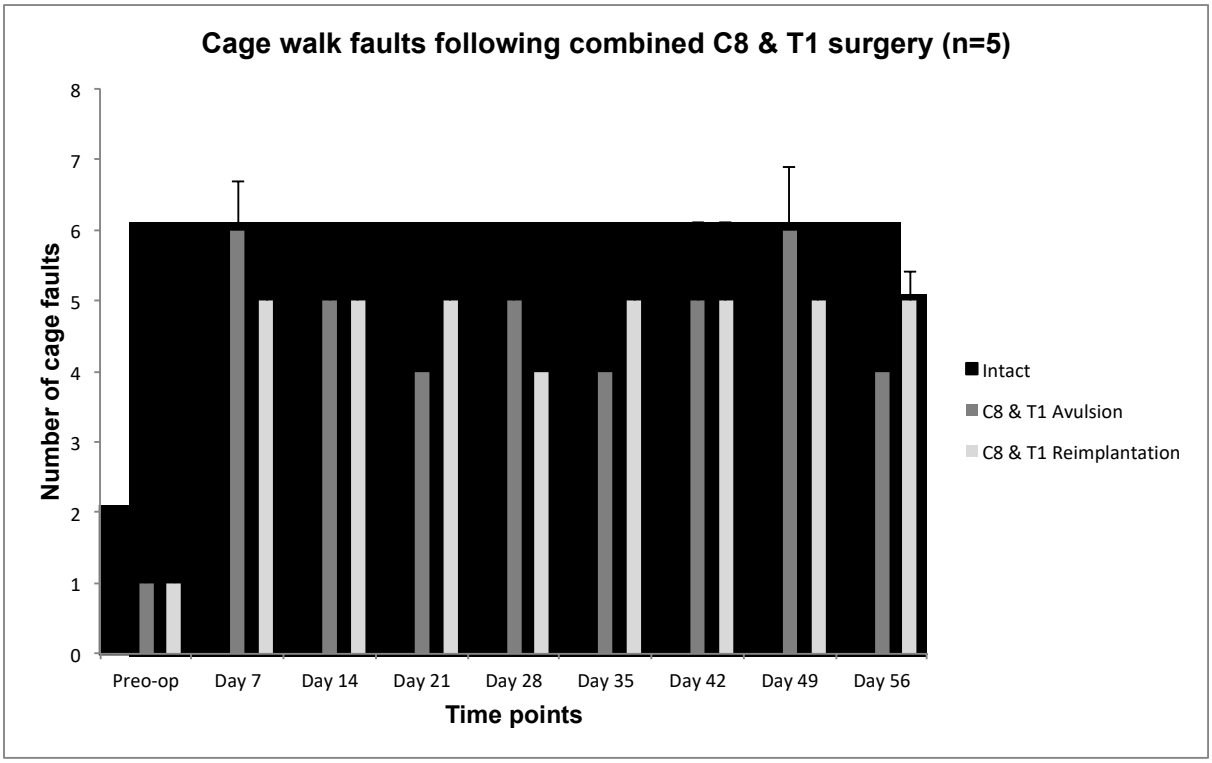

Figure 5.19. Cage walk faults following combined C8 & T1 ventral root surgery. Graph showing number of cage-walk faults in intact, combined C8 &T1 avulsion and C8 & T1 ventral root reimplantation groups, over the 56-day period (n = 5 in each group)

Following combined C8 & T1 surgery there was a significant difference between the number of cage walk faults compared to control (mean 6 ± 0.8 faults in the avulsion and 5 ± 1.1in the reimplantation groups, $p<0.05$). (Figure 5.19) This difference was maintained at all periods over the 56-day testing period. These rats also had a higher rate of autotomy.

5.5.4 Vertical Paw Placing

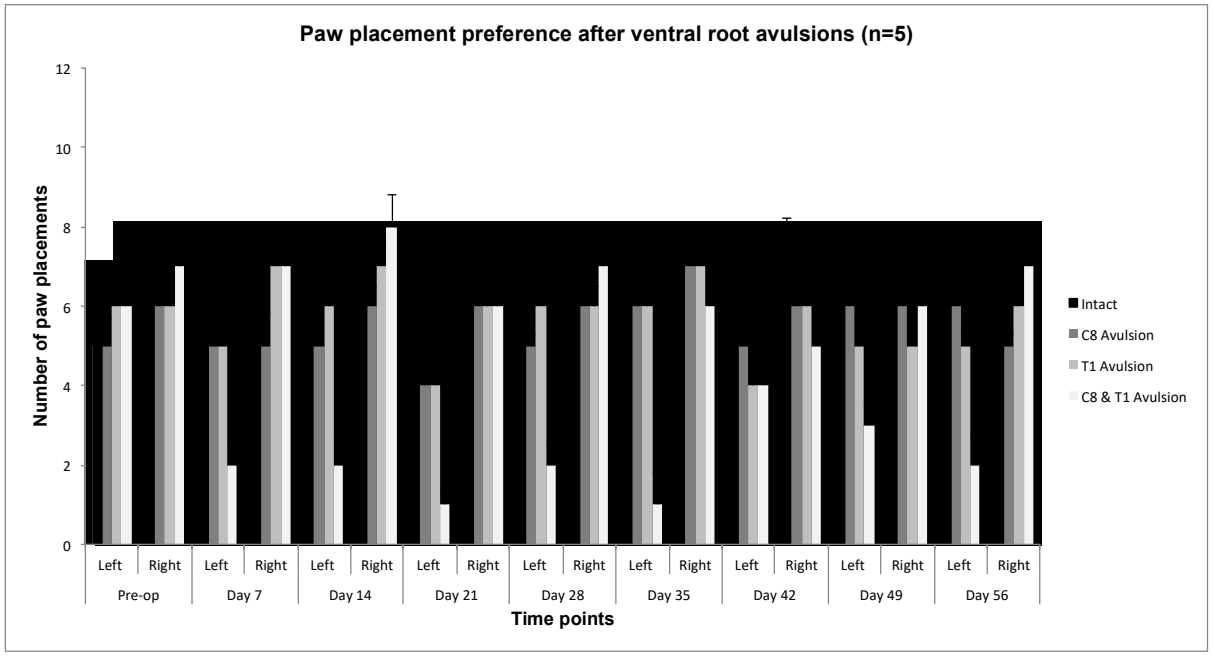

Figure 5.20. Paw placement following ventral root surgery. Graph demonstrating preference of paw placement in the intact rat, after C8 avulsion, T1 avulsion and combined C8 & T1 avulsion. (n = 5 in all groups, mean ± SD shown on graphs)

Preoperatively there was no significant difference in preferential paw placement although there was a tendency for most rats to use the right paw ($p = 0.67$). On days 7 & 14, all rats had a tendency to use the right paw following avulsion surgery although there was no significant difference in paw preference between the right and left paws in the C8 and T1 avulsion groups. ($p = 0.67$). However, there was a significant difference in preferential paw placement in the combined left C8 & T1 avulsion group, who preferred to use the right paw ($p<0.05$). At all other time points there was no significant different in the paw placement in the C8 and T1 avulsion groups. At all other time points in the combined left C8 & T1 avulsion model all rats preferably used the right paw and this was significantly different at all time points ($p<0.05$). (Figure 5.20)

5.5.5 Discussion

We have conducted a number of tests to try to establish the most suitable functional tests for our brachial plexus repair model.

Gait analysis enabled us to identify a number of demonstrable differences following ventral root avulsion and reimplantation. Over the 8-week testing period there was a statistically significant difference between paw spread in the C8 avulsion and reimplantation groups at a number of time points, which persisted to the final testing period. The paw spread in the reimplantation group improved significantly compared to the avulsion group from week five onwards but did not return to baseline at the final time point. However, paw spread differences between the T1 avulsion and reimplantation groups were not statistically significant. We felt that a T1 nerve root injury would not be suitable to analyse paw spread for our ventral root repair model. The groups where both C8 and T1 ventral nerve roots were either avulsed or reimplanted had significant paw deformity, which meant that the paw spread could not be quantified. Furthermore, the paw spread in these groups was morphologically different compared to a single root surgery and these rats had high rates of autotomy compared with rats having single root surgeries.

For the intermediate toe spread, measurements were significantly lower in both avulsion and reimplantation groups compared to control but there was no significant difference in ITS between the C8 and T1 avulsion and reimplantation groups ($p = 0.167$ and $p = 0.234$). The combined C8 & T1 surgery resulted in a greater reduction in ITS compared to the single levels but there was no significant difference between the avulsion and reimplantation groups. Similarly for the paw angles, the single level avulsions and reimplantation resulted in a significant reduction in paw angle compared

to control but there was no difference at any time point and the final time point in the C8 ($p = 0.328$) & T1 ($p = 0.234$) avulsion and reimplantation groups. Similar to the ITS, in the combined C8 & T1 groups there was a significant reduction in PA compared to control, but these groups had more deformity and the paw angles were difficult to measure.

From these preliminary studies we felt that paw spread in the left C8 avulsion and reimplantation groups gave us a quantifiable difference. The paw spread improved in the C8 reimplantation groups compared with the avulsion group. The ITS and PA were not useful as an outcome measure.

The grip strength results demonstrate that there is a significant difference in left paw grip strength with C8 ventral root avulsion and this difference improved in the C8 ventral root reimplantation. In both groups the difference between them at several time points and at the final timepoint was significant. The T1 ventral root model did not lead to a significant decrease in grip strength difference at day 56, between the avulsion and reimplantation groups. The combined C8 & T1 models showed no significant difference in left paw grip strength between the avulsion and reimplantation groups but were associated with high rates of paw deformity, difficulty in grasping and autotomy.

Paw grip is supplied predominantly by the median nerve. In the rat the T1 root provides a smaller component to the median nerve and a larger component to the ulnar nerve. (Greene, 1968) The left paw grip in the avulsion and reimplantation groups did fall significantly compared to baseline following T1 avulsion and reimplantation but it was greater than in the C8 avulsion group. On this evidence there is likely to be a T1 component to the paw flexors. Given the fact that T1 reimplantation had no significant

improvement in paw grip we felt that the left T1 ventral root model with regards to grip testing would not be an ideal functional test for our brachial plexus repair model.

Cage walk fault testing is a sign for both motor and sensory system preservation following cervical root surgery. (Metz et al., 2000) However, previous studies have shown that at least four dorsal roots need to be avulsed in order for sensorimotor function to be impaired in the rat forepaw. (Ibrahim et al., 2009b) Our studies demonstrated that avulsion of a single dorsal and motor root had no significant impact on cage walk faults. Avulsion of two dorsal and ventral roots lead to a significant increase in the number of faults but this was not improved by reimplantation. On the basis of this assessment we concluded that cage walk faults were not a suitable functional test for our brachial plexus avulsion model. Similarly, a single C8 or T1 ventral root avulsion had no impact on preferential paw placement pre- and post-surgery in our model. In the combined C8 & T1 group there was a significant difference. Based on this and other functional studies we felt that preferential paw placement would not be a suitable test for our brachial plexus avulsion model.

5.6 Conclusion

From these experiments we concluded that paw spread and grip strength following surgery and repair at the C8 level were the most suitable functional tests to assess outcomes for our brachial plexus repair model.

CHAPTER SIX

CHAPTER 6: OLFACTORY ENSHEATHING CELLS FOR CENTRAL NERVOUS SYSTEM REPAIR: USING THE VENTRAL ROOT MODEL FOR INTRASPINAL BRACHIAL PLEXUS REPAIR

6.1 Introduction

Brachial plexus injuries occurring at the CNS-PNS junction are often referred to as a longitudinal spinal cord injury. (Carlstedt, 2007) Such injuries can lead to substantial motor neurone death and cause significant neurological impairment, pain and

morbidity. Spontaneous recovery after such injuries is unlikely and this has led to a number of experimental treatments in patients. The commonest surgical treatments for brachial plexus repair include nerve transfers using extraplexal donor nerves, which lead to functional recovery of proximal arm muscles but not hand function. (Seddon, 1963, Songcharoen et al., 1996, Songcharoen et al., 2001, Gu and Ma, 1996, Waikakul et al., 1999, Friedman et al., 1990, Samardzic et al., 2000, El-Gammal and Fathi, 2002, Samii et al., 2003, Bertelli and Ghizoni, 2003, Midha, 2004, Malessy et al., 2004, Bertelli and Ghizoni, 2007) In order to attempt a more effective treatment, Carlstedt et al. described an intradural ventral root reimplantation. (Carlstedt and Noren, 1995, Carlstedt et al., 1995, Carlstedt et al., 2000) It is postulated that reimplantation leads to improved motor neurone survival and regrowth of axons through the spinal cord which in theory can make contact and innervate target muscles. Some of the adult patients in these studies showed good recovery of proximal muscle function and relief of neuropathic pain but return of hand function was only reported in one pre-adolescent patient. (Carlstedt et al., 2004, Htut et al., 2006)

Following on from groundbreaking work by Tello, Ramón y Cajal, and David and Aguayo, a number of preclinical studies in the last two decades have attempted to identify cellular therapies for CNS repair and regeneration. (David and Aguayo, 1981, Ramon Y Cajal, 1928, Tello, 1911a) Schwann cells, neural stem/progenitor cells (NSPCs), and neural and glial restricted precursors have been extensively studied. (Bray et al., 1987, Li and Raisman, 1994, Barakat et al., 2005, Takami et al., 2002, Cao et al., 2005, Iwanami et al., 2005, Karimi-Abdolrezaee et al., 2006, Parr et al., 2007) Over the last two decades OECs have become popular as an experimental cell for spinal cord repair and regeneration.

OECs, which are found in the mammalian nasal mucosa and olfactory bulb, are found in the PNS, continuously regenerate in adult life and are intimately associated with astrocytes in the CNS. (Doucette, 1991, Raisman, 1985, Franssen et al., 2007) A number of investigators therefore explored the possibility of using them as a cellular strategy to promote axonal regeneration in damaged spinal cords of adult rats. (Boyd et al., 2003, Bunge, 2001, Franklin and Barnett, 2000, Raisman, 2001, Ramon-Cueto and Valverde, 1995, Richter and Roskams, 2008, Ruitenberg et al., 2006) In animal models OECs have been shown to promote axonal growth, promote neuroprotection and less glial scar formation, and interact with astrocytes and remyelinate of axons. (King-Robson, 2011, Ramon-Cueto and Nieto-Sampedro, 1994, Lakatos et al., 2003, Devon and Doucette, 1992) Reimplantation of avulsed ventral roots into the spinal cord has demonstrated that axons can grow into the reimplanted ventral roots. (Carlstedt et al., 1986) OECs reimplanted into lumbosacral ventral root repairs have been shown to increase the number of axons entering the reimplanted roots. (Bigbee et al., 2007) Thus in theory OEC transplantation could lead to improved outcomes for intraspinal ventral root reimplantation after avulsion injury.

However, despite these encouraging studies a number of controversies regarding OECs exist including the source of OECs, culture and isolation methods, composition of cultured cells and technique of application. (Li et al., 2005, Novikova et al., 2011, Raisman et al., 2011, Ibrahim et al., 2009a, Ramon-Cueto and Nieto-Sampedro, 1994) Controversy also remains as to whether mucosal or bulb OECs should be used for spinal cord repair and regeneration. Studies have shown that mucosal OECs reduced the size of the glial scar, spinal cord cavitation and promote growth of motor and sensory axons through the lesion site. However, they do not survive for long periods or migrate long distances. (Ramer et al., 2004) Bulb OECs have been shown to

promote axonal growth through the lesion site, restore spinal reflexes and improve locomotor function. (Lu et al., 2001, Lu et al., 2002) Although mucosal OECs have the potential advantage of ease of access in humans compared with bulb OECs for human transplants, human clinical studies using OECs for spinal cord repair have their own controversies (see Chapter 1). (Huang et al., 2003a, Feron et al., 2005, Lima et al., 2006, Tabakow et al., 2014)

In previous chapters we developed a C8 ventral root model in a rat, including histological, immunohistochemistry and functional tests. We have also assessed the continuity of axonal projections across the repair site using Fast Blue® retrograde tracers. In this chapter we will augment the C8 ventral root repair model with mucosal and bulb OECs to assess the effect on recovery.

6.2 Materials & Methods

In this chapter eight primary techniques were used: microsurgery, cell culture, histology, immunohistochemistry, retrograde labelling of axonal tracts, light & fluorescence microscopy and functional testing.

All the work performed in this chapter was approved by the Animal Welfare Ethical Review Body (AWERB). All experiments in this study were conducted in accordance with the UK's Animals (Scientific Procedures) Act 1986 with ethical approval from Institute of Neurology, University College London. We followed the ARRIVE Guidelines when conducting these experiments.

In an earlier chapter (see Chapter 2), we developed our microsurgical technique to perform a consistent and reproducible C8 ventral root surgery in a rat and a number of tests to assess the efficacy of the surgery. (Oprych et al., 2015) In a series of

experiments in this chapter, the left C8 cervical ventral roots were either avulsed or reimplanted on the dorsolateral surface of the spinal cord and in other groups this reimplantation was augmented with either mucosal or bulb OECs to assess their efficacy for repair and regeneration. Histology with haematoxylin and eosin (H&E) and immunohistochemistry with GFAP and NF were used to assess nerve repair and regeneration at the surgery site. (Bignami et al., 1972, Schlaepfer and Lynch, 1977, Harris, 1900) Retrograde tracer Fast Blue® was used to assess continuity of motor neurone axons across the repair site and survival of motor neurone cell bodies in the spinal cord. (see Chapter 4) Gait analysis and grip strength testing were functional tests deployed to quantify the C8 ventral root injury and repair in the different study groups. (Meyer et al., 1979, Anderson et al., 2005, de Medinaceli et al., 1982) (see Chapter 5) Statistical tests were carried out using SPSS Statistics 22.0. (IBM, Armonk, NY, USA) Before the final study was conducted sample size was calculated based on provisional results from previous chapters.

6.2.1 Sample size calculations for the rat brachial plexus ventral root repair model

Our primary outcomes to assess the rat brachial plexus ventral repair model are paw spread, grip strength and retrograde labelling of motor neurones in the spinal cord. It is important to give considered thought to the design of animal studies because if experimental numbers are too small, the study may fail to detect scientifically important results or if it too large it may lead to an unnecessary use of animals and resources. (Fitts, 2011) A power analysis is therefore a useful step to estimate the sample size of the study. In order to ensure that the work conducted in the remainder of this chapter was performed effectively, efficiently and humanely we proceeded to calculate the

sample size by using data obtained in our previously conducted functional and retrograde labelling studies.

In our power analysis two groups were being compared, namely the C8 avulsion and the C8 reimplantation. The calculation of sample size depends on knowledge of number of variables, namely the effect size, standard deviation, the significance level, chosen power, alternative hypothesis and sample size. (Festing and Altman, 2002)

The effect size is a measure of the differences of the means in these two groups. Standard deviation measures the variance between the means and samples with a low standard deviation have a low variance and will therefore need a smaller sample size. Conversely a large variance will require a larger sample size. The significance level is usually set at an arbitrary value of 5% and denotes a Type I error; this is the chance of obtaining a false positive result due to a sampling error. It is the therefore the cut-off value below which the null hypothesis will be rejected. The power of an experiment is the likelihood it will detect the specified effect size for the given significance level and standard deviation. Choice of a power level is arbitrary and can range from 80-95% in animal studies. 1- power is the likelihood that a false-negative result can occur, referred to as a Type II error. (Petrie, 2009)

6.2.2 Type of power analyses

The three main types of power to consider when powering an animal study include priori, post-hoc and sensitivity. A priori power analysis is done when a study is being planned and can give you a basic idea of sample size when basic statistics are available. Post-hoc power analyses are carried out after the study has been concluded. These are also useful in that the expected and the actual effect may be

different. A sensitivity power analysis is used when for instance, the sample size is limited for other reasons, such as cost or availability of animal subjects. (Petrie, 2009)

6.2.3 Calculating the sample size

There are two main methods of calculating sample size in animal studies. The most scientific method is by performing a power analysis. (Festing and Altman, 2002, Jones et al., 2003, Festing, 2006) Alternatively less accurate calculations can be performed using simple formulas. (Charan and Kantharia, 2013)

Sample size can be calculated from statistical software packages such as G Power. (Faul et al., 2007) This calculates power based on Cohen's principles. (Cohen, 1998) SPSS allows you to calculate observed and post-hoc power, so we elected to use G Power for our brachial plexus ventral root study. From our previous studies we found that 20 of the animals in the preliminary study groups had to be culled, so the sample size calculation was corrected for attrition rate with the following formula: (Charan and Kantharia, 2013)

Corrected sample size = sample size/(1 – (% attrition/100))

6.2.4 Power calculations based on paw spread

Power calculations for paw spread were based on provisional data from functional studies performed in Chapter 5. With the α value set at 0.05 and the mean and standard deviations for paw spread entered into G Power in a one tailed T-test we determined that for a power of 80% and 90% we would need sample sizes of 12 and 16 respectively. Our functional studies showed an attrition rate of twenty percent. For

or an 80% and 90% power we would therefore need to have an adjusted sample size of 16 and 20 respectively in each of the experimental groups to adequately power the study. (Figure 6.1)

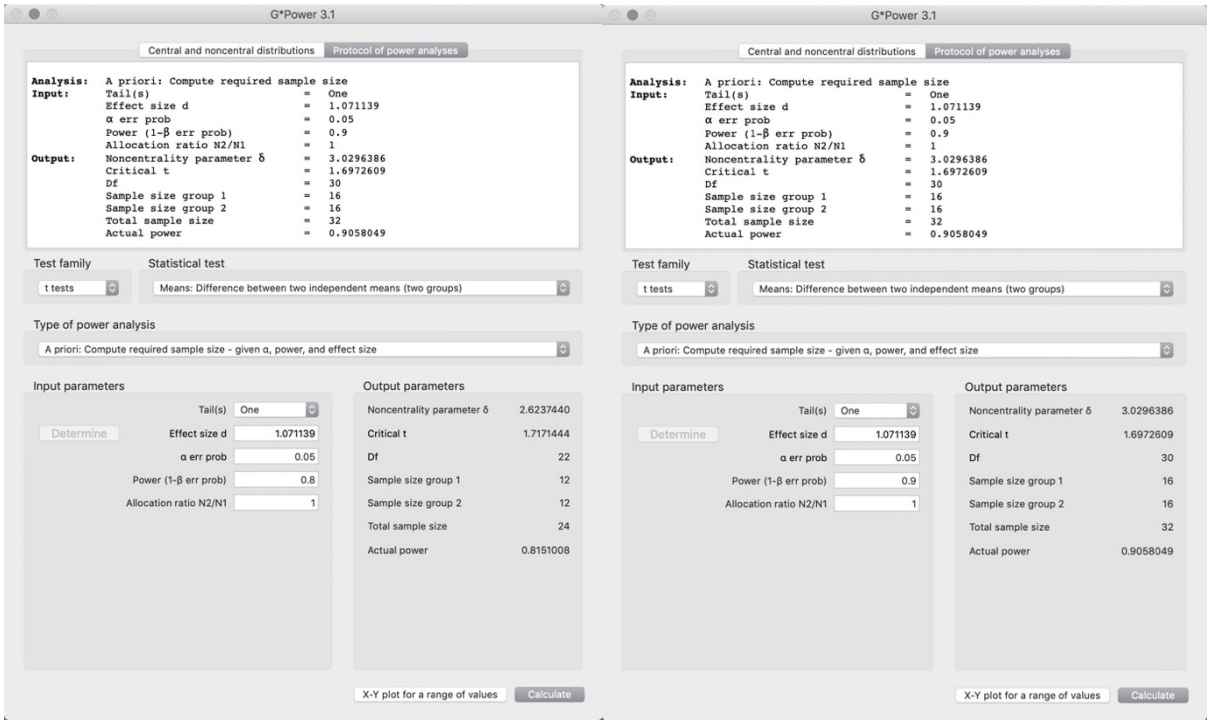

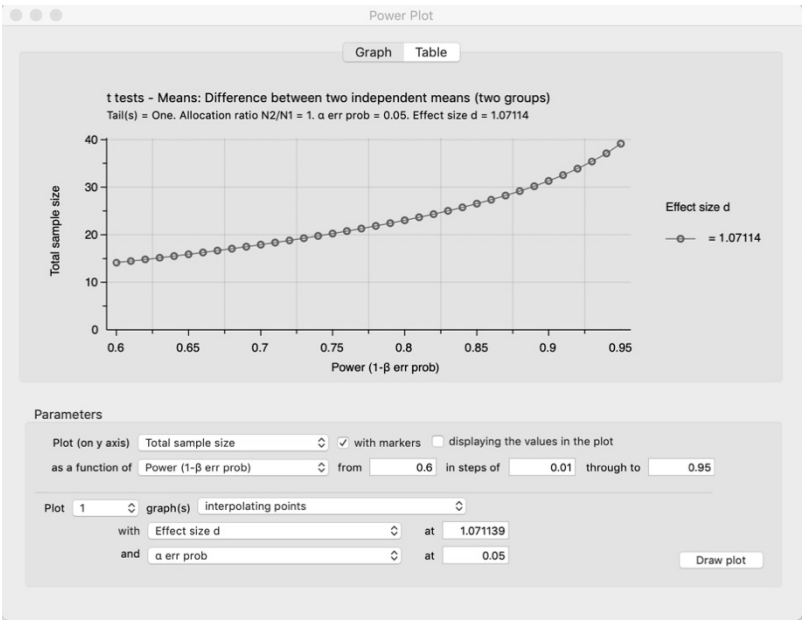

Figure 6.1. Power calculations based on paw spread. Outputs from G Power for paw spread, when the power is arbitrarily set at 80 and 90%. Graph depicts higher sample size as the power of the study increases, thus reducing the Type II error.

6.2.5 Power calculations based on left paw grip strength

Power calculations for left grip strength were based on provisional results from functional studies performed in Chapter 5. With the α value set at 0.05 and the mean and standard deviations for paw spread entered into G Power in a one tailed T-test we determined that for a power of 80% and 90% we would need sample sizes of 11 and 15 respectively to compare the avulsion and reimplantation models. Our functional studies showed an attrition rate of twenty percent. For or an 80% and 90% power we would therefore need to have an adjusted sample size of 13.75 and 18.75 respectively in each of the experimental groups to adequately power the study. (Figure 6.2)

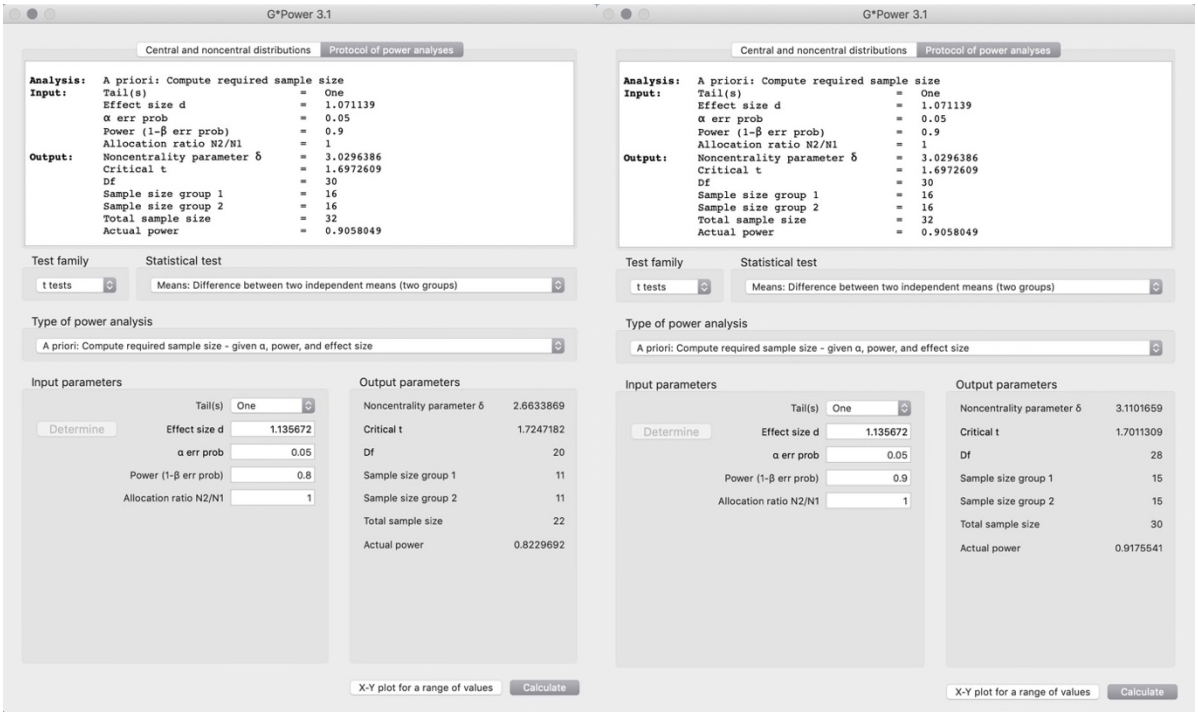

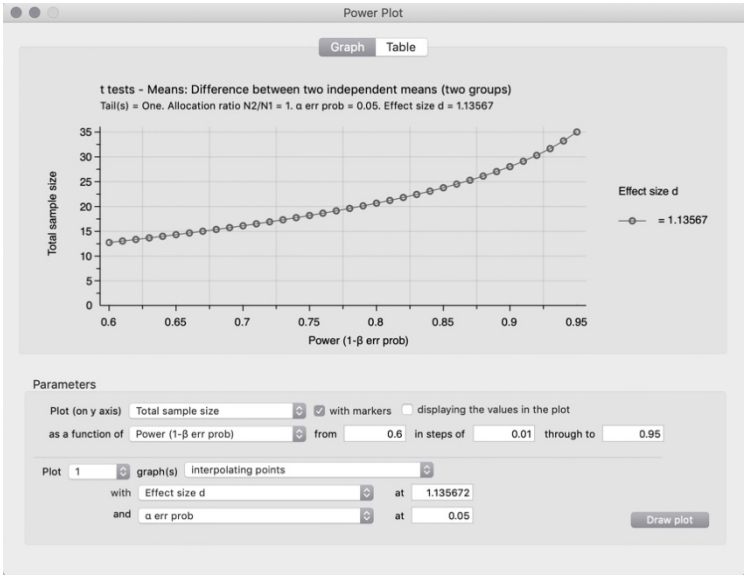

Figure 6.2. Power calculations based on grip strength. Outputs from G-Power for left paw grip strength, when the power is arbitrarily set at 80 and 90%. Graph depicts higher sample size as the power of the study increases, thus reducing the Type II error.

6.2.6 Power calculations based on labelling with retrograde tracers

Power calculations for left grip strength were based on results from the tracer studies performed in Chapter 4. With the α value set at 0.05 and the mean and standard deviations for paw spread entered into G Power in a one tailed T-test we determined that for a power of 80% and 90% we would need sample sizes of 11 and 15 respectively to compare the avulsion and reimplantation models. Our functional studies showed an attrition rate of twenty percent. For or an 80% and 90% power we would therefore need to have an adjusted sample size of 13.75 and 18.75 respectively in each of the experimental groups to adequately power the study. (Figure 6.3)

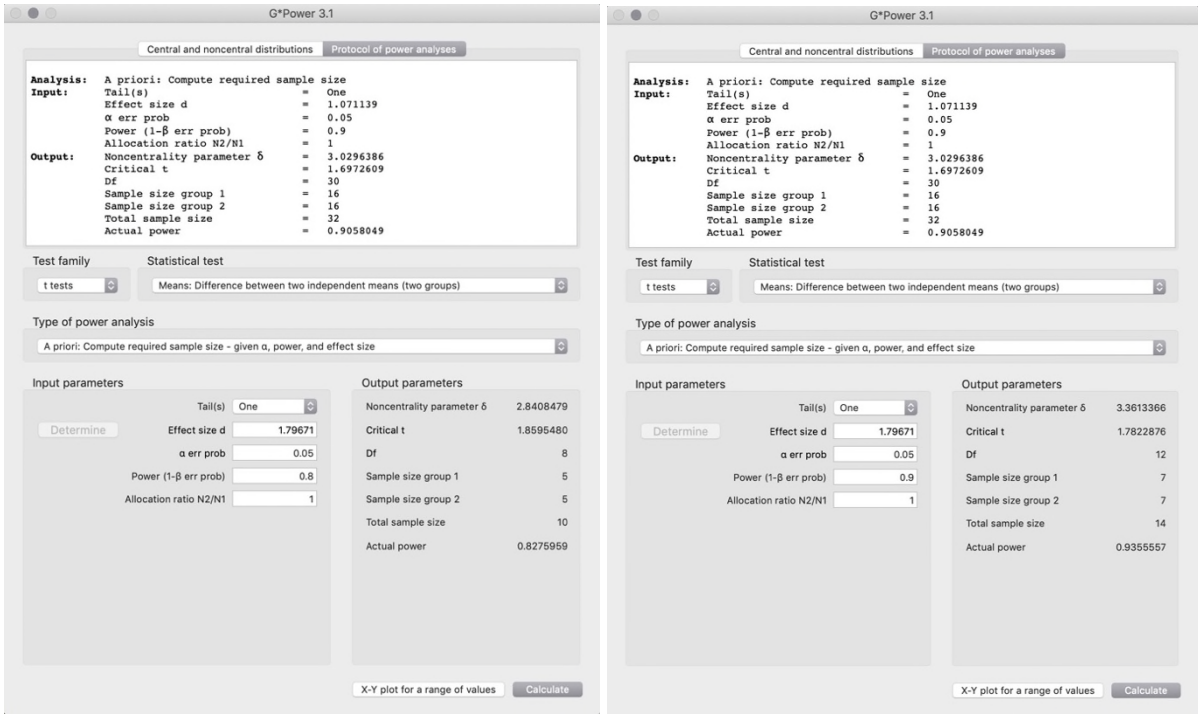

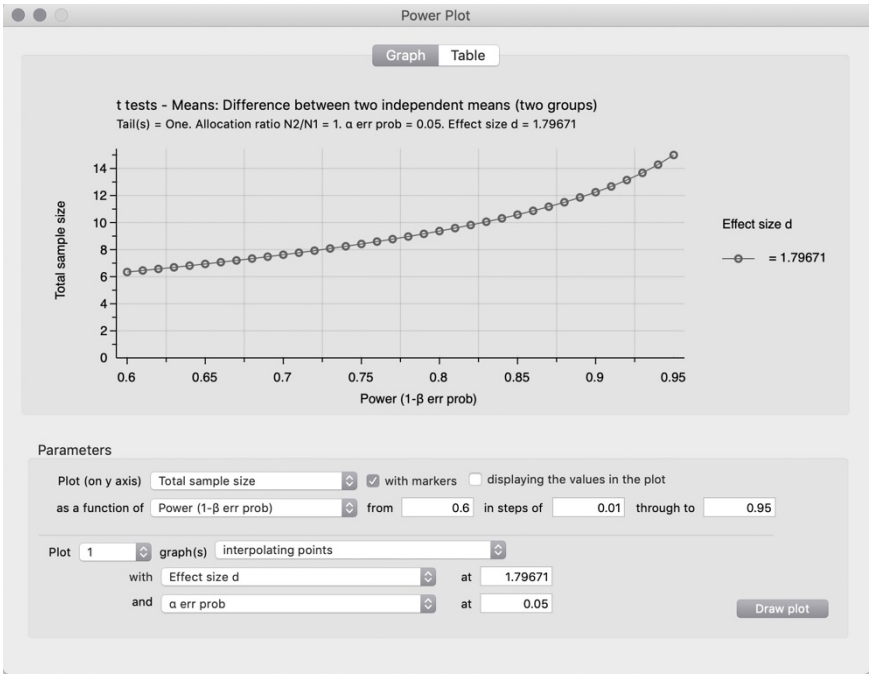

Figure 6.3. Power calculations based on retrograde tracers. Outputs from G Power for Fast Blue® tracer labelling, when the power is arbitrarily set at 80 and 90%. Graph depicts higher sample size as the power of the study increases, thus reducing the Type II error.

6.2.7 Power calculations for the brachial plexus repair model

For paw spread, with a p value of <0.05, the effect size if 1.07, there was a 90% chance of detecting a significant difference with a sample size of 20 rats per group. For the left paw grip and retrograde tracers, the effect size was greater, so lower numbers were required to power the study. Based on the adjusted power calculations for attrition rates, we concluded that a sample size of 20 rats per group would give us enough power to detect a significant difference for our brachial plexus repair model, without underpowering the study or causing unnecessary harm by using excess animals.

6.2.8 Experimental study groups

Four experimental groups were utilised for this study. The first group was the control and comprised of 20 rats undergoing a C8 ventral root avulsion. (ASD, n = 20)) The second group comprised the C8 ventral root reimplantation group, where the C8 ventral root was avulsed and reimplanted into the dorsolateral aspect of the spinal cord. (RSD, n = 20) Group 3 comprised rats who underwent a C8 ventral root reimplantation which was augmented with autologous mucosal OECs (MSD, n = 20) and Group 4 was made up by rats having a reimplantation augmented with bulb OECs (BSD, n = 20).

6.2.9 Animal Subjects

All experiments in this study were conducted in accordance with the UK's Animals (Scientific Procedures) Act 1986 with ethical approval from Institute of Neurology, University College London. Rats were all locally bred isogenic and phenotypically identical adult female Sprague-Dawley's (SD) weighing 200-250g at the start of the experiments. Throughout the experiments the rats had unrestricted access to food and water. Appropriate measures were taken to minimise pain and discomfort and experiments were terminated if the animal subjects developed pain, self-harm or autotomy.

6.2.10 Inhalational Anaesthesia

Isoflurane inhalational anaesthetic was used to deliver and maintain anaesthesia for all surgeries. (IsoFlo®, Abbott Laboratories Ltd, UK) Anaesthetic was delivered via a facemask from a pre-calibrated anaesthetic machine at a rate of 1.5 to 2.5L/min. The

anaesthetic facemask and the rat were held in place by a custom-made plasticine frame (see Chapter 2).

6.2.11 Surgery for avulsion and reimplantation of the C8 ventral root and addition of OECs

Under inhalational anaesthesia and using an operating microscope (Carl Zeiss Ltd, Cambridge, UK) all rats in the 4 groups underwent a posterior cervical approach to the spinal cord. (as describe in detail in Chapter 2, (Oprych et al., 2015)) In Group 1 (ASD, n = 20) the C8 ventral root was avulsed and placed on the dorsolateral aspect of the spinal cord and a millilitre of Tisseel® was applied to keep the nerve in position. In Group 2 (RSD, n = 20) the C8 ventral root was avulsed and inserted into the dorsolateral aspect of the spinal cord after a careful pial opening, and a millilitre of Tisseel® was applied to keep the nerve in position. In Group 3 (MSD, n = 20) we performed the same procedure as in Group 2 but the repair was augmented with mucosal OEC and in Group 4 (BSD, n = 4) bulb OECs were applied using the technique described below.

6.2.12 Olfactory Ensheathing Cell culture

Olfactory tissue from adult female SD rats (200-250g) was used for bulb and mucosal cultures. Surgical instruments used for dissection were sterilised by autoclaving by heating for 20 minutes at 120^0C, and the laminar flow hood where the cells were prepared was cleaned with 70% ethanol.

6.2.13 Olfactory mucosa & bulb cultures

Growing medium specific for mucosal OECs (DFF10; Dulbeccos' Modified Eagle Medium with F12 Nutrient (DMEM/F12) with 10% Foetal Calf Serum) is prepared. Rats

were placed under terminal anaesthesia with CO_2 and decapitated. The skin is removed, and muscle excised down to bone. The nasal septum is dissected and placed in ice-cold Hank's Balanced Salt Solution (HBSS). The olfactory mucosa covering the posterior nasal septum is identified by its yellow colour and separated from the anterior respiratory epithelial mucosa, which is discarded. Following two washes in HBSS, the tissue is incubated at 37°C in 2.4µl/ml dispase II solution for 30 min. The superficial layers of the olfactory epithelium become crinkled and are easily peeled away from the lamina propria. The lamina propria, which contains the OECs and ONFs associated with the olfactory nerves, is washed in HBSS and incubated at 37°C for 30 min in 0.05% collagenase and dispase in HBSS. Trituration in DFF10 yields a cell suspension, which is centrifuged at 250g for 5 minutes. The cells are re-suspended in DFF10 and plated on uncoated 35mm dishes. The following day the supernatant is removed and plated on poly-L-lysine coated 35mm dishes and maintained in minimal volume of culture medium. The dishes are incubated at 37^0C in an atmosphere containing 5% CO_2. At day 5, the medium is replaced with fresh warm DFF10 and replaced thereafter every 2-3 days for the next 12-14 days. When the cells are ready for transplantation they have a concentration of $2.5x10^4$ cells/µl. (See Appendix 7)

Growing medium specific for bulb OECs (DFF10; Dulbeccos' Modified Eagle Medium with F12 Nutrient (DMEM/F12) with 10% Foetal Calf Serum was prepared. Rats are placed under terminal anaesthesia with CO_2 and decapitated. The skin is removed, and muscle excised down to bone. The nasal bones are cut anteriorly, and the skull opened posteriorly, and olfactory bulbs carefully removed and transferred to a dish containing Hanks Balanced Salt Solution. Under the dissecting microscope remnants of adherent meningeal membranes are removed. The outer nerve and glomerular layers of the olfactory bulb are excised. The tissue is dissociated in 0.1% Trypsin at 37^0C for 15 minutes. After trypsinization excess volume of DFF10 is added and partly removed to leave a small suspension. Deoxyribonuclease I is added and the suspension triturated. More DFF10 is added and the suspension centrifuged at 120g for five minutes. The supernatant is removed and re-suspended in DFF10 before being plated on poly-L-lysine coated dishes at a concentration of approximately 1.5 olfactory bulbs per dish. The dishes are incubated at 37^0C in an atmosphere containing 5% CO_2 for 4-5 days before new warm DFF10 is added and replaced thereafter every 2-3 days

for the next 12-14 days. When the cells are ready for transplantation they have a concentration of $2.5x10^4$ cells/µl. (see Appendix 8) (see Figure 6.4)

6.2.14 OEC Transfection with Lentivirus to Express Green Fluorescent Protein

OECs were transfected with a lentivirus (copGFP; SantaCruz Biotechnology, USA) to label them with green fluorescent protein (GFP) so that they could be identified during immunochemical preparation. Two to three days before scraping, OEC cultures were washed with serum free, DMEM-F12 medium (Gibco-BRL, UK) and incubated for 24 hours in media containing recombinant, replication-incompetent lentivirus vectors expressing enhanced GFP. The virus labelled up to 25% of the cells. (Figure 6.4 c)

6.2.15 Preparation of OECs for transplantation

The gel-like matrix of cell culture containing the OECs and ONFs was scraped off the dish with polyethene spatula, (Costar, Corning, NY) divided into four roughly equal sized pieces with a concentration of $2.5x10^4$ cells/µl and transplanted to the recipient site. Transplanting the cells in this matrix avoids loss of cells during transfer but also prevented immediate diffusion of cells away from the transplant site. (Figure 6.4 c, d). The cells were picked up using our custom-made hook before being placed on the reimplanted nerve root. (see Chapter 2)

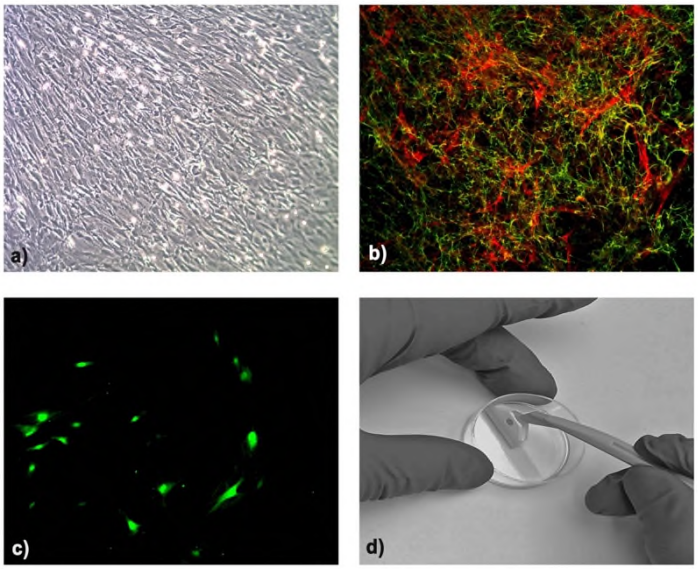

Figure 6.4. Microscopic imaging and harvesting of OECs. a) Light microscopy showing a culture of bulb cells at Day 17 (x40). b) Bulb cultures characterised with p75 (green) and Fibronectin (red) at Day 17. c) GFP labelled bulb cultures as seen under the fluorescent microscope. d) Scraping technique for harvesting cells.

6.2.16 Functional tests to assess recovery in forepaw function after C8 ventral root surgery

We conducted gait analysis and paw grip strength testing in every rat in the four groups, from the preoperative period and weekly up to 8 weeks after the surgery.

Gait analysis testing was performed as described in detail in Chapter 5. (de Medinaceli et al., 1982, Chan et al., 2005, Metz et al., 2000) From the paw prints generated we assessed the paw spread in each rat in the four treatment groups.

Left paw and bilateral grip strength testing was performed using a Grip Strength Meter (GSM) as described in detail in Chapter 5. (TSE Systems Inc, Chesterfield, MO) (Anderson et al., 2005, Meyer et al., 1979) Measurements were taken preoperatively and weekly up to 8-weeks in each rat in the four groups.

6.2.17 Retrograde labelling of motor neurones with Fast Blue® to assess continuity of motor neurones across the surgery site

In order to assess the continuity of motor neurones across the site of surgery in the four different study groups we injected Fast Blue® (Polysciences Inc, USA) retrograde tracer into the extraforaminal C8 nerve. This was done at week 8 and the rats were culled 7 days later. (Methods described in detail in Chapter 4)

6.2.18 Parenteral Anaesthesia

Animals were anaesthetised with a terminal dose of CO_2 administered at a dose of 4L/min by inhalation. This provided deep and irreversible anaesthesia and was used for all rats about to undergo pericardial perfusion for histological processing.

6.2.19 Pericardial perfusion & fixation

Pericardial perfusion and fixation of the spinal cord was performed after terminal anaesthesia. (see Appendix 3)

6.2.20 Tissue preparation & cryopreservation for sectioning using a cryostat microtome

Under a dissecting microscope the cervical spine was dissected to remove excess muscle and the tissue prepared for histological sectioning. (see Appendix 4)

6.2.21 Haematoxylin & Eosin staining

Alternate slides through the relevant cervical spine sections in each group were analysed after staining with Haematoxylin & Eosin. (Merck, Darmstadt, Germany) (see Appendix 5)

6.2.22 Double staining with GFAP and Neurofilament

Alternate slides through the relevant cervical spine sections in each group were analysed after double staining with glial fibrillary acidic protein and neurofilament. (see Appendix 9)

6.2.23 Statistical analysis

All statistical tests were carried out using SPSS Statistics 22.0. (IBM, Armonk, NY, USA).

6.3 Results

6.3.1 Left Paw Spread Recovery

Left paw spread recovery and paw spread gait analysis at Day 56 are demonstrated in Figures 6.5 & 6.6.

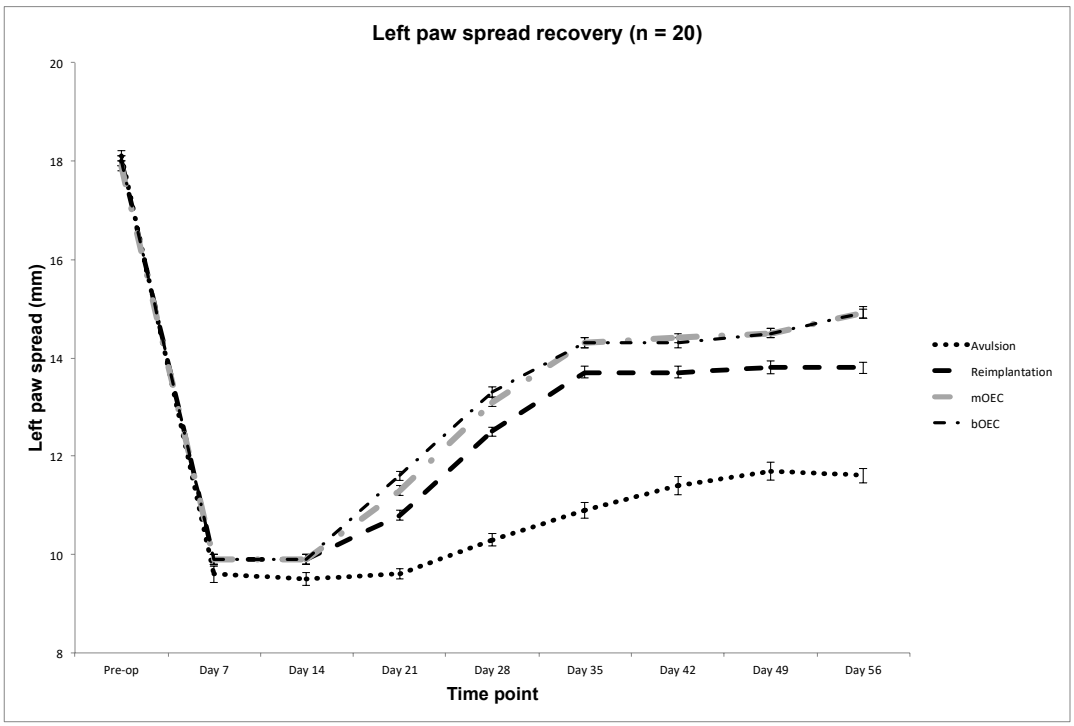

Figure 6.5. Left paw spread recovery. Graph showing left paw spread recovery in the different treatment groups over various time points (n =20 in each group at the start of experiments). Error bars indicate mean ± SEM indicated on graph. (mOEC: mucosal OEC; bOEC: bulb OEC)

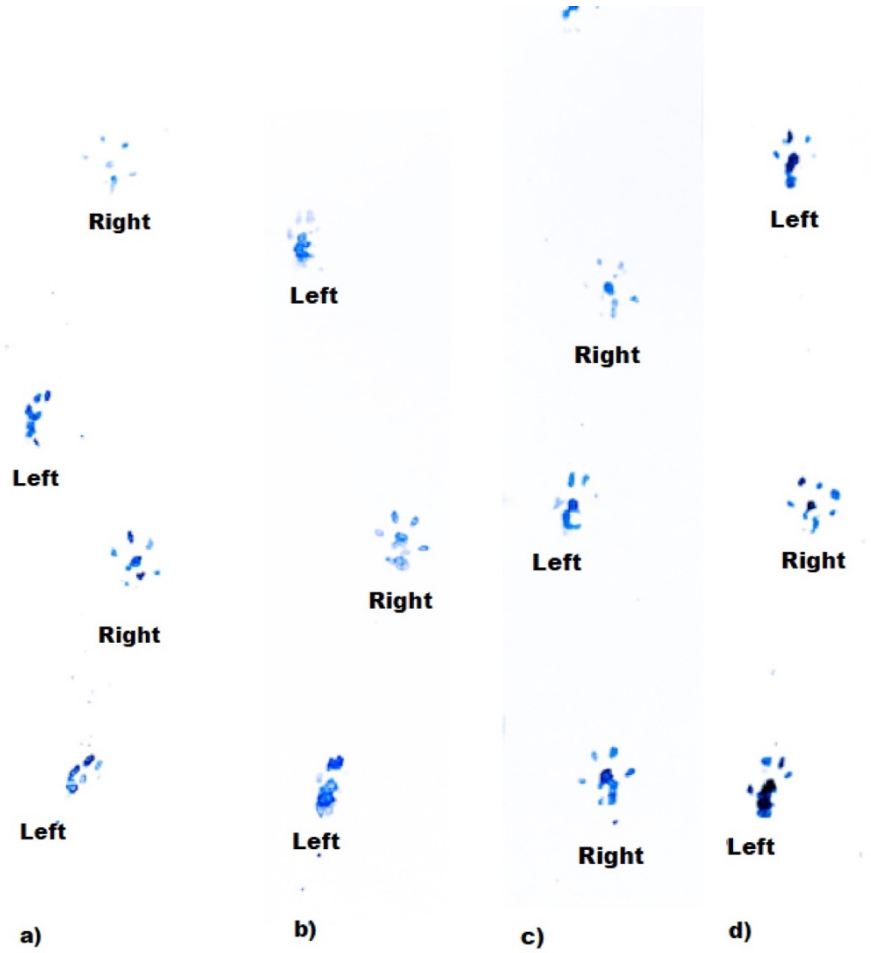

Figure 6.6. Gait strips analysis of paw spread recovery at day 56. a) avulsion; b) reimplantation; c) mucosal OEC; d) bulb OEC. The paw spread in the left paw in the mucosal and bulb groups has improved compared to the reimplantation group. The reimplantation group is improved compared to the avulsion group.

6.3.1.1 Left paw spread

Pre-operatively there was no statistically significant difference in paw spread between the avulsion (18.1 ± 0.7 SD), reimplantation (18.0 ± 0.6 SD), mOEC (18.0 ± 0.6 SD)

and bOEC (18.0 ± 0.8 SD) groups. (Welch's ANOVA F(3, 189.025) = 0.147, p = 0.931) (See Figures 6.5 & 6.6)

At day 7 the mean paw spread was significantly less than preoperatively but there was no statistically significant difference in paw spread between the avulsion (9.6 ± 0.1.5 SD), reimplantation (9.9 ± 1.0 SD), mOEC (10.0 ± 0.9 SD) and bOEC (9.9 ± 1.1 SD groups. (Welch's ANOVA F(3, 182.343) = 1.283, p = 0.282)

At day 14 there was no statistically significant difference in paw spread between the avulsion (9.5 ± 1.2 SD), reimplantation (9.9 ± 0.8 SD), mOEC (9.9 ± 0.8 SD) and bOEC (9.9 ± 0.9 SD) groups. (Welch's ANOVA F(3, 182.272) = 2.449, p = 0.065)

At day 21 there was a statistically significant difference in paw spread between the avulsion (9.6 ± 0.8 SD), reimplantation (10.8 ± 0.7 SD), mOEC (11.3 ± 0.7 SD) and bOEC (11.6 ± 0.9 SD) groups. (Welch's ANOVA F(3, 187.453) = 93.238, p<0.005). The left paw spread in the avulsion groups was significantly lower than the other three groups (p<0.005). The paw spread in the mOEC and bOEC was significantly better than the reimplantation groups (p<0.005) but there was no difference between these two groups at this stage (p = 0.052).

At day 28 there was a statistically significant difference between the avulsion (10.3 ± 1.1 SD), reimplantation (12.5 ± 0.8 SD), mOEC (13.1 ± 0.7 SD) and bOEC (13.2 ± 0.8 SD) groups. (Welch's ANOVA F(3, 180.166) = 132.383, p<0.005). The left paw spread was significantly lower than the reimplantation, mOEC and bOEC groups (p<0.005). The mOEC and bOEC paw spread was significantly improved compared to the reimplantation group (*p<0.005*) but there was no difference between the mOEC and bOEC groups (p = 0.142)

At day 35 there was a statistically significant difference between the avulsion (10.9 ± 1.5 SD), reimplantation (13.7 ± 1.1 SD), mOEC (14.3 ± 0.7 SD) and bOEC (14.2 ± 0.6 SD) groups. (Welch's ANOVA $F(3, 169.967) = 2.449$, $p<0.005$). The paw spread in the avulsion group was significantly worse than in the other three groups ($p<0.005$). The mOEC and bOEC groups were significantly more improved than the reimplantation group ($p<0.005$). However, there was no difference in paw spread recovery between the mOEC and bOEC groups. ($p = 0.769$)

At day 42 there was a statistically significant difference between the avulsion (11.4 ± 1.6 SD), reimplantation (13.8 ± 1.1 SD), mOEC (14.4 ± 0.6 SD) and bOEC (14.3 ± 1.5 SD) groups. (Welch's ANOVA $F(3, 169.031) = 76.088$, $p<0.005$). The paw spread recovery in the avulsion group was significantly less than in the other three groups (*$p<0.005$*). The mOEC and bOEC group paw recovery was significantly better than the reimplantation group ($p<0.005$ and $p = 0.04$ respectively) but there was no difference between the mOEC and bOEC groups ($p = 0.333$).

At day 49 there was a statistically significant difference between the avulsion (11.7 ± 1.3 SEM), reimplantation (13.9 ± 1.1 SD), mOEC (14.5 ± 0.7 SD) and bOEC (14.5 ± 0.7 SD) groups. (Welch's ANOVA $F(3, 161.628) = 75.403$, $p<0.005$). The avulsion paw spread recovery was significantly less than the other three groups ($p<0.005$). The paw spread difference in the reimplantation group was significantly lower compared to the mOEC and bOEC groups ($p<0.005$). However, there was no difference in paw spread recovery between the mOEC and bOEC groups. ($p = 1.000$)

At day 56 there was a statistically significant difference between the avulsion (11.6 ± 1.3 SD), reimplantation (13.9 ± 1.1 SD), mOEC (14.9 ± 0.7 SD) and bOEC (14.9 ± 0.8 SD) groups. (Welch's ANOVA $F(3, 174.477) = 149.006$, $p<0.005$). The paw spread in

the avulsion group was considerably less than preoperatively and compared to the other groups at this time point ($p<0.005$). The reimplantation group recovery was better than the avulsion ($p<0.005$) but the mOEC and bOEC group recovery was better ($p<0.005$) although there was no significant difference between the mOEC and bOEC groups ($p = 1.000$)

Tables 6.1, 6.2 & 6.3 show the left paw spread data in the different groups over the test period, ANOVA robust equality of means and & Games-Howell Test multiple pairwise comparisons, respectively.

Left Paw Spread		Pre-op	Day 7	Day 14	Day 21	Day 28	Day 35	Day 42	Day 49	Day 56
Avulsion	**Mean**	**18.1**	**9.6**	**9.5**	**9.6**	**10.3**	**10.9**	**11.4**	**11.7**	**11.6**
	SEM	.075	.168	.141	.099	.132	.169	.191	.186	.153
	Std. Deviation	.655	1.460	1.223	.854	1.145	1.465	1.654	1.615	1.327
Reimplantation	**Mean**	**18.0**	**9.9**	**9.9**	**10.8**	**12.5**	**13.7**	**13.8**	**13.9**	**13.9**
	SEM	.071	.115	.094	.077	.088	.130	.130	.131	.124
	Std. Deviation	.615	1.00	.814	.665	.760	1.124	1.125	1.133	1.073
mOEC	**Mean**	**18.0**	**10.0**	**9.9**	**11.3**	**13.1**	**14.3**	**14.4**	**14.5**	**14.9**
	SEM	.061	.091	.075	.069	.064	.064	.064	.057	.069
	Std. Deviation	.642	.953	.789	.720	.675	.670	.667	.601	.724
bOEC	**Mean**	**18.0**	**9.9**	**9.9**	**11.6**	**13.2**	**14.2**	**14.3**	**14.5**	**14.9**
	SEM	.0758	.111	.086	.086	.083	.061	.061	.153	.0772
	Std. Deviation	.75872	1.11464	.87496	.86199	.82975	.61332	.61332	1.52723	.77198

Table 6.1. Left paw spread data analysis. Means, standard error of the means (SEM) and standard deviations (Std. Deviation) for left paw spread in the different groups at various time points.

		Statistic[a]	df1	df2	Sig.
L Paw Preop	**Welch**	.15	3	189.03	.931
L Paw Day 7	**Welch**	1.28	3	182.34	.282
L Paw Day 14	**Welch**	2.45	3	182.27	.065
L Paw Day 21	**Welch**	93.24	3	187.45	.000
L Paw Day 28	**Welch**	132.38	3	180.17	.000
L Paw Day 35	**Welch**	123.59	3	169.97	.000
L Paw Day 42	**Welch**	76.09	3	169.03	.000
L Paw Day 49	**Welch**	75.40	3	161.63	.000
L Paw Day 56	**Welch**	149.01	3	174.48	.000

a. Asymptotically F distributed.

Table 6.2. Robust test of equality of means as per Welch ANOVA test, for left paw spread. (L paw: left paw; df: degrees freedom; sig: significance)

	(I) LPaw	(J) LPaw	Mean Difference (I-J)	Std. Error	Sig.	95% Confidence Interval	
						Lower Bound	Upper Bound
L Paw Preop	Avulsion	Reimplantation	.053	.104	.956	-.216	.323
		mOEC	.062	.097	.918	-.190	.315
		bOEC	.043	.1071	.978	-.235	.321
	Reimplantation	Avulsion	-.053	.1038	.956	-.323	.216
		mOEC	.009	.0938	1.000	-.234	.252
		bOEC	-.010	.1039	1.000	-.279	.259
	mOEC	Avulsion	-.062	.0974	.918	-.315	.190
		Reimplantation	-.009	.0938	1.000	-.253	.234
		bOEC	-.019	.0975	.997	-.272	.233
	bOEC	Avulsion	-.043	.1072	.978	-.321	.234
		Reimplantation	.010	.1039	1.000	-.260	.279
		mOEC	.019	.098	.997	-.234	.271

L Paw Day 7	**Avulsion**	**Reimplantation**	-.360	.204	.296	-.892	.171
		mOEC	-.359	.192	.244	-.859	.139
		bOEC	-.287	.202	.490	-.813	.239
	Reimplantation	**Avulsion**	.360	.20434	.296	-.172	.891
		mOEC	.001	.147	1.000	-.381	.382
		bOEC	.073	.160	.968	-.343	.489
	mOEC	**Avulsion**	.359	.192	.244	-.140	.858
		Reimplantation	-.001	.147	1.000	-.382	.380
		bOEC	.073	.144	.958	-.299	.445
	bOEC	**Avulsion**	.287	.202	.490	-.239	.812
		Reimplantation	-.073	.160	.968	-.490	.343
		mOEC	-.073	.144	.958	-.445	.299
L Paw Day 14	**Avulsion**	**Reimplantation**	-.453*	.170	.042	-.894	-.011
		mOEC	-.367	.160	.106	-.783	.050
		bOEC	-.357	.166	.144	-.789	.075
	Reimplantation	**Avulsion**	.453*	.170	.042	.0119	.894
		mOEC	.086	.120	.889	-.225	.399
		bOEC	.097	.128	.875	-.236	.429
	mOEC	**Avulsion**	.367	.160	.106	-.050	.783
		Reimplantation	-.087	.120	.889	-.399	.225
		bOEC	.010	.115	1.000	-.289	.309
	bOEC	**Avulsion**	.357	.166	.144	-.075	.789
		Reimplantation	-.097	.128	.875	-.429	.236
		mOEC	-.010	.115	1.000	-.309	.289
L Paw Day 21	**Avulsion**	**Reimplantation**	-1.227*	.125	.000	-1.551	-.901

		mOEC	-1.734	.120	.000	-2.04	-1.423
		bOEC	-2.02	.131	.000	-2.360	-1.679
	Reimplantation	**Avulsion**	1.227*	.125	.000	.901	1.551
		mOEC	-.510*	.103	.000	-.777	-.242
		bOEC	-.793*	.115	.000	-1.092	-.493
	mOEC	**Avulsion**	1.743*	.120	.000	1.423	2.048
		Reimplantation	.509*	.103	.000	.2423	.777
		bOEC	-.284	.110	.052	-.569	.002
	bOEC	**Avulsion**	2.020*	.131	.000	1.679	2.360
		Reimplantation	.793*	.115	.000	.493	1.092
		mOEC	.284	.110	.052	-.002	.569
L Paw Day 28	**Avulsion**	**Reimplantation**	-2.171*	.159	.000	-2.586	-1.760
		mOEC	-2.707*	.147	.000	-3.091	-2.324
		bOEC	-2.93*	.156	.000	-3.339	-2.527
	Reimplantation	**Avulsion**	2.173*	.159	.000	1.760	2.586
		mOEC	-.535*	.109	.000	-.817	-.251
		bOEC	-.760*	.121	.000	-1.073	-.446
	mOEC	**Avulsion**	2.708*	.147	.000	2.324	3.091
		Reimplantation	.535*	.109	.000	.251	.817
		bOEC	-.225	.105	.142	-.497	.046
	bOEC	**Avulsion**	2.933*	.156	.000	2.527	3.339
		Reimplantation	.760*	.121	.000	.446	1.073
		mOEC	.225	.105	.142	-.046	.497
L Paw Day 35	**Avulsion**	**Reimplantation**	-2.747*	.213	.000	-3.301	-2.192
		mOEC	-3.385*	.181	.000	-3.858	-2.912

		bOEC	-3.300*	.180	.000	-3.770	-2.829
	Reimplantation	**Avulsion**	2.747*	.213	.000	2.192	3.301
		mOEC	-.639	.145	.000	-1.016	-.261
		bOEC	-.553*	.144	.001	-.928	-.178
	mOEC	**Avulsion**	3.385*	.181	.000	2.912	3.858
		Reimplantation	.639*	.145	.000	.261	1.016
		bOEC	.085	.089	.769	-.143	.314
	bOEC	**Avulsion**	3.300*	.180	.000	2.829	3.770
		Reimplantation	.553*	.144	.001	.178	.928
		mOEC	-.085	.089	.769	-.314	.143
L Paw Day 42	**Avulsion**	**Reimplantation**	-2.320*	.231	.000	-2.921	-1.718
		mOEC	-2.969*	.201	.000	-3.496	-2.442
		bOEC	-2.820*	.201	.000	-3.345	-2.294
	Reimplantation	**Avulsion**	2.320*	.231	.000	1.718	2.921
		mOEC	-.649*	.145	.000	-1.026	-.271
		bOEC	-.500*	.144	.004	-.875	-.125
	mOEC	**Avulsion**	2.969	.201	.000	2.442	3.496
		Reimplantation	.649*	.145	.000	.271	1.026
		bOEC	.149	.088	.333	-.079	.378
	bOEC	**Avulsion**	2.820*	.201	.000	2.294	3.345
		Reimplantation	.500	.144	.004	.125	.875
		mOEC	-.149	.088	.333	-.378	.079
L Paw Day 49	**Avulsion**	**Reimplantation**	-2.240*	.228	.000	-2.832	-1.647
		mOEC	-2.874	.195	.000	-3.384	-2.363
		bOEC	-2.877	.241	.000	-3.502	-2.250

	Reimplantation	**Avulsion**	2.240*	.228	.000	1.647	2.832
		mOEC	-.634*	.143	.000	-1.007	-.260
		bOEC	-.637*	.201	.010	-1.158	-.114
	mOEC	**Avulsion**	2.874*	.195	.000	2.363	3.384
		Reimplantation	.634*	.142	.000	.260	1.007
		bOEC	-.003	.163	1.000	-.427	.422
	bOEC	**Avulsion**	2.877*	.241	.000	2.250	3.502
		Reimplantation	.637*	.201	.010	.114	1.158
		mOEC	.003	.163	1.000	-.422	.427
L Paw Day 56	**Avulsion**	**Reimplantation**	-2.320*	.197	.000	-2.832	-1.807
		mOEC	-3.335*	.168	.000	-3.774	-2.896
		bOEC	-3.327*	.172	.000	-3.774	-2.879
	Reimplantation	**Avulsion**	2.320*	.197	.000	1.807	2.832
		mOEC	-1.016*	.142	.000	-1.385	-.646
		bOEC	-1.007*	.146	.000	-1.386	-.626
	mOEC	**Avulsion**	3.336*	.168	.000	2.896	3.774
		Reimplantation	1.016*	.142	.000	.646	1.385
		bOEC	.009	.103	1.000	-.259	.277
	bOEC	**Avulsion**	3.327*	.172	.000	2.879	3.774
		Reimplantation	1.007*	.146	.000	.626	1.386
		mOEC	-.009	.103	1.000	-.277	.259

*. The mean difference is significant at the 0.05 level.

Table 6.3. Games-Howell post-hoc multiple comparison tests between paw spread in the different groups at different time points

6.3.2 Left paw grip strength

6.3.2.1 Left paw grip strength pre-operative

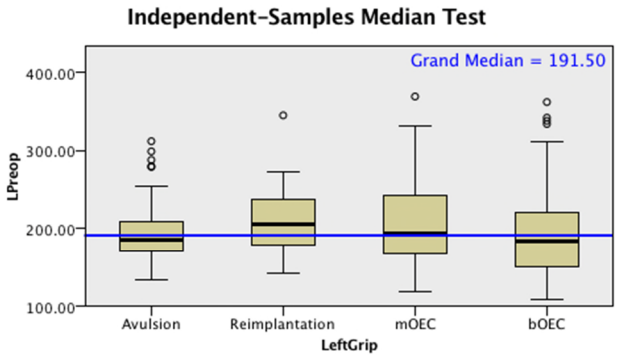

Total N	320
Median	191.500
Test Statistic	5.237
Degrees of Freedom	3
Asymptotic Sig. (2-sided test)	.155

1. Multiple comparisons are not performed because the overall test does not show significant differences across samples.

A Kruskal Wallis H test was run to determine whether there were differences in the left paw grip strength in the four groups pre-operatively. The table shows the total number of grip strength measured in the four groups (n = 320). Distributions were similar as between the groups, as assessed by visual inspection of the results. Median rank scores in the preoperative groups were similar in the avulsion, reimplantation, mOEC and bOEC groups. The Kruskal-Wallis test showed that there was no statistically significant difference between the median rank scores in preoperative groups, $X^2(3) = 5.327$, $p = 0.155$.

6.3.2.2 Left paw grip strength - day 7

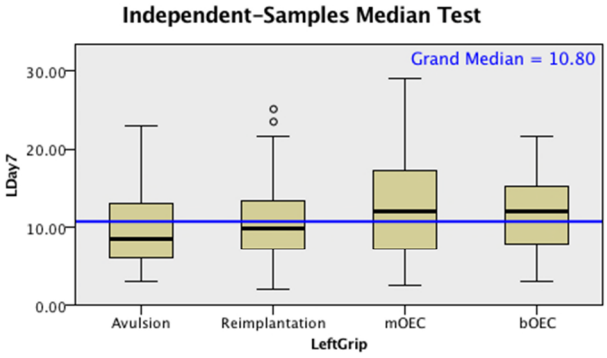

Total N	308
Median	10.800
Test Statistic	7.658
Degrees of Freedom	3
Asymptotic Sig. (2-sided test)	.054

1. Multiple comparisons are not performed because the overall test does not show significant differences across samples.

The table shows the total number of grip strength measured in the four groups (n = 308). The Kruskal-Wallis H test showed that there was no statistically significant difference between the median rank scores at Day 7, $X^2(3) = 10.8$, $p = 0.054$.

6.3.2.3 Left paw grip strength - day 14

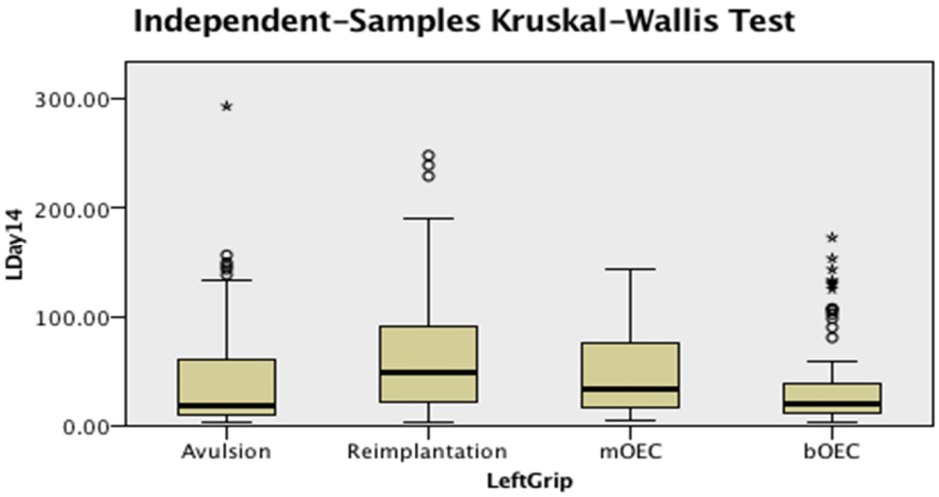

Total N	304
Test Statistic	27.558
Degrees of Freedom	3
Asymptotic Sig. (2-sided test)	.000

1. The test statistic is adjusted for ties.

Graph and table showing the median rank scores in the avulsion, reimplantation, mOEC and bOEC groups at day 14. The table shows the total number of grip strength measured in the four groups (n = 304), the independent Kruskal-Wallis H test statistic (Test statistic, H = 27.558) and the Asymptotic Significance ($p<0.005$).

Pairwise comparisons were performed using Dunn's (1964) procedure with a Bonferroni correction for multiple comparisons. Adjusted p-values are presented. Values are mean ranks unless otherwise stated. The post-hoc analysis revealed statistically significant differences in the left paw grip strength between the avulsion (125.46) and the reimplantation (192.44) groups ($p<0.005$), and the bOEC (130.23) and reimplantation (192.44) ($p<0.005$). However, there were no differences between the avulsion and mOEC groups and the avulsion and bOEC groups, or any other group combination.

6.3.2.4 Left paw grip strength - day 21

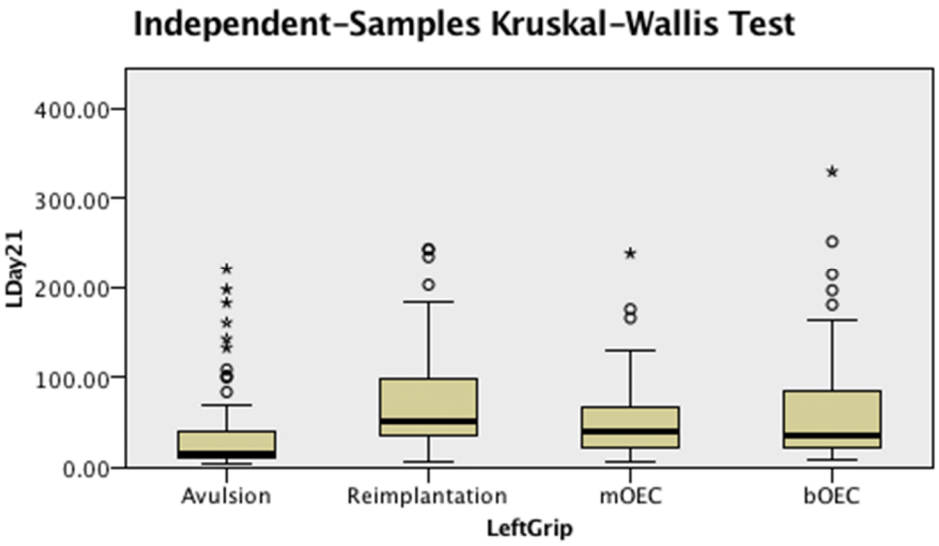

Total N	314
Test Statistic	44.288
Degrees of Freedom	3
Asymptotic Sig. (2-sided test)	.000

1. The test statistic is adjusted for ties.

Graph and table showing the median scores in the avulsion, reimplantation, mOEC and bOEC groups at day 21. The table shows the total number of grip strength measured in the four groups (n = 314), the independent Kruskal-Wallis H test statistic (Test statistic, H 44.288) and the Asymptotic Significance ($p<0.005$)

Pairwise comparisons were performed using Dunn's (1964) procedure with a Bonferroni correction for multiple comparisons. Adjusted p-values are presented. Values are mean ranks unless otherwise stated. The post-hoc analysis revealed statistically significant differences in the left paw grip strength between the avulsion (99.31) and the reimplantation (196.55) groups ($p<0.005$), and the avulsion (99.31) and mOEC (161.33) ($p<0.005$), and the avulsion (99.31) and bOEC (167.54) ($p<0.005$). However, there were no differences between the other group combinations.

6.3.2.5 Left paw grip strength - day 28

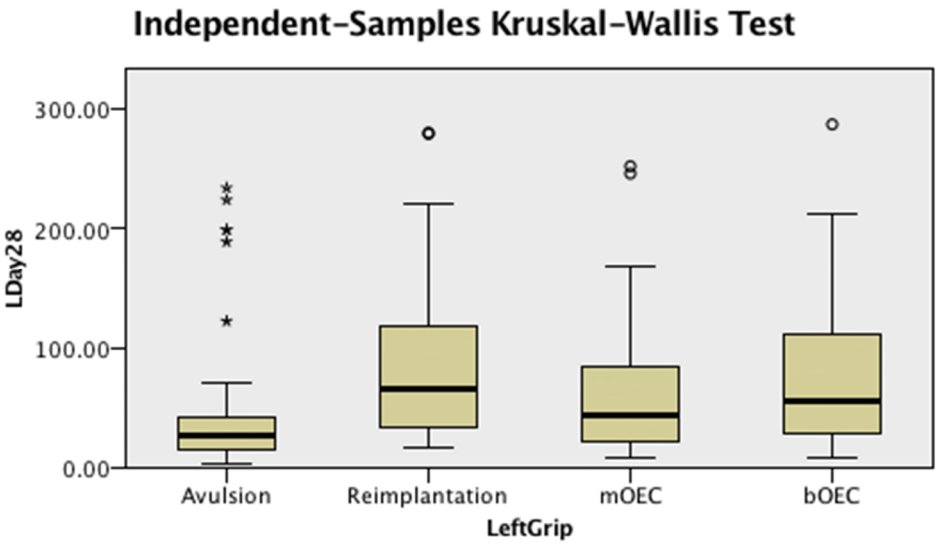

Total N	286
Test Statistic	39.752
Degrees of Freedom	3
Asymptotic Sig. (2-sided test)	.000

1. The test statistic is adjusted for ties.

Graph and table showing the median scores in the avulsion, reimplantation, mOEC and bOEC groups at day 28. The table shows the total number of grip strength measured in the four groups (n = 286), the independent Kruskal-Wallis H test statistic (Test statistic, H = 39.752) and the Asymptotic Significance ($p<0.005$).

Pairwise comparisons were performed using Dunn's (1964) procedure with a Bonferroni correction for multiple comparisons. Adjusted p-values are presented. Values are mean ranks unless otherwise stated. The post-hoc analysis revealed statistically significant differences in the left paw grip strength between the avulsion (93.45) and the reimplantation (175.35) groups ($p<0.005$), and the avulsion (93.45) and mOEC (135.42) ($p = 0.018$), and the avulsion (93.45) and bOEC (163.04) ($p<0.005$). There was also a significant difference between the mOEC (135.42) and the reimplantation (175.35) groups ($p = 0.021$). However, there were no differences between the other group combinations.

6.3.2.6 Left paw grip strength - day 35

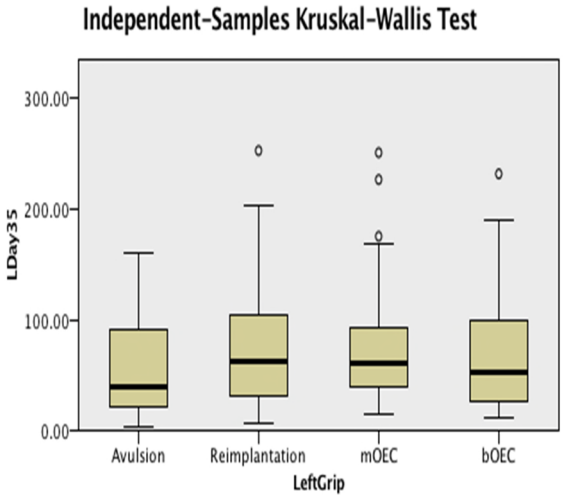

Total N	249
Test Statistic	6.764
Degrees of Freedom	3
Asymptotic Sig. (2-sided test)	.080

1. The test statistic is adjusted for ties.
2. Multiple comparisons are not performed because the overall test does not show significant differences across samples.

Graph and table showing the median scores in the avulsion, reimplantation, MOEC and bOEC groups at Day 35. The table shows the total number of grip strength measured in the four groups (n = 249), the independent Kruskal-Wallis H test statistic (Test statistic, H = 7.764) and the Asymptotic Significance (p = 0.08), which suggests that there is no difference across samples.

6.3.2.7 Left paw grip strength - day 42

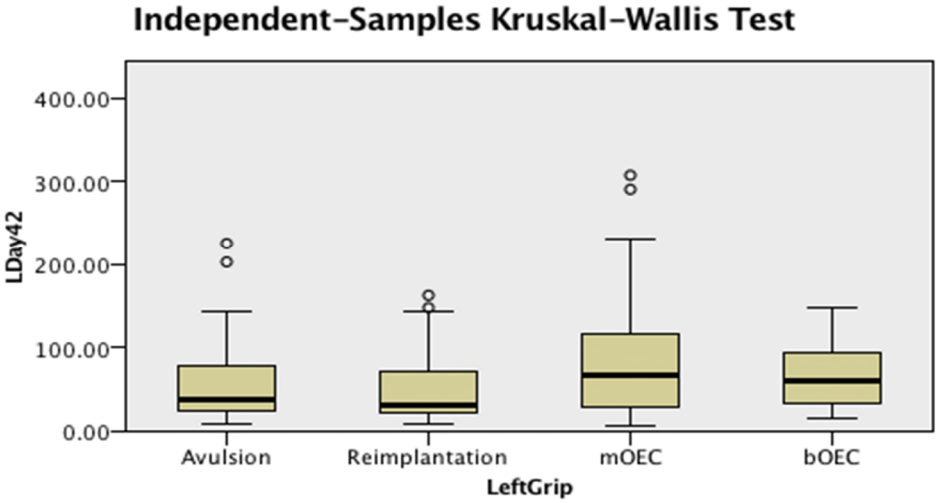

Total N	231
Test Statistic	12.807
Degrees of Freedom	3
Asymptotic Sig. (2-sided test)	.005

1. The test statistic is adjusted for ties.

Graph and table showing the median scores in the avulsion, reimplantation, MOEC and bOEC groups at Day 42. The table shows the total number of grip strength measured in the four groups (n = 231), the independent Kruskal-Wallis H test statistic (Test statistic, H = 12.807) and the Asymptotic Significance (p = 0.005).

Pairwise comparisons were performed using Dunn's (1964) procedure with a Bonferroni correction for multiple comparisons. Adjusted p-values are presented. Values are mean ranks unless otherwise stated. The post-hoc analysis revealed statistically significant differences in the left paw grip strength between the reimplantation (93.45) and bOEC (130.06) groups ($p = 0.021$), and the reimplantation (93.45) and mOEC (131.32) ($p = 0.028$). There was also a significant difference between the avulsion and reimplantation, avulsion and mOEC or avulsion and bOEC groups, and no differences between the other group combinations.

6.3.2.8 Left paw grip strength - day 49

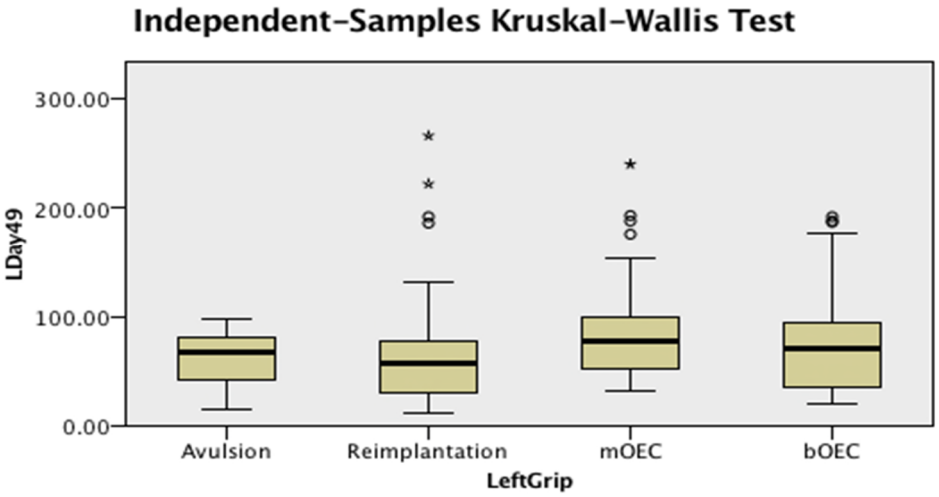

Total N	208
Test Statistic	10.720
Degrees of Freedom	3
Asymptotic Sig. (2-sided test)	.013

1. The test statistic is adjusted for ties.

Graph and table showing the median scores in the avulsion, reimplantation, MOEC and bOEC groups at Day 49. The table shows the total number of grip strength measured in the four groups (N = 208), the independent Kruskal-Wallis H test statistic (Test statistic, H = 10.72) and the Asymptotic Significance (p = 0.013).

Pairwise comparisons were performed using Dunn's (1964) procedure with a Bonferroni correction for multiple comparisons. Adjusted p-values are presented. Values are mean ranks unless otherwise stated. The post-hoc analysis revealed statistically significant differences in the left paw grip strength between the reimplantation (87.56) and mOEC (124.36) groups ($p = 0.017$). There was no significant difference between the avulsion and reimplantation, avulsion and mOEC and avulsion an bOEC groups, and no differences between the other group combinations.

6.3.2.9 Left paw grip strength - day 56

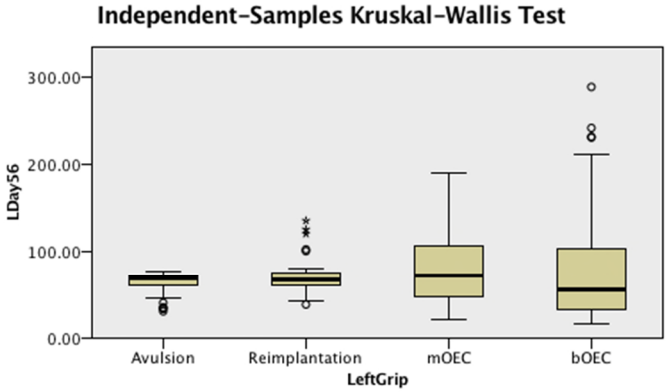

Total N	188
Test Statistic	3.823
Degrees of Freedom	3
Asymptotic Sig. (2-sided test)	.281

1. The test statistic is adjusted for ties.
2. Multiple comparisons are not performed because the overall test does not show significant differences across samples.

Graph and table showing the median scores in the avulsion, reimplantation, MOEC and bOEC groups at Day 56. The table shows the total number of grip strength measured in the four groups (N = 188), the independent Kruskal-Wallis H test statistic (Test statistic, H = 9.032) and the Asymptotic Significance (p = 0.281).

Pairwise comparisons were performed using Dunn's (1964) procedure with a Bonferroni correction for multiple comparisons. Adjusted p-values are presented. Values are mean ranks unless otherwise stated. The post-hoc analysis revealed that

there was no statistically significant differences in the left paw grip strength between all the groups tested.

The left paw grip strength recovery in the different groups over the test period is charted in Figure 6.7. Left paw grip strength data is shown in Table 6.4.

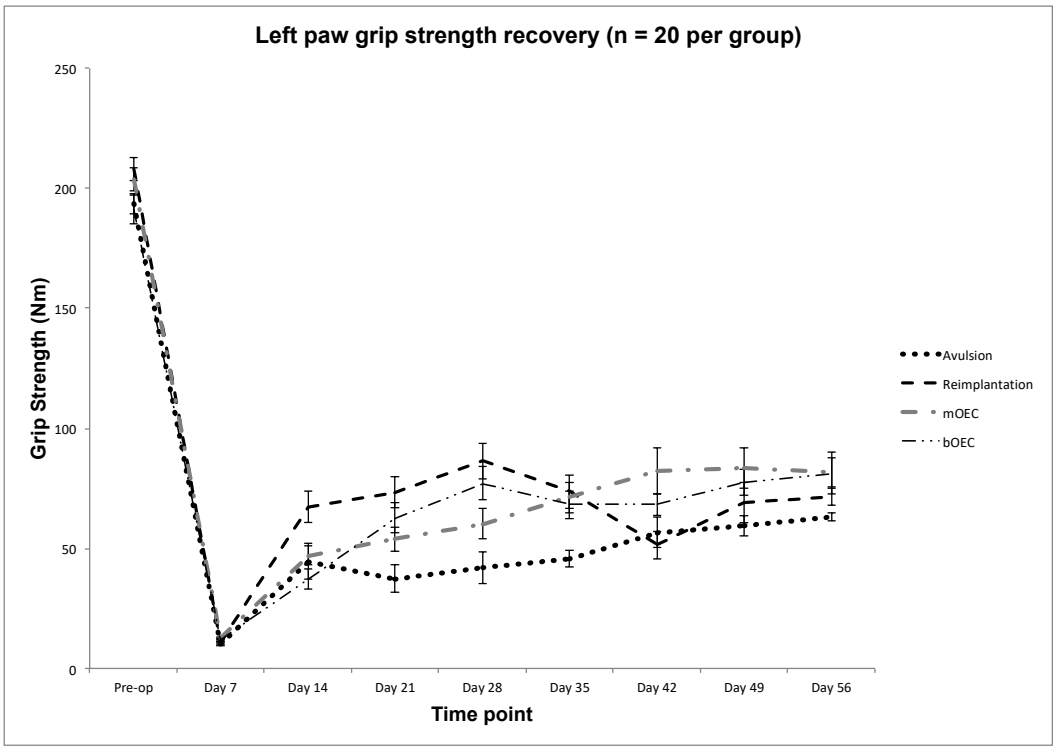

Figure 6.7. Left paw grip strength recovery. Graph showing left paw grip strength recovery in the different groups over the test period. Mean ± SD is indicated on chart. (mOEC: mucosal OEC; bOEC: bulb OEC)

Left Grip Strength		Preop	Day 7	Day 14	Day 21	Day 28	Day 35	Day 42	Day 49	Day 56
Avulsion	Mean	193.64	10.17	44.72	37.26	41.95	45.89	56.74	59.47	63.19
	SEM	4.20	.67	7.45	5.77	6.54	3.62	6.25	4.16	1.69
	Std. Deviation	36.42	5.68	57.24	48.65	52.76	28.08	46.35	29.45	11.8
Reimplantation	Mean	208.24	10.70	67.48	73.35	86.49	73.55	51.39	68.91	71.66
	SEM	4.98	.54	6.75	6.40	7.50	7.13	5.77	8.39	3.61
	Std. Deviation	37.97	4.72	58.51	55.51	65.02	52.87	42.84	55.66	21.38
mOEC	Mean	203.92	12.66	47.08	53.77	60.21	71.21	82.77	83.42	81.68
	SEM	4.96	.72	4.10	5.01	6.20	6.41	9.60	8.423	6.27
	Std. Deviation	48.93	6.40	36.46	44.25	52.63	51.29	69.23	58.96	41.64
bOEC	Mean	191.12	11.96	37.27	62.72	77.09	68.16	68.24	77.50	81.33
	SEM	5.88	.49	4.23	6.22	6.76	5.93	4.53	5.56	8.80
	Std. Deviation	55.85	4.63	40.37	59.03	58.16	49.69	37.71	44.84	68.16

Table 6.4. Left paw grip strength recovery data analysis. Means, standard error of the mean (SEM) and standard deviation (Std. Deviation) of left paw grip strength recovery in the different groups at the different test points.

6.3.3 Bilateral Paw Grip Strength

The data for bilateral paw grip in the pre-operative and Day 7 groups followed a normal distribution. However, in the other groups this was not the case. However, Levenes test for equality of variances was positive ($p<0.05$) indicating that the within group variances were greater than the in between group variances and the groups were not homogenous. In the remaining groups the data did not follow a normal distribution. Transformation of the data was attempted but given the shape of the transformed data a non-parametric test was selected to analyse the data. Based on the distributions of the data in these groups it was decided to use the Kruskal-Wallis test. The distribution of the data set in all the groups meant that the test was used to compare mean ranks at the relevant time points. Bilateral grip strength recovery in all the groups is charted in Figure 6.8. Table 6.5 shows the mean, standard error of the mean and standard deviations for bilateral paw strength recovery.

6.3.3.1 Bilateral paw grip strength - preoperative

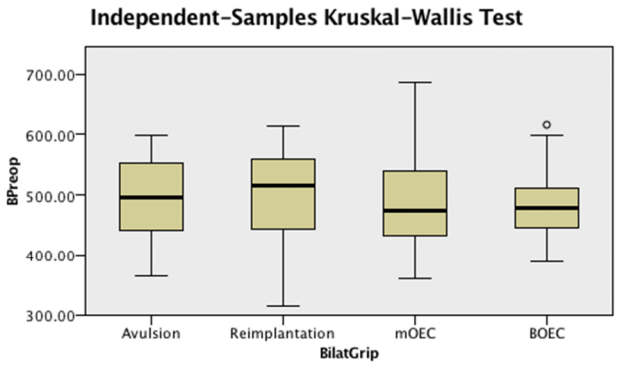

Total N	327
Test Statistic	3.684
Degrees of Freedom	3
Asymptotic Sig. (2-sided test)	.298

1. The test statistic is adjusted for ties.
2. Multiple comparisons are not performed because the overall test does not show significant differences across samples.

A Kruskal Wallis H test was run to determine whether there were differences in the preoperative bilateral paw grip strength in the four groups. Distributions were similar between the groups, as assessed by visual inspection of the results. Mean rank scores in the preoperative groups were similar in the avulsion (92.8), reimplantation (103.1), mOEC (96.5) and bOEC (87.9) groups. The independent Kruskal-Wallis H test showed that there was no statistically significant difference between the mean rank scores in preoperative groups (Test statistic, H 3.684), Asymptotic Significance (p = 0.298).

6.3.3.2 Bilateral paw grip strength - day 7

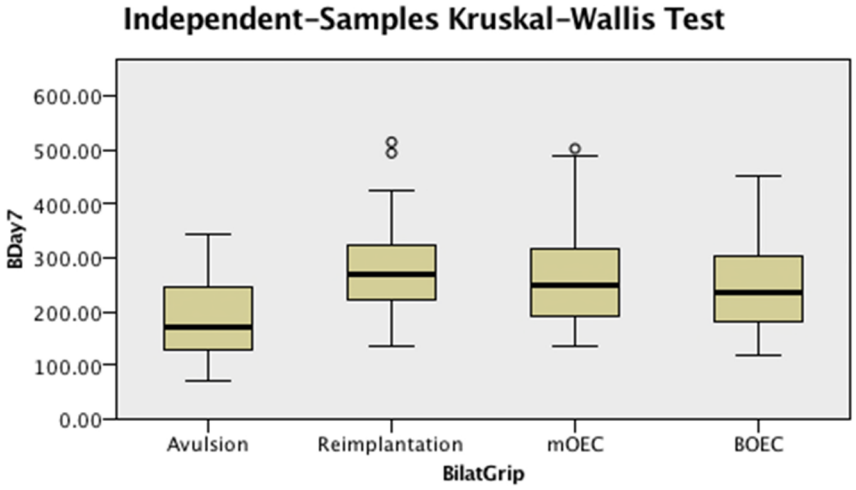

Total N	290
Test Statistic	42.371
Degrees of Freedom	3
Asymptotic Sig. (2-sided test)	.000

1. The test statistic is adjusted for ties.

Graph and table showing the mean rank scores in the bilateral grip strength scores in the avulsion, reimplantation, mOEC and bOEC groups at Day 7. The table shows the total number of grip strength measured in the four groups (n = 290), the independent Kruskal-Wallis H test statistic (Test statistic, H 42.371) and the Asymptotic Significance ($p < 0.005$).

Pairwise comparisons were performed using Dunn's (1964) procedure with a Bonferroni correction for multiple comparisons. Adjusted p-values are presented. Values are mean ranks unless otherwise stated. The post-hoc analysis revealed statistically significant differences in the bilateral paw grip strength between the avulsion (85.5) and the reimplantation (178.8) groups ($p<0.005$), and the avulsion (85.5) and mOEC (159.99) ($p<0.005$), and the avulsion (85.5) and bOEC (146.99) ($p<0.005$). However, there were no differences between the other group combinations.

6.3.3.3 Bilateral paw grip strength - day 14

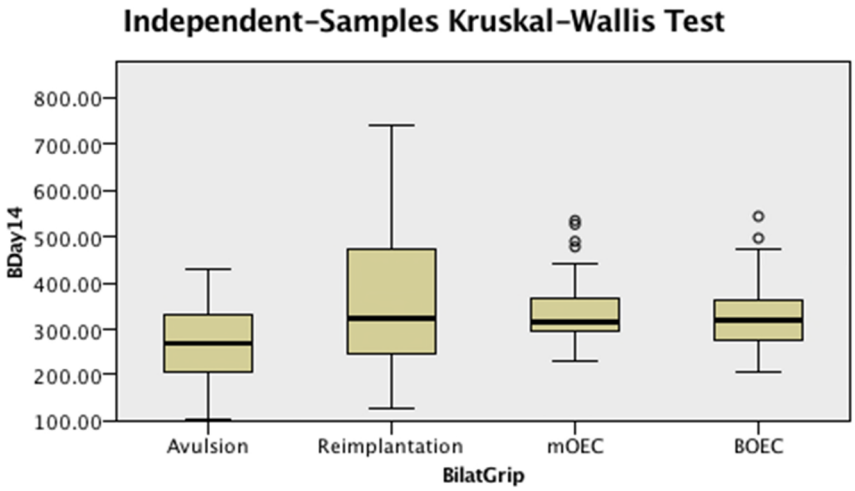

Total N	309
Test Statistic	24.074
Degrees of Freedom	3
Asymptotic Sig. (2-sided test)	.000

1. The test statistic is adjusted for ties.

Graph and table showing the mean rank scores in the bilateral grip strength scores in the avulsion, reimplantation, mOEC and bOEC groups at Day 14. The table shows the total number of grip strength measured in the four groups (n = 309), the independent Kruskal-Wallis H test statistic (Test statistic, H 24.074) and the Asymptotic Significance ($p<0.005$).

Pairwise comparisons were performed using Dunn's (1964) procedure with a Bonferroni correction for multiple comparisons. Adjusted p-values are presented. Values are mean ranks unless otherwise stated. The post-hoc analysis revealed statistically significant differences in the bilateral paw grip strength between the avulsion (104.69) and the reimplantation (167.06) groups ($p<0.005$), and the avulsion (104.69) and mOEC (173.55) ($p<0.005$), and the avulsion (104.69) and bOEC (160.41) ($p<0.005$). However, there were no differences between the other group combinations.

6.3.3.4 Bilateral paw grip strength – day 21

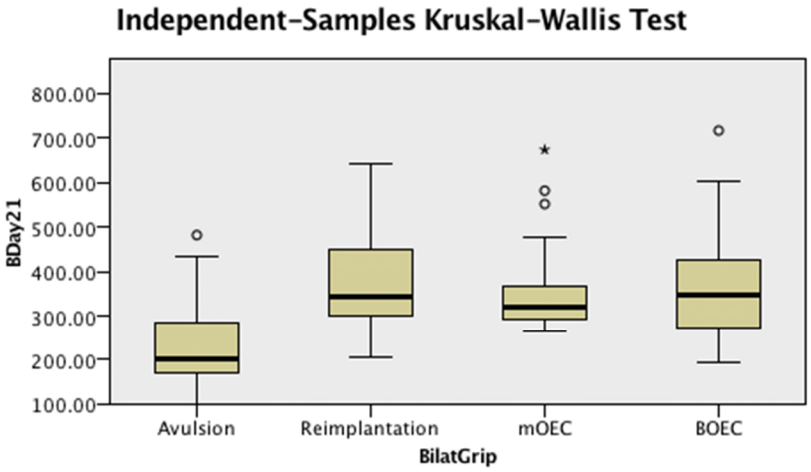

Total N	313
Test Statistic	74.202
Degrees of Freedom	3
Asymptotic Sig. (2-sided test)	.000

1. The test statistic is adjusted for ties.

Graph and table showing the mean rank scores of bilateral grip strength in the avulsion, reimplantation, mOEC and bOEC groups at day 21. The table shows the total number of grip strength measured in the four groups (N = 313), the independent Kruskal-Wallis H test statistic (Test statistic, H 74.202) and the Asymptotic Significance ($p<0.005$).

Pairwise comparisons were performed using Dunn's (1964) procedure with a Bonferroni correction for multiple comparisons. Adjusted p-values are presented.

Values are mean ranks unless otherwise stated. The post-hoc analysis revealed statistically significant differences in the bilateral paw grip strength between the avulsion (79.8) and the reimplantation (192.33) groups ($p<0.005$), and the avulsion (79.8) and mOEC (169.55) ($p<0.005$), and the avulsion (79.8) and bOEC (181.31) ($p<0.005$). However, there were no differences between the other group combinations.

6.3.3.5 Bilateral paw grip strength – day 28

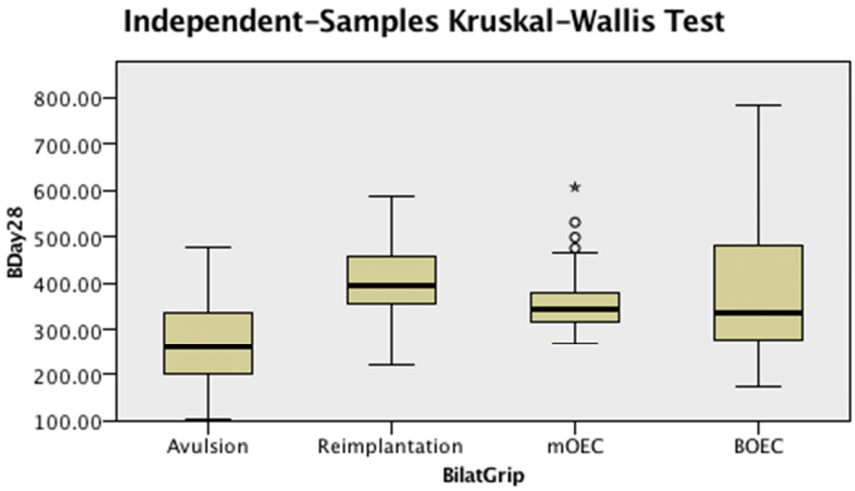

Total N	286
Test Statistic	56.387
Degrees of Freedom	3
Asymptotic Sig. (2-sided test)	.000

1. The test statistic is adjusted for ties.

Graph and table showing the mean rank scores of bilateral grip strength in the avulsion, reimplantation, mOEC and bOEC groups at day 28. The table shows the total number of grip strength measured in the four groups (n = 286), the independent Kruskal-Wallis H test statistic (Test statistic, H 56.387) and the Asymptotic Significance ($p<0.005$).

Pairwise comparisons were performed using Dunn's (1964) procedure with a Bonferroni correction for multiple comparisons. Adjusted p-values are presented.

Values are mean ranks unless otherwise stated. The post-hoc analysis revealed statistically significant differences in the bilateral paw grip strength between the avulsion (81.1) and the reimplantation (185.30) groups ($p<0.005$), and the avulsion (81.1) and mOEC (147.58) ($p<0.005$), and the avulsion (81.1) and bOEC (151.03) ($p<0.005$). There was also a significant difference between the reimplantation (185.3) and the mOEC (147.58) groups ($p = 0.034$). However, there were no differences between the other group combinations.

6.3.3.6 Bilateral paw grip strength – Day 35

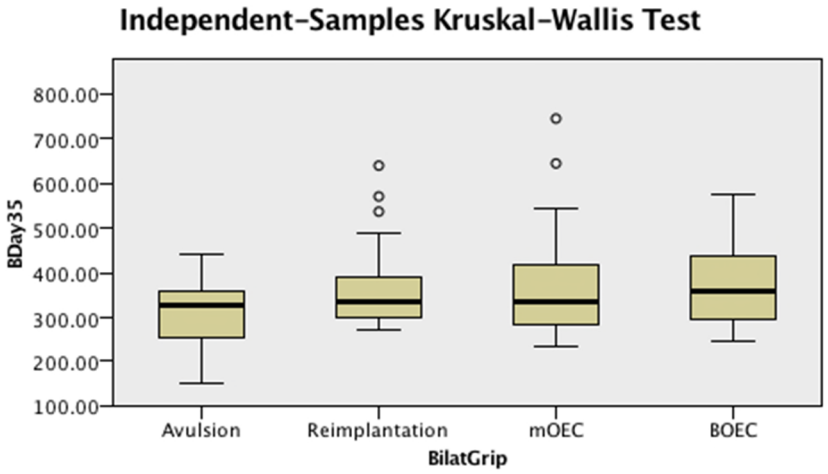

Total N	244
Test Statistic	12.428
Degrees of Freedom	3
Asymptotic Sig. (2-sided test)	.006

1. The test statistic is adjusted for ties.

Graph and table showing the mean rank scores of bilateral grip strength in the avulsion, reimplantation, mOEC and bOEC groups at day 28. The table shows the total number of grip strength measured in the four groups (n = 244), the independent Kruskal-Wallis H test statistic (Test statistic, H 12.428) and the Asymptotic Significance (p = 0.006).

Pairwise comparisons were performed using Dunn's (1964) procedure with a Bonferroni correction for multiple comparisons. Adjusted p-values are presented. Values are mean ranks unless otherwise stated. The post-hoc analysis revealed statistically significant differences in the bilateral paw grip strength between the avulsion (97.72) and the bOEC (121.97) groups ($p<0.005$) However, there were no differences between the other group combinations.

6.3.3.7 Bilateral paw grip strength – day 42

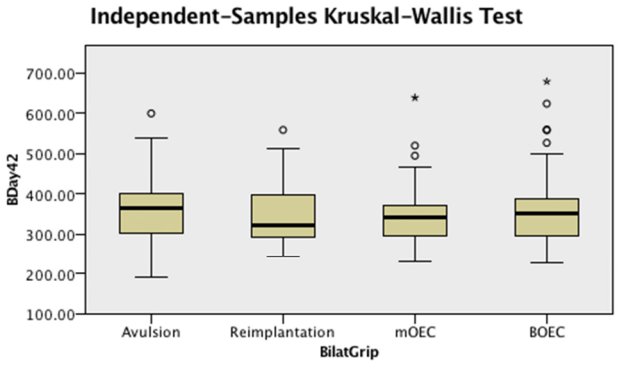

Total N	233
Test Statistic	2.186
Degrees of Freedom	3
Asymptotic Sig. (2-sided test)	.535

1. The test statistic is adjusted for ties.
2. Multiple comparisons are not performed because the overall test does not show significant differences across samples.

Graph and table showing the mean rank scores of bilateral grip strength in the avulsion, reimplantation, mOEC and bOEC groups at day 28. The table shows the

total number of grip strength measured in the four groups (n = 233), the independent Kruskal-Wallis H test statistic (Test statistic, H 2.186) and the Asymptotic Significance (p = 0.535).

6.3.3.8 Bilateral paw grip strength – day 49

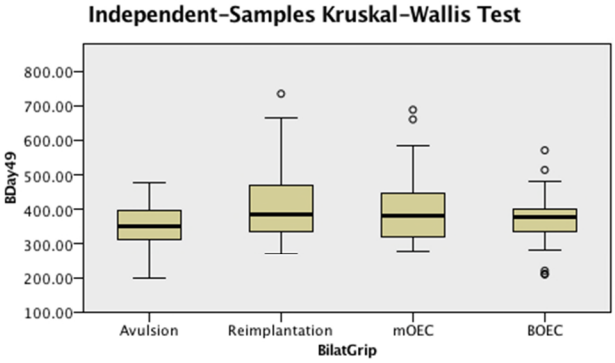

Total N	208
Test Statistic	7.014
Degrees of Freedom	3
Asymptotic Sig. (2-sided test)	.071

1. The test statistic is adjusted for ties.
2. Multiple comparisons are not performed because the overall test does not show significant differences across samples.

Graph and table showing the mean rank scores of bilateral grip strength in the avulsion, reimplantation, mOEC and bOEC groups at day 28. The table shows the total number of grip strength measured in the four groups (N = 208), the independent

Kruskal-Wallis H test statistic (Test statistic, H 7.104) and the Asymptotic Significance (p = 0.071).

6.3.3.9 Bilateral paw grip strength – day 56

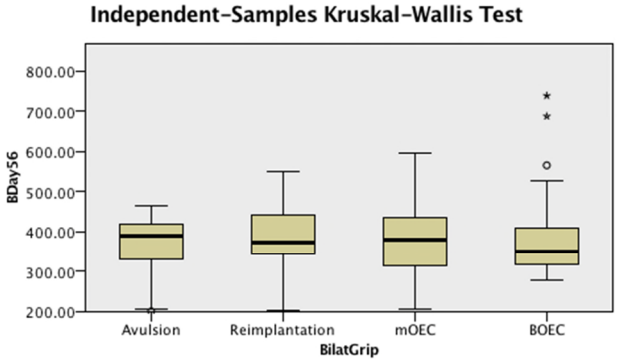

Total N	187
Test Statistic	1.855
Degrees of Freedom	3
Asymptotic Sig. (2-sided test)	.603

1. The test statistic is adjusted for ties.
2. Multiple comparisons are not performed because the overall test does not show significant differences across samples.

Graph and table showing the mean rank scores of bilateral grip strength in the avulsion, reimplantation, mOEC and bOEC groups at day 28. The table shows the total number of grip strength measured in the four groups (n = 187), the independent

Kruskal-Wallis H test statistic (Test statistic, H 1.855) and the Asymptotic Significance (p = 0.603).

Bilateral grip strength is charted in Figure 6.8 and the data represented in Table 6.5 below.

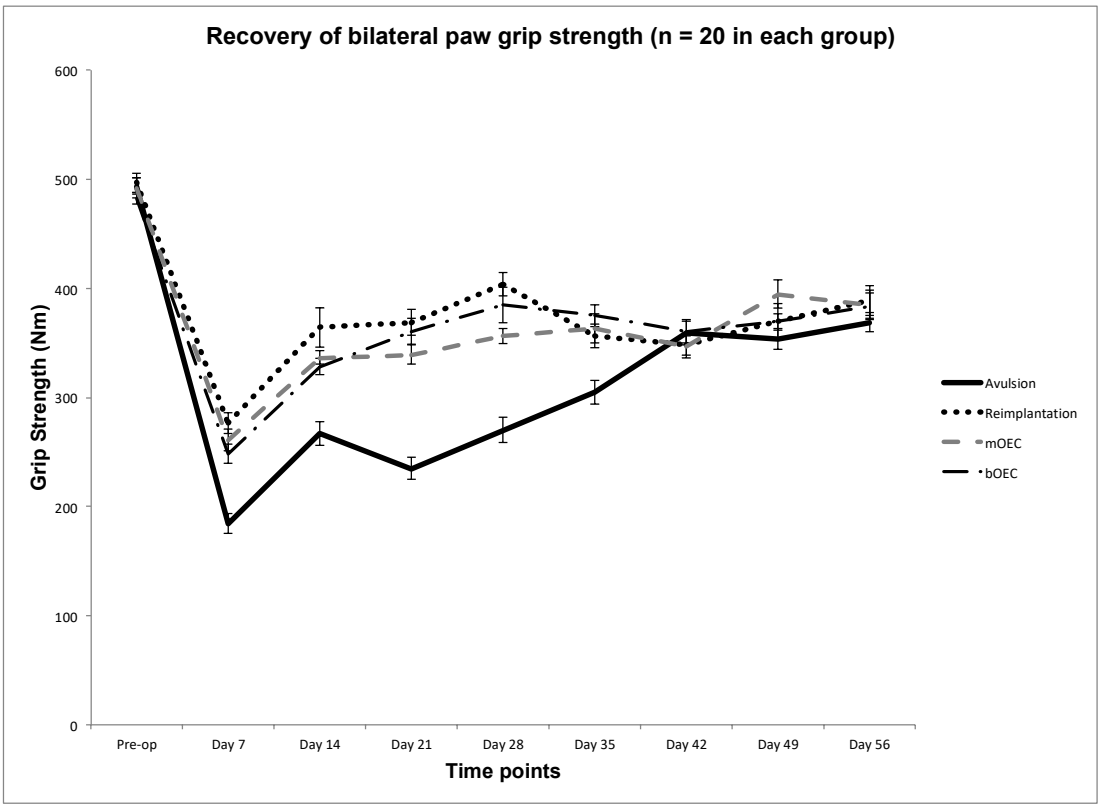

Figure 6.8. Bilateral paw grip strength recovery. Graph showing bilateral grip strength recovery in the different groups over the various test time points. Mean ± SEM shown on chart. (mOEC: mucosal OEC; bOEC: bulb OEC)

Bilateral Grip Strength		Preop	Day 7	Day 14	Day 21	Day 28	Day 35	Day 42	Day 49	Day 56
Avulsion	**Mean**	493.68	184.17	266.86	234.77	270.20	304.38	359.30	353.18	368.78
	Std. Deviation	65.84	67.94	83.66	90.94	95.45	82.46	88.30	65.00	63.41
	SEM	7.60	9.0	10.89	10.57	11.93	10.64	11.80	9.19	8.96
Reimplantation	**Mean**	496.61	276.52	364.09	369.02	403.48	356.18	348.70	369.80	388.45
	Std. Deviation	77.41	79.23	156.86	104.44	90.57	78.71	73.98	107.08	77.83
	SEM	9.38	9.68	18.11	12.06	10.45	10.61	9.97	15.96	13.15
mOEC	**Mean**	491.82	260.65	336.63	339.02	356.05	363.42	346.43	394.85	385.28
	Std. Deviation	85.04	84.69	59.95	72.77	61.37	103.78	74.99	91.97	86.60
	SEM	8.86	9.65	6.50	8.45	7.23	13.51	10.30	13.27	13.36
bOEC	**Mean**	482.26	248.03	328.30	360.50	384.36	374.90	360.11	369.36	382.88
	Std. Deviation	50.04	81.73	70.83	110.55	142.52	84.44	85.07	63.16	94.58
	SEM	5.21	8.66	7.46	11.65	16.45	10.09	10.24	7.83	12.21

Table 6.5 Bilateral grip strength recovery data analysis. Table showing the mean, standard deviations (Std. Deviation) and standard errors of the mean (SEM) in the different groups over the different time points.

6.3.4 Retrograde labelling of motor neurone cell bodies to assess continuity of repair

All the results within the different groups were normally distributed (Table 6.6). In order to run a one-way ANOVA, we decided to perform a Test of Homogeneity of Variances (Table 6.7). However, the assumption of homogeneity of variances was violated, as per Levene's test for quality of variances ($p<0.005$). Subsequently a modified one-way ANOVA, a Welch ANOVA was performed. This test statistic demonstrated that there was a statistically significant difference in the labelling in the different groups, Welch's $F(7, 30.223) = 170.98$, $p<0.005$, as per the Robust Tests of Equality of Means (Table 6.7). The Games-Howell post hoc test was subsequently run to compare all possible combinations of group differences, as the assumption of homogeneity of variances was violated. This post hoc test provides confidence intervals for the differences between group means and shows whether the differences are statistically significant. The Games-Howell post hoc test is presented below (Table 6.8). Retrograde labelling of motor neurones in the different groups is charted in Figure 6.9 a&b.

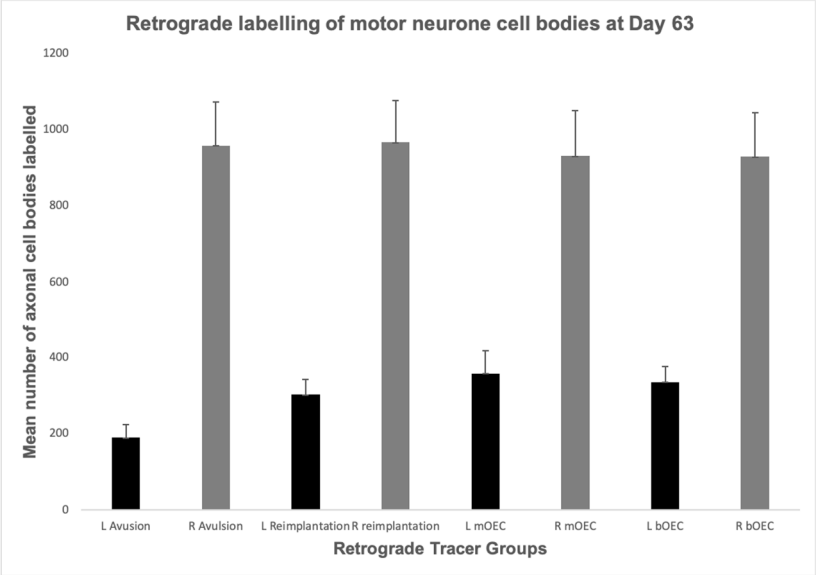

Figure 6.9a. Retrograde labelling of motor neurone cell bodies at day 63. Graph showing the mean number of motor neurone cell bodies labelled by retrograde tracer Fast Blue® in the left and right-side motor neurone pool corresponding to the C8 nerve root. Average labelled motor neurone cell body numbers indicated on chart. L: left, surgery side; R: right, control normal side. Error bars represent SD. (Avulsion n = 14; Reimplantation n = 13; mOEC n = 15; bOEC n = 14, day 63)

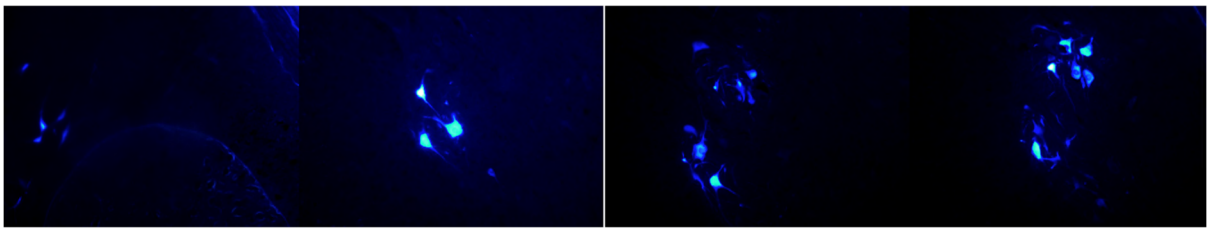

Figure 6.9b. Retrograde labelling of motor neurone cell bodies at day 63. Flourescense microscope images of Fast Blue® labelling in the avulsion, reimplantation, mOEC and bOEC groups.

Group	n	Mean	Standard Deviation	Standard Error	95% Confidence Interval for Mean		Minimum	Maximum
					Lower Bound	Upper Bound		
L Avulsion	14	190.1	32.6	10.3	166.7	213.4	146.0	243.0
R Avulsion	14	958.8	113.8	36.0	877.3	1040.2	853.0	1190.0
L Reimplant	13	302.1	41.1	14.5	297.7	366.4	289.0	401.0
R Reimplant	13	967.5	109.3	38.6	876.1	1058.8	799.0	1178.0
L mOEC	15	358.3	59.6	17.9	318.2	398.4	296.0	477.0
R mOEC	15	930.6	117.8	35.5	851.4	1009.8	799.0	1191.0
L bOEC	14	335.2	41.8	12.0	308.6	361.8	298.0	422.0
R bOEC	14	929.6	114.9	33.1	856.6	1002.6	799.0	1201.0

Table 6.6. Retrograde labelling of motor neurone cell bodies data analysis. Mean, standard deviation, standard error of the mean and confidence intervals. L: left; R: right. n represents the final number of rats in each group at day 63. (n=20 at start of study)

	Levene Statistic	df1	df2	Significance
Based on Mean	3.545	7	74	.002
Based on Median	1.891	7	74	.083
Based on Median and adjusted df	1.891	7	44.8	.094
Based on trimmed mean	3.135	7	74	.006

Table 6.7. Statistical analysis of retrograde tracers. Table showing that Levene's test is significant, and that the different Fast Blue® retrograde tracer groups do not have equal variances. (Above) Statistical analysis of retrograde tracers. Robust tests of equality of means for retrograde tracers. (Below)

Welch's ANOVA indicated that there was a significant difference between the labelled motor neurone cell bodies in the 4 different groups. Subsequently, a pairwise comparison post hoc analysis using the Games-Howells test was conducted to look for differences between the groups (Table 6.8). The test showed that there was a significant difference between the avulsion group and the reimplantation, mOEC and bOEC groups. ($p<0.0005$) There was also a significant difference between the reimplantation and mOEC and bOEC groups. ($p<0.005$). Although the mOEC and mOEC groups were significantly different from the avulsion and reimplantation groups there was no significant difference between the mOEC and bOEC groups. ($p = 0.956$)

(I) Tracers	(J) Tracers	Mean			95% Confidence Interval

		Difference (I-J)	Std. Error	Sig.	Lower Bound	Upper Bound
L Avulsion	**R Avulsion**	-768.70*	37.45	.000	-907.84	-629.55
	L Reimplantation	-142.02*	17.82	.000	-205.49	-78.55
	R Reimplantation	-777.40*	40.00	.000	-935.69	-619.10
	L mOEC	-168.26*	20.73	.000	-240.19	-96.33
	R mOEC	-740.53*	37.00	.000	-875.14	-605.92
	L bOEC	-145.15*	15.88	.000	-198.72	-91.57
	R bOEC	-739.56*	34.73	.000	-863.46	-615.66
R Avulsion	**L Avulsion**	768.70*	37.45	.000	629.55	907.84
	L Reimplantation	626.67*	38.82	.000	485.65	767.69
	R Reimplantation	-8.70	52.82	1.000	-192.53	175.13
	L mOEC	600.43*	40.24	.000	457.28	743.58
	R mOEC	28.16	50.58	.999	-143.41	199.74
	L bOEC	623.55*	37.97	.000	483.91	763.18
	R bOEC	29.13	48.95	.999	-136.49	194.76
L Reimplant	**L Avulsion**	142.02*	17.82	.000	78.55	205.49
	R Avulsion	-626.67*	38.82	.000	-767.69	-485.65
	R Reimplantation	-635.37*	41.29	.000	-794.23	-476.51
	L mOEC	-26.23	23.12	.040	-105.68	53.21
	R mOEC	-598.51*	38.39	.000	-735.40	-461.61
	L bOEC	-3.12	18.89	0.40	-68.92	62.67
	R bOEC	-597.54*	36.21	.000	-724.32	-470.76
R Reimplant	**L Avulsion**	777.40*	40.00	.000	619.10	935.69
	R Avulsion	8.70	52.82	1.000	-175.13	192.53
	L Reimplantation	635.37*	41.29	.000	476.51	794.23
	L mOEC	609.13*	42.63	.000	449.34	768.9256

	R mOEC	36.86	52.50	.996	-145.08	218.8077
	L bOEC	632.25*	40.49	.000	473.96	790.5369
	R bOEC	37.83	50.93	.994	-138.96	214.6347
L mOEC	**L Avulsion**	168.26*	20.73	.000	96.33	240.1943
	R Avulsion	-600.43*	40.24	.000	-743.58	-457.2853
	L Reimplantation	26.23	23.12	.040	-53.21	105.6886
	R Reimplantation	-609.13*	42.63	.000	-768.92	-449.3471
	R mOEC	-572.27*	39.82	.000	-711.64	-432.9001
	L bOEC	23.11	21.66	.956	-50.90	97.1328
	R bOEC	-571.30*	37.73	.000	-701.09	-441.5086
R mOEC	**L Avulsion**	740.53*	37.00	.000	605.92	875.1495
	R Avulsion	-28.16	50.58	.999	-199.74	143.4166
	L Reimplantation	598.51*	38.39	.000	461.61	735.4071
	R Reimplantation	-36.86	52.50	.996	-218.80	145.0804
	L mOEC	572.27*	39.82	.000	432.90	711.6454
	L bOEC	595.38*	37.53	.000	460.12	730.6492
	R bOEC	.96	48.61	1.000	-162.30	164.2426
L bOEC	**L Avulsion**	145.15*	15.88	.000	91.57	198.7244
	R Avulsion	-623.55	37.97	.000	-763.18	-483.9159
	L Reimplantation	3.12	18.89	0.040	-62.67	68.9289
	R Reimplantation	-632.25*	40.49	.000	-790.53	-473.9631
	L mOEC	-23.11	21.66	.956	-97.13	50.9055
	R mOEC	-595.38*	37.53	.000	-730.64	-460.1235
	R bOEC	-594.41*	35.30	.000	-719.16	-469.6652
R bOEC	**L Avulsion**	739.56*	34.73	.000	615.67	863.4676
	R Avulsion	-29.13	48.95	.999	-194.76	136.4942

	L Reimplantation	597.54*	36.21	.000	470.76	724.3222
	R Reimplantation	-37.83	50.93	.994	-214.63	138.9681
	L mOEC	571.30*	37.73	.000	441.50	701.0974
	R mOEC	-.96	48.61	1.000	-164.24	162.3032
	L bOEC	594.41*	35.30	.000	469.66	719.1682

Table 6.8. Multiple comparisons from the Games-Howell post hoc test for retrograde tracer labelling of motor neurone cell bodies. *The mean difference is significant at the 0.05 level.

6.3.5 Rat attrition rates in the different experimental groups

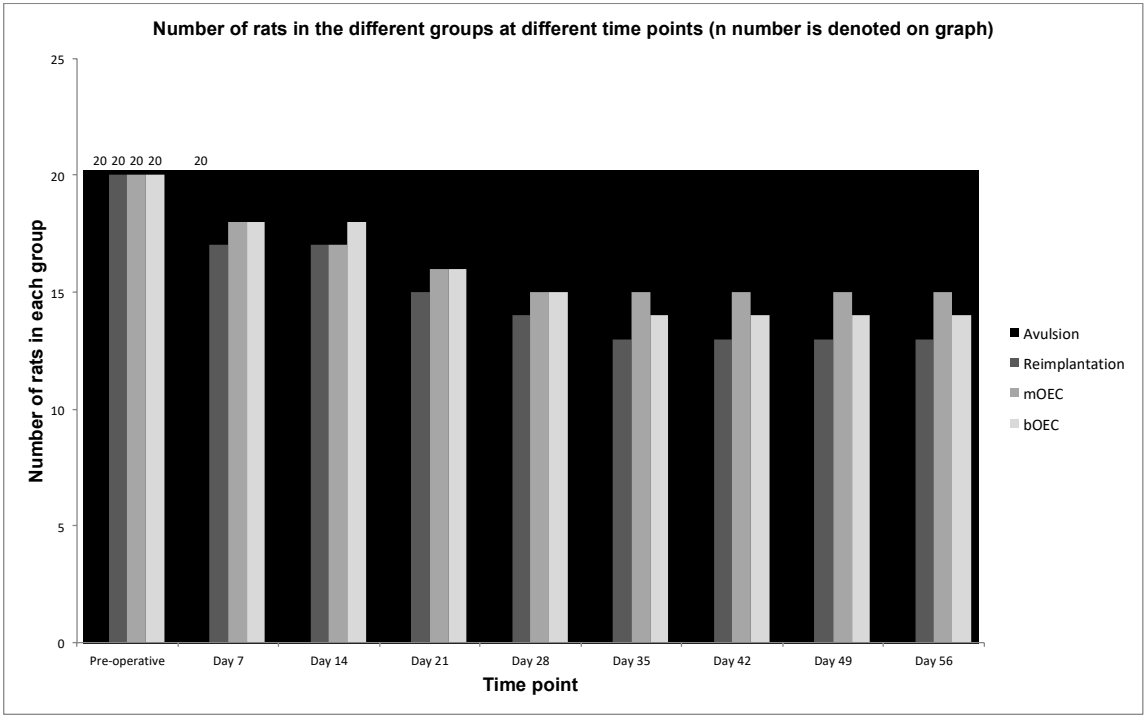

Figure 6.10. Rat attrition rates in the different groups. Chart showing the number of rats in the different groups at each time point. Attrition rates were due to immediate peri-operative complications, infection, limb deformities and autotomy. The attrition rates in the different groups are comparable at every time point and by day 56 of the study.

6.3.6 Rat forepaw deformities in the different experimental groups

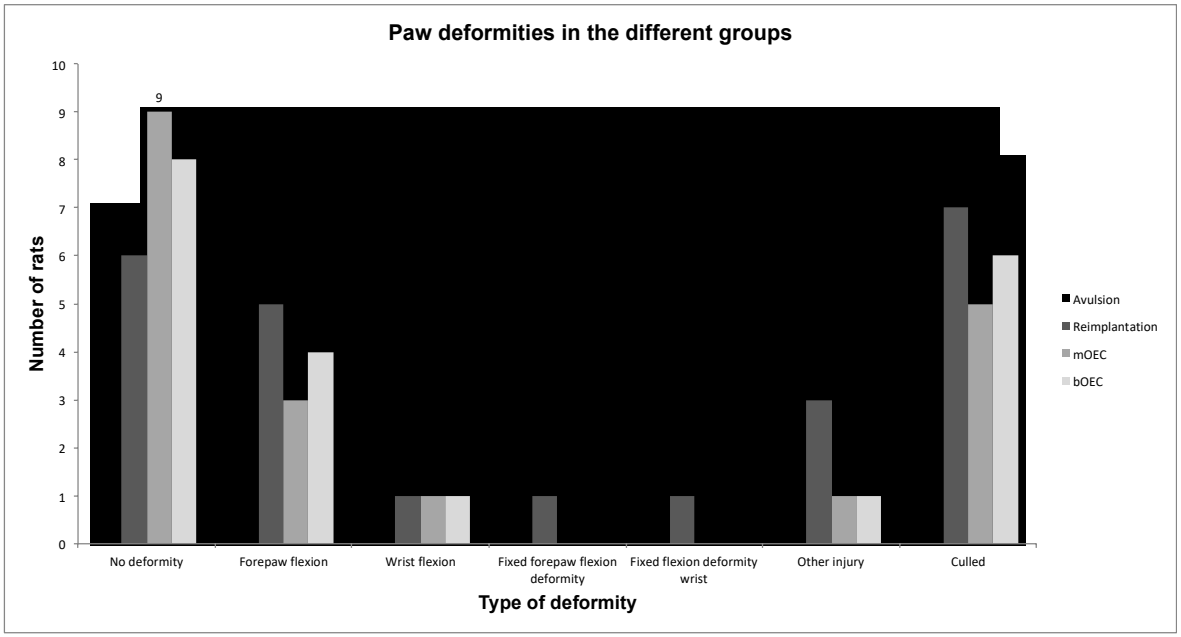

Figure 6.11. Rat forepaw deformity in the different groups during the test period. The mOEC and bOEC had the largest number of rats with no paw deformity (9 and 8 respectively, compared to avulsion (5) and reimplantation (6). The highest number of forepaw flexion deformities were in the avulsion (7) and reimplantation (5) groups. Wrist flexion deformity was highest in the avulsion group (2) and all other groups had 1 rat with this problem. Only rats in the avulsion and reimplantation groups had a fixed forepaw and wrist flexion deformity. Other injuries included autotomy of the forepaw and in some cases in the avulsion group the hind paw. The total attrition rate in the different groups over the 56 days of the study is identified as the number of rats culled.

Figure 6.12. Photograph showing normal paw spread of a Sprague-Dawley rat.

Figure 6.13. Photograph showing left paw flexion deformity after C8 dorsal root transection and ventral root surgery.

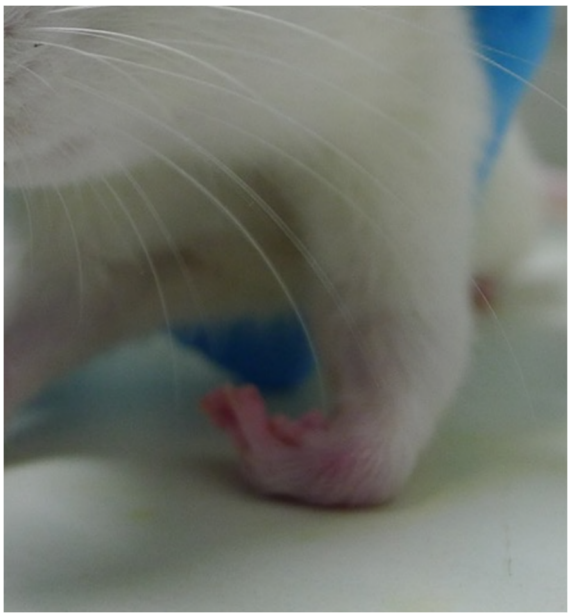

Figure 6.14. Photograph showing left wrist flexion deformity in a rat with a left C8 dorsal root transection and ventral root avulsion.

Figure 6.15. Photograph showing fixed flexion deformity at the left elbow, wrist and fingers in a Sprague-Dawley rat after C8 dorsal root transection and ventral root avulsion.

Figure 6.16. Left forepaw autotomy after C8 dorsal root transection and ventral root avulsion.

Figure 6.17. Photograph demonstrating autotomy in left hind paw of the Sprague-Dawley rat following left C8 dorsal root transection and ventral root avulsion.

6.3.7 Histology & Immunohistochemistry

6.3.7.1 Avulsion group

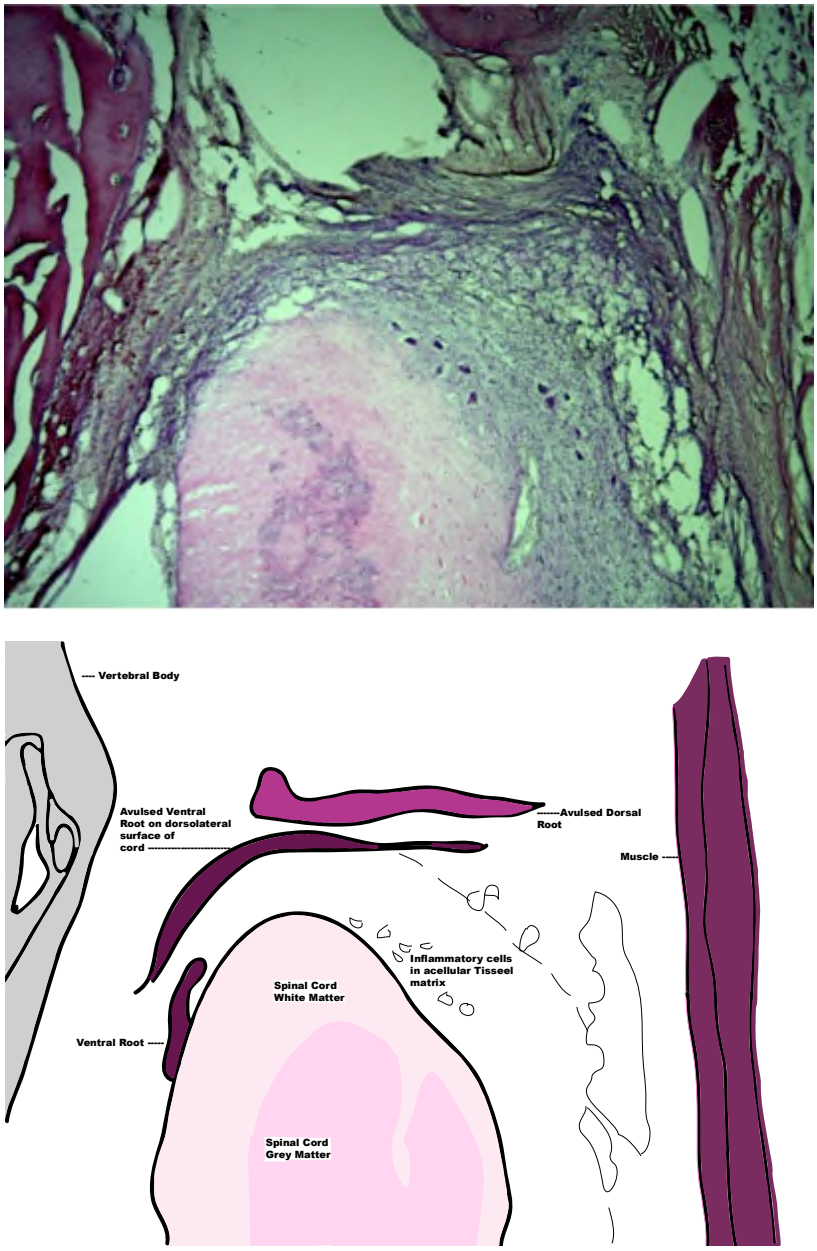

Figure 6.18. Avulsion group histology, schematics & immunohistochemistry images. a & b: a) Cross section of rat cervical spinal cord demonstrating avulsed C8 ventral root on the dorsolateral aspect of the spinal cord, with overlying avulsed dorsal root. Inflammatory cells in an amorphous matrix composed of Tisseel® and break down products is visible. The ventral root is juxtaposed to the cord but has not been

reimplanted into the dorsolateral aspect of the cord. (Haematoxylin & Eosin x4) b) Schematic of image a) identifying structures that can be seen in the cross section.

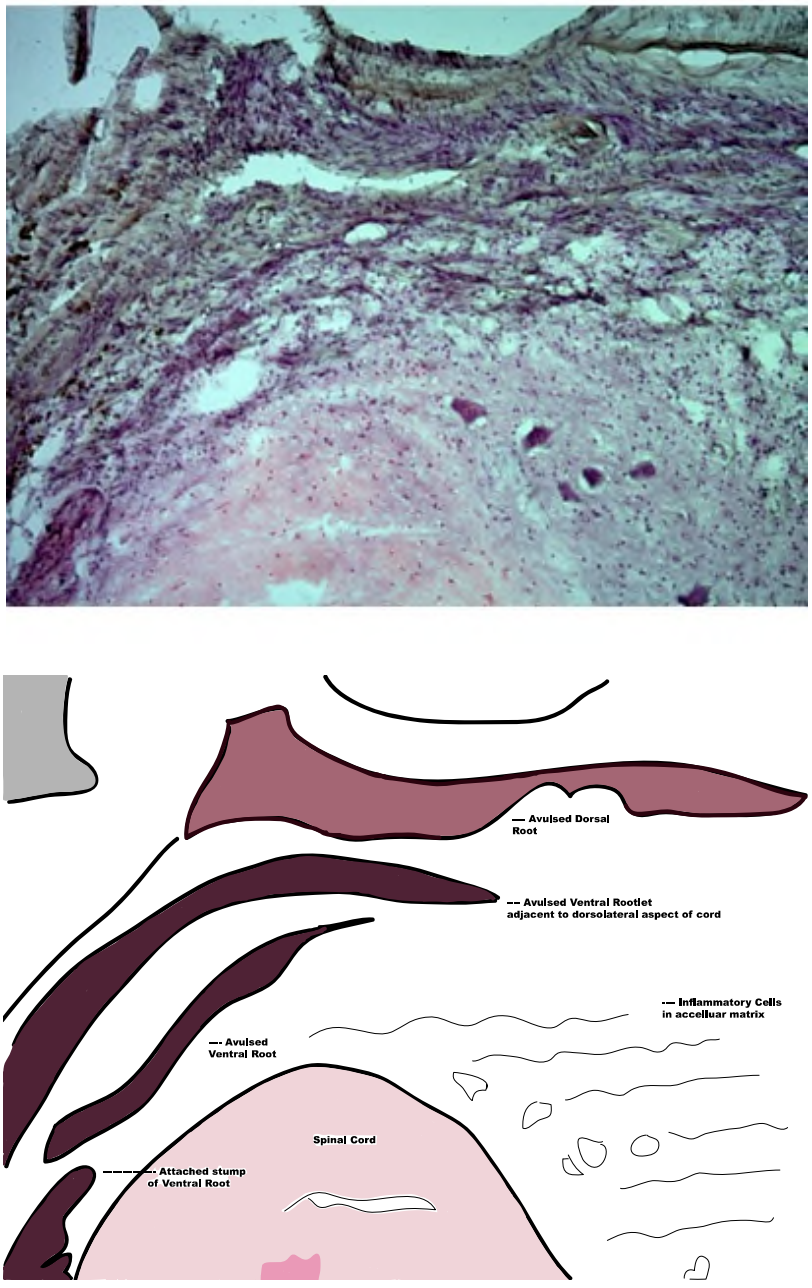

Figure 6.18. c & d: c) Higher power cross section of rat cervical spinal cord demonstrating avulsed C8 ventral root on the dorsolateral aspect of cord. A clear gap between the root and cord is identified, despite the application of Tisseel® at the time of surgery, implying there is no continuity of ventral root fibres with the spinal cord. Amorphous acellular material, representing Tisseel® breakdown products and inflammatory reaction characterised by the presence of mononuclear cells is

demonstrated. (Haematoxylin & Eosin x10) d) Schematic of image b) identifying structures that can be seen in the cross section.

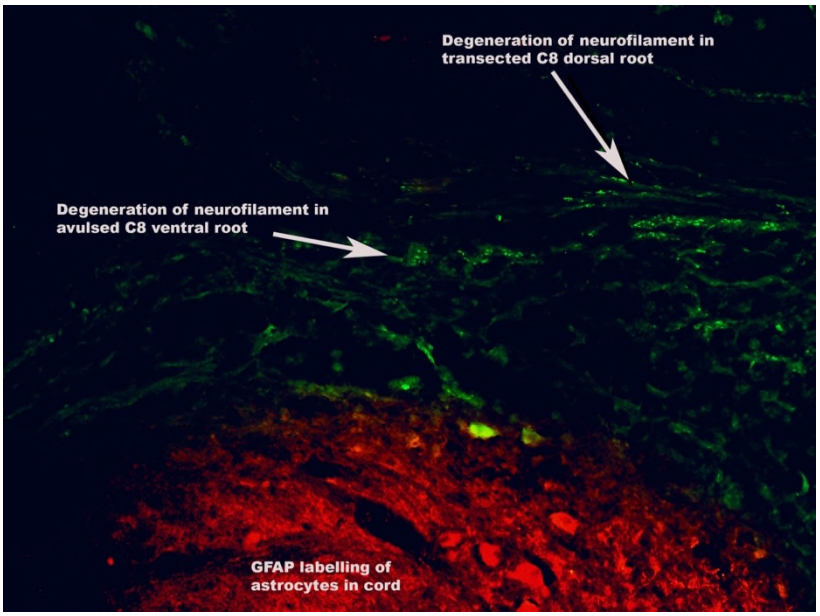

Figure 6.18. e) Double staining with neurofilament (green) and GFAP (red)) x10, as viewed on the fluorescence microscope. In the avulsed ventral root the neurofilament is severely degenerated and is not in a regular organised pattern. GFAP labelling demonstrates astrocytic cells within the cord, but none in the avulsed ventral root. Large mononuclear cells can also be seen in the background artefact, likely representing inflammatory mononuclear cells.

6.3.7.2 Reimplantation group

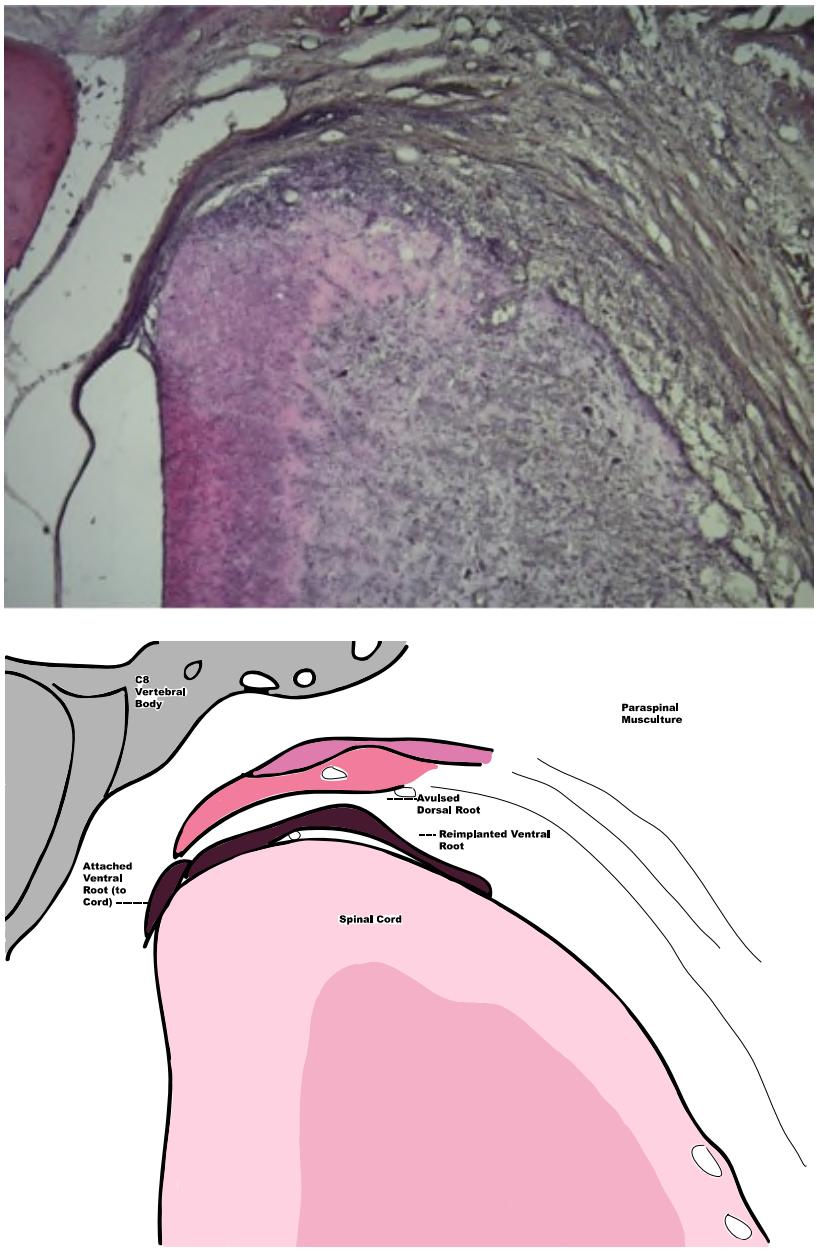

Figure 6.19. Reimplantation group histology, schematics & immunohistochemistry images a & b: Cross section of rat cervical spinal cord demonstrating reimplanted C8 ventral root on the dorsolateral aspect of cord, with overlying avulsed dorsal root. The ventral root is juxtaposed to the cord, as the pia has been opened and the root reimplanted. (Haematoxylin & Eosin x4) b) Schematic of image a) identifying structures that can be seen in the cross section.

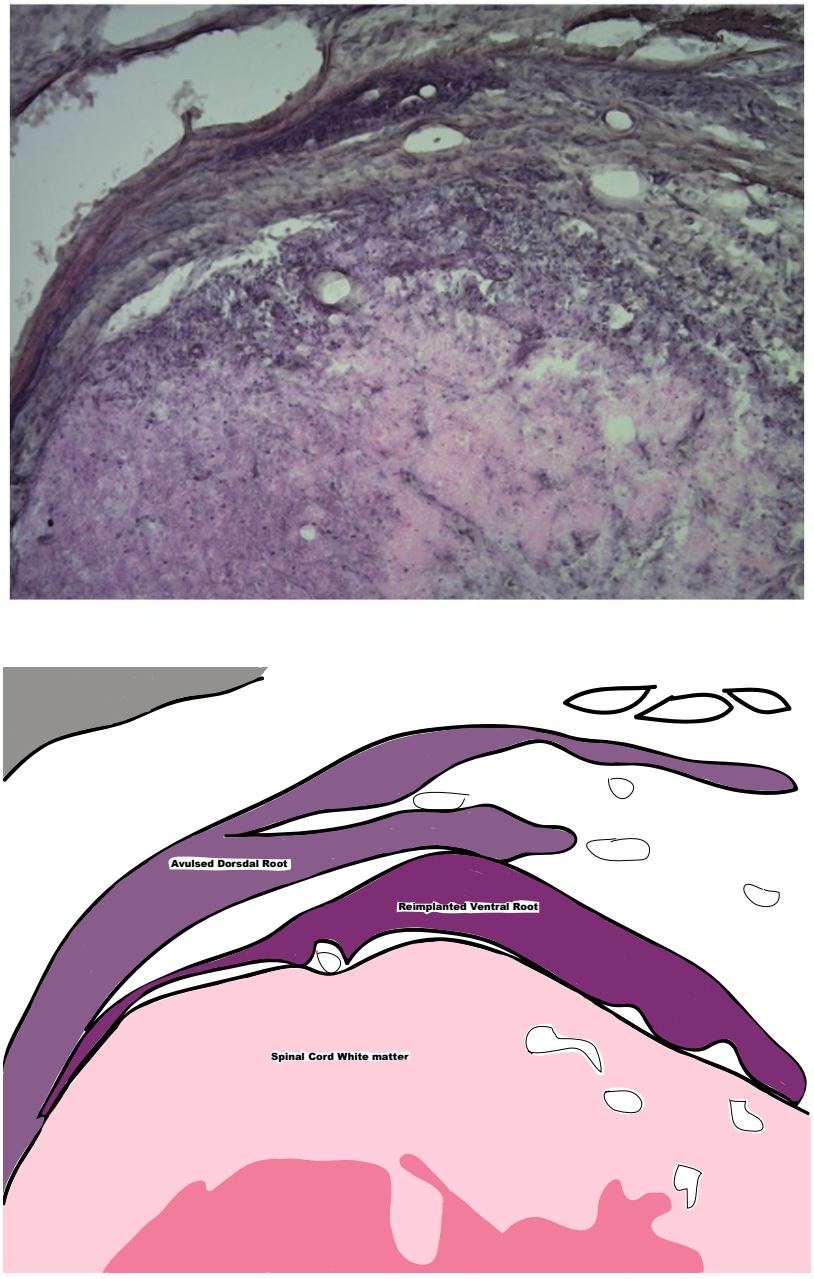

Figure 6.19. c & d: c) Higher power cross section of rat cervical spinal cord demonstrating reimplanted C8 ventral root on dorsolateral aspect of cord, with the ventral root juxtaposed to the dorsolateral cord surface. (Haematoxylin & Eosin x10). An eosinophilic response denoting a chronic inflammatory infiltrate is identified at the reimplantation site. d) Schematic of image b) identifying structures that can be seen in the cross section.

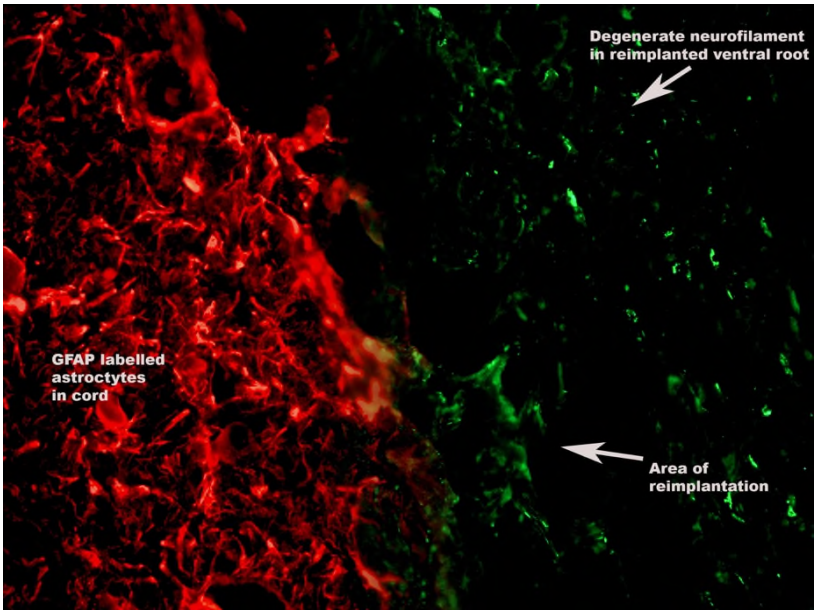

Figure 6.19. e) At high power (x20) degeneration of the neurofilament (green) in the reimplanted C8 ventral root is noted. In contrast to the avulsion group there is still an organised structure to this arrangement. In addition connections between the reimplanted ventral root and the spinal cord are visible in this image. GFAP (red) labelling shows astrocytes in the adjacent spinal cord, but not the reimplanted ventral root.

6.3.7.3 Mucosal OEC group

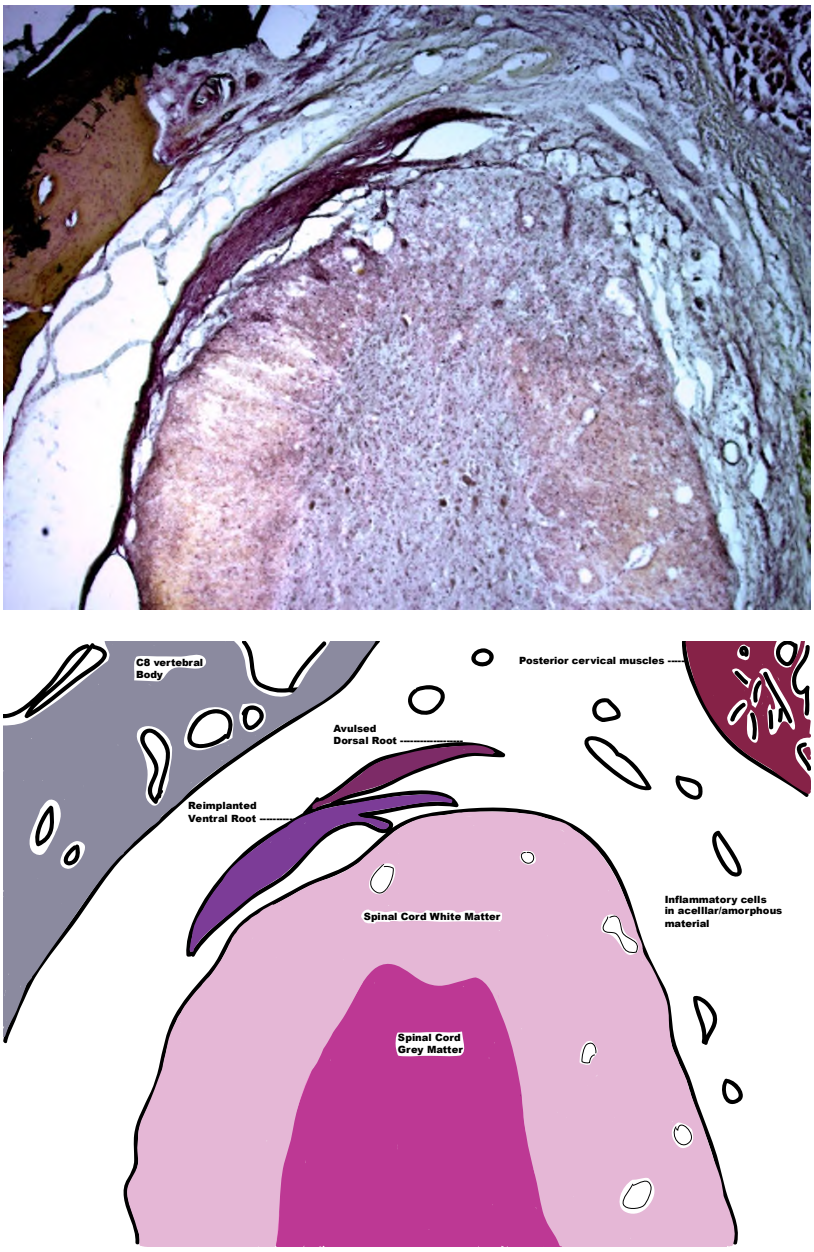

Figure 6.20. Mucosal OEC group histology, schematics & immunohistochemistry images. a & b: Cross section of rat cervical spinal cord demonstrating reimplanted C8 ventral root on the dorsolateral aspect of cord, the reimplantation has been augmented with mucosal OECs (not visible). The ventral root is juxtaposed to the cord. (Haematoxylin & Eosin x4) b) Schematic of image a) identifying structures that can be seen in the cross section.

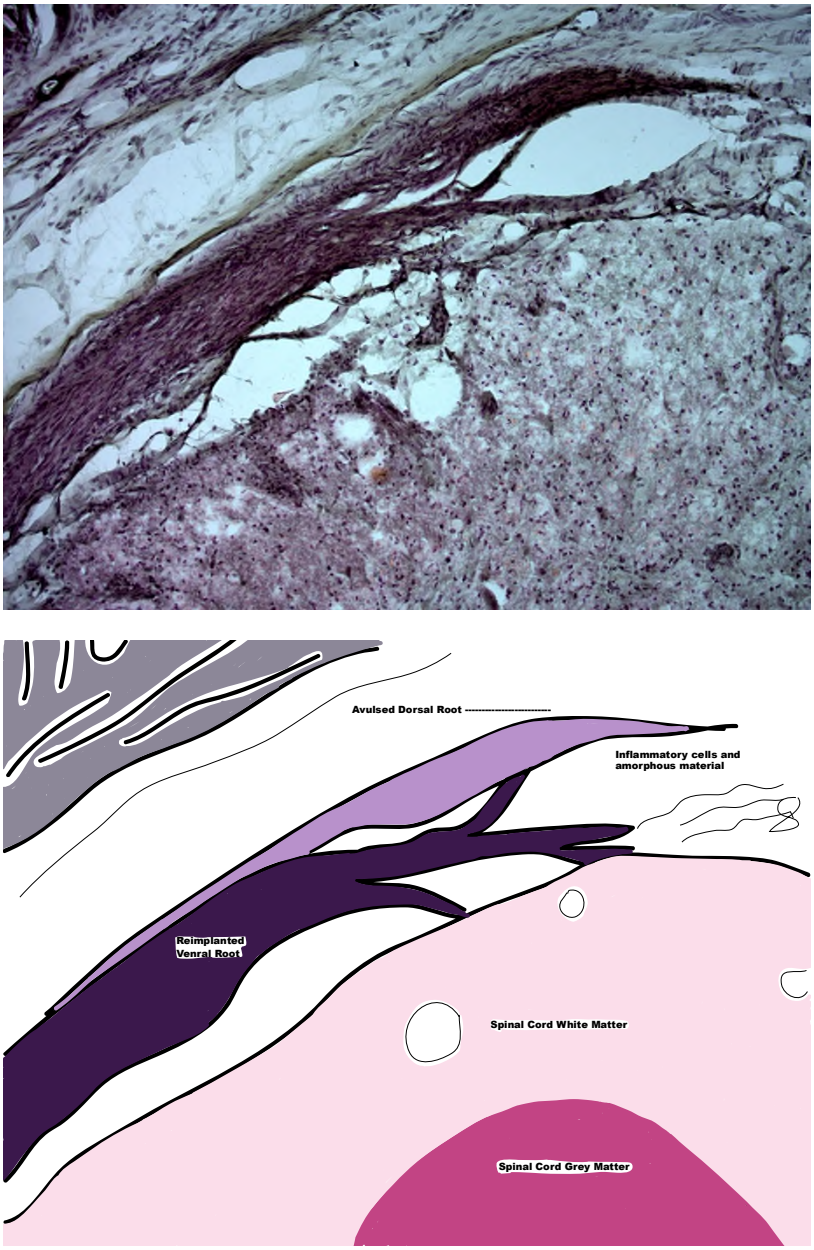

Figure 6.20. c & d: Higher power cross section of rat cervical spinal cord demonstrating reimplanted C8 ventral root on dorsolateral aspect of cord, with rootlets reimplanted into the cord surface. (Haematoxylin & Eosin x10). An eosinophilic response denoting a chronic inflammatory infiltrate is identified. d) Schematic of image b) identifying structures that can be seen in the cross section.

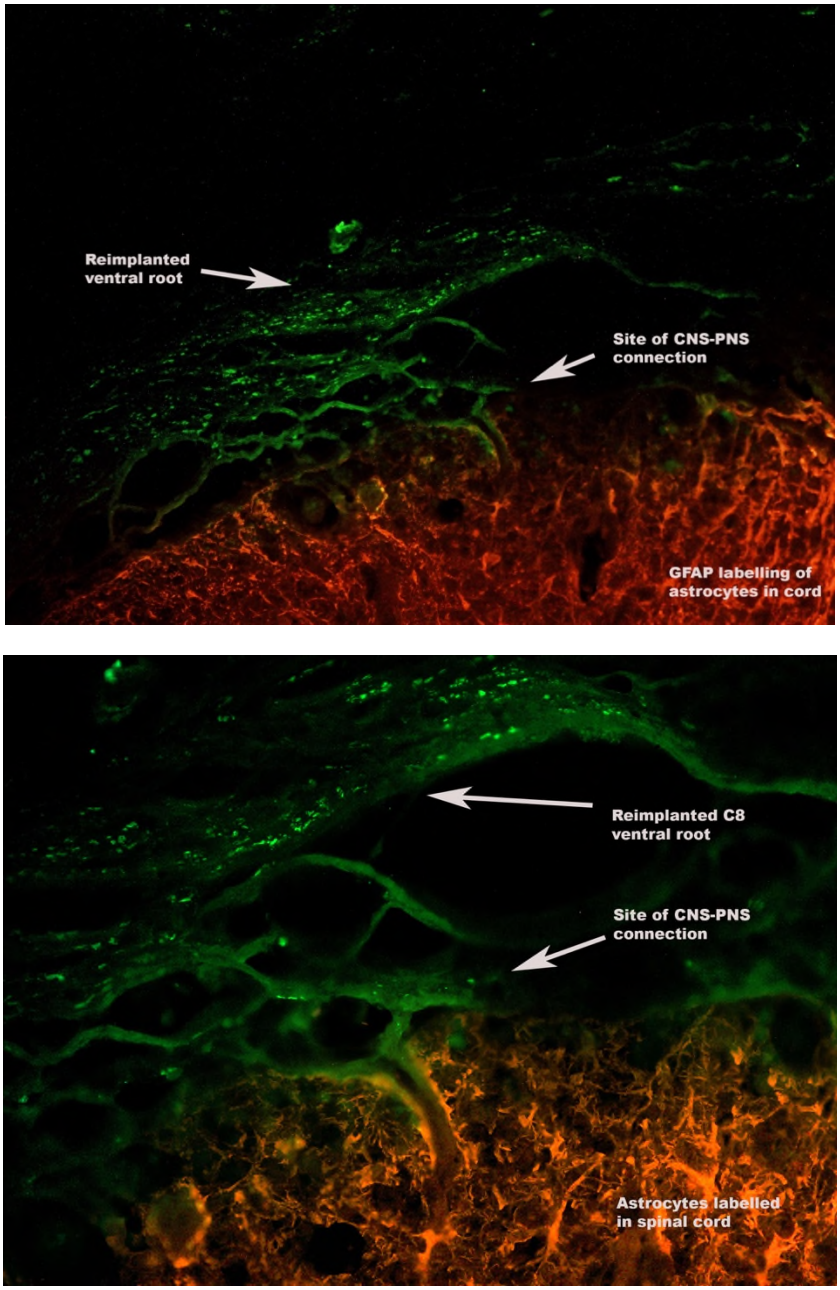

Figure 6.20. e) Neurofilament (green) and GFAP (red) staining x10, as viewed on the fluorescence microscope. In the reimplanted C8 ventral root the neurofilament shows a degree of organisation which is not seen in the avulsion groups. However, compared to a normal ventral root the fibres are more degenerate and less organised, but less so compared with an avulsed ventral root. GFAP labelling demonstrates astrocytic cells within the cord. f) At higher power (x20) Neurofilament (green) arrangement in the reimplanted ventral root is noted at the CNS-PNS interface. Neurofilament in the reimplanted ventral root can also be seen entering the spinal cord.

6.3.7.4 Bulb OEC group

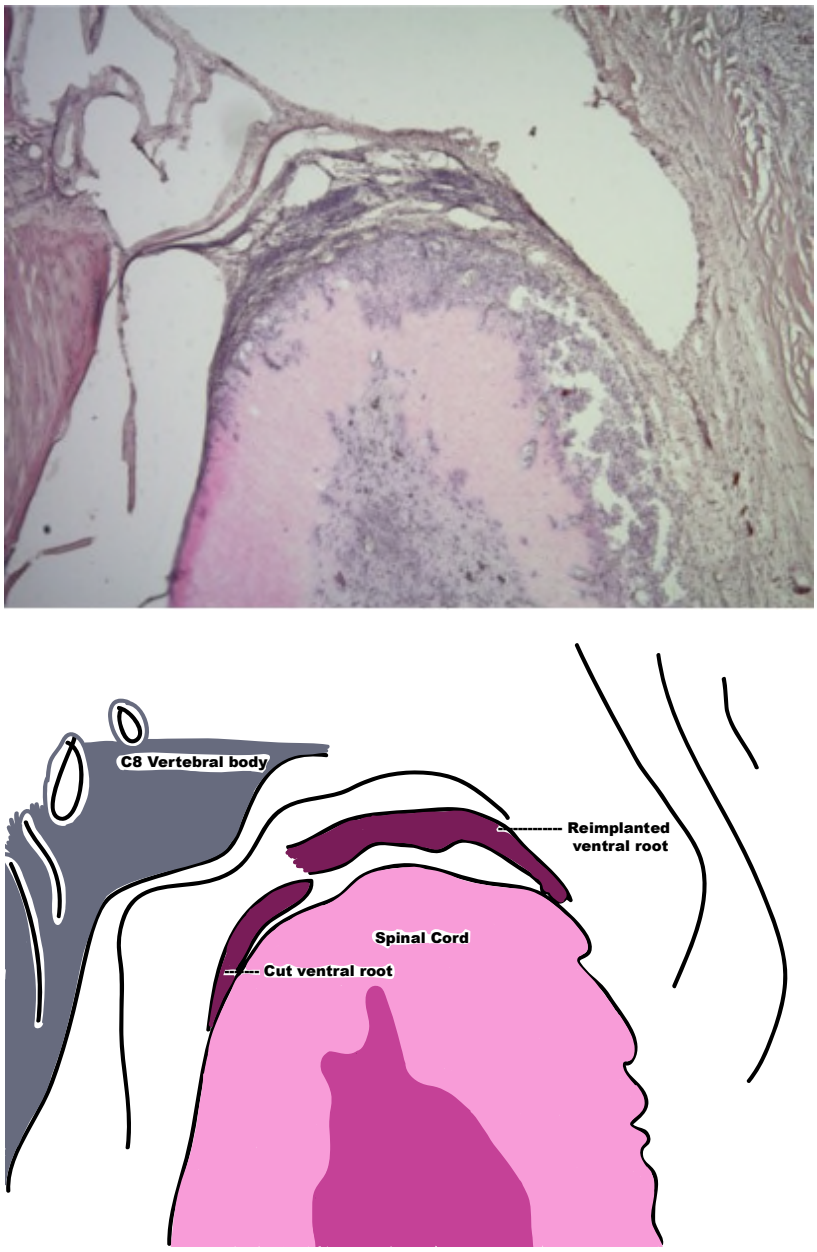

Figure 6.21. Bulb OEC group histology, schematics & immunohistochemistry images. a & b: Cross section of rat cervical spinal cord demonstrating reimplanted C8 ventral root on the dorsolateral aspect of cord, the reimplantation has been augmented with bulb OECs (not visible). (Haematoxylin &Eosin x4) b) Schematic of image a) identifying structures that can be seen in the cross section.

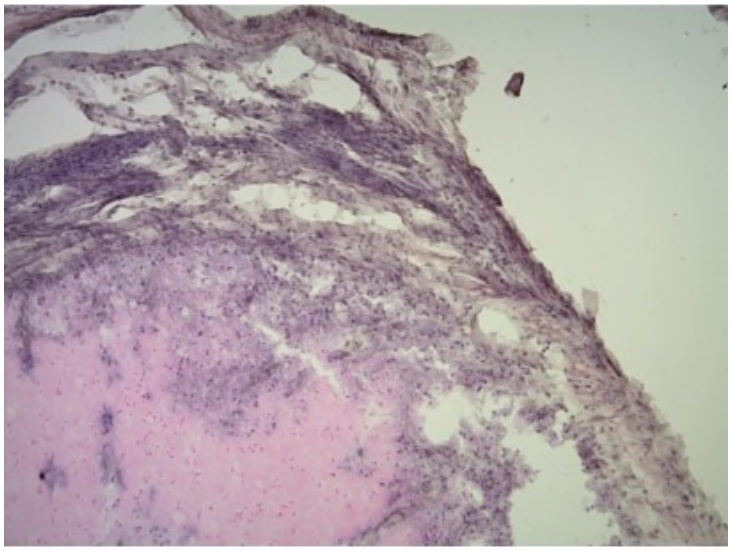

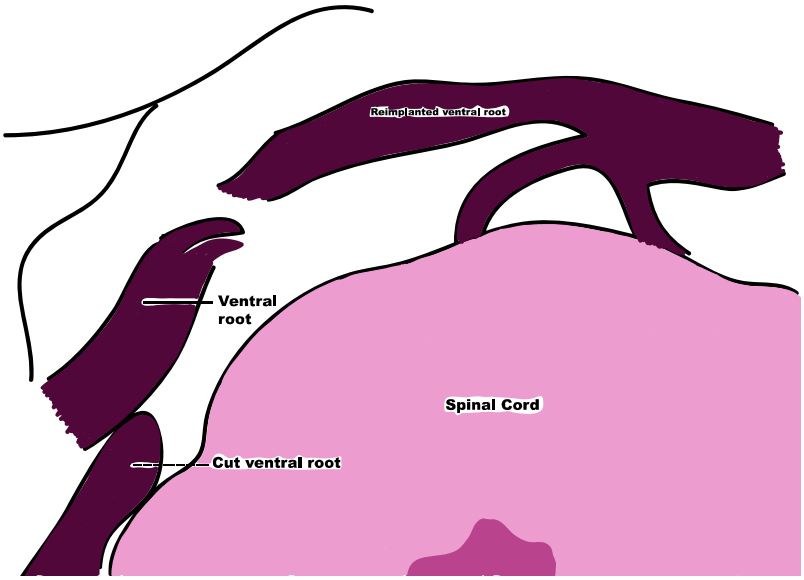

Figure 6.21. c & d: Higher power cross section of rat cervical spinal cord demonstrating reimplanted C8 ventral root on dorsolateral aspect of cord, with rootlets reimplanted into the cord surface. (Haematoxylin & Eosin x10). An eosinophilic response denoting a chronic inflammatory infiltrate is identified. d) Schematic of image c) identifying structures that can be seen in the cross section.

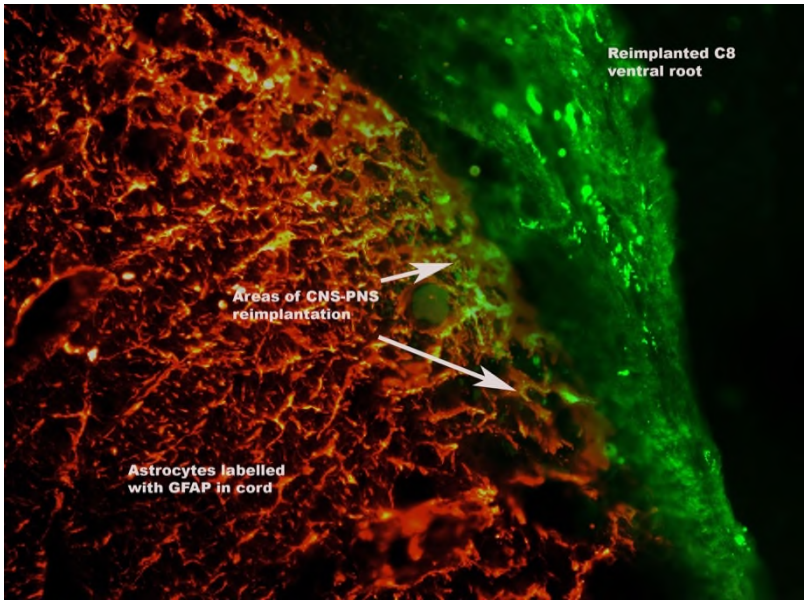

Figure 6.21. e) Neurofilament (green) and GFAP (red) staining x20, as viewed on the fluorescence microscope. In the reimplanted C8 ventral root the neurofilament in the ventral root can be seen entering the cord at the CNS-PNS interface. The neurofilament arrangement shows a degree of organisation. However, compared to a normal ventral root the fibres are more degenerate and less organised, GFAP labelling demonstrates astrocytic cells within the cord.

6.3.7.5 Additional histological images of selected spinal cord sections

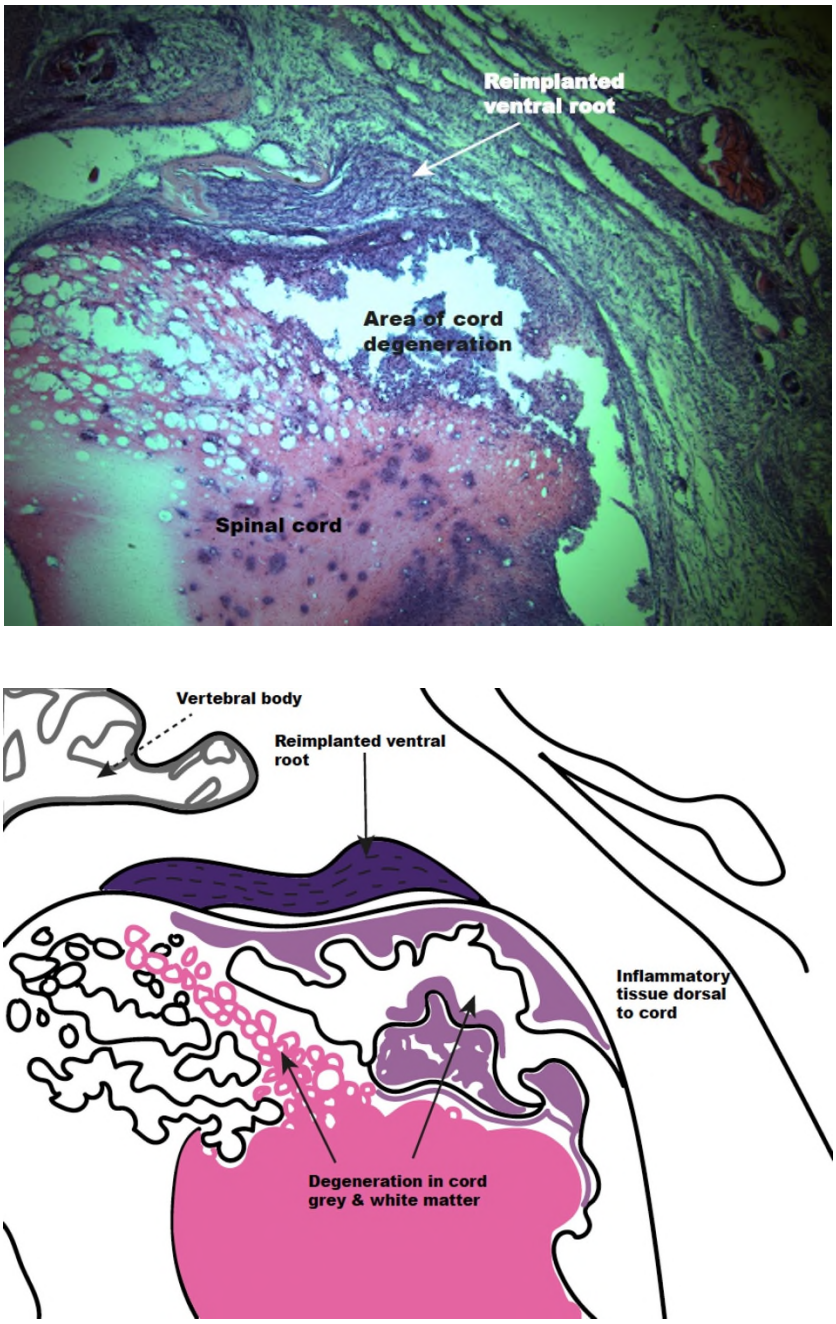

Figure 6.22. Cervical cord necrosis histology and schematic. a & b) Cross section of rat cervical spinal cord demonstrating reimplanted C8 ventral root on the dorsolateral aspect of cord. (Haematoxylin &Eosin x4) The rat was culled at day 7 because it demonstrated a left sided hemiparesis. The reimplantation has led to a significant spinal cord injury. b) Schematic of image a) identifying structures that can be seen in the cross section.

6.4 Discussion

Repair of the CNS remains a major challenge and although a myriad of preclinical and clinical trials have been conducted over the past three decades a successful treatment strategy remains elusive. A cervical ventral root avulsion injury occurring at the CNS-PNS transition zone is considered a longitudinal spinal cord injury. (Carlstedt, 2007) If left untreated it leads to rapid death of up to 90% the motor neurone cell bodies in the anterior horn of the spinal cord, with significant neurological impairment and morbidity. (Koliatsos et al., 1994) Failure of axons to regenerate across the injury site is attributed to a number of factors including lack of trophic support, vascular damage, and a non-permissive environment created by the formation of a glial scar. (Carlstedt, 2008)

Although a number of surgical strategies have been devised to treat brachial plexus avulsion injury, including ventral root reimplantation, there is currently no cure. (Kachramanoglou et al., 2011b, Carlstedt, 1997) The versatility of cellular therapies makes them an ideal candidate for the treatment of CNS injury. Several preclinical and clinical studies have highlighted the potential therapeutic role of OECs for repair of CNS injuries. (Li et al., 2004, Ibrahim et al., 2009a, Li et al., 1997, Ramon-Cueto and Avila, 1998, Imaizumi et al., 1998, Kato et al., 2000, Barnett et al., 2000) In our series of experiments, we have augmented a rat model of C8 ventral root reimplantation after avulsion injury, with mOEC and bOEC to assess their ability for CNS repair. We have used functional tests, retrograde labelling of axonal tracts to assess continuity of repair across the injury site, histology and immunohistochemistry to provide evidence of repair across the surgical site.

6.4.1 Assessing functional recovery using left paw spread recovery

Paw spread recovery was a primary outcome measure in the study. The data analysis suggests that the avulsion group had the least recovery, followed by the reimplantation group. Following surgery, at day's 7 and 14, there was no significant difference in the left paw spread in any of the groups. ($p = 0.282$) However, by day 21 the recovery in paw spread of the reimplantation group was significantly better than the avulsion group ($p<0.005$) and mOEC and bOEC groups were significantly better than the reimplantation group ($p<0.005$). However, there was no difference in the recovery in the mOEC and bOEC groups ($p = 0.052$) From day 21 onwards the paw spread recovery in the reimplantation group was significantly better than the avulsion group, at every time point up to and including day 56. The paw spread in the mOEC and bOEC recovered better than the reimplantation group and the paw spread recovery in these groups was significantly better than the reimplantation group at every time point from day 21 onwards up to day 56.

The enhanced recovery in the reimplantation group compared to the avulsion group is likely attributed to the survival of anterior horn motor neurone cell bodies, as confirmed by the retrograde labelling of cell bodies (see later). Reimplantation of the ventral root can arrest the process of motor neurone cell death caused by root avulsion. (Koliatsos et al., 1994) Growth of the cut axons or sprouting of dendritic processes from the soma can lead to new connections between cell bodies and peripheral axons in the ventral root stump. (Linda et al., 1985, Linda et al., 1992) The histology and immunohistochemistry staining with neurofilament and GFAP confirmed the apposition of the reimplanted root into the spinal cord and this likely to have

contributed to motor neurone survival and recovery of paw spread in the reimplantation group. (Figures 6.18 to 6.21)

From our studies the effect of mOEC and bOECs on the improved paw spread recovery is apparent but the mechanism by this was achieved remains unclear. Although the reimplanted nerve roots could be seen in the examined cross sections the GFP labelled OECs could not be identified. (discussed later) Neurofilament could be seen entering the spinal cord at the CNS-PNS interface in these and the reimplantation group, so we have to assume that the improved recovery in paw spread in these groups is attributed to the presence of OECs. Although earlier studies suggested that OECs promoted axonal outgrowth from the injury site many recent studies have suggested functional recovery in the absence of significant axonal regeneration, with proposed mechanisms including neuroprotection, reduced glial scar formation, angiogenesis and local sprouting and plasticity. (Barnett et al., 2000, Boyd et al., 2005, Li et al., 1997, Ramon-Cueto and Avila, 1998, Raisman and Li, 2007, Au and Roskams, 2003) Other studies have demonstrated that transplantation of bulb OECs into corticospinal tract lesions induced regeneration of axons and restoration of function. (Li et al., 1998) However, mucosal OECs transplanted into the same lesions produced functional repair without regeneration of the damaged axons, indicating that mucosal OECs may have the ability to enhance plasticity. (Yamamoto et al., 2009) As the recovery of paw spread in the mOEC and bOEC groups was better than the reimplantation group, but was not significantly different between the two groups, it is likely that the presence of OECs has led to an improvement in the functional outcomes as well as survival of motor neurone cell bodies (discussed later).

6.4.2 Assessing functional recovery by analysing left paw grip strength recovery

Left paw grip strength recovery was another primary outcome in this study. Although there was a significant reduction in left forepaw grip strength at day 7 in all groups, there was a gradual but differing rate of recovery in the groups over the 8-week test period. By day 56 there was no significant difference in left paw grip strength recovery between the groups and paw strength remained significantly reduced compared with the preoperative values.

As expected, there was no significant difference in mean preoperative left paw grip strength in the avulsion, reimplantation, mOEC and bOEC preoperatively. At day 7, the left paw grip strengths were significantly lower than preoperatively but there was no difference between the groups. C8 motor root avulsion lead to weakness in all the groups, and despite reimplanting the nerve root or adding either mOECs or bOECs, this intervention had no effect on paw recovery at this early stage.

The rate of left paw strength recovery did vary in the different groups. The reimplantation group was significantly better than the avulsion ($p<0.005$) and the bOEC ($p<0.005$) at day 14 and by day 21 the reimplantation, mOEC and bOEC left paw grip recovery was significantly better than the avulsion group ($p<0.005$). By day 28 paw recovery in all groups was better than avulsion ($p<0.005$) and the bOEC paw strength had recovered and was comparable to the reimplantation and mOEC groups. However the reimplantation group paw strength recovery was significantly better than the mOEC group ($p = 0.021$). However, by days 35 & 42 there was no significant recovery in left paw strength between the four groups. At Day 49, the mOEC recovery was significantly better than the reimplantation group. ($p = 0.017$)

However, at day 56 the mean left paw grip strength had recovered in all groups, with the mean left paw grip strength in avulsion, reimplantation, mOEC and bOEC showing no significant difference.

From the preliminary functional tests studies (Chapter 5), the difference in left paw grip strength recovery between the avulsion and reimplantation groups had meant that for a power of 90% a and a 20% attrition rate, a sample size of 18.75 would be enough to detect a difference between the avulsion and reimplantation groups. The attrition rate in our study was such that by day 14 we had 18 or less rats in each of the four groups, primary due to autotomy or self-harm (see later). By day 56 there were 14 rats in the avulsion, 13 in the reimplantation, 15 in the mOEC and 14 in the bOEC. This attrition rate may have influenced the effect size and the subsequent underpowering of the study may have contributed to the findings. Similarly, the sample size to detect the effect size was a direct comparison between the avulsion and reimplantation groups. At this stage of the study we did not have data for the mOEC and bOEC groups, so it may well be the case that the sample size needed to detect a significant difference in these groups may actually be higher.

Rats in the avulsion and reimplantation groups had higher levels of forepaw and wrist flexion deformities compared to the mOEC and bOEC groups. These groups subsequently had higher initial attrition rates. Deafferentation is known to increase the rate of self-mutilation injury in rats so the combination of a dorsal root transection and ventral root avulsion may have led to greater forepaw deformity and an inability to grip the grip strength meter appropriately, with greater degrees of autotomy. (Dennis and Melzack, 1979, Lombard et al., 1979) Subsequently, the rats in the avulsion group had higher attrition rates between days 14 and 21, so that the grip strength measurements from the remaining rats in the group, who by definition had less paw deformity, better

grip ability and less autotomy, improved the average left paw grip strength in this group.

Rats in the reimplantation group had a better recovery rate between days 7 and 28 compared to the mOEC and bOEC rates but after this point they improved in all groups. Although the neurotrophic effects of mOEC and bOEC may have led to less paw deformity and better ability to grip the grip strength meter, with lower initial attrition rates in this group, the addition of OECs did not make a significant difference to left paw grip strengths recovery by day 56.

Rat forepaw function is a directly related to median nerve function, of which the C8 nerve root is an important contributor to the forepaw flexors. (Greene, 1968) However, it may be the case that left forepaw grip strength testing was not sufficient to quantify the degree of deficit with a C8 lesion and this may not have been the most sensitive functional test to assess recovery of C8 ventral root function.

Similarly, other authors have shown recovery in forepaw function after repair of dorsal cervical roots augmented with OECs. (Ibrahim et al., 2009a) Dorsal roots provide sensory input important for ambulation and grasp function. In our model the dorsal root has to be transected so we can have access to the ventral root which is located on the ventral aspect of the cord. We do not reimplant the dorsal root back into the cord so in theory some of the functional deficits we have shown could be from dorsal root avulsion. However, the same surgical procedure was applied to all four of groups and we were able to show differences in functional recovery and motor neurone survival in the different test groups. So the improvements we have seen are probably from reimplantation and/or augmentation with OECs. However, motor recovery could

also be due to learned behaviours, for example where muscles are innervated by more than one nerve root.

6.4.3 Assessing functional recovery by assessing bilateral grip strength recovery

Bilateral paw strength was not one of our primary or secondary outcome measures because we failed to find a significant difference in bilateral grip strength in our provisional functional studies. (Chapter 5) However, we conducted this test at the same time as the left paw grip strength analysis, as we wanted to assess whether addition of mOEC or bOEC would made a difference to bilateral paw strength recovery.

Preoperative bilateral paw grip strength in the four groups was comparable with means in the avulsion, reimplantation, mOEC and bOEC showing no significant difference. ($p = 0.29$) At days 7,14, 21 and 28 the bilateral paw strength recovery in the avulsion group was significantly lower than the reimplantation, mOEC and bOEC groups. ($p<0.005$) This finding mirrored the finding of the left paw grip strength testing, in that the left paw strength in the avulsion group was significantly less in the first few weeks of the study, but as the left paw grip strength improved, the bilateral grip strength also improved. At day 28 bilateral paw strength in the reimplantation group was significantly better than the mOEC group ($p = 0.034$) but there were no differences in recovery up to this point between the other treatment groups. By Day 35 the avulsion bilateral paw strength had recovered to the reimplantation group, but it remained significantly weaker than the bOEC group ($p<0.005$). At days 42, 49 and 56, although the mean bilateral paw strength compared to preoperative scores was lower in all four groups, there was no significant difference in bilateral paw strength recovery between the

avulsion and the reimplantation, mOEC and bOEC groups respectively. ($p = 0.535$; $p = 0.071$; $p = 0.603$)

However, unlike with the failure to detect a difference in the recovery of left paw strength recovery, the results in the bilateral paw strength recovery were not a surprise as the preliminary functional tests we had performed in Chapter 5 indicated that bilateral paw strength recovery was no different in the avulsion and reimplantation groups. An obvious reason to detect no difference could be simply that the deficit created by a C8 root surgery was not significant enough to be detected by the bilateral grip strength testing. We had previously shown (Chapter 5) that left paw strength recovery for a power of 90% would need a sample size of at least 15 but the difference between the bilateral paw strength recovery between the avulsion and reimplantation group recovery in the provisional tests was not shown to be significant using the grip strength model. The addition of mOEC and bOEC made no difference to the recovery of bilateral paw strength.

The attrition rate in the four study groups was such that even for the left paw grip strength testing the minimum sample size needed was at least 15 to compare between the avulsion and reimplantation groups but by day 35 the only group with 15 rats was the mOEC group and at day 56 there were 14 rats in the avulsion, 13 in the reimplantation, 15 in the mOEC and 14 in the bOEC. It is likely therefore that with a C8 ventral root lesion, the bilateral grip strength functional test, powering of the study, sample size and rat attrition rate is likely to have influenced the effect size and the significance of the results.

6.4.4 Assessment of continuity of axonal fibres across the site of ventral root repair

Assessment of the number of rescued motor neurones was another primary outcome in this study. At day 56 bilateral C8 nerves in rats in each group were labelled in the extraforaminal part of the nerve root using retrograde tracer Fast Blue®. After one week the rats were culled and analysed. As expected, the results showed there was no significant difference between labelling of motor neurone cell bodies in the control right side of the cord in any of the groups ($p>0.900$). However, there was a significant reduction in motor neurone cell bodies in the treated left side in all groups and the recovery pattern also differed. In the avulsion group, the mean number of motor neurone cell bodies labelled with Fast Blue® was significantly less than in the reimplantation group. ($p<0.05$) From this result we can conclude that reimplantation of the ventral root lead to a greater survival of motor neurone cell bodies in the reimplantation group. Similarly, the mean number of motor neurone cell bodies labelled in the reimplantation group was significantly lower than in the mOEC ($p = 0.040$) and the bOEC ($p = 0.040$) groups. Augmentation with mOEC and bOEC lead to a significantly greater number of labelled motor neurones in the anterior horn of the spinal cord, corresponding to the C8 root neurone pool. However, there was no significant difference between the mOEC and bOEC groups ($p = 0.956$).

A ventral root injury will lead to degeneration and death of motor neurone cell bodies. Motor neurones are rapidly killed by ventral root avulsion with a loss of up to 90% of the cell bodies. (Koliatsos et al., 1994) This loss is due to a combination of excitotoxicity, vascular injury, loss of neurotrophic factors and the inflammatory response to avulsion which leads to an astrocytic response with glial proliferation.

(Koliatsos et al., 1994, Linda et al., 1985, Olsson et al., 2000) Over the next few weeks more than 50% of motor neurones are lost with a progressive loss over time. (Bergerot et al., 2004) So in theory, due to this time dependent survival of motor neurones, a ventral root avulsion and reimplantation in the same operation setting as in our study, should lead to a greater survival of motor neurones. However, in the reimplantation group in our study, at day 56 after reimplantation around 33% of motor neurones were detected compared to 11% in the avulsion group and 36% in the mOEC and 39% in the bOEC groups.

Thus reimplantation of a ventral root can lead to survival of motor neurones and in theory lead to the production of new axons across the CNS-PNS repair site. A single surviving motor neurone is thought to lead to the formation of multiple myelinated axons, either from the cut end or from the cell body itself. (Linda et al., 1992)

Addition of mOEC and bOEC led to a significantly greater survival of motor neurone cell bodies in the anterior horn of the spinal cord compared to the reimplantation group, although there was no difference in the number of surviving motor neurones in the mOEC and bOEC groups. This was corroborated by the enhanced paw spread recovery in the mOEC and bOEC groups. This phenomenon could be due to a number of reasons. Although regeneration could not clearly be identified, a number of factors unrelated to axonal regeneration may be responsible for the enhanced motor neurone survival. For example, this could be due to reduced scar formation improved vascularity through the release of endothelial growth factor or other neurotrophic factors due to the presence of OECs. (Lipson et al., 2003, Au and Roskams, 2003, Lakatos et al., 2003)

6.4.5 Assessment of rat attrition rates and forepaw deformities: an observational assessment

In the preoperative period there were 20 rats in each group. At day 7, no rats in the avulsion groups were culled compared to three in the reimplantation group (15%) and two in both the mOEC and bOEC (10%) groups. The reimplantation, mOEC and bOEC groups had a slightly different surgery to the avulsion group. Whereas in the avulsion group the C8 dorsal root was transected and the motor rootlets avulsed, all the other groups had an additional reimplantation procedure whereby the motor root was inserted via a direct pial opening into the dorsolateral aspect of the rat spinal cord. This procedure invariably lead to a degree of spinal cord contusion/injury, when the pial surface of the cord was disrupted to reimplant the ventral root into the cord. By day 14 the attrition rate in all the groups was similar (20-25%) and this was maintained until day 56 whereby it was 30% (n = 6) in the avulsion, 35% in the reimplantation (n = 7), 25% in the mOEC (n = 5) and 30% in the bOEC (n =6), which was not statistically different.

The attrition rate in the avulsion group increased from zero at day 7, to 1 at day 14 and was 4 by day 21. Three rats were culled between the days 14 and 21. Although this group did not have a controlled pial opening during surgery to explain the initial higher attrition rates in the other groups, they did have a higher rate of deformity and autotomy between Days 14 and 21, but after this point attrition rates were similar in all groups. (Figure 6.10)

Over the study period rats in the avulsion group were observed to have a higher number of deformities. Only five rats in the avulsion group had no deformity over the

study period, compared to six in the reimplantation and nine and eight in the mOEC and bOEC groups respectively. (Figure 6.11)

Avulsion group rats had a higher number of forepaw deformities, which consisted of either forepaw or wrist flexion or a combination of the two (n = 9), compared with only four in the mOEC and five in the bOEC groups. (Figures 6.12 – 6.17) Additionally, two rats each in the avulsion and reimplantation groups had a fixed forepaw or wrist flexion deformity, which was not seen in either of the mOEC or bOEC groups. Between days 14 and 21, rats in the avulsion group had sustained more injuries to their left forepaw, including bleeding, biting and loss of digits, which are probably in the context of phantom limb pain and/or a lack of sensation in the paws and had to be culled. Other injuries in the avulsion group included left hind paw autotomy. One of these rats was found to have a spinal cord injury on cross section but the other did not. Similarly this effect was also seen in one of the reimplantation group rats but was not observed in the mOEC and bOEC groups. In addition one of the rats in the avulsion group exhibited biting of its tail and had to be culled but this was not seen in any rats in the other groups.

The majority of rats in the avulsion group that were culled had a self-inflicted mutilation injury but the exact mechanism of autotomy is debatable. There may be a link between autotomy and pain but this remains to be proven. Autotomy has been described in animals following deafferentation injury, and a deafferentation caused by dorsal root injury is an established chronic pain model in which this behaviour is observed. A number of early studies demonstrated that rats who had had dorsal root rhizotomy self-mutilated the limb on the ipsilateral side of the lesion. (Dennis and Melzack, 1979, Lombard et al., 1979) It is hypothesized that the pain caused by deafferentation leads to self-mutilation as the animal attempts to remove the affected part of the limb,

thereby representing an animal form of anaesthesia dolorosa. (Wall et al., 1979) The two behaviours that are usually observed are chewing of the affected body part and scratching of the area in the boundary of the region abutting the deafferented and normal sensory zone. It has also been observed that the greater the brachial plexus injury the greater the degree of self-mutilation but in rats with brachial plexus lesions where nerves are spared, they are likely to have more scratching than self-mutilation. (Rabin and Anderson, 1985) Considering the fact that the reimplantation, mOEC and bOEC also had a dorsal root transection, this effect was observed in lower frequencies than in the avulsion group. It may be the case that reimplantation of the ventral root has a protective effect to this regard. The addition of OECs may also protect from this. It may be the case that mOEC and bOEC confer a protective advantage to the spinal cord/nerve roots, which meant that these rats did not have a significant deformity at this early time point.

However, a recent description has raised doubts as to whether the widely accepted theory that damage to the afferent nerve root leads to autotomy in humans. (Kachramanoglou et al., 2011a) The authors observed that self-mutilation occurred in their patient who had no pain or sensation to light touch, confirmed by neurophysiological studies, and it may simply be an attempt to remove part of a limb which has no sensation, akin to like nail-biting in humans.

6.4.6 Histology and Immunochemistry analysis of spinal cord sections

Histological and immunohistochemical analysis was done using haematoxylin and eosin and neurofilament and glial fibrillary acidic protein. In addition transplanted OECs were labelled with green fluorescent protein prior to transplantation.

In the avulsion group (Figure 6.18) histological sections confirmed the presence of transected dorsal root and avulsed ventral root, which was juxtaposed to the cord. There was presence of inflammatory exudate dorsal to the cord, representing blood and Tisseel® breakdown products, as well as formation of scar tissue, which was present in the different treatment groups. Double staining with NF and GFAP showed that the neurofilament in both the dorsal and ventral roots was highly disorganised and degenerated, which is what we expect to see in a cut nerve root at this time point. The neuronal axons in the ventral root in this group had lost continuity with the motor neurone cell body and the microscopic structure of the neurofilament reflected this change. GFAP staining demonstrated the presence of astrocytic cells in the spinal cord, which is the usual case. There was no clear evidence of central nerve fibres entering the reimplanted root on any of the reviewed sections and this represents a lack of continuity of the ventral root with the spinal cord, which was reflected in the poor paw spread recovery and reduced motor neurone survival. Furthermore, the spinal cord in these sections showed a greater deal of vacuolation and gliosis compared to the reimplantation and mOEC/bOEC groups which infers that reimplantation of the root and addition of mOEC/bOEC transplants may confer a degree of neuroprotection to the neurones in the cord.

In the reimplantation group, analysis of the histological sections at low and high power demonstrated that the ventral root was visible juxtaposed to the dorsolateral aspect of the spinal cord (Figure 6.19) and fibres could be seen entering the spinal cord. Double staining with NF and GFAP demonstrated neurofilament fibres from the ventral root attempting to bridge across from the PNS to the CNS at the reimplantation site. The organisation of the neurofilament in the reimplanted root was more regular although the presence of degenerated axons represented by the less linear arrangement was

evident, compared to normal sections. However, compared to the avulsion group the organisation and structure of the neurofilament, and hence the ventral root structure, was better, which is likely a reflection of improved motor neurone survival compared with the avulsion group. The presence of continuity between the PNS and CNS was corroborated further by the enhanced paw spread recovery in this group and the improved survival of motor neurone cell bodies labelled with Fast Blue® retrograde tracer.

In the mOEC and bOEC group histological sectioning showed a similar picture to the reimplantation groups. There was an obvious presence of connections from the ventral root into the spinal cord. However, the neurofilament staining demonstrated a more organised structure in the ventral roots of the mOEC and bOEC groups, which was markedly different to the reimplantation groups. Neurofilament fibres from the reimplanted ventral root could clearly be seen entering the cord from the ventral root in both these groups. The histological sections in these two groups showed less gliosis and chronic inflammatory cells within the grey and white mater of the spinal cord implying improved survival of cells within the cord. (Figures 6.20 & 6.21) Although the reasons for this are unclear, this phenomenon was not seen to the same degree in the reimplantation group, so it is likely that the cells responsible for this, as well as the improved paw spread recovery and enhanced motor neurone survival in these groups, are the OECs. On examination of the NF and GFAP staining in the OEC group sections a similar effect was seen in both groups and no clear structural differences in the ventral roots could be identified.

Green fluorescent protein (GFP) is a protein found in the jellyfish Aequorea Victoria. It exhibits green fluorescence when exposed to light. It was added to the OEC cultures prior to transplantation so we could identify the OECs at the end of the experiments.

However, on examination of the sections we failed to identify the fluorescence and subsequently the OECs could not be identified. Previous studies in our lab on the lumbar nerve roots have transplanted OECs in a similar way to us, and we applied the fibrin glue Tisseel® to reinforce the repair and to keep the transplanted cells in place. However, unlike in other studies in our lab we used decalcifer to soften the cervical bones so they could be sectioned and examined under the microscope without damaging the spinal surgery site. Initial observations had demonstrated that bones could not be cut in a cryostat for sectioning, and removal of the spinal cord and nerve roots after perfusing the rats had led to a disruption of the surgical repair. It could be that the acidic decalcifier denatured the Green Fluorescent Protein so that we could not detect it after tissue processing thereby confirming the presence of OECs at the end of the study. In addition it may be the case that the cells were unable to express GFP at Day 63 of transplantation or that the transplanted cells were washed away with CSF flow.

6.5 Conclusion

Reimplantation of the left C8 ventral root lead to a significantly improved left paw spread and survival of motor neurone cell bodies in the anterior horn of the spinal cord. Addition of mOEC and bOEC to augment the repair leads to a significant recovery in paw spread, increased survival of motor neurones, and less forepaw deformity and autotomy compared to the reimplantation and avulsion groups.

CHAPTER SEVEN

CHAPTER 7: FUTURE WORK

7.1 Introduction

The work carried out in this thesis has led to the development brachial plexus ventral root repair model. Future work will include ways to refine some of the techniques by developing new functional tests, assessment of the effect of decalcifying agents on the fluorescence of OEC green fluorescent protein, powering the study with data from the mOEC and bOEC data, and the use of other cell types to assess CNS repair in this model.

7.2 Developing additional functional tests to quantify the C8 ventral root injury

There are no functional tests available to assess the behavioural outcomes following C8 ventral root injury in a rat. Our experiments showed that gait analysis could be used to assess recovery of forepaw spread following C8 ventral root surgery. There are a number of other tests for gait assessment which we considered, including intermediate toe spread and limb rotation angle. However, in this study we felt that preliminary gait analysis functional tests we had performed with a small number of rats, were not useful in detecting an effect after ventral root surgery. This could be revisited with the larger study we performed in Chapter 6, to see whether a difference can be detected with a larger sample size. Additionally, gait analysis tests using video analysis software such as the Catwalk® or Digi Gait® (Mouse Specifics Inc., Boston, USA) systems could be deployed in a less labour intensive manner to assess whether other gait analytics could be deployed to assess the C8 ventral root model. (Hamers et al., 2001, Hamers et al., 2006)

Although the paw grip strength testing using the Meyer Method (Meyer et al., 1979) initially showed promise, in the final study we failed to find a difference in the groups. The data from these results could be used in power calculations to calculate the sample size to appropriately power a future study. Furthermore, a number of other tests for forepaw function have been described in the literature. (Nichols et al., 2005) These could be revisited in a separate study and the effects of a C8 ventral root surgery studied to find other optimal functional tests to assess recovery in forepaw function.

Additionally, neurophysiology testing (nerve conduction tests and electromyography) of the brachial plexus and more specifically the C8 motor root after repair would give additional information of nerve repair and regeneration, and this should be considered in future studies using this model.

7.3 Power calculations to estimate sample size for future work using the C8 ventral root repair model

Our work in this study was powered using preliminary outcomes from functional tests and assessment of continuity of axonal fibres across the repair site using a ventral root avulsion and reimplantation model. Using the additional data we have obtained from our results with mOEC and bOECs transplants, we should be able calculate sample size requirements to adequately power future studies to assess the efficacy of OECs and other cell types in our model of ventral root repair. For example, the sample size may have contributed to the effect size in one of our functional tests, so more data will help us refine and improve this model for future work.

7.4 Detecting transplanted OECs

Our initial studies showed that OEC labelled with GFP fluoresced for several months in vitro. Other researchers in our lab have used them to label OECs for other spinal procedures in rodents where decalcifying agents were not necessary to decalcify and soften the vertebra in preparation for sectioning. An important step for this model would be to establish a technique whereby the spine did not have to be decalcified in order to obtain the spinal tissue to process it if histology and immunohistochemistry. Exploring the potential to amplify the fluorescence using antibodies to attach to the GFP after tissue processing with decalcifier could also be a possibility but at the time of writing this thesis we could not identify a product on the market for this purpose. n

7.5 Improving OEC characterisation and administration techniques

Despite successful reports of the benefits of OEC transplants for CNS repair, a number of negative studies have raised questions. The application methods in preclinical studies has varied enormously, from placing cultured cells onto the injury site, injecting them or administering them on a matrix. (Ramon-Cueto and Nieto-Sampedro, 1994, Li et al., 2007, Ibrahim et al., 2009b) Further assessment of administration techniques is required to evaluate the optimal delivery of these and other cell types. A number of biomaterials have been proposed as scaffolds, including QL6, hyaluronan/methylcellulose and other scaffolds have been described to provide guidance for regenerating/growing nerve fibres. (Badhiwala et al., 2018)

The culture and composition of OEC cultures is also a point of contention. There still remains controversy regarding culture media and length of culture time prior to transplantation. The superiority of mucosal over bulb OEC cultures transplants is still

a matter of debate. Whereas some researchers have used purified OECs, others have stated that the regenerative potential of unpurified cultures is based on co-transplantation of other cell types in the culture mix. Furthermore, the effect of pharmacological and molecular therapeutics agents to enhance the efficacy of OECs still needs to be investigated.

7.6 Transplantation of human OECs

If we assume that OECs are beneficial for CNS repair, the next logical step is to consider their utilisation in patients with brachial plexus injury. OECs can safely be obtained from the nasal mucosa of the olfactory epithelium but there are a number of different ways including culture from cadaveric specimens, culture of biopsies from the olfactory mucosa of normal human patients or those with brachial plexus injury, or direct harvest and use of unprepared olfactory mucosa containing OECs. (Lima et al., 2006, Miedzybrodzki et al., 2006, Choi et al., 2008) However, there remain a number of controversies associated with each of these methods. Biopsies from the nasal mucosa of young, spinal cord injury patients are likely to have a better yield of OECs than from patients undergoing endoscopic surgery for nasal pathology. Increasing age and neurodegenerative pathologies have been associated with poor yields but most spinal injuries are in a younger group of patients. (Kovacs, 2004) Likewise, the surgical technique and location of the mucosal biopsy can have implications for the yield of OECs. (Choi et al., 2008) Yields from cadaveric specimens have traditionally not been as encouraging and there are issues with transplant rejection following transplants with allograft mucosal cells. (Miedzybrodzki et al., 2006) Direct autologous transplants with olfactory tissue is appealing but under these circumstances the yield

of OECs, other cellular components of the mucosa and potential for transmission of infection are risks which need to be considered. (Choi and Gladwin, 2015)

Prior to human transplantations of OECs for brachial plexus repair, the rat model we have devised could be utilised to study the effects on neural repair and regeneration of human OECs. This would provide us with a safety profile as well as allow us to study any reparative effects of these cells *in vivo* prior to clinical trials being started.

7.7 Other cell types and therapeutic agents to consider for the ventral root model

The rat model of brachial plexus repair we have devised could be used to study the effects of other cellular therapeutic agents on brachial plexus ventral root repair. Mesenchymal stem cells, Schwann cells, neural stem cells, oligodendrocyte progenitor cells and embryonic stem cells have all been utilised in recent studies to effect spinal cord repair. Phase III trials to assess the neuroprotective and regenerative effects of riluzole, minocycline and Cethrin have been undertaken. (Casha et al., 2012, Lord-Fontaine et al., 2008, Schwartz and Fehlings, 2001) These agents could be used in our model either in isolation or combination with OECs to assess their efficacy in brachial plexus repair.

CHAPTER EIGHT

CHAPTER 8: APPENDICES

8.1 Appendix 1

Phosphate Buffered Saline (PBS) 0.01M pH 7.3

To each litre of distilled water add:

1. $NaH_2PO_4.2H_20$ (0.359g)
2. $Na_2HPO_4.12H_20$ (3.19g)
3. NaCl (9.0g)

8.2 Appendix 2

4% Paraformaldehyde (PFA) pH 7.2-7.4

1. 200g of PFA powder
2. 2L distilled water
3. 10ml of 1M NaOH
4. Heat to 60^0C until fully dissolved in the fume hood
5. When dissolved add more distilled water to make up to 2.5L
6. Leave to cool overnight
7. Filter
8. Add 2.5L of 0.2M phosphate buffer

8.3 Appendix 3

Intracardiac perfusion

1. After terminal anaesthesia with $C0_2$, a wide thoracotomy is performed and the heart is exposed.
2. An incision made in the right atrium and to the left ventricle.
3. A blunt hypodermic needle (0 gauge; cut flat and polished smooth) is inserted into the ascending aorta through the left ventricle.
4. The circulating blood volume is flushed out by perfusion with 100ml of 0.1M phosphate-buffered saline followed by perfusion with 4% paraformaldehyde fixative.
5. The rat is then decapitated, the torso removed to deliver the cervical spine with vertebral column and attached muscles, and post-fixed in PFA for at least 24 hours prior to further tissue processing.

8.4 Appendix 4

Tissue preparation for sectioning using a cryostat microtome

1. Under a dissecting microscope the cervical spine is dissected to remove excess muscle and trimmed down to a size to fit the cryotome.
2. The dissected tissue is placed in Decalcifier-II (Surgipath Europe Ltd., Cambridgeshire, UK) for 18 hours followed by suspension in 10% and 20% sucrose overnight for cryopreservation.
3. The sample is then placed in OCT (Bright Cryo-M-Bed; Jencons Scientific Ltd, Leighton Buzzard, UK) on an agitator for 30 minutes before being rapidly frozen with crushed dry ice.
4. The sample is mounted on a specimen holder in OCT (Bright Cryo-M-Bed); Jencons Scientific Ltd, Leighton Buzzard, UK) and cut in coronal sections a plane thickness of 16μm.
5. The sections are mounted on to slides and dried for at least 4 hours prior to staining with H&E, GFAP, NF and other labelling.

8.5 Appendix 5

Haematoxylin & Eosin staining

Haemalum colours nuclei of cells blue and eosin stains the other eosinophilic compounds various stains of pink, orange or red.

Reagents

1. Mayer's Haemalum solution – 200 ml
2. Acid Alcohol – 200ml ethanol, 2ml 1M HCL
3. Ammonia Solution – 200ml distilled water, 2ml Ammonia solution
4. Eosin – 200ml Eosin, 0.4ml Glacial Acetic Acid
5. Alcohol solutions (50%, 70%, 96%, 100%)
6. Histoclear
7. London tap water for washes

Procedure

1. Fix slides in PFA (15 mins)
2. Rehydrate in PBS (3 x 10 min)
3. Stain 1-2min in Haemalum
4. Rinse in distilled water
5. Acid solution 2 sec
6. Rinse in distilled water
7. Ammonium solution 20 sec (to 'blue' the stain)
8. Rinse in distilled water
9. Place in Eosin for 2-3min
10. Rinse in distilled water
11. Dehydrate in ascending alcohol 2min in each solution (50%, 70% 96%, 100%)
12. Histoclear at end for 5 min
13. Dry & mount same day and leave to dry

8.6 Appendix 6

Bulb and mucosal olfactory ensheathing cell culture media

	50ml	100ml	250ml	561.6ml
DMEM/F12	44	88	222.5	500
FCS	5	10	25	56
P/S	0.5	1	2.5	5.6

Instructions:

1. Prepare filter
2. Add DMEF-12 Glutamax media to the filter device
3. Add penicillin/streptomycin
4. Add foetal calf serum (FCS) at end (otherwise it may block filter)
5. Plug in Integra Vacusafe, hold filter as it may tip over and start filtering.
6. Store in 4^0C fridge and warm to 37^0Cwhen required.

8.7 Appendix 7

Mucosal OEC culture

1. Growing medium specific for mucosal OECs (DFF10; Dulbeccos' Modified Eagle Medium with F12 Nutrient (DMEM/F12) (Gibco-BRL, UK), with 10% Foetal Calf Serum (FCS; Invitrogen, Rockville, MD) is prepared (Jani and Raisman, 2004)

2. The rats were placed under terminal anaesthesia with CO_2 and decapitated.
3. The skin is removed, and muscle excised down to bone.
4. The nasal septum is dissected and placed in ice-cold Hank's Balanced Salt Solution (HBSS; Gibco-BRL, UK).
5. The olfactory mucosa covering the posterior nasal septum is identified by its yellow colour and separated from the anterior respiratory epithelial mucosa, which is discarded.
6. Following two washes in HBSS, the tissue is incubated at 37°C in 2.4 U/ml dispase II (Roche, Penzberg, Germany) solution for 30 min.
7. The superficial layers of the olfactory epithelium become crinkled and are easily peeled away from the lamina propria.
8. The lamina propria, which contains the OECs and ONFs associated with the olfactory nerves, is washed in HBSS and incubated at 37°C for 30 min in 0.05% collagenase (Type II; Sigma, UK) and dispase (Roche, UK) in HBSS (Gibco-BRL, UK).
9. Trituration in DFF10 yields a cell suspension, which is centrifuged at 250g for 5 minutes. The cells are re-suspended in DFF10 and plated on uncoated 35mm dishes.
10. The following day the supernatant is removed and plated on poly-L-lysine (Sigma UK) coated 35mm dishes and maintained in minimal volume of culture medium.
11. The dishes are incubated at 37^0C in an atmosphere containing 5% CO_2.
12. At day 5, the medium is replaced with fresh warm DFF10 and replaced thereafter every 2-3 days for the next 12-14 days.

8.8 Appendix 8

Bulb OEC culture

1. Growing medium specific for bulb OECs (DFF10; Dulbeccos' Modified Eagle Medium with F12 Nutrient (DMEM/F12) (Gibco-BRL, UK), with 10% Foetal Calf Serum (FCS; Invitrogen, Rockville, MD) is prepared. (Barnett and Roskams, 2002, Jani and Raisman, 2004)
2. Rats are placed under terminal anaesthesia with CO_2 and decapitated.
3. The skin is removed, and muscle excised down to bone.
4. The nasal bones are cut anteriorly, and the skull opened posteriorly, and olfactory bulbs carefully removed and transferred to a dish containing Hanks Balanced Salt Solution. (HBBS) (Gibco-BRL, UK)
5. Under the dissecting microscope remnants of adherent meningeal membranes are removed. The outer nerve and glomerular layers of the olfactory bulb are excised.
6. The tissue is dissociated in 0.1% Trypsin at 37^0C for 15 minutes.
7. After trypsinization excess volume of DFF10 is added and partly removed to leave a small suspension.
8. Deoxyribonuclease I (DNAse; Invitrogen, Rockville, MD) is added and the suspension triturated.
9. More DFF10 is added and the suspension centrifuged at 120g for five minutes.
10. The supernatant is removed and re-suspended in DFF10 before being plated on poly-L-lysine (PLL) coated dishes at a concentration of approximately 1.5 olfactory bulbs per dish.
11. The dishes are incubated at 37^0C in an atmosphere containing 5% CO_2 for 4-5 days before new warm DFF10 is added and replaced thereafter every 2-3 days for the next 12-14 days.

Appendix 9

Glial Fibrillary Acidic Protein & Neurofilament dual labelling protocol

1. Place cross sections on slides in a solution of 4% paraformaldehyde (PFA) for 15 minutes.
2. Once fixed remove the PFA and wash the culture dishes with phosphate buffered saline (PBS). (3 washes x 10 minutes)
3. While the cells are being fixed in PFA make up a blocking solution of 2% milk in PBS with 0.01% Triton X-100, and leave the dishes in blocking solution for 1 hour.
4. Make up the primary antibody solutions using the blocking solution, and keep in the fridge until required.
5. Add 250µl of primary antibody solution to the culture dishes with and leave in the fridge overnight, on a humidified tray.
6. The next day, wash the slides with PBS (3 x 10 min) on an agitator
7. Make up the secondary antibody solution using blocking solution and leave in the fridge (dark).
8. Add 250µl secondary antibody to the culture dishes and leave for 2 hours.
9. Wash once in PBS
10. You can either view directly under fluorescence microscope and take pictured (in which case leave a 1 ml of PBS on the cells) OR mount with Fluorosave mounting media and apply a cover slip and leave to dry in a dark room (24-48hrs) before viewing.

REFERENCES

ANDERSON, K. D., GUNAWAN, A. & STEWARD, O. 2005. Quantitative assessment of forelimb motor function after cervical spinal cord injury in rats: relationship to the corticospinal tract. *Exp Neurol,* 194**,** 161-74.

ANDERSON, K. D., SHARP, K. G., HOFSTADTER, M., IRVINE, K. A., MURRAY, M. & STEWARD, O. 2009. Forelimb locomotor assessment scale (FLAS): novel assessment of forelimb dysfunction after cervical spinal cord injury. *Exp Neurol,* 220**,** 23-33.

ANDREWS, B. T., WEINSTEIN, P. R., ROSENBLUM, M. L. & BARBARO, N. M. 1988. Intradural arachnoid cysts of the spinal canal associated with intramedullary cysts. *J Neurosurg,* 68**,** 544-9.

AU, E. & ROSKAMS, A. J. 2003. Olfactory ensheathing cells of the lamina propria in vivo and in vitro. *Glia,* 41**,** 224-36.

BABIN-EBELL, J., BOUGIOUKAKIS, P., URBANSKI, P., FROEHNER, S. & DIEGELER, A. 2010. Foreign material reaction to BioGlue(R) as a possible cause of cardiac tamponade. *Thorac Cardiovasc Surg,* 58**,** 489-91.

BADHIWALA, J. H., AHUJA, C. S. & FEHLINGS, M. G. 2018. Time is spine: a review of translational advances in spinal cord injury. *J Neurosurg Spine,* 30**,** 1-18.

BAKAR, B., KOSE, E. A., BALCI, M., ATASOY, P., SARKARATI, B., ALHAN, A., KILINC, K. & KESKIL, I. S. 2013. Evaluation of the neurotoxicity of the polyethylene glycol hydrogel dural sealant. *Turk Neurosurg,* 23**,** 16-24.

BALLERMANN, M., MCKENNA, J. & WHISHAW, I. Q. 2001. A grasp-related deficit in tactile discrimination following dorsal column lesion in the rat. *Brain Res Bull,* 54**,** 237-42.

BARAKAT, D. J., GAGLANI, S. M., NERAVETLA, S. R., SANCHEZ, A. R., ANDRADE, C. M., PRESSMAN, Y., PUZIS, R., GARG, M. S., BUNGE, M. B. & PEARSE, D. D. 2005. Survival, integration, and axon growth support of glia transplanted into the chronically contused spinal cord. *Cell Transplant,* 14**,** 225-40.

BARBER, P. C. & LINDSAY, R. M. 1982. Schwann cells of the olfactory nerves contain glial fibrillary acidic protein and resemble astrocytes. *Neuroscience,* 7**,** 3077-90.

BARNETT, S. C., ALEXANDER, C. L., IWASHITA, Y., GILSON, J. M., CROWTHER, J., CLARK, L., DUNN, L. T., PAPANASTASSIOU, V., KENNEDY, P. G. & FRANKLIN, R. J. 2000. Identification of a human olfactory ensheathing cell that can effect transplant-mediated remyelination of demyelinated CNS axons. *Brain,* 123 (Pt 8)**,** 1581-8.

BARNETT, S. C. & RIDDELL, J. S. 2007. Olfactory ensheathing cell transplantation as a strategy for spinal cord repair--what can it achieve? *Nat Clin Pract Neurol,* 3**,** 152-61.

BARNETT, S. C. & ROSKAMS, A. J. 2002. Olfactory ensheathing cells. Isolation and culture from the rat olfactory bulb. *Methods Mol Biol,* 198**,** 41-8.

BASSO, D. M. 2004. Behavioral testing after spinal cord injury: congruities, complexities, and controversies. *J Neurotrauma,* 21**,** 395-404.

BASSO, D. M., BEATTIE, M. S. & BRESNAHAN, J. C. 1995. A sensitive and reliable locomotor rating scale for open field testing in rats. *J Neurotrauma,* 12**,** 1-21.

BAVARIA, J. E., BRINSTER, D. R., GORMAN, R. C., WOO, Y. J., GLEASON, T. & POCHETTINO, A. 2002. Advances in the treatment of acute type A dissection: an integrated approach. *Ann Thorac Surg,* 74**,** S1848-52; discussion S1857-63.

BENTIVOGLIO, M., KUYPERS, H. G., CATSMAN-BERREVOETS, C. E., LOEWE, H. & DANN, O. 1980. Two new fluorescent retrograde neuronal tracers which are transported over long distances. *Neurosci Lett,* 18**,** 25-30.

BENTOLILA, V., NIZARD, R., BIZOT, P. & SEDEL, L. 1999. Complete traumatic brachial plexus palsy. Treatment and outcome after repair. *J Bone Joint Surg Am,* 81**,** 20-8.

BERGER, A., FLORY, P. J. & SCHALLER, E. 1990. Muscle transfers in brachial plexus lesions. *J Reconstr Microsurg,* 6**,** 113-6.

BERGEROT, A., SHORTLAND, P. J., ANAND, P., HUNT, S. P. & CARLSTEDT, T. 2004. Co-treatment with riluzole and GDNF is necessary for functional recovery after ventral root avulsion injury. *Exp Neurol,* 187**,** 359-66.

BERMAN, J. S., BIRCH, R. & ANAND, P. 1998. Pain following human brachial plexus injury with spinal cord root avulsion and the effect of surgery. *Pain,* 75**,** 199-207.

BERRETTA, S., PERCIAVALLE, V. & POPPELE, R. E. 1991. Origin of cuneate projections to the anterior and posterior lobes of the rat cerebellum. *Brain Res,* 556**,** 297-302.

BERTELLI, J. A. & GHIZONI, M. F. 2003. Brachial plexus avulsion injury repairs with nerve transfers and nerve grafts directly implanted into the spinal cord yield partial recovery of shoulder and elbow movements. *Neurosurgery,* 52**,** 1385-9; discussion 1389-90.

BERTELLI, J. A. & GHIZONI, M. F. 2007. Transfer of the accessory nerve to the suprascapular nerve in brachial plexus reconstruction. *J Hand Surg Am,* 32**,** 989-98.

BERTELLI, J. A. & MIRA, J. C. 1993. Behavioral evaluating methods in the objective clinical assessment of motor function after experimental brachial plexus reconstruction in the rat. *J Neurosci Methods,* 46**,** 203-8.

BERTELLI, J. A. & MIRA, J. C. 1994. Brachial plexus repair by peripheral nerve grafts directly into the spinal cord in rats. Behavioral and anatomical evidence of functional recovery. *J Neurosurg,* 81**,** 107-14.

BERTELLI, J. A. & MIRA, J. C. 1995. The grasping test: a simple behavioral method for objective quantitative assessment of peripheral nerve regeneration in the rat. *J Neurosci Methods,* 58**,** 151-5.

BERTHOLD, C. H. & CARLSTEDT, T. 1977. Observations on the morphology at the transition between the peripheral and the central nervous system in the cat. II. General organization of the transitional region in S1 dorsal rootlets. *Acta Physiol Scand Suppl,* 446**,** 23-42.

BIGBEE, A. J., HOANG, T. X. & HAVTON, L. A. 2007. At-level neuropathic pain is induced by lumbosacral ventral root avulsion injury and ameliorated by root reimplantation into the spinal cord. *Exp Neurol,* 204**,** 273-82.

BIGNAMI, A., ENG, L. F., DAHL, D. & UYEDA, C. T. 1972. Localization of the glial fibrillary acidic protein in astrocytes by immunofluorescence. *Brain Res,* 43**,** 429-35.

BJUGSTAD, K. B., LAMPE, K., KERN, D. S. & MAHONEY, M. 2010. Biocompatibility of poly(ethylene glycol)-based hydrogels in the brain: an analysis of the glial response across space and time. *J Biomed Mater Res A,* 95**,** 79-91.

BLITS, B., CARLSTEDT, T. P., RUITENBERG, M. J., DE WINTER, F., HERMENS, W. T., DIJKHUIZEN, P. A., CLAASENS, J. W., EGGERS, R., VAN DER SLUIS, R., TENENBAUM, L., BOER, G. J. & VERHAAGEN, J. 2004. Rescue and sprouting of motoneurons following ventral root avulsion and reimplantation combined with intraspinal adeno-associated viral vector-mediated expression of glial cell line-derived neurotrophic factor or brain-derived neurotrophic factor. *Exp Neurol,* 189**,** 303-16.

BOYD, J. G., DOUCETTE, R. & KAWAJA, M. D. 2005. Defining the role of olfactory ensheathing cells in facilitating axon remyelination following damage to the spinal cord. *FASEB J,* 19**,** 694-703.

BOYD, J. G., JAHED, A., MCDONALD, T. G., KROL, K. M., VAN EYK, J. E., DOUCETTE, R. & KAWAJA, M. D. 2006. Proteomic evaluation reveals that olfactory ensheathing cells but not Schwann cells express calponin. *Glia,* 53**,** 434-40.

BOYD, J. G., LEE, J., SKIHAR, V., DOUCETTE, R. & KAWAJA, M. D. 2004. LacZ-expressing olfactory ensheathing cells do not associate with myelinated axons after implantation into the compressed spinal cord. *Proc Natl Acad Sci U S A,* 101**,** 2162-6.

BOYD, J. G., SKIHAR, V., KAWAJA, M. & DOUCETTE, R. 2003. Olfactory ensheathing cells: historical perspective and therapeutic potential. *Anat Rec B New Anat,* 271**,** 49-60.

BRAILOWSKY, S. & KNIGHT, R. T. 1987. Recovery from GABA-mediated hemiplegia in young and aged rats: effects of catecholaminergic manipulations. *Neurobiol Aging,* 8**,** 441-7.

BRAY, G. M., VILLEGAS-PEREZ, M. P., VIDAL-SANZ, M. & AGUAYO, A. J. 1987. The use of peripheral nerve grafts to enhance neuronal survival, promote growth and permit terminal reconnections in the central nervous system of adult rats. *J Exp Biol,* 132**,** 5-19.

BRUSHART, T. M. & MESULAM, M. M. 1980. Alteration in connections between muscle and anterior horn motoneurons after peripheral nerve repair. *Science,* 208**,** 603-5.

BUNGE, M. B. 2001. Bridging areas of injury in the spinal cord. *Neuroscientist,* 7**,** 325-39.

CALOF, A. L., BONNIN, A., CROCKER, C., KAWAUCHI, S., MURRAY, R. C., SHOU, J. & WU, H. H. 2002. Progenitor cells of the olfactory receptor neuron lineage. *Microsc Res Tech,* 58**,** 176-88.

CAO, Q., XU, X. M., DEVRIES, W. H., ENZMANN, G. U., PING, P., TSOULFAS, P., WOOD, P. M., BUNGE, M. B. & WHITTEMORE, S. R. 2005. Functional recovery in traumatic spinal cord injury after transplantation of multineurotrophin-expressing glial-restricted precursor cells. *J Neurosci,* 25**,** 6947-57.

CAO, X. C. & LING, L. J. 2003. Anatomic basis and technical aspects of a new brachial plexus avulsion injury model in the rat. *Plast Reconstr Surg,* 111**,** 2488-90.

CARLSTEDT, T. 1997. Nerve fibre regeneration across the peripheral-central transitional zone. *J Anat,* 190 (Pt 1)**,** 51-6.

CARLSTEDT, T. 2007. *Central Nerve Plexus Injury,* London, Imperial College Press.

CARLSTEDT, T. 2008. Root repair review: basic science background and clinical outcome. *Restor Neurol Neurosci,* 26**,** 225-41.

CARLSTEDT, T. 2016. New Treatments for Spinal Nerve Root Avulsion Injury. *Front Neurol,* 7**,** 135.

CARLSTEDT, T., ANAND, P., HALLIN, R., MISRA, P. V., NOREN, G. & SEFERLIS, T. 2000. Spinal nerve root repair and reimplantation of avulsed ventral roots into the spinal cord after brachial plexus injury. *J Neurosurg,* 93**,** 237-47.

CARLSTEDT, T., ANAND, P., HTUT, M., MISRA, P. & SVENSSON, M. 2004. Restoration of hand function and so called "breathing arm" after intraspinal repair of C5-T1 brachial plexus avulsion injury. Case report. *Neurosurg Focus,* 16**,** E7.

CARLSTEDT, T., DALSGAARD, C. J. & MOLANDER, C. 1987. Regrowth of lesioned dorsal root nerve fibers into the spinal cord of neonatal rats. *Neurosci Lett,* 74**,** 14-8.

CARLSTEDT, T., GRANE, P., HALLIN, R. G. & NOREN, G. 1995. Return of function after spinal cord implantation of avulsed spinal nerve roots. *Lancet,* 346**,** 1323-5.

CARLSTEDT, T., LINDA, H., CULLHEIM, S. & RISLING, M. 1986. Reinnervation of hind limb muscles after ventral root avulsion and implantation in the lumbar spinal cord of the adult rat. *Acta Physiol Scand,* 128**,** 645-6.

CARLSTEDT, T. & NOREN, G. 1995. Repair of ruptured spinal nerve roots in a brachial plexus lesion. Case report. *J Neurosurg,* 82**,** 661-3.

CARLSTEDT, T. P., HALLIN, R. G., HEDSTROM, K. G. & NILSSON-REMAHL, I. A. 1993. Functional recovery in primates with brachial plexus injury after spinal cord implantation of avulsed ventral roots. *J Neurol Neurosurg Psychiatry,* 56**,** 649-54.

CASHA, S., ZYGUN, D., MCGOWAN, M. D., BAINS, I., YONG, V. W. & HURLBERT, R. J. 2012. Results of a phase II placebo-controlled randomized trial of minocycline in acute spinal cord injury. *Brain,* 135**,** 1224-36.

CHAN, C. C., KHODARAHMI, K., LIU, J., SUTHERLAND, D., OSCHIPOK, L. W., STEEVES, J. D. & TETZLAFF, W. 2005. Dose-dependent beneficial and detrimental effects of ROCK inhibitor Y27632 on axonal sprouting and functional recovery after rat spinal cord injury. *Exp Neurol,* 196**,** 352-64.

CHARAN, J. & KANTHARIA, N. D. 2013. How to calculate sample size in animal studies? *J Pharmacol Pharmacother,* 4**,** 303-6.

CHENG, H., CAO, Y. & OLSON, L. 1996. Spinal cord repair in adult paraplegic rats: partial restoration of hind limb function. *Science,* 273**,** 510-3.

CHEW, D. J., LEINSTER, V. H., SAKTHITHASAN, M., ROBSON, L. G., CARLSTEDT, T. & SHORTLAND, P. J. 2008. Cell death after dorsal root injury. *Neurosci Lett,* 433**,** 231-4.

CHOI, D. & GLADWIN, K. 2015. Olfactory ensheathing cells: Part II--source of cells and application to patients. *World Neurosurg,* 83**,** 251-6.
CHOI, D., LI, D., LAW, S., POWELL, M. & RAISMAN, G. 2008. A prospective observational study of the yield of olfactory ensheathing cells cultured from biopsies of septal nasal mucosa. *Neurosurgery,* 62**,** 1140-4; discussion 1144-5.
CHOI, D., LI, D. & RAISMAN, G. 2002. Fluorescent retrograde neuronal tracers that label the rat facial nucleus: a comparison of Fast Blue, Fluoro-ruby, Fluoro-emerald, Fluoro-Gold and DiI. *J Neurosci Methods,* 117**,** 167-72.
CHONG, M. S., WOOLF, C. J., HAQUE, N. S. & ANDERSON, P. N. 1999. Axonal regeneration from injured dorsal roots into the spinal cord of adult rats. *J Comp Neurol,* 410**,** 42-54.
CHUAH, M. I. & ZHENG, D. R. 1992. The human primary olfactory pathway: fine structural and cytochemical aspects during development and in adults. *Microsc Res Tech,* 23**,** 76-85.
CHUANG, T. Y., HUANG, M. C., CHEN, K. C., CHANG, Y. C., YEN, Y. S., LEE, L. S. & CHENG, H. 2002. Forelimb muscle activity following nerve graft repair of ventral roots in the rat cervical spinal cord. *Life Sci,* 71**,** 487-96.
CLARKE, P. G. 1992. How inaccurate is the Abercrombie correction factor for cell counts? *Trends Neurosci,* 15**,** 211-2.
COGGESHALL, R. E. & LEKAN, H. A. 1996. Methods for determining numbers of cells and synapses: a case for more uniform standards of review. *J Comp Neurol,* 364**,** 6-15.
COHEN, J. 1998. *Statistical Power Analysis for the Behavioural Sciences*.
COLLINS, A., LI, D., MCMAHON, S. B., RAISMAN, G. & LI, Y. 2017. Transplantation of Cultured Olfactory Bulb Cells Prevents Abnormal Sensory Responses During Recovery From Dorsal Root Avulsion in the Rat. *Cell Transplant,* 26**,** 913-924.
CULLHEIM, S., CARLSTEDT, T., LINDA, H., RISLING, M. & ULFHAKE, B. 1989. Motoneurons reinnervate skeletal muscle after ventral root implantation into the spinal cord of the cat. *Neuroscience,* 29**,** 725-33.
DAVID, S. & AGUAYO, A. J. 1981. Axonal elongation into peripheral nervous system "bridges" after central nervous system injury in adult rats. *Science,* 214**,** 931-3.
DE MEDINACELI, L., FREED, W. J. & WYATT, R. J. 1982. An index of the functional condition of rat sciatic nerve based on measurements made from walking tracks. *Exp Neurol,* 77**,** 634-43.
DE VRIES, J., MENOVSKY, T., GROTENHUIS, J. A. & VAN OVERBEEKE, J. J. 1998. Protective coating of cranial nerves with fibrin glue (Tissucol) during cranial base surgery: technical note. *Neurosurgery,* 43**,** 1242-6.
DE VRIES, J., MENOVSKY, T., VAN GULIK, S. & WESSELING, P. 2002. Histological effects of fibrin glue on nervous tissue: a safety study in rats. *Surg Neurol,* 57**,** 415-22; discussion 422.
DELLON, A. L. & MACKINNON, S. E. 1989. Selection of the appropriate parameter to measure neural regeneration. *Ann Plast Surg,* 23**,** 197-202.
DENNIS, S. G. & MELZACK, R. 1979. Self-mutilation after dorsal rhizotomy in rats: effects of prior pain and pattern of root lesions. *Exp Neurol,* 65**,** 412-21.
DEVON, R. & DOUCETTE, R. 1992. Olfactory ensheathing cells myelinate dorsal root ganglion neurites. *Brain Res,* 589**,** 175-9.
DIENER, P. S. & BREGMAN, B. S. 1998. Fetal spinal cord transplants support the development of target reaching and coordinated postural adjustments after neonatal cervical spinal cord injury. *J Neurosci,* 18**,** 763-78.
DOI, K., MURAMATSU, K., HATTORI, Y., OTSUKA, K., TAN, S. H., NANDA, V. & WATANABE, M. 2000. Restoration of prehension with the double free muscle technique following complete avulsion of the brachial plexus. Indications and long-term results. *J Bone Joint Surg Am,* 82**,** 652-66.
DOUCETTE, J. R. 1984. The glial cells in the nerve fiber layer of the rat olfactory bulb. *Anat Rec,* 210**,** 385-91.
DOUCETTE, R. 1991. PNS-CNS transitional zone of the first cranial nerve. *J Comp Neurol,* 312**,** 451-66.

DOUCETTE, R. 1995. Olfactory ensheathing cells: potential for glial cell transplantation into areas of CNS injury. *Histol Histopathol,* 10**,** 503-7.

DUNNING, M. D., LAKATOS, A., LOIZOU, L., KETTUNEN, M., FFRENCH-CONSTANT, C., BRINDLE, K. M. & FRANKLIN, R. J. 2004. Superparamagnetic iron oxide-labeled Schwann cells and olfactory ensheathing cells can be traced in vivo by magnetic resonance imaging and retain functional properties after transplantation into the CNS. *J Neurosci,* 24**,** 9799-810.

EL-GAMMAL, T. A. & FATHI, N. A. 2002. Outcomes of surgical treatment of brachial plexus injuries using nerve grafting and nerve transfers. *J Reconstr Microsurg,* 18**,** 7-15.

FAROOQUE, M. 2000. Spinal cord compression injury in the mouse: presentation of a model including assessment of motor dysfunction. *Acta Neuropathol,* 100**,** 13-22.

FAUL, F., ERDFELDER, E., LANG, A. G. & BUCHNER, A. 2007. G*Power 3: a flexible statistical power analysis program for the social, behavioral, and biomedical sciences. *Behav Res Methods,* 39**,** 175-91.

FERON, F., PERRY, C., COCHRANE, J., LICINA, P., NOWITZKE, A., URQUHART, S., GERAGHTY, T. & MACKAY-SIM, A. 2005. Autologous olfactory ensheathing cell transplantation in human spinal cord injury. *Brain,* 128**,** 2951-60.

FESTING, M. F. 2006. Design and statistical methods in studies using animal models of development. *ILAR J,* 47**,** 5-14.

FESTING, M. F. & ALTMAN, D. G. 2002. Guidelines for the design and statistical analysis of experiments using laboratory animals. *ILAR J,* 43**,** 244-58.

FIRESTEIN, S. 2001. How the olfactory system makes sense of scents. *Nature,* 413**,** 211-8.

FITTS, D. A. 2011. Ethics and animal numbers: informal analyses, uncertain sample sizes, inefficient replications, and type I errors. *J Am Assoc Lab Anim Sci,* 50**,** 445-53.

FRANCESCHINI, I. A. & BARNETT, S. C. 1996. Low-affinity NGF-receptor and E-N-CAM expression define two types of olfactory nerve ensheathing cells that share a common lineage. *Dev Biol,* 173**,** 327-43.

FRANKLIN, R. J. & BARNETT, S. C. 1997. Do olfactory glia have advantages over Schwann cells for CNS repair? *J Neurosci Res,* 50**,** 665-72.

FRANKLIN, R. J. & BARNETT, S. C. 2000. Olfactory ensheathing cells and CNS regeneration: the sweet smell of success? *Neuron,* 28**,** 15-8.

FRANSSEN, E. H., DE BREE, F. M. & VERHAAGEN, J. 2007. Olfactory ensheathing glia: their contribution to primary olfactory nervous system regeneration and their regenerative potential following transplantation into the injured spinal cord. *Brain Res Rev,* 56**,** 236-58.

FRIEDMAN, A. H., NUNLEY, J. A., 2ND, GOLDNER, R. D., OAKES, W. J., GOLDNER, J. L. & URBANIAK, J. R. 1990. Nerve transposition for the restoration of elbow flexion following brachial plexus avulsion injuries. *J Neurosurg,* 72**,** 59-64.

FRITZ, N., ILLERT, M. & REEH, P. 1986a. Location of motoneurones projecting to the cat distal forelimb. II. Median and ulnar motornuclei. *J Comp Neurol,* 244**,** 302-12.

FRITZ, N., ILLERT, M. & SAGGAU, P. 1986b. Location of motoneurones projecting to the cat distal forelimb. I. Deep radial motornuclei. *J Comp Neurol,* 244**,** 286-301.

GABEREL, T., BORGEY, F., THIBON, P., LESTEVEN, C., LECOUTOUR, X. & EMERY, E. 2011. Surgical site infection associated with the use of bovine serum albumine-glutaraldehyde surgical adhesive (BioGlue) in cranial surgery: a case-control study. *Acta Neurochir (Wien),* 153**,** 156-62; discussion 162-3.

GALE, K., KERASIDIS, H. & WRATHALL, J. R. 1985. Spinal cord contusion in the rat: behavioral analysis of functional neurologic impairment. *Exp Neurol,* 88**,** 123-34.

GALTREY, C. M. & FAWCETT, J. W. 2007. Characterization of tests of functional recovery after median and ulnar nerve injury and repair in the rat forelimb. *J Peripher Nerv Syst,* 12**,** 11-27.

GENSEL, J. C., TOVAR, C. A., HAMERS, F. P., DEIBERT, R. J., BEATTIE, M. S. & BRESNAHAN, J. C. 2006. Behavioral and histological characterization of unilateral cervical spinal cord contusion injury in rats. *J Neurotrauma,* 23**,** 36-54.

GHARBAWIE, O. A., WHISHAW, P. A. & WHISHAW, I. Q. 2004. The topography of three-dimensional exploration: a new quantification of vertical and horizontal exploration, postural support, and exploratory bouts in the cylinder test. *Behav Brain Res,* 151**,** 125-35.

GHULAM MUHAMMAD, A. K., YOSHIMINE, T., MARUNO, M., TAKEMOTO, O. & HAYAKAWA, T. 1997. Topical application of fibrin adhesive in the rat brain: effects on different cellular elements of the wound. *Neurol Res,* 19**,** 84-8.

GIMLICH, R. L. & BRAUN, J. 1985. Improved fluorescent compounds for tracing cell lineage. *Dev Biol,* 109**,** 509-14.

GLOVER, J. C., PETURSDOTTIR, G. & JANSEN, J. K. 1986. Fluorescent dextran-amines used as axonal tracers in the nervous system of the chicken embryo. *J Neurosci Methods,* 18**,** 243-54.

GONCALVES, M. B., MALMQVIST, T., CLARKE, E., HUBENS, C. J., GRIST, J., HOBBS, C., TRIGO, D., RISLING, M., ANGERIA, M., DAMBERG, P., CARLSTEDT, T. P. & CORCORAN, J. P. 2015. Neuronal RARbeta Signaling Modulates PTEN Activity Directly in Neurons and via Exosome Transfer in Astrocytes to Prevent Glial Scar Formation and Induce Spinal Cord Regeneration. *J Neurosci,* 35**,** 15731-45.

GONG, Q., BAILEY, M. S., PIXLEY, S. K., ENNIS, M., LIU, W. & SHIPLEY, M. T. 1994. Localization and regulation of low affinity nerve growth factor receptor expression in the rat olfactory system during development and regeneration. *J Comp Neurol,* 344**,** 336-48.

GORDON, D. C. & RICHMOND, F. J. 1990. Topography in the phrenic motoneuron nucleus demonstrated by retrograde multiple-labelling techniques. *J Comp Neurol,* 292**,** 424-34.

GRAZIADEI, P. P. & GRAZIADEI, G. A. 1979. Neurogenesis and neuron regeneration in the olfactory system of mammals. I. Morphological aspects of differentiation and structural organization of the olfactory sensory neurons. *J Neurocytol,* 8**,** 1-18.

GREENE, E. 1968. *Anatomy of the rat.,* New York, Hafner.

GU, Y. D. & MA, M. K. 1996. Use of the phrenic nerve for brachial plexus reconstruction. *Clin Orthop Relat Res***,** 119-21.

GUENARD, V., MONTAG, D., SCHACHNER, M. & MARTINI, R. 1996. Onion bulb cells in mice deficient for myelin genes share molecular properties with immature, differentiated non-myelinating, and denervated Schwann cells. *Glia,* 18**,** 27-38.

GUNDERSEN, H. J., BAGGER, P., BENDTSEN, T. F., EVANS, S. M., KORBO, L., MARCUSSEN, N., MOLLER, A., NIELSEN, K., NYENGAARD, J. R., PAKKENBERG, B. & ET AL. 1988. The new stereological tools: disector, fractionator, nucleator and point sampled intercepts and their use in pathological research and diagnosis. *APMIS,* 96**,** 857-81.

GUO, W. L., QI, Z. P., YU, L., SUN, T. W., QU, W. R., LIU, Q. Q., ZHU, Z. & LI, R. 2019. Melatonin combined with chondroitin sulfate ABC promotes nerve regeneration after root-avulsion brachial plexus injury. *Neural Regen Res,* 14**,** 328-338.

HAASE, P. & PAYNE, J. N. 1990. Comparison of the efficiencies of true blue and diamidino yellow as retrograde tracers in the peripheral motor system. *J Neurosci Methods,* 35**,** 175-83.

HALLIN, R. G., CARLSTEDT, T., NILSSON-REMAHL, I. & RISLING, M. 1999. Spinal cord implantation of avulsed ventral roots in primates; correlation between restored motor function and morphology. *Exp Brain Res,* 124**,** 304-10.

HAMERS, F. P., KOOPMANS, G. C. & JOOSTEN, E. A. 2006. CatWalk-assisted gait analysis in the assessment of spinal cord injury. *J Neurotrauma,* 23**,** 537-48.

HAMERS, F. P., LANKHORST, A. J., VAN LAAR, T. J., VELDHUIS, W. B. & GISPEN, W. H. 2001. Automated quantitative gait analysis during overground locomotion in the rat: its application to spinal cord contusion and transection injuries. *J Neurotrauma,* 18**,** 187-201.

HANINEC, P., HOUST'AVA, L., STEJSKAL, L. & DUBOVY, P. 2003. Rescue of rat spinal motoneurons from avulsion-induced cell death by intrathecal administration of IGF-I and Cerebrolysin. *Ann Anat,* 185**,** 233-8.

HARRIS, H. 1900. On the rapid conversion of haematoxylin into haematin in staining reactions. . *Journal of Applied Microscopic Laboratory Methods.,* 3**,** 777-780.

HAVTON, L. & KELLERTH, J. O. 1987. Regeneration by supernumerary axons with synaptic terminals in spinal motoneurons of cats. *Nature,* 325**,** 711-4.

HEWITT, C. W., MARRA, S. W., KANN, B. R., TRAN, H. S., PUC, M. M., CHRZANOWSKI, F. A., JR., TRAN, J. L., LENZ, S. D., CILLEY, J. H., JR., SIMONETTI, V. A. & DELROSSI, A. J. 2001. BioGlue surgical adhesive for thoracic aortic repair during coagulopathy: efficacy and histopathology. *Ann Thorac Surg,* 71**,** 1609-12.

HICKS, S. P. & D'AMATO, C. J. 1975. Motor-sensory cortex-corticospinal system and developing locomotion and placing in rats. *Am J Anat,* 143**,** 1-42.

HILLEL, A. T., UNTERMAN, S., NAHAS, Z., REID, B., COBURN, J. M., AXELMAN, J., CHAE, J. J., GUO, Q., TROW, R., THOMAS, A., HOU, Z., LICHTSTEINER, S., SUTTON, D., MATHESON, C., WALKER, P., DAVID, N., MORI, S., TAUBE, J. M. & ELISSEEFF, J. H. 2011. Photoactivated composite biomaterial for soft tissue restoration in rodents and in humans. *Sci Transl Med,* 3**,** 93ra67.

HOANG, T. X., AKHAVAN, M., WU, J. & HAVTON, L. A. 2008. Minocycline protects motor but not autonomic neurons after cauda equina injury. *Exp Brain Res,* 189**,** 71-7.

HOOVER, J. E. & DURKOVIC, R. G. 1991. Morphological relationships among extensor digitorum longus, tibialis anterior, and semitendinosus motor nuclei of the cat: an investigation employing the retrograde transport of multiple fluorescent tracers. *J Comp Neurol,* 303**,** 255-66.

HORIKAWA, K. & POWELL, E. W. 1986. Comparison of techniques for retrograde labeling using the rat's facial nucleus. *J Neurosci Methods,* 17**,** 287-96.

HTUT, M., MISRA, P., ANAND, P., BIRCH, R. & CARLSTEDT, T. 2006. Pain phenomena and sensory recovery following brachial plexus avulsion injury and surgical repairs. *J Hand Surg Br,* 31**,** 596-605.

HTUT, M., MISRA, V. P., ANAND, P., BIRCH, R. & CARLSTEDT, T. 2007. Motor recovery and the breathing arm after brachial plexus surgical repairs, including re-implantation of avulsed spinal roots into the spinal cord. *J Hand Surg Eur Vol,* 32**,** 170-8.

HUANG, D. W., MCKERRACHER, L., BRAUN, P. E. & DAVID, S. 1999. A therapeutic vaccine approach to stimulate axon regeneration in the adult mammalian spinal cord. *Neuron,* 24**,** 639-47.

HUANG, H., CHEN, L., WANG, H., XIU, B., LI, B., WANG, R., ZHANG, J., ZHANG, F., GU, Z., LI, Y., SONG, Y., HAO, W., PANG, S. & SUN, J. 2003a. Influence of patients' age on functional recovery after transplantation of olfactory ensheathing cells into injured spinal cord injury. *Chin Med J (Engl),* 116**,** 1488-91.

HUANG, M. C., CHANG, P. T., TSAI, M. J., KUO, H. S., KUO, W. C., LEE, M. J., LO, M. J., LEE, I. H., HUANG, W. C., LEE, L. M., SHIH, Y. H., LEE, L. S. & CHENG, H. 2007. Sensory and motor recovery after repairing transected cervical roots. *Surg Neurol,* 68 Suppl 1**,** S17-24; discussion S24.

HUANG, M. C., CHEN, K. C., CHUANG, T. Y., CHANG, W. C., LEE, L. S., HUANG, W. C. & CHENG, H. 2003b. Cervical root repair in adult rats after transection: recovery of forelimb motor function. *Exp Neurol,* 180**,** 101-9.

HUANG, M. C., LO, M. J., LIN, Y. L., CHANG, S. E., HUANG, W. C., KUO, W. C., TSAI, M. J., KUO, H. S., SHIH, Y. H. & CHENG, H. 2009. Functional recovery after the repair of transected cervical roots in the chronic stage of injury. *J Neurotrauma,* 26**,** 1795-804.

HUANG, Z. H., WANG, Y., CAO, L., SU, Z. D., ZHU, Y. L., CHEN, Y. Z., YUAN, X. B. & HE, C. 2008. Migratory properties of cultured olfactory ensheathing cells by single-cell migration assay. *Cell Res,* 18**,** 479-90.

IBRAHIM, A. G., KIRKWOOD, P. A., RAISMAN, G. & LI, Y. 2009a. Restoration of hand function in a rat model of repair of brachial plexus injury. *Brain,* 132**,** 1268-76.

IBRAHIM, A. G., RAISMAN, G. & LI, Y. 2009b. Permanent loss of fore-paw grasping requires complete deprivation of afferent input from a minimum of four dorsal roots of the rat brachial plexus. *Exp Neurol,* 215**,** 142-5.

ILLERT, M., FRITZ, N., ASCHOFF, A. & HOLLANDER, H. 1982. Fluorescent compounds as retrograde tracers compared with horseradish peroxidase (HRP). II. A parametric study in the peripheral motor system of the cat. *J Neurosci Methods,* 6**,** 199-218.

IMAIZUMI, T., LANKFORD, K. L., WAXMAN, S. G., GREER, C. A. & KOCSIS, J. D. 1998. Transplanted olfactory ensheathing cells remyelinate and enhance axonal conduction in the demyelinated dorsal columns of the rat spinal cord. *J Neurosci,* 18**,** 6176-85.

ITO, K., HORIUCHI, T., OYANAGI, K., NOMIYAMA, T. & HONGO, K. 2013. Comparative study of fibrin and chemical synthetic sealant on dural regeneration and brain damage. *J Neurosurg Spine,* 19**,** 736-43.

IVANCO, T. L., PELLIS, S. M. & WHISHAW, I. Q. 1996. Skilled forelimb movements in prey catching and in reaching by rats (Rattus norvegicus) and opossums (Monodelphis domestica): relations to anatomical differences in motor systems. *Behav Brain Res,* 79**,** 163-81.

IWANAMI, A., KANEKO, S., NAKAMURA, M., KANEMURA, Y., MORI, H., KOBAYASHI, S., YAMASAKI, M., MOMOSHIMA, S., ISHII, H., ANDO, K., TANIOKA, Y., TAMAOKI, N., NOMURA, T., TOYAMA, Y. & OKANO, H. 2005. Transplantation of human neural stem cells for spinal cord injury in primates. *J Neurosci Res,* 80**,** 182-90.

JAGER, S. B., RONCHI, G., VAEGTER, C. B. & GEUNA, S. 2014. The mouse median nerve experimental model in regenerative research. *Biomed Res Int,* 2014**,** 701682.

JAHED, A., ROWLAND, J. W., MCDONALD, T., BOYD, J. G., DOUCETTE, R. & KAWAJA, M. D. 2007. Olfactory ensheathing cells express smooth muscle alpha-actin in vitro and in vivo. *J Comp Neurol,* 503**,** 209-23.

JANI, H. R. & RAISMAN, G. 2004. Ensheathing cell cultures from the olfactory bulb and mucosa. *Glia,* 47**,** 130-7.

JIVAN, S., NOVIKOVA, L. N., WIBERG, M. & NOVIKOV, L. N. 2006. The effects of delayed nerve repair on neuronal survival and axonal regeneration after seventh cervical spinal nerve axotomy in adult rats. *Exp Brain Res,* 170**,** 245-54.

JONES, S. R., CARLEY, S. & HARRISON, M. 2003. An introduction to power and sample size estimation. *Emerg Med J,* 20**,** 453-8.

KACHRAMANOGLOU, C., CARLSTEDT, T., KOLTZENBURG, M. & CHOI, D. 2011a. Self-mutilation in patients after nerve injury may not be due to deafferentation pain: a case report. *Pain Med,* 12**,** 1644-8.

KACHRAMANOGLOU, C., CARLSTEDT, T., KOLTZENBURG, M. & CHOI, D. 2017. Long-Term Outcome of Brachial Plexus Reimplantation After Complete Brachial Plexus Avulsion Injury. *World Neurosurg,* 103**,** 28-36.

KACHRAMANOGLOU, C., LI, D., ANDREWS, P., EAST, C., CARLSTEDT, T., RAISMAN, G. & CHOI, D. 2011b. Novel strategies in brachial plexus repair after traumatic avulsion. *Br J Neurosurg,* 25**,** 16-27.

KAISER, R., WALDAUF, P., ULLAS, G. & KRAJCOVA, A. 2020. Epidemiology, etiology, and types of severe adult brachial plexus injuries requiring surgical repair: systematic review and meta-analysis. *Neurosurg Rev,* 43**,** 443-452.

KALSI, P., THOM, M. & CHOI, D. 2017. Histological effects of fibrin glue and synthetic tissue glues on the spinal cord: are they safe to use? *Br J Neurosurg,* 31**,** 695-700.

KARIMI-ABDOLREZAEE, S., EFTEKHARPOUR, E., WANG, J., MORSHEAD, C. M. & FEHLINGS, M. G. 2006. Delayed transplantation of adult neural precursor cells promotes remyelination and functional neurological recovery after spinal cord injury. *J Neurosci,* 26**,** 3377-89.

KATO, T., HONMOU, O., UEDE, T., HASHI, K. & KOCSIS, J. D. 2000. Transplantation of human olfactory ensheathing cells elicits remyelination of demyelinated rat spinal cord. *Glia,* 30**,** 209-18.

KATOH, S. & EL MASRY, W. S. 1994. Neurological recovery after conservative treatment of cervical cord injuries. *J Bone Joint Surg Br,* 76**,** 225-8.

KATOH, S. & EL MASRY, W. S. 1995. Motor recovery of patients presenting with motor paralysis and sensory sparing following cervical spinal cord injuries. *Paraplegia,* 33**,** 506-9.

KAWAJA, M. D., BOYD, J. G., SMITHSON, L. J., JAHED, A. & DOUCETTE, R. 2009. Technical strategies to isolate olfactory ensheathing cells for intraspinal implantation. *J Neurotrauma,* 26**,** 155-77.

KEYVAN-FOULADI, N., RAISMAN, G. & LI, Y. 2003. Functional repair of the corticospinal tract by delayed transplantation of olfactory ensheathing cells in adult rats. *J Neurosci,* 23**,** 9428-34.

KHAN, H., CHAUBEY, S. & DESAI, J. 2011. Early failure of coronary artery bypass grafts: an albumin cross-linked glutaraldehyde (BioGlue) related complication. *J Card Surg,* 26**,** 264-6.

KIM, D., SCHALLERT, T., LIU, Y., BROWARAK, T., NAYERI, N., TESSLER, A., FISCHER & MURRAY, M. 2001. Transplantation of genetically modified fibroblasts expressing BDNF in adult rats with a subtotal hemisection improves specific motor and sensory functions. *Neurorehabil Neural Repair,* 15**,** 141-50.

KIM, J., DADSETAN, M., AMEENUDDIN, S., WINDEBANK, A. J., YASZEMSKI, M. J. & LU, L. 2010. In vivo biodegradation and biocompatibility of PEG/sebacic acid-based hydrogels using a cage implant system. *J Biomed Mater Res A,* 95**,** 191-7.

KING-ROBSON, J. 2011. Encouraging regeneration in the central nervous system: is there a role for olfactory ensheathing cells? *Neurosci Res,* 69**,** 263-75.

KLIMO, P., JR., KHALIL, A., SLOTKIN, J. R., SMITH, E. R., SCOTT, R. M. & GOUMNEROVA, L. C. 2007. Wound complications associated with the use of bovine serum albumin-glutaraldehyde surgical adhesive in pediatric patients. *Neurosurgery,* 60**,** 305-9; discussion 309.

KLIOT, M., SMITH, G. M., SIEGAL, J. D. & SILVER, J. 1990. Astrocyte-polymer implants promote regeneration of dorsal root fibers into the adult mammalian spinal cord. *Exp Neurol,* 109**,** 57-69.

KOLIATSOS, V. E., PRICE, W. L., PARDO, C. A. & PRICE, D. L. 1994. Ventral root avulsion: an experimental model of death of adult motor neurons. *J Comp Neurol,* 342**,** 35-44.

KOVACS, T. 2004. Mechanisms of olfactory dysfunction in aging and neurodegenerative disorders. *Ageing Res Rev,* 3**,** 215-32.

KOZIN, S. H., PORTER, S., CLARK, P. & THODER, J. J. 1999. The contribution of the intrinsic muscles to grip and pinch strength. *J Hand Surg Am,* 24**,** 64-72.

KRIEGSFELD, L. J., ELIASSON, M. J., DEMAS, G. E., BLACKSHAW, S., DAWSON, T. M., NELSON, R. J. & SNYDER, S. H. 1999. Nocturnal motor coordination deficits in neuronal nitric oxide synthase knock-out mice. *Neuroscience,* 89**,** 311-5.

KRISTENSSON, K., GHETTI, B. & WISNIEWSKI, H. M. 1974. Study on the propagation of Herpes simplex virus (type 2) into the brain after intraocular injection. *Brain Res,* 69**,** 189-201.

KRISTENSSON, K. & OLSSON, Y. 1971. Uptake and retrograde axonal transport of peroxidase in hypoglossal neurons. Electron microscopical localization in the neuronal perikaryon. *Acta Neuropathol,* 19**,** 1-9.

KUMAR, A., MAARTENS, N. F. & KAYE, A. H. 2003. Reconstruction of the sellar floor using Bioglue following transsphenoidal procedures. *J Clin Neurosci,* 10**,** 92-5.

LAKATOS, A., BARNETT, S. C. & FRANKLIN, R. J. 2003. Olfactory ensheathing cells induce less host astrocyte response and chondroitin sulphate proteoglycan expression than Schwann cells following transplantation into adult CNS white matter. *Exp Neurol,* 184**,** 237-46.

LARSEN, W. 1998. *Essentials of Human Embryology,* Edinburgh, Churchill Livingstone.

LAUVIN, M. A., ZEMMOURA, I., CAZALS, X. & COTTIER, J. P. 2015. Delayed cauda equina compression after spinal dura repair with BioGlue: magnetic resonance imaging and computed tomography aspects of two cases of "glue-oma". *Spine J,* 15**,** e5-8.

LEMAIRE, S. A., OCHOA, L. N., CONKLIN, L. D., SCHMITTLING, Z. C., UNDAR, A., CLUBB, F. J., JR., LI WANG, X., COSELLI, J. S. & FRASER, C. D., JR. 2007. Nerve and conduction tissue injury caused by contact with BioGlue. *J Surg Res,* 143**,** 286-93.

LEUNG, C. T., COULOMBE, P. A. & REED, R. R. 2007. Contribution of olfactory neural stem cells to tissue maintenance and regeneration. *Nat Neurosci,* 10**,** 720-6.

LI, L., WU, W., LIN, L. F., LEI, M., OPPENHEIM, R. W. & HOUENOU, L. J. 1995. Rescue of adult mouse motoneurons from injury-induced cell death by glial cell line-derived neurotrophic factor. *Proc Natl Acad Sci U S A,* 92**,** 9771-5.

LI, R. H., SLIWKOWSKI, M. X., LO, J. & MATHER, J. P. 1996. Establishment of Schwann cell lines from normal adult and embryonic rat dorsal root ganglia. *J Neurosci Methods,* 67**,** 57-69.

LI, Y., CARLSTEDT, T., BERTHOLD, C. H. & RAISMAN, G. 2004. Interaction of transplanted olfactory-ensheathing cells and host astrocytic processes provides a bridge for axons to regenerate across the dorsal root entry zone. *Exp Neurol,* 188**,** 300-8.

LI, Y., DECHERCHI, P. & RAISMAN, G. 2003a. Transplantation of olfactory ensheathing cells into spinal cord lesions restores breathing and climbing. *J Neurosci,* 23**,** 727-31.

LI, Y., FIELD, P. M. & RAISMAN, G. 1997. Repair of adult rat corticospinal tract by transplants of olfactory ensheathing cells. *Science,* 277**,** 2000-2.

LI, Y., FIELD, P. M. & RAISMAN, G. 1998. Regeneration of adult rat corticospinal axons induced by transplanted olfactory ensheathing cells. *J Neurosci,* 18**,** 10514-24.

LI, Y., FIELD, P. M. & RAISMAN, G. 2005. Olfactory ensheathing cells and olfactory nerve fibroblasts maintain continuous open channels for regrowth of olfactory nerve fibres. *Glia,* 52**,** 245-51.

LI, Y. & RAISMAN, G. 1994. Schwann cells induce sprouting in motor and sensory axons in the adult rat spinal cord. *J Neurosci,* 14**,** 4050-63.

LI, Y., SAUVE, Y., LI, D., LUND, R. D. & RAISMAN, G. 2003b. Transplanted olfactory ensheathing cells promote regeneration of cut adult rat optic nerve axons. *J Neurosci,* 23**,** 7783-8.

LI, Y., YAMAMOTO, M., RAISMAN, G., CHOI, D. & CARLSTEDT, T. 2007. An experimental model of ventral root repair showing the beneficial effect of transplanting olfactory ensheathing cells. *Neurosurgery,* 60**,** 734-40; discussion 740-1.

LIGUORI, R., DELGAIZO, S., FUSCO, G. & DE BELLIS, M. 1984. "Tissucol" in spinal surgery. *J Neurosurg Sci,* 28**,** 187-90.

LIMA, C., PRATAS-VITAL, J., ESCADA, P., HASSE-FERREIRA, A., CAPUCHO, C. & PEDUZZI, J. D. 2006. Olfactory mucosa autografts in human spinal cord injury: a pilot clinical study. *J Spinal Cord Med,* 29**,** 191-203; discussion 204-6.

LINDA, H., CULLHEIM, S. & RISLING, M. 1992. A light and electron microscopic study of intracellularly HRP-labeled lumbar motoneurons after intramedullary axotomy in the adult cat. *J Comp Neurol,* 318**,** 188-208.

LINDA, H., RISLING, M. & CULLHEIM, S. 1985. 'Dendraxons' in regenerating motoneurons in the cat: do dendrites generate new axons after central axotomy? *Brain Res,* 358**,** 329-33.

LIPSON, A. C., WIDENFALK, J., LINDQVIST, E., EBENDAL, T. & OLSON, L. 2003. Neurotrophic properties of olfactory ensheathing glia. *Exp Neurol,* 180**,** 167-71.

LIU, S., PEULVE, P., JIN, O., BOISSET, N., TIOLLIER, J., SAID, G. & TADIE, M. 1997. Axonal regrowth through collagen tubes bridging the spinal cord to nerve roots. *J Neurosci Res,* 49**,** 425-32.

LIVESEY, F. J. & FRAHER, J. P. 1992. Experimental traction injuries of cervical spinal nerve roots: a scanning EM study of rupture patterns in fresh tissue. *Neuropathol Appl Neurobiol,* 18**,** 376-86.

LOBSIGER, C. C. D. 2009. *Neurofilaments: Organization and Function in Neurons*, Elsevier Ltd.

LOMBARD, M. C., NASHOLD, B. S., JR., ALBE-FESSARD, D., SALMAN, N. & SAKR, C. 1979. Deafferentation hypersensitivity in the rat after dorsal rhizotomy: a possible animal model of chronic pain. *Pain,* 6**,** 163-74.

LORD-FONTAINE, S., YANG, F., DIEP, Q., DERGHAM, P., MUNZER, S., TREMBLAY, P. & MCKERRACHER, L. 2008. Local inhibition of Rho signaling by cell-permeable recombinant protein BA-210 prevents secondary damage and promotes functional recovery following acute spinal cord injury. *J Neurotrauma,* 25**,** 1309-22.

LU, J., FERON, F., HO, S. M., MACKAY-SIM, A. & WAITE, P. M. 2001. Transplantation of nasal olfactory tissue promotes partial recovery in paraplegic adult rats. *Brain Res,* 889**,** 344-57.

LU, J., FERON, F., MACKAY-SIM, A. & WAITE, P. M. 2002. Olfactory ensheathing cells promote locomotor recovery after delayed transplantation into transected spinal cord. *Brain,* 125**,** 14-21.

LUK, A., DAVID, T. E. & BUTANY, J. 2012. Complications of Bioglue postsurgery for aortic dissections and aortic valve replacement. *J Clin Pathol,* 65**,** 1008-12.

MALESSY, M. J., DE RUITER, G. C., DE BOER, K. S. & THOMEER, R. T. 2004. Evaluation of suprascapular nerve neurotization after nerve graft or transfer in the treatment of brachial plexus traction lesions. *J Neurosurg,* 101**,** 377-89.

MATHIS, D. & SHOELSON, S. E. 2011. Immunometabolism: an emerging frontier. *Nat Rev Immunol,* 11**,** 81.

MENOVSKY, T., DE VRIES, J. & BLOSS, H. G. 1999. Treatment of postoperative subgaleal cerebrospinal fluid fistulas by using fibrin sealant. Technical note. *J Neurosurg,* 90**,** 1143-5.

METZ, G. A., DIETZ, V., SCHWAB, M. E. & VAN DE MEENT, H. 1998. The effects of unilateral pyramidal tract section on hindlimb motor performance in the rat. *Behav Brain Res,* 96**,** 37-46.

METZ, G. A., MERKLER, D., DIETZ, V., SCHWAB, M. E. & FOUAD, K. 2000. Efficient testing of motor function in spinal cord injured rats. *Brain Res,* 883**,** 165-77.

MEYER, O. A., TILSON, H. A., BYRD, W. C. & RILEY, M. T. 1979. A method for the routine assessment of fore- and hindlimb grip strength of rats and mice. *Neurobehav Toxicol,* 1**,** 233-6.

MIDHA, R. 2004. Nerve transfers for severe brachial plexus injuries: a review. *Neurosurg Focus,* 16**,** E5.

MIEDZYBRODZKI, R., TABAKOW, P., FORTUNA, W., CZAPIGA, B. & JARMUNDOWICZ, W. 2006. The olfactory bulb and olfactory mucosa obtained from human cadaver donors as a source of olfactory ensheathing cells. *Glia,* 54**,** 557-65.

MILLS, C. D., HAINS, B. C., JOHNSON, K. M. & HULSEBOSCH, C. E. 2001. Strain and model differences in behavioral outcomes after spinal cord injury in rat. *J Neurotrauma,* 18**,** 743-56.

MIRAGALL, F., KADMON, G., HUSMANN, M. & SCHACHNER, M. 1988. Expression of cell adhesion molecules in the olfactory system of the adult mouse: presence of the embryonic form of N-CAM. *Dev Biol,* 129**,** 516-31.

MONTOYA, C. P., CAMPBELL-HOPE, L. J., PEMBERTON, K. D. & DUNNETT, S. B. 1991. The "staircase test": a measure of independent forelimb reaching and grasping abilities in rats. *J Neurosci Methods,* 36**,** 219-28.

MUIR, G. D. & WEBB, A. A. 2000. Mini-review: assessment of behavioural recovery following spinal cord injury in rats. *Eur J Neurosci,* 12**,** 3079-86.

NANCE, D. M. & BURNS, J. 1990. Fluorescent dextrans as sensitive anterograde neuroanatomical tracers: applications and pitfalls. *Brain Res Bull,* 25**,** 139-45.

NARAKAS, A. 1988. The use of fibrin glue in repair of peripheral nerves. *Orthop Clin North Am,* 19**,** 187-99.

NARAKAS, A. O. & HENTZ, V. R. 1988. Neurotization in brachial plexus injuries. Indication and results. *Clin Orthop Relat Res***,** 43-56.

NASH, H. H., BORKE, R. C. & ANDERS, J. J. 2001. New method of purification for establishing primary cultures of ensheathing cells from the adult olfactory bulb. *Glia,* 34**,** 81-7.

NICHOLS, C. M., MYCKATYN, T. M., RICKMAN, S. R., FOX, I. K., HADLOCK, T. & MACKINNON, S. E. 2005. Choosing the correct functional assay: a comprehensive assessment of functional tests in the rat. *Behav Brain Res,* 163**,** 143-58.

NOVIKOVA, L., NOVIKOV, L. & KELLERTH, J. O. 1997a. Effects of neurotransplants and BDNF on the survival and regeneration of injured adult spinal motoneurons. *Eur J Neurosci,* 9**,** 2774-7.

NOVIKOVA, L., NOVIKOV, L. & KELLERTH, J. O. 1997b. Persistent neuronal labeling by retrograde fluorescent tracers: a comparison between Fast Blue, Fluoro-Gold and various dextran conjugates. *J Neurosci Methods,* 74**,** 9-15.

NOVIKOVA, L. N., LOBOV, S., WIBERG, M. & NOVIKOV, L. N. 2011. Efficacy of olfactory ensheathing cells to support regeneration after spinal cord injury is influenced by method of culture preparation. *Exp Neurol,* 229**,** 132-42.

OLSSON, T., LUNDBERG, C., LIDMAN, O. & PIEHL, F. 2000. Genetic regulation of nerve avulsion-induced spinal cord inflammation. *Ann N Y Acad Sci,* 917**,** 186-96.

OPRYCH, K. M., KALSI, P. S., KACHRAMANOGLOU, C. & CHOI, D. 2015. Technical Improvements to a Rat Brachial Plexus Avulsion Model via a Posterior Surgical Approach. *Plast Reconstr Surg Glob Open,* 3**,** e576.

PAPALIA, I., TOS, P., SCEVOLA, A., RAIMONDO, S. & GEUNA, S. 2006. The ulnar test: a method for the quantitative functional assessment of posttraumatic ulnar nerve recovery in the rat. *J Neurosci Methods,* 154**,** 198-203.

PARR, A. M., KULBATSKI, I. & TATOR, C. H. 2007. Transplantation of adult rat spinal cord stem/progenitor cells for spinal cord injury. *J Neurotrauma,* 24**,** 835-45.

PASSAGE, J., JALALI, H., TAM, R. K., HARROCKS, S. & O'BRIEN, M. F. 2002. BioGlue Surgical Adhesive--an appraisal of its indications in cardiac surgery. *Ann Thorac Surg,* 74**,** 432-7.

PEARSE, D. D., LO, T. P., JR., CHO, K. S., LYNCH, M. P., GARG, M. S., MARCILLO, A. E., SANCHEZ, A. R., CRUZ, Y. & DIETRICH, W. D. 2005. Histopathological and behavioral characterization of a novel cervical spinal cord displacement contusion injury in the rat. *J Neurotrauma,* 22**,** 680-702.

PEARSE, D. D., SANCHEZ, A. R., PEREIRA, F. C., ANDRADE, C. M., PUZIS, R., PRESSMAN, Y., GOLDEN, K., KITAY, B. M., BLITS, B., WOOD, P. M. & BUNGE, M. B. 2007. Transplantation of Schwann cells and/or olfactory ensheathing glia into the contused spinal cord: Survival, migration, axon association, and functional recovery. *Glia,* 55**,** 976-1000.

PETRIE, A. S., C. 2009. *Medical Statistics at a Glance,* United Kingdom, Wiley-Blackwell.

PINTER, S., GLOVICZKI, B., SZABO, A., MARTON, G. & NOGRADI, A. 2010. Increased survival and reinnervation of cervical motoneurons by riluzole after avulsion of the C7 ventral root. *J Neurotrauma,* 27**,** 2273-82.

PIXLEY, S. K. 1992. The olfactory nerve contains two populations of glia, identified both in vivo and in vitro. *Glia,* 5**,** 269-84.

PREUL, M. C., BICHARD, W. D. & SPETZLER, R. F. 2003. Toward optimal tissue sealants for neurosurgery: use of a novel hydrogel sealant in a canine durotomy repair model. *Neurosurgery,* 53**,** 1189-98; discussion 1198-9.

PREUL, M. C., CAMPBELL, P. K., BICHARD, W. D. & SPETZLER, R. F. 2007. Application of a hydrogel sealant improves watertight closures of duraplasty onlay grafts in a canine craniotomy model. *J Neurosurg,* 107**,** 642-50.

PUIGDELLIVOL-SANCHEZ, A., PRATS-GALINO, A., RUANO-GIL, D. & MOLANDER, C. 2000. Fast blue and diamidino yellow as retrograde tracers in peripheral nerves: efficacy of combined nerve injection and capsule application to transected nerves in the adult rat. *J Neurosci Methods,* 95**,** 103-10.

RABIN, A. G. & ANDERSON, E. G. 1985. Autotomy following limb denervation: effects of previous exposure to neurectomy. *Pain,* 21**,** 105-15.

RAISMAN, G. 1985. Specialized neuroglial arrangement may explain the capacity of vomeronasal axons to reinnervate central neurons. *Neuroscience,* 14**,** 237-54.

RAISMAN, G. 2001. Olfactory ensheathing cells - another miracle cure for spinal cord injury? *Nat Rev Neurosci,* 2**,** 369-75.

RAISMAN, G., CARLSTEDT, T., CHOI, D. & LI, Y. 2011. Clinical prospects for transplantation of OECs in the repair of brachial and lumbosacral plexus injuries: opening a door. *Exp Neurol,* 229**,** 168-73.

RAISMAN, G. & LI, Y. 2007. Repair of neural pathways by olfactory ensheathing cells. *Nat Rev Neurosci,* 8**,** 312-9.

RAMER, L. M., AU, E., RICHTER, M. W., LIU, J., TETZLAFF, W. & ROSKAMS, A. J. 2004. Peripheral olfactory ensheathing cells reduce scar and cavity formation and promote regeneration after spinal cord injury. *J Comp Neurol,* 473**,** 1-15.

RAMER, M. S., BISHOP, T., DOCKERY, P., MOBARAK, M. S., O'LEARY, D., FRAHER, J. P., PRIESTLEY, J. V. & MCMAHON, S. B. 2002. Neurotrophin-3-mediated regeneration and recovery of proprioception following dorsal rhizotomy. *Mol Cell Neurosci,* 19**,** 239-49.

RAMON Y CAJAL, S. 1928. *Degeneration and regeneration of the nervous system,* London, Oxford University Press.

RAMON-CUETO, A. & AVILA, J. 1998. Olfactory ensheathing glia: properties and function. *Brain Res Bull,* 46**,** 175-87.

RAMON-CUETO, A. & NIETO-SAMPEDRO, M. 1992. Glial cells from adult rat olfactory bulb: immunocytochemical properties of pure cultures of ensheathing cells. *Neuroscience,* 47**,** 213-20.

RAMON-CUETO, A. & NIETO-SAMPEDRO, M. 1994. Regeneration into the spinal cord of transected dorsal root axons is promoted by ensheathing glia transplants. *Exp Neurol,* 127**,** 232-44.

RAMON-CUETO, A., PEREZ, J. & NIETO-SAMPEDRO, M. 1993. In vitro enfolding of olfactory neurites by p75 NGF receptor positive ensheathing cells from adult rat olfactory bulb. *Eur J Neurosci,* 5**,** 1172-80.

RAMON-CUETO, A. & VALVERDE, F. 1995. Olfactory bulb ensheathing glia: a unique cell type with axonal growth-promoting properties. *Glia,* 14**,** 163-73.

REID, B., GIBSON, M., SINGH, A., TAUBE, J., FURLONG, C., MURCIA, M. & ELISSEEFF, J. 2015. PEG hydrogel degradation and the role of the surrounding tissue environment. *J Tissue Eng Regen Med,* 9**,** 315-8.

REIER, P. S., LJ; GUTH, L. 1983. The astrocytic scar as an impediment to regeneration in the central nervous system. *In:* KAO, C. (ed.) *Spinal Cord Reconstruction. .* New York.: Raven Press. .

RICHMOND, F. J., GLADDY, R., CREASY, J. L., KITAMURA, S., SMITS, E. & THOMSON, D. B. 1994. Efficacy of seven retrograde tracers, compared in multiple-labelling studies of feline motoneurones. *J Neurosci Methods,* 53**,** 35-46.

RICHTER, M. W., FLETCHER, P. A., LIU, J., TETZLAFF, W. & ROSKAMS, A. J. 2005. Lamina propria and olfactory bulb ensheathing cells exhibit differential integration and migration and promote differential axon sprouting in the lesioned spinal cord. *J Neurosci,* 25**,** 10700-11.

RICHTER, M. W. & ROSKAMS, A. J. 2008. Olfactory ensheathing cell transplantation following spinal cord injury: hype or hope? *Exp Neurol,* 209**,** 353-67.

RISLING, M., CULLHEIM, S. & HILDEBRAND, C. 1983. Reinnervation of the ventral root L7 from ventral horn neurons following intramedullary axotomy in adult cats. *Brain Res,* 280**,** 15-23.

RISLING, M., FRIED, K., LINDA, H., CARLSTEDT, T. & CULLHEIM, S. 1993. Regrowth of motor axons following spinal cord lesions: distribution of laminin and collagen in the CNS scar tissue. *Brain Res Bull,* 30**,** 405-14.

RUITENBERG, M. J. & VUKOVIC, J. 2008. Promoting central nervous system regeneration: lessons from cranial nerve I. *Restor Neurol Neurosci,* 26**,** 183-96.

RUITENBERG, M. J., VUKOVIC, J., SARICH, J., BUSFIELD, S. J. & PLANT, G. W. 2006. Olfactory ensheathing cells: characteristics, genetic engineering, and therapeutic potential. *J Neurotrauma,* 23**,** 468-78.

SAMARDZIC, M., RASULIC, L., GRUJICIC, D. & MILICIC, B. 2000. Results of nerve transfers to the musculocutaneous and axillary nerves. *Neurosurgery,* 46**,** 93-101; discussion 101-3.

SAMII, A., CARVALHO, G. A. & SAMII, M. 2003. Brachial plexus injury: factors affecting functional outcome in spinal accessory nerve transfer for the restoration of elbow flexion. *J Neurosurg,* 98**,** 307-12.

SANANPANICH, K., GALEA, M. P., MORRISON, W. A. & MESSINA, A. 2007. Quantitative characterization of regenerating axons after end-to-side and end-to-end coaptation in a rat brachial plexus model: a retrograde tracer study. *J Neurotrauma,* 24**,** 864-75.

SASAKI, M., BLACK, J. A., LANKFORD, K. L., TOKUNO, H. A., WAXMAN, S. G. & KOCSIS, J. D. 2006a. Molecular reconstruction of nodes of Ranvier after remyelination by transplanted olfactory ensheathing cells in the demyelinated spinal cord. *J Neurosci,* 26**,** 1803-12.

SASAKI, M., HAINS, B. C., LANKFORD, K. L., WAXMAN, S. G. & KOCSIS, J. D. 2006b. Protection of corticospinal tract neurons after dorsal spinal cord transection and engraftment of olfactory ensheathing cells. *Glia,* 53**,** 352-9.

SCHAFER, M., KLEIN, H. J. & RICHTER, H. P. 1985. [Fibrin glue in neurosurgery. Areas of use and experiences]. *Fortschr Med,* 103**,** 545-7.

SCHILLER, W., RUDORF, H., KIDERLEN, M. J., WELZEL, C. B., SCHMITZ, C., PROBST, C. & WELZ, A. 2007a. Short-term tissue response of lapine carotid artery microanastomoses to BioGlue. *Thorac Cardiovasc Surg,* 55**,** 298-303.

SCHILLER, W., RUDORF, H., WELZEL, C. B., KIDERLEN, M. J., PROBST, C., DEWALD, O. & WELZ, A. 2007b. Sutureless anastomoses of rabbit carotid arteries with BioGlue. *J Thorac Cardiovasc Surg,* 134**,** 1513-8.

SCHLAEPFER, W. W. & LYNCH, R. G. 1977. Immunofluorescence studies of neurofilaments in the rat and human peripheral and central nervous system. *J Cell Biol,* 74**,** 241-50.

SCHMUED, L., KYRIAKIDIS, K. & HEIMER, L. 1990. In vivo anterograde and retrograde axonal transport of the fluorescent rhodamine-dextran-amine, Fluoro-Ruby, within the CNS. *Brain Res,* 526**,** 127-34.

SCHWARTZ, G. & FEHLINGS, M. G. 2001. Evaluation of the neuroprotective effects of sodium channel blockers after spinal cord injury: improved behavioral and neuroanatomical recovery with riluzole. *J Neurosurg,* 94**,** 245-56.

SCHWOB, J. E. 2002. Neural regeneration and the peripheral olfactory system. *Anat Rec,* 269**,** 33-49.

SEDDON, H. J. 1963. Nerve Grafting. *J Bone Joint Surg Br,* 45**,** 447-61.

SMITH, P. M., SIM, F. J., BARNETT, S. C. & FRANKLIN, R. J. 2001. SCIP/Oct-6, Krox-20, and desert hedgehog mRNA expression during CNS remyelination by transplanted olfactory ensheathing cells. *Glia,* 36**,** 342-53.

SON, Y. J. 2015. Synapsing with NG2 cells (polydendrocytes), unappreciated barrier to axon regeneration? *Neural Regen Res,* 10**,** 346-8.

SONGCHAROEN, P., MAHAISAVARIYA, B. & CHOTIGAVANICH, C. 1996. Spinal accessory neurotization for restoration of elbow flexion in avulsion injuries of the brachial plexus. *J Hand Surg Am,* 21**,** 387-90.

SONGCHAROEN, P., WONGTRAKUL, S., MAHAISAVARIYA, B. & SPINNER, R. J. 2001. Hemi-contralateral C7 transfer to median nerve in the treatment of root avulsion brachial plexus injury. *J Hand Surg Am,* 26**,** 1058-64.

SONIGRA, R. J., BRIGHTON, P. C., JACOBY, J., HALL, S. & WIGLEY, C. B. 1999. Adult rat olfactory nerve ensheathing cells are effective promoters of adult central nervous system neurite outgrowth in coculture. *Glia,* 25**,** 256-69.

SOREIDE, A. J. 1981. Variations in the axon reaction in animals of different ages. A light microscopic study on the facial nucleus of the rat. *Acta Anat (Basel),* 110**,** 40-7.

STOSSEL, M., REHRA, L. & HAASTERT-TALINI, K. 2017. Reflex-based grasping, skilled forelimb reaching, and electrodiagnostic evaluation for comprehensive analysis of functional recovery-The 7-mm rat median nerve gap repair model revisited. *Brain Behav,* 7**,** e00813.

STYLLI, S. S., KUMAR, A., GONZALES, M. & KAYE, A. H. 2004. The biocompatibility of BioGlue with the cerebral cortex: a pilot study. *J Clin Neurosci,* 11**,** 631-5.

TABAKOW, P., RAISMAN, G., FORTUNA, W., CZYZ, M., HUBER, J., LI, D., SZEWCZYK, P., OKUROWSKI, S., MIEDZYBRODZKI, R., CZAPIGA, B., SALOMON, B., HALON, A., LI, Y., LIPIEC, J., KULCZYK, A. & JARMUNDOWICZ, W. 2014. Functional regeneration of supraspinal connections in a patient with transected spinal cord following transplantation of bulbar olfactory ensheathing cells with peripheral nerve bridging. *Cell Transplant,* 23**,** 1631-55.

TAKAHASHI, S., IWANAGA, T., TAKAHASHI, Y., NAKANO, Y. & FUJITA, T. 1984. Neuron-specific enolase, neurofilament protein and S-100 protein in the olfactory mucosa of human fetuses. An immunohistochemical study. *Cell Tissue Res,* 238**,** 231-4.

TAKAMI, T., OUDEGA, M., BATES, M. L., WOOD, P. M., KLEITMAN, N. & BUNGE, M. B. 2002. Schwann cell but not olfactory ensheathing glia transplants improve hindlimb locomotor performance in the moderately contused adult rat thoracic spinal cord. *J Neurosci,* 22**,** 6670-81.

TATLISUMAK, T. F., M. 2006. *Handbook of Experimental Neurology: Methods and Techniques in Animal Research,* Cambridge, Cambridge University Press.

TELLO, F. 1911a. La influencia del neurotropismo en la regeneracion de los nervisos. *Trab Lab Invest Biol,* 9**,** 123-128.

TELLO, F. 1911b. La influencia del neurtotropismo en la regenracion de los nerviosos. *Trab Lab Invest Biol,* 9**,** 123-128.

TSAI, E. C., VAN BENDEGEM, R. L., HWANG, S. W. & TATOR, C. H. 2001. A novel method for simultaneous anterograde and retrograde labeling of spinal cord motor tracts in the same animal. *J Histochem Cytochem,* 49**,** 1111-22.

UBINK, R. & HOKFELT, T. 2000. Expression of neuropeptide Y in olfactory ensheathing cells during prenatal development. *J Comp Neurol,* 423**,** 13-25.

URDZIKOVA, L. & VANICKY, I. 2006. Post-traumatic moderate systemic hyperthermia worsens behavioural outcome after spinal cord injury in the rat. *Spinal Cord,* 44**,** 113-9.

UZAN, M., HANCI, M., KUDAY, C., AKAR, Z., SHAMSI, A. A., OZLEN, F., OZ, B. & DENIZ, E. 1996. A new aneurysm wrapping material: polyglactin 910 + fibrin sealant. *Neurosurg Rev,* 19**,** 89-91.

VAN DE MEENT, H., HAMERS, F. P., LANKHORST, A. J., BUISE, M. P., JOOSTEN, E. A. & GISPEN, W. H. 1996. New assessment techniques for evaluation of posttraumatic spinal cord function in the rat. *J Neurotrauma,* 13**,** 741-54.

VAN DER KOOY, D., KUYPERS, H. G. & CATSMAN-BERREVOETS, C. E. 1978. Single mammillary body cells with divergent axon collaterals. Demonstration by a simple, fluorescent retrograde double labeling technique in the rat. *Brain Res,* 158**,** 189-96.

VINCENT, A. J., WEST, A. K. & CHUAH, M. I. 2005. Morphological and functional plasticity of olfactory ensheathing cells. *J Neurocytol,* 34**,** 65-80.

WAIKAKUL, S., WONGTRAGUL, S. & VANADURONGWAN, V. 1999. Restoration of elbow flexion in brachial plexus avulsion injury: comparing spinal accessory nerve transfer with intercostal nerve transfer. *J Hand Surg Am,* 24**,** 571-7.

WALL, P. D., SCADDING, J. W. & TOMKIEWICZ, M. M. 1979. The production and prevention of experimental anesthesia dolorosa. *Pain,* 6**,** 175-82.

WANG, M., XU, W., ZHENG, M., TENG, F., XU, J. & GU, Y. 2011. Phrenic nerve end-to-side neurotization in treating brachial plexus avulsion: an experimental study in rats. *Ann Plast Surg,* 66**,** 370-6.

WANG, R., KING, T., OSSIPOV, M. H., ROSSOMANDO, A. J., VANDERAH, T. W., HARVEY, P., CARIANI, P., FRANK, E., SAH, D. W. & PORRECA, F. 2008. Persistent restoration of sensory function by immediate or delayed systemic artemin after dorsal root injury. *Nat Neurosci,* 11**,** 488-96.

WEWETZER, K. & BRANDES, G. 2006. Axonal signalling and the making of olfactory ensheathing cells: a hypothesis. *Neuron Glia Biol,* 2**,** 217-24.

WEWETZER, K., KERN, N., EBEL, C., RADTKE, C. & BRANDES, G. 2005. Phagocytosis of O4+ axonal fragments in vitro by p75- neonatal rat olfactory ensheathing cells. *Glia,* 49**,** 577-87.

WHISHAW, I. Q. 2000. Loss of the innate cortical engram for action patterns used in skilled reaching and the development of behavioral compensation following motor cortex lesions in the rat. *Neuropharmacology,* 39**,** 788-805.

WHISHAW, I. Q. & GORNY, B. 1994. Arpeggio and fractionated digit movements used in prehension by rats. *Behav Brain Res,* 60**,** 15-24.

YAMAMOTO, M., RAISMAN, G., LI, D. & LI, Y. 2009. Transplanted olfactory mucosal cells restore paw reaching function without regeneration of severed corticospinal tract fibres across the lesion. *Brain Res,* 1303**,** 26-31.

YANG, J., LI, X., HOU, Y., YANG, Y., QIN, B., FU, G., QI, J., ZHU, Q., LIU, X. & GU, L. 2015. Development of a novel experimental rat model for brachial plexus avulsion injury. *Neuroreport,* 26**,** 501-9.

YANG, J. T., FANG, J. T., LI, L., CHEN, G., QIN, B. G. & GU, L. Q. 2019. Contralateral C7 transfer combined with acellular nerve allografts seeded with differentiated adipose stem cells for repairing upper brachial plexus injury in rats. *Neural Regen Res,* 14**,** 1932-1940.